THE UNIVERSITY OF MICHIGAN
AUG 30 1960
ENGINEERING LIBRARY

JOURNAL OF FLUID MECHANICS

VOLUME 8 PART 4

AUGUST 1960

PUBLISHED BY

CAMBRIDGE UNIVERSITY PRESS

BENTLEY HOUSE, 200 EUSTON ROAD, LONDON, N.W.1

AMERICAN BRANCH: 32 EAST 57TH STREET, NEW YORK 22, N.Y.

Price 30*s.* (*U.S.A.* $5.00)

The JOURNAL OF FLUID MECHANICS exists for the publication of theoretical and experimental investigations of all aspects of the mechanics of fluids, and is issued in four parts per volume.

EDITOR

DR G. K. BATCHELOR

Department of Applied Mathematics and Theoretical Physics, University of Cambridge, Free School Lane, Cambridge, England

ASSISTANT EDITORS

DR T. B BENJAMIN, DR I. PROUDMAN, DR P. G. SAFFMAN

Department of Applied Mathematics and Theoretical Physics, University of Cambridge, Free School Lane, Cambridge, England

ASSOCIATE EDITORS

PROF. G. F. CARRIER

Pierce Hall, Harvard University, Cambridge 38, *Massachusetts, U.S.A.*

DR W. C. GRIFFITH

Research and Development Laboratory, Missile Systems Division, Lockheed Aircraft Corporation, Palo Alto, California, U.S.A.

M. J. LIGHTHILL

Royal Aircraft Establishment, Farnborough, Hampshire, England

PROF. R. R. LONG

School of Engineering, The Johns Hopkins University, Baltimore 18, *Maryland, U.S.A.*

Authors wishing to have papers published in the JOURNAL should communicate them to any one of the persons named above, choosing one in their own country where possible.

Authors are urged to ensure that their papers are written clearly and attractively, in order that their work will be readily accessible to readers.

Manuscripts should be typed in double spacing on one side of the paper only, with references listed at the end in alphabetical order of authors. Drawings should be done on a large scale in Indian ink on tracing cloth or drawing paper, the lettering being shown clearly in pencil for reproduction by the printer; the list of captions should be typed at the end of the manuscript. Proofs of papers from overseas will usually be despatched to authors by airmail. There is no charge for publication. Authors are entitled to receive 50 offprints of a paper in the JOURNAL free of charge, and additional offprints can be purchased if ordered in advance.

SUBSCRIPTIONS

The subscription price for a volume of four parts is £5. 10*s*. net, post free, payable in advance; separate parts 30*s*. net, plus postage. Subscriptions may be sent to any bookseller, or to the Cambridge University Press, Bentley House, 200 Euston Road, London, N.W. 1.

Subscribers in the United States should send their orders to the Cambridge University Press, American Branch, 32 East 57th Street, New York 22. The subscription price per volume is $18.50, post free, payable in advance; separate parts $5.00, plus postage.

Quotations for available back volumes and parts may be obtained on application to the Cambridge University Press.

Gravity waves in a stratified fluid

By CHIA-SHUN YIH
Department of Engineering Mechanics, University of Michigan

(Received 18 December 1959)

A unified treatment of wave motion in a stratified fluid, with or without density discontinuities, is achieved by reducing the governing differential system to a Sturm–Liouville system. With the aid of Sturm's comparison theorem, it is found (without detailed calculations) that, for any stratification, the phase velocity increases as the wave-number decreases and that, for the same wave-number, the phase velocity increases as the density gradient is increased everywhere and decreases as the density is increased everywhere by a constant amount. Sturm's oscillation theorem provides upper and lower bounds for the phase velocity for a given stratification, a given wave-number, and a given number of zeros of the eigenfunction (or a given number of stationary surfaces in the fluid). The inequalities giving these bounds are used to explain the well-known tendency for surfaces of density discontinuities to behave as rigid boundaries when the stratification in each layer is slight. The rigid-boundary behaviour of interfaces in such cases enables one to obtain the approximate eigenvalue spectrum by superimposing the spectra of the individual layers (with the interfaces treated as rigid) on the spectrum of the interfacial (or free surface) waves, obtained by ignoring the slight continuous stratification in each layer. It is pointed out that the Ritz method can be used for calculating the eigenvalues even when the density is discontinuous, and examples are given to show the accuracy of the Ritz method. The nature of the spectrum when the depth is infinite is also clarified.

In the course of the development of the theory, the effects of compressibility and of three-dimensionality are determined and given explicitly, the rate of growth of unstable stratifications is related to the phase velocity of waves in stable ones, and equipartition of energy is proved. Motion due to a wave-maker is discussed in order to bring out the connexion between the type of the governing partial differential equation and the nature (local or not local) of the disturbances. The effect of surface tension and the stability of a stratified fluid under vertical oscillation are also discussed.

1. Introduction

The propagation of gravity waves in a system consisting of many distinct layers of fluids was investigated by Webb (1884) and Greenhill (1887) many years ago. Recently, Benton (1953) considered the propagation of long waves in a system of flowing layers, and by a limiting process generalized the result to apply to

waves propagating in a flowing fluid with continuous stratification. His approach provides a desirable link between results for distinct layers and those for a continuously stratified fluid. However, a unified theory is still lacking, and a convenient method for determining the phase velocity remains to be adopted. In this paper, the approach is diametrically opposite to that of Benton. Instead of considering a continuous stratification as a limit of a discontinuous one, as Benton did, one deals with continuous stratifications directly and treats surfaces of density discontinuity as limits of regions of large density gradients. If the effect of viscosity is neglected, the governing differential system is a Sturm–Liouville system, and Sturm's theorems can be used for the prediction of the ranges in which the phase velocities for the various modes must lie, for comparing the phase velocity in one stratified fluid with that of the corresponding mode in another, and for explaining a well-known behaviour of the surfaces of density discontinuity. The theory of infinitesimal waves presented herein also includes a technique to obtain the phase velocity to any degree of accuracy, an example of wave motion generated by a simple wave-maker, and an investigation of stability under vertical vibration.

2. The governing differential system

The differential system governing the propagation of gravity waves in a continuously stratified fluid at rest is well known (Lamb 1945, p. 378). Since the effect of compressibility will be discussed later, it is desirable to derive the differential system for wave propagation in a stratified and compressible fluid at rest, on the assumption that the change of state for each material particle is isentropic (the entire fluid not necessarily having the same entropy). The equations for incompressible fluids can then be immediately obtained by letting the sound velocity approach infinity.

With x, y, and z denoting Cartesian co-ordinates, z being measured vertically upward, and u, v and w denoting the corresponding velocity components, the mean density $\bar{\rho}(z)$ and mean pressure $\bar{p}(z)$ are related by the hydrostatic condition

$$\bar{p}' = -g\bar{\rho}. \tag{1}$$

The linearized equation of continuity is

$$\frac{\partial \rho}{\partial t} + \bar{\rho}\left(\frac{\partial u}{\partial x} + \frac{\partial v}{\partial y} + \frac{\partial w}{\partial z}\right) + w\bar{\rho}' = 0, \tag{2}$$

in which ρ is the density fluctuation and the accent indicates differentiation with respect to z. Since the velocity and the density perturbation are assumed to be small, their products and products of their derivatives have been neglected in the equation of continuity, and will be neglected in all the equations to be presented in this section. The linearized equation of isentropy is

$$\frac{\partial p}{\partial t} + w\bar{p}' = \frac{\partial p}{\partial t} - g\bar{\rho}w = c_s^2\left(\frac{\partial \rho}{\partial t} + w\bar{\rho}'\right), \tag{3}$$

in which p is the pressure fluctuation and c_s the sound velocity, which can vary with z. The equations of motion are, for an inviscid fluid,

$$\bar{\rho}\frac{\partial}{\partial t}(u, v, w) = -\left(\frac{\partial}{\partial x}, \frac{\partial}{\partial y}, \frac{\partial}{\partial z}\right) p + (0, 0, -g\rho). \tag{4}$$

From the first two of equations (4), it follows immediately upon cross-differentiation that

$$\frac{\partial}{\partial t}\left(\frac{\partial(\bar{\rho}u)}{\partial y} - \frac{\partial(\bar{\rho}v)}{\partial x}\right) = 0.$$

If the motion is started from rest, or if u and v (as well as other dependent variables) are assumed to have an exponential time factor,

$$\frac{\partial(\bar{\rho}u)}{\partial y} - \frac{\partial(\bar{\rho}v)}{\partial x} = 0,$$

and a potential ϕ exists for u and v

$$\bar{\rho}u = -\frac{\partial\phi}{\partial x}, \quad \bar{\rho}v = -\frac{\partial\phi}{\partial y}.$$

The motion is therefore irrotational when *viewed from above*, in much the same way that Hele–Shaw flows are irrotational when viewed in a direction perpendicular to the (closely spaced) plane boundaries. The equation of continuity then assumes the form

$$\nabla^2\phi = \bar{\rho}\frac{\partial w}{\partial z} + w\bar{\rho}' + \frac{\partial\rho}{\partial t}, \quad \left(\nabla^2 = \frac{\partial^2}{\partial x^2} + \frac{\partial^2}{\partial y^2}\right), \tag{2a}$$

and integration of the first two of equations (4) produces

$$\frac{\partial\phi}{\partial t} = p,$$

with the function of integration $F(z, t)$ absorbed in $\partial\phi/\partial t$. After differentiation with respect to t and utilization of equations (3) and (2a), this equation assumes the form

$$\frac{\partial^2\phi}{\partial t^2} = g\bar{\rho}w + c_s^2\left(\nabla^2\phi - \bar{\rho}\frac{\partial w}{\partial z}\right). \tag{5}$$

Substituting $\partial\phi/\partial t$ for p in the third of equations (4), one has

$$\frac{\partial}{\partial t}\left(\frac{\partial\phi}{\partial z} + \bar{\rho}w\right) + g\rho = 0. \tag{6}$$

From equations (6) and (2a), the equation

$$\frac{\partial^3\phi}{\partial t^2\partial z} + g\nabla^2\phi - g\frac{\partial}{\partial z}(\bar{\rho}w) + \frac{\partial^2}{\partial t^2}(\bar{\rho}w) = 0$$

is obtained, whereas differentiation of equation (5) produces

$$\frac{\partial^3\phi}{\partial t^2\partial z} - g\frac{\partial}{\partial z}(\bar{\rho}w) - \frac{\partial}{\partial z}(c_s^2\nabla^2\phi) + \frac{\partial}{\partial z}\left(\bar{\rho}c_s^2\frac{\partial w}{\partial z}\right) = 0.$$

From these one obtains by subtraction

$$\nabla^2\left[g\phi+\frac{\partial}{\partial z}(c_s^2\phi)\right]+\frac{\partial^2}{\partial t^2}(\bar{\rho}w)-\frac{\partial}{\partial z}\left(\bar{\rho}c_s^2\frac{\partial w}{\partial z}\right)=0.$$

Equation (5) and the equation following (7) give

$$\frac{\partial^2}{\partial t^2}\left(g\phi+c_s^2\frac{\partial\phi}{\partial z}\right)-g^2\bar{\rho}w-c_s^2g\bar{\rho}'w+c_s^2\frac{\partial^2}{\partial t^2}(\bar{\rho}w)=0,$$

from which follows

$$-(c_s^2)'\frac{\partial^2}{\partial t^2}\nabla^2\phi=\frac{\partial^4}{\partial t^4}(\bar{\rho}w)-\frac{\partial^3}{\partial t^2\partial z}\left(\bar{\rho}c_s^2\frac{\partial w}{\partial z}\right)+(g^2\bar{\rho}+c_s^2g\bar{\rho}')\nabla^2w-c_s^2\bar{\rho}\frac{\partial^2}{\partial t^2}\nabla^2w. \quad (7)$$

In the problems treated in this paper, ϕ, w, p and ρ are assumed to have a common factor $S(x,y)$ which satisfies the equation

$$(\nabla^2+\alpha^2)S(x,y)=0. \quad (8)$$

If the time-dependence of ϕ and w is assumed to be contained in the exponential factor $e^{-i\sigma t}$, so that

$$(\phi,w)=e^{-i\sigma t}S(x,y)\,[\phi(z),w(z)],$$

elimination of ϕ from equations (5) and (7) with the aid of (8) produces, with w now indicating $w(z)$,

$$\left(\frac{\alpha^2c_s^2}{\sigma^2}-1\right)[\sigma^2c_s^2(\bar{\rho}w')'+(\sigma^4-\alpha^2g^2-c_s^2\alpha^2\sigma^2)\bar{\rho}w-c_s^2\alpha^2g\bar{\rho}'w]$$
$$+(c_s^2)'\bar{\rho}(\alpha^2gw-\sigma^2w')=0. \quad (9)$$

For three-dimensional sinusoidal waves, the appropriate form for $S(x,y)$ is $\exp i(kx+ly)$, so that, with $\sigma=kc$,

$$(u,v,w,p,\rho)=[u(z),v(z),w(z),p(z),\rho(z)]\exp i(kx+ly-kct).$$

If, for brevity, u is written for $u(z)$, etc., the relationships between the several unknowns are

$$c\bar{\rho}u=p,\quad lu=kv,\quad ikc\bar{\rho}w=c(\bar{\rho}u)'+g\rho,\quad -ikcp-g\bar{\rho}w=c_s^2(-ikc\rho+w\bar{\rho}'),$$

and

$$i\rho u=\frac{kc_s^2\bar{\rho}}{(k^2+l^2)c_s^2-k^2c^2}\left(\frac{gw}{c_s^2}-w'\right),$$

which are recorded here for general convenience. With $\alpha^2=k^2+l^2$ and $\sigma=kc$, equation (9) has the form

$$\left[\frac{(k^2+l^2)c_s^2}{k^2c^2}-1\right]\{k^2c^2c_s^2(\bar{\rho}w')'+(kc)^4\bar{\rho}w-(k^2+l^2)[(g^2+k^2c^2c_s^2)\bar{\rho}w-c_s^2g\bar{\rho}'w]\}$$
$$+(c_s^2)'\bar{\rho}[(k^2+l^2)gw-k^2c^2w']=0. \quad (9a)$$

If c_s is constant, equation (9a) assumes the simpler form

$$(\bar{\rho}w')'-\frac{k^2+l^2}{k^2}\left(k^2\bar{\rho}-\frac{g}{c^2}\bar{\rho}'\right)w+\frac{c^2}{c_s^2}\left(k^2-\frac{(k^2+l^2)g^2}{k^2c^4}\right)\bar{\rho}w=0. \quad (10)$$

If the fluid is bounded by two rigid barriers at $z = 0$ and $z = d$, the boundary conditions are

$$w(0) = 0, \quad w(d) = 0.$$

Boundary conditions at free surfaces and interfaces will be presented later.

For an incompressible fluid, $c_s = \infty$, and equation (10) reduces to

$$(\bar{\rho}w')' - \frac{k^2+l^2}{k^2}\left(k^2\bar{\rho} + \frac{g}{c^2}\bar{\rho}'\right)w = 0, \tag{11}$$

which for two-dimensional motion can be further reduced to the simple form

$$(\bar{\rho}w')' - \left(k^2\bar{\rho} + \frac{g}{c^2}\bar{\rho}'\right)w = 0. \tag{12}$$

For two-dimensional motion of a compressible fluid with constant c_s, equation (10) has the form

$$(\bar{\rho}w')' - \left(k^2\bar{\rho} + \frac{g}{c^2}\bar{\rho}'\right)w + \frac{c^2}{c_s^2}\left(k^2 - \frac{g^2}{c^4}\right)\bar{\rho}w = 0. \tag{13}$$

3. General considerations

Although equation (10) appears rather complex as it stands, for many problems its solution can be reduced to that of equation (12). First of all, the effect of three-dimensionality can be determined once and for all. From equation (9) it is seen that for a given stratification σ^2 is a function of α^2 (in this case k^2+l^2) alone. (The sum k^2+l^2 really is the square of the wave-number of a corresponding two-dimensional wave travelling in the direction with direction numbers k, l, and zero.) Thus, without any loss of generality, the problem of determining σ given k and l is reduced to the problem of determining σ for a two-dimensional wave motion with wave-number $k_2 = \alpha$, from equation (9). The rule of conversion, first enunciated and proved by Squire (1933) in connexion with a problem of hydrodynamic stability, is as follows. The σ for a three-dimensional disturbance of wave-numbers k and l is the same as that for a two-dimensional disturbance of wave-number $(k^2+l^2)^{\frac{1}{2}}$, the actual phase velocity c (in the x-direction) is σ/k which is greater than the c for an actual two-dimensional disturbance of wave-number $(k^2+l^2)^{\frac{1}{2}}$ by the factor $(k^2+l^2)^{\frac{1}{2}}/k$.

Turning now to equation (13), one seeks to determine the effect of compressibility in a simple way, without any detailed calculations. In this connexion it must be remembered that the sound velocity is in general a function of location. For liquids it can without great error be taken to be constant, and at all events the effect of compressibility is small. For gases, c_s is constant only for an isothermal atmosphere. Under the assumption that c_s is constant, and with a fictitious wave-number k_i for a corresponding wave motion in incompressible fluid defined as

$$k_i^2 = k^2 + \frac{c^2}{c_s^2}\left(\frac{g^2}{c^4} - k^2\right), \tag{14}$$

equation (13) is reduced to the form

$$(\bar{\rho}w')' - \left(k_i^2\bar{\rho} + \frac{g}{c^2}\bar{\rho}'\right)w = 0.$$

After c is determined from this equation for a chosen k_i, the actual k can then be calculated simply from equation (14). Of course, the assumed k_i should be greater than g/cc_s (in most cases) for a *wave* motion. Otherwise k^2 would be negative (since c is in most cases less than c_s) and the motion would not be a wave motion. With k found, σ is also known. This procedure evidently involves a process of trial and error if c is to be found for a given k, or k is to be found for a given σ, but it certainly is a convenient means of determining the effect of compressibility. Since g/k is the c^2 for free-surface waves in a semi-infinite fluid, and the c^2 for internal or interfacial waves is usually smaller, $k_i^2 > k^2$ in most cases of practical interest. In a subsequent paragraph it will be shown that the c^2 determined from equation (12) decreases with k^2. Thus, whenever c_s is constant and $g > kc^2$, the effect of compressibility is to *reduce* the phase velocity, and the amount of reduction can be simply determined in the manner described above.

Attention will then be focused on equation (12) in the major part of this paper. Since this corresponds to two-dimensional flows of an incompressible fluid, the stream function will be introduced for convenience

$$\psi = f(z)\exp ik(x-ct).$$

The velocity components being

$$u = -\frac{\partial\psi}{\partial z} = -f'(z)\exp ik(x-ct), \quad w = \frac{\partial\psi}{\partial x} = ikf(z)\exp ik(x-ct),$$

the function $w(z)$ in equation (12) can be replaced by $f(z)$

$$(\bar{\rho}f')' - \left(k^2\bar{\rho} + \frac{g\bar{\rho}'}{c^2}\right)f = 0. \tag{12a}$$

If, further, the new variable

$$\eta = \frac{z}{d}$$

is introduced, and accents are now used to denote differentiations with respect to η, equation (12a) becomes

$$(\bar{\rho}f')' - \left(m^2\bar{\rho} + \frac{gd}{c^2}\bar{\rho}'\right)f = 0, \tag{15}$$

in which $m = kd$ is the dimensionless wave-number.

The boundary conditions at the rigid boundaries are, in terms of η,

$$f(0) = 0, \quad f(1) = 0. \tag{16}$$

At a surface of density discontinuity the density below the surface will be denoted by $\bar{\rho}_l$ and that above by $\bar{\rho}_u$. The vertical velocity w at the interface is $\partial\zeta/\partial t$, in which ζ is the deviation of the interface from its mean position. With ζ expressed as $\zeta_0\exp ik(x-ct)$, the kinematic condition is

$$-c\zeta_0 = f, \tag{17}$$

to be applied at the interface. Apart from the exponential factor, the pressure at the interface is then, from equations (1), (17), and the first of equations (4),

$$\bar{\rho}_u\left(-cf' + \frac{g}{c}f\right)_u$$

for the upper fluid, and

$$\bar{\rho}_l\left(-cf'+\frac{g}{c}f\right)_l$$

for the lower. Continuity of the vertical velocity demands the continuity of the stream function:

$$f_u = f_l.$$

Hence the equality of pressures across the interface demands that

$$(\bar{\rho}f')_u-(\bar{\rho}f')_l+(\bar{\rho}_l-\bar{\rho}_u)\frac{gd}{c^2}f=0, \tag{18}$$

in terms of η. Equation (18) has been obtained by a fairly complicated argument. But if $\bar{\rho}$ and f' in equation (15) are allowed to be discontinuous, and only the continuity of f is maintained, integration of that equation in the Stieltjes sense across the interface produces (18) immediately. There are then two possible approaches. One can consider the system of differential equations governing the motion in the various continuously stratified layers, together with the interfacial conditions derived above. Or one can consider the motion of the entire fluid to be governed by equation (15), and allow solutions with discontinuous f' at the interfaces. The former is the conventional approach, but the latter approach is adopted in this paper, and it appears to be the more powerful and fruitful.

By the use of the present approach the whole power of the Sturm–Liouville theory can be borrowed to achieve a unified treatment of wave motion in stratified fluids. Without detailed calculations, certain conclusions can be drawn in regard to the variation of the phase velocity with wave-length and with the density distribution, the range in which the phase velocity must lie can be predicted, and certain well-known effects of density discontinuities can be explained. Furthermore, the Ritz method can be applied for calculating the phase velocities even when the density has discontinuities. The unified treatment is the main contribution of this paper. Many of the results obtained as a consequence of this treatment are new, or have a greater generality than has previously been achieved.

In order to have a Sturm–Liouville system, the upper boundary is assumed to be always rigid, and a free surface is considered to be a liquid-gas interface covered by a fluid layer of small but non-zero* density which is bounded above by a rigid plane. The location of the upper boundary is, in the presence of a free surface, assumed to have little effect on the phase velocities. Thus the boundary condition at the upper boundary is always $f(1) = 0$, and the governing differential system is a Sturm–Liouville system consisting of equations (15) and (16) in the former of which $\bar{\rho}$ may have finite discontinuities. The integral form of equation (15) is

$$f(\eta)=\int_0^\eta\frac{1}{\bar{\rho}}\left[\bar{\rho}(0)f'(0)+\int_0^\eta(m^2\bar{\rho}+\lambda\bar{\rho}')f\,d\eta\right]d\eta. \tag{19}$$

* Dr F. Ursell has pointed out to the author that the assumption of non-zero density for the top layer, made here for convenience, is really not necessary, and the developments presented here can well be extended to include cases in which a free surface in the ordinary sense is present. In this connexion, see Sz.-Nagy (1947).

in which $\lambda = gd/c^2$, and $\bar{\rho}$ is assumed to be greater than zero. In the presence of density discontinuities, the integration in equation (20) is in the Stieltjes sense, and the function $f(\eta)$ obtained (by step-wise integration, for instance) is continuous with discontinuous derivatives at the locations where the density is discontinuous. The boundary condition $f(0) = 0$ is automatically satisfied. Since $\bar{\rho}'$ is uniformly negative, it is easy to see that a sufficiently large λ will force f to be zero at $\eta = 1$, and that at least a first eigenvalue exists. The eigenfunction satisfies equation (15) everywhere except at the density discontinuities, where equation (18) is automatically satisfied.

To show that equations (19) and (16) possess infinitely many eigenvalues corresponding to eigenfunctions with the number of zeros increasing with the index of the eigenvalues, even when $\bar{\rho}$ is discontinuous, one may approximate the given stratification by an infinite sequence of continuous stratifications with increasingly greater density gradients near the discontinuities of the given stratification. For a specified number of zeros for f in the closed interval (0 to 1 inclusive), the eigenvalues (of λ) for the sequence must approach a limit* (by the Weierstrass–Bolzano theorem), which is the eigenvalue for the given stratification, for the specified number of zeros of f in the interval. That the limit is unique follows essentially from the fact that, for a specified number of zeros of f, the eigenvalue varies continuously with a continuous variation of the density distribution—a fact that can be proved easily. Consequently much of the Sturm–Liouville theory can be carried over to the case of discontinuous density. This fortunate situation is entirely due to the fact that the interfacial conditions (18) are implied in equation (15), and automatically satisfied by equation (19).

For a given density distribution and a given wave-number, the admissible values of c are determined by equations (15) and (16) . These values are the phase velocities of waves propagating in the fluid (otherwise at rest). If c has an imaginary part, the waves will grow† in amplitude. It is easy to show that if $\bar{\rho}'$ is everywhere negative c is real, and if $\bar{\rho}'$ is everywhere positive c is purely imaginary. Thus, if equation (15) is multiplied by the complex conjugate of f and integrated between 0 and 1, and equations (16) are utilized, we have

$$-\int_0^1 \bar{\rho}\,|f'|^2\,d\eta - m^2\int_0^1 \bar{\rho}\,|f|^2\,d\eta - \frac{gd}{c^2}\int_0^1 \bar{\rho}'\,|f|^2\,d\eta = 0, \tag{20}$$

which states that if $\bar{\rho}'$ is negative throughout, c^2 is positive and c is real, and that if $\bar{\rho}'$ is positive throughout, c is purely imaginary and the fluid is unstable. Clearly the same conclusion would have been reached if equation (11) for three-dimensional disturbances had been used instead of equation (15). If $\bar{\rho}'$ is partly negative and partly positive, equation (20) still demands that c^2 be real. It must also be negative, since it must be unstable on physical grounds. If $\bar{\rho}$ is discontinuous, the terms

$$-\frac{gd}{c^2}\sum_{i=1}^{M}(\Delta\bar{\rho})_i f_i^2$$

* That this limit exists can be proved by the aid of an easily constructed density distribution, which by Sturm's comparison theorem (for continuous $\bar{\rho}$) must have an eigenvalue (finite) greater than those for the sequence.

† The simplest way to see this is to note that k may be assigned negative values, so that whatever the sign of the imaginary part of c, the waves will grow.

must be added to the left-hand side of equation (20), and the conclusions are unchanged. In the above expression, i indicates the ith interface, $\Delta\bar{\rho}$ is the density jump (negative), and M is the total number of density discontinuities. The terms to be added arise from integration by parts and application of equation (18). Alternatively and preferably, the last integral in (20) can be considered to be in the Stieltjes sense. In this discussion, the density of the top layer can be taken to be zero without introducing any difficulty.

For an inversion of an originally stable stratification or, equivalently, for a reversal of the direction of gravity, equation (15) shows that the eigenvalue c^2 must change sign but retains its magnitude. Thus the fluid will be unstable, and the amplification factor $-ikc$ is exactly the same as the time frequency $\sigma\,(=kc)$ for the stable stratification. Calculations of phase velocities for given k's therefore also provides results for the amplification factor when the stratification is unstable. In the following sections, $\bar{\rho}'$ will be assumed to be negative throughout.

Without any detailed calculations, conclusions can be at once drawn from equations (15) and (16) that for the same stratification and the same mode* the smaller the wave-number m (hence the longer the wave-length), the greater the phase velocity c. This conclusion is the direct consequence of Sturm's fundamental theorem (Ince 1944, pp. 224–5) that the solutions of

$$\frac{d}{dx}\left(K\frac{df}{dx}\right)-Gf=0 \tag{21}$$

oscillate more rapidly when K and G are diminished algebraically. In the present discussion K is $\bar{\rho}$, which is the same for all wave-lengths. The quantity G is

$$m^2\bar{\rho}+\frac{gd}{c^2}\bar{\rho}',$$

which certainly diminishes as m diminishes. Inspection of the proof of the theorem reveals that it is still valid for the specified K and G if $\bar{\rho}$ has finite discontinuities. For the greatest value of c, the boundary conditions call for exactly one oscillation in the interval (0, 1). If for a certain m and c the boundary conditions are satisfied, for a smaller m and the same gd and c there would be one zero at $\eta=0$ (as required) and one other between 0 and 1, but not at 1, since the new G would be uniformly smaller than the old. In order to satisfy the boundary condition at $\eta=1$, c must be greater if gd is the same, since G increases uniformly with c. The fastest waves are therefore the longest waves. If the fluid is flowing at a uniform velocity U greater than the phase velocity of the longest waves of gravest mode, no infinitesimal disturbances can travel upstream. The flow is then supercritical and internal hydraulic jumps may occur under suitable downstream conditions. The reason for this is that finite disturbances travel faster than infinitesimal ones, and can travel with a speed equal to U to make a stationary jump possible. If U is less than the greatest possible c but larger than the greatest c for higher modes, internal hydraulic jumps may still occur.

From equations (15) and (16) it can be seen immediately that for a given $\bar{\rho}(\eta)$ and a given m, c is simply proportional to $\sqrt{(gd)}$. The values of gd/c^2 are deter-

* The mode of the wave is determined by the number of zeros of the function f.

mined by the governing differential system, and are the eigenvalues, the lowest of which corresponds to the greatest possible phase velocity. According to Sturm's main theorem of oscillation (Ince 1944, p. 233), the number of zeros in the open interval $0 < \eta < 1$ for the function $f(\eta)$ is greater by one as the index (arranged according to increasing magnitude) of the eigenvalue for $\lambda = gd/c^2$ is increased by one. (Since the end-points are always zeros by specification, the number of zeros in the closed interval $0 \leqslant \eta \leqslant 1$ also increases by one when the index of λ is increased by one.) If the first mode is associated with the first eigenvalue, etc., higher and higher modes correspond to more and more nodal planes of wave motion, and smaller and smaller phase velocities. In the following sections, the definition of 'mode' given above will be retained throughout, even in the presence of surfaces of density discontinuity. Whenever *distinguishable*, waves principally associated with surfaces of discontinuity are called interfacial waves in general or free-surface waves in particular (when the density on one side is very small), and waves principally associated with continuous stratifications are called internal waves.

Sturm's fundamental theorem is again useful for comparing the phase velocities for the same wave-number but different stratifications. According to the theorem, for the same m and gd/c^2, the number of zeros of $f(\eta)$ for a smaller $\bar{\rho}$ and a greater $|\bar{\rho}'|$ in the interval (0, 1) is at least as great as that for a greater $\bar{\rho}$ and smaller $|\bar{\rho}'|$. This means that if the eigenvalues for $\bar{\rho}_1$ and $\bar{\rho}_2$ are λ_1 and λ_2, respectively, and if $\bar{\rho}_1 > \bar{\rho}_2$ and $|\bar{\rho}_1'| < |\bar{\rho}_2'|$, then $\lambda_2 < \lambda_1$ and $c_2 > c_1$. This is very understandable from a physical point of view. From a review of the derivation of equation (15), it is clear that $\bar{\rho}$ is associated with the role of density as a measure of inertia, whereas $g\bar{\rho}'$ is a measure of the restoring force responsible for the existence of wave motion. A smaller $\bar{\rho}$ and greater $|\bar{\rho}'|$ therefore correspond to a greater time frequency of oscillation and (for the same m) a greater phase velocity. If density discontinuities are present, the comparison theorem is useful only if they occur at the same locations for the two stratifications under comparison. In that case the inequality for $\bar{\rho}'$ must be supplemented by

$$|\Delta\bar{\rho}|_1 < |\Delta\bar{\rho}|_2$$

at all locations of density discontinuities.

With the aid of the Sturm–Liouville theory, the ranges in which phase velocities for the various modes must lie can be determined for the case of continuous density. If the lowest density is a and the highest density b, and if the algebraically least and greatest values of the density gradient are $-\beta$ and $-\beta+\epsilon$, then for the nth mode (with $n+1$ zeros in the closed interval $0 \leqslant \eta \leqslant 1$)

$$\frac{gd\beta}{ac^2} - m^2 \geqslant n^2\pi^2, \quad \frac{gd(\beta-\epsilon)}{bc^2} - m^2 \leqslant (n+1)^2\pi^2,$$

or

$$\frac{gd\beta}{a(n^2\pi^2+m^2)} \geqslant c^2 \geqslant \frac{gd(\beta-\epsilon)}{b[(n+1)^2\pi^2+m^2]}. \tag{22}$$

Although these inequalities have been derived for continuous $\bar{\rho}$, they are still valid in the presence of density jumps, provided the $n+1$ zeros all occur in one layer with continuous density. For small ϵ and small $b-a$, and for large n or m,

the inequalities give a rather sharp estimate of c. These inequalities are obtained by comparing the zeros of the eigenfunctions with those of sine functions (which are solutions of a Sturm–Liouville system), and by applying Sturm's fundamental theorem (Ince 1944, p. 227.)

4. Surfaces of density discontinuity

It has been observed (Lamb 1945) that for two superposed layers of homogeneous fluids differing slightly in density and with a free surface on top, there are two distinct modes of gravity waves. For the one mode the phase velocity and the amplitude distribution with height are nearly the same as those of waves propagating on the free surface of a homogeneous fluid, the slight density difference of the two fluids producing only a slight correction. For the other mode the situation is entirely different. The free surface is now nearly horizontal, with negligible waviness, the greatest amplitude occurs at the interface, and the phase velocity is very much smaller. These conclusions follow from detailed calculations given in Lamb's book. What will happen in the general case of many interfaces (not excluding a free surface) separating many continuously but slightly stratified layers? Is it possible to reach similar conclusions? And, if so, is it possible to do so without detailed calculations? The answers to these questions are in the affirmative.

The simplest case of two continuously and slightly stratified layers with a single interface (which can be considered a free-surface if $\overline{\rho}_u$ is small) will be considered first. The first eigenvalue for $\lambda\,(=gd/c^2)$ calls for exactly two zeros situated at the end-points. Thus, the first mode corresponds essentially to interfacial waves only slightly affected by the slight continuous density variations. The subsequent modes are markedly different from the first one. For the next mode there is a zero of $f(\eta)$ between 0 and 1 (Sturm's oscillation theorem; see Ince (1944), p. 233). Since the continuous density gradient is small throughout, the inequalities (22) immediately show that $c^2 \sim \beta$ and is very small. Since f' is of the order* of 1, equation (18) shows that f is very small at the interface and of the order c^2. Equation (17) then shows that ζ_0 is of the order of c, and is therefore small. Thus the interface is almost horizontal, as if it were a rigid surface. For subsequent eigenvalues the number of zeros continually increases, and the same argument can be applied to reach the same conclusion. Furthermore, from the inequalities (22) it can be seen that, even if the density gradient is not very small, the phase velocity is still small (and hence the interface still behaves essentially as a rigid boundary) at large wave-numbers for any mode, and for high modes at the same wave-number.

The case next in complexity is that of three continuously stratified layers contained between two rigid boundaries and separated by two surfaces of density discontinuity. This includes the case of two layers with a free surface

* The function f can of course be multiplied by any constant. For convenience, its maximum value will be taken to be of order 1. For not too high a mode $f'(\eta)$ will then be of order 1. If the mode is high, f' may be considerably greater than 1, but then β is supposed to be very small, and the higher the mode, the smaller c^2 is for the same β. In fact, the product c^2f'/gd is of the order of β/n.

on top, for the highest of the three layers can be considered to consist of a fluid of very small density. For the first mode, the only zeros of $f(\eta)$ occur at $\eta = 0$ and $\eta = 1$. By Sturm's oscillation theorem another zero must appear in the interval $(0, 1)$ for the second eigenvalue. In which layer will this zero appear? Depending on the thicknesses of the layers and the magnitude of the density gradient in each layer, this middle zero can occur in any of the three layers. However, for very small density gradients in the layers, it can be concluded that the middle zero must occur in the middle layer. For, with the density discontinuities at the interfaces kept constant, the density gradient in each layer can be made to approach zero. As these gradients become smaller and smaller, a stage will be reached when the middle zero will be situated in the middle layer and will stay there as the gradients are further reduced, since otherwise either the highest or the lowest layer would have two zeros, and, in the limiting case, with two zeros in a homogeneous fluid, there could be no wave motion. Only one mode of wave motion would then exist in the limiting case of three homogeneous layers of fluids, in contradiction to established facts.

If the continuous density gradients are not small, liberal sufficient conditions can be found under which the middle zero must be located in the middle layer. In the case of three layers of thicknesses d_1, d_2 and d_3, it can be shown that

$$\left[\frac{(-\bar{\rho}')_{\min}}{\bar{\rho}_{\max}}\right]_{\text{upper layers}} > \left(\frac{d_3}{d_1+d_2}\right)^2 \left[\frac{(-\bar{\rho}')_{\max}}{\bar{\rho}_{\min}}\right]_{\text{lowest layer}} \tag{23}$$

and

$$\left[\frac{(-\bar{\rho}')_{\min}}{\bar{\rho}_{\max}}\right]_{\text{lower layers}} > \left(\frac{d_1}{d_2+d_3}\right)^2 \left[\frac{(-\bar{\rho}')_{\max}}{\bar{\rho}_{\min}}\right]_{\text{top layer}} \tag{24}$$

are sufficient conditions for long waves. If there is indeed an additional zero in the lowest layer, then Sturm's oscillation theorem states that

$$\left[\frac{g(-\bar{\rho}')_{\max}}{c^2\bar{\rho}_{\min}}\right]_{\text{lowest layer}} > \frac{\pi^2}{d_3^2}. \tag{25}$$

From equation (23) it then follows that

$$\left[\frac{g(-\bar{\rho}')_{\min}}{c^2\bar{\rho}_{\max}}\right]_{\text{upper layers}} > \frac{\pi^2}{(d_1+d_2)^2}, \tag{26}$$

which is sufficient to guarantee an additional zero (other than the one at $\eta = 1$) in the upper two layers, in contradiction to hypothesis. Hence the middle zero must not occur in the bottom layer under the stated condition. The proof for the statement concerning equation (24) is entirely similar. For the general case of n layers of thicknesses $d_i (i = 1, \ldots, n)$, criteria similar to inequalities (25) and (26) can be used to determine the regions in which the additional zero or zeros must be located.

For the case of three layers, the next higher mode brings in a fourth zero. If the previous three zeros are in different layers, this fourth one must cause one of the layers to have two zeros. Then the inequalities (22) show that for small density gradients (small β) c^2 must indeed be very small. From the interfacial conditions stated by equation (18) it can be seen that the two interfaces now behave almost like rigid boundaries—a situation which is maintained in the

subsequent modes. For the general case, it can be shown by reasoning similar to that employed in the preceding two paragraphs that, for very small density variation in each layer, zeros in addition to those at the end-points will appear one after the other as the modes are higher and higher, until each layer has one and only one zero. The next higher eigenvalue, bringing in another zero, corresponds to a mode with one of its layers having two nodal points (or zeros). The surfaces of density discontinuity will then behave like rigid boundaries, and will so behave for subsequent modes. The number of modes for which the surfaces of density discontinuity do not behave like rigid boundaries is $n-1$ for n layers of fluid—the same as the number of these surfaces. The phase velocities for these modes are, for small density variation in each layer, nearly the same as those for wave motion in n homogeneous fluid layers with the same depths and the same mean densities as the layers under consideration.

The conclusions reached in this section remain essentially valid if the effect of surface tension Γ is included in the interfacial boundary conditions, which then assume the form

$$(\bar{\rho}f')_u-(\bar{\rho}f')_l+\left[\frac{\Gamma m^2}{c^2d}+(\bar{\rho}_l-\bar{\rho}_u)\frac{gd}{c^2}\right]f=0. \tag{27}$$

If there is only one surface of density discontinuity and if the density gradient elsewhere is small, the effect of surface tension, as far as interfacial waves are concerned, is to increase g by the amount

$$\frac{\Gamma m^2}{(\bar{\rho}_l-\bar{\rho}_u)\,d^2}=\frac{\Gamma k^2}{\bar{\rho}_l-\bar{\rho}_u}.$$

If there are two or more surfaces of discontinuity, approximate phase velocities of the interfacial waves can be found by assuming the density in each layer to be constant and equal to the mean density (provided that the density variation in each layer is small), and by imposing the boundary conditions (27) instead of (18). For internal waves the effect of surface tension is to stiffen the interfaces further (as can also be seen from the fact that the coefficient of f in equation (27) is increased by surface tension), and if the interfaces behave like rigid barriers without surface tension, they will do so even more effectively with the aid of surface tension. Thus the phase velocities for truly internal waves are hardly affected by surface tension.

5. Equipartition of energy

Equation (20), used in a previous section to prove the reality of c, also contains the theorem of equipartition of energy. For isopycnic particles

$$(u,w,\zeta)=\left[-f'(z),ikf(z),-\frac{f(z)}{c}\right]\exp ik(x-ct).$$

Integration of u^2, w^2 and ζ^2 with respect to x over a wave-length produces the common factor $\frac{1}{2}$. With the multiplication of this common factor, equation (20) can be written, in dimensional terms

$$\frac{g}{2}\int_0^d\bar{\rho}'\zeta^2dz=\frac{1}{2}\left(\int_0^d\bar{\rho}f'^2dz+k^2\int_0^d\bar{\rho}f^2dz\right). \tag{28}$$

The left-hand side of this equation represents the excess of potential energy* per unit wave-length in the x-direction over that of the mean configuration, or the potential energy of wave motion. The right-hand side obviously represents the kinetic energy per unit length. The equation therefore states that there is equipartition of energy. Although the proof given is for progressive waves, a slight modification of the form of u, w and ζ will make it valid for standing waves also.

Equation (20) was derived for the case of rigid barriers at $z = 0$ and $z = d$, and for a continuous stratification. If there are density discontinuities, the integral on the left-hand side of equation (28) must be taken to be in the Stieltjes sense, but the equipartition of energy is unaffected. In this discussion, the density of the top layer can be taken to be zero without introducing any difficulty.

For the same wave-number m general wave motion in a stratified fluid may be composed of many modes, each of which corresponds to an eigenvalue of gd/c^2 (or of c). It will be shown that the kinetic and potential energies of the component modes are entirely separable. In other words there are no energy couplings between the component modes at all. The proof for the case of a continuously stratified fluid between rigid boundaries is straightforward. The differential system consisting of equations (15) and (16) is self-adjoint, and it is well known that for such a system the eigenfunctions are orthogonal. In the present instance this means that (with r and s indicating the modes)

$$\int_0^1 \bar{\rho}' f_r(\eta)\, f_s(\eta)\, d\eta = 0, \tag{29}$$

or that there is no coupling of the various modes as far as potential energy of the wave motion is concerned. To obtain the corresponding result for kinetic energy, equation (15) will be written in the form

$$(\bar{\rho} f_r')' - (m^2 \bar{\rho} + \lambda_r \bar{\rho}') f_r = 0. \tag{30}$$

If equation (30) is multiplied by f_s and integrated, and if equations (16) are utilized, the result

$$\int_0^1 \bar{\rho}(f_r' f_s' + m^2 f_r f_s)\, d\eta = 0 \tag{31}$$

is obtained, which states that there is also no coupling between the different modes in connexion with kinetic energy.

In the presence of surfaces of density discontinuity, the governing differential system is no longer self-adjoint in the ordinary sense, but the de-coupling of potential and kinetic energies can be proved with the aid of the boundary conditions (18). Cross-multiplication of equation (30) and the equation

$$(\bar{\rho} f_s')' - (m^2 \bar{\rho} + \lambda_s \bar{\rho}') f_s = 0 \tag{32}$$

* The factor $\frac{1}{2}$ can best be explained by considering the potential energy of water waves. The water in the troughs are raised to the crests, each element ζdx by the height ζ. Thus the total potential energy is proportional to the integral of ζ^2 over a half wave-length. Hence the factor $\frac{1}{2}$.

by f_s and f_r and integration of the difference of the results produces, after utilization of equation (20) at all the interfaces,

$$\sum_{i=1}^{M} (\Delta\overline{\rho} f_r f_s)_i + \sum_{j=1}^{n} \int_{\eta_{j-1}}^{\eta_j} \overline{\rho}' f_r f_s d\eta = 0, \tag{33}$$

which is the same as equation (29) if the latter is considered to be in the Stieltjes sense. From equations (30) and (33), equation (31) is again obtained. Thus the normality of the energy spectra is established even in the presence of density discontinuities, as indeed is to be expected.

So far the normality of the energy spectra has been established only for the same wave-number. It remains to mention that if the wave-numbers are different, the net coupling effect is finite over a distance in the x-direction however long, and is therefore zero per unit distance.

The conclusion of equipartition of energy is valid for three-dimensional waves also. The proof is entirely similar. One needs only to start with equation (11) instead of equation (15), and use $lu = kv$.

6. The case of infinite depth

As has been remarked by Lamb (1945) for incompressible fluids, and as can be easily verified from equation (9*a*) for a semi-infinite fluid with any stratification (whether compressible or not), the system consisting of equation (9*a*) (with $l = 0$ and w changed to f), the conditions at infinity

$$f(z) \to 0 \quad \text{as} \quad z \to -\infty, \tag{34}$$

and the *usual* free-surface condition

$$f'(0) - \frac{g}{c^2} f(0) = 0 \tag{35}$$

possess the solution $$f(z) = e^{kz}, \quad c^2 = g/k. \tag{36}$$

The fact that the solution is independent of the mean density distribution and that it corresponds to irrotational motion is certainly rather surprising. But the explanation is not far to seek. The solution is the same as the well-known solution for wave motion in a semi-infinite homogeneous fluid. If it is valid also for a non-homogeneous fluid, there must be something very special about it. The special feature is that in co-ordinates *moving with the waves* the streamlines of the (steady) flow corresponding to the solution are lines of constant pressure, as can be readily demonstrated. This situation is not affected if the density is a function of the stream function alone (which is the case for an incompressible fluid in steady motion) or for a compressible fluid with isentropic change of state along a streamline (hence p is a function of ρ alone along a streamline). The distribution of mean density or mean entropy in the vertical direction is quite immaterial, so long as the density or entropy does not change along a streamline in the moving frame of reference. For convenience only two-dimensional waves have been discussed. The essential features of the flow are, however, unchanged if the waves are three-dimensional.

Actually, though the solution given by equation (36) is the only one which is independent of density stratification, another interesting one exists if c_s is con-

stant. Equation (13), with w changed to f, and the boundary conditions (34) and (35) are evidently satisfied by

$$f(z) = \exp\{(g/c_s^2)\,z\}, \quad c = c_s. \tag{37}$$

The motion represented by this solution, which is incidentally independent of the wave-number, is not irrotational. That it is independent of the density variation (so long as it is consistent with constant c_s or with an isothermal atmosphere) is again because streamlines in a frame moving with the waves are isobars. It has often been said that sound waves are longitudinal. The wave motion discovered here propagates with sound velocity, and is strongly affected by compressibility, and yet, since c_s is large and therefore $u \sim f'(z)$ is small, it is predominately transverse.

In the case of finite depth the eigenvalues are discrete and, if the stratification is continuous over any portion of the fluid, infinite in number. If the depth is infinite, the spectrum of the eigenvalues is continuous, with a number of discrete eigenvalues equal to the number of density discontinuities (or possibly greater than it if the fluid is compressible). For demonstration, a fluid with the density variation

$$\bar{\rho} = \rho_0 e^{-bz} \quad (b \text{ positive})$$

and with a free surface at $z = 0$ may be considered. For this particular density variation, the atmosphere is isothermal and the sound velocity constant, as can be seen by applying the hydrostatic equation $dp = -g\bar{\rho}\,dz$. Thus equation (13) can be solved exactly. (The free surface should, of course, be removed to $z = \infty$ to make the problem realistic.) However, the purpose of this section is to show the continuity of the spectrum of σ. Hence the fluid will be assumed to be incompressible for simplicity, and the fluid to extend to $z = -\infty$. Equation (12a) possesses the solution

$$f(z) = A\,e^{a_1 z} + B^{a_2 z}$$

in which

$$(a_1, a_2) = \frac{1}{2}\left[b \pm \sqrt{\left\{b^2 - 4k^2\left(\frac{gb}{\sigma^2} - 1\right)\right\}}\right] \quad (\sigma = kc). \tag{38}$$

If $gb < \sigma^2$, equation (34) demands that $B = 0$, and the surface condition (35) demands that

$$a_1 = \frac{gk^2}{\sigma^2} \quad \text{or} \quad c^2 = \frac{g}{k}.$$

The solution is therefore the one discussed before in the present section. However, if $gb > \sigma^2$, both a_1 and a_2 have a positive real part, so that the condition at $z = -\infty$ is automatically satisfied, and the surface condition assumes the form

$$Aa_1 + Ba_2 - (A + B)\frac{gk^2}{\sigma^2} = 0.$$

Given any k, b and σ, B can be solved in terms of A or vice versa. Thus any σ equal to or less than $\sqrt{(gb)}$ will do, and the spectrum of σ is continuous from zero to $\sqrt{(gb)}$. For any k the spectrum of c is then continuous from zero to $\sqrt{(gb)}/k$. For $k < b$, the value gk for σ^2 satisfies the requirement $gb/\sigma^2 \geqslant 1$. Thus the situation can be summarized as follows. (1) For any k, gk is an eigenvalue for σ^2. It corresponds to a motion identical to that of ordinary surface waves, and is an

isolated mode if $k > b$. (2) Any σ^2 less than gb corresponds to a possible wave motion. For $k \leqslant b$, the eigenvalue (for σ^2) for the free-surface mode is imbedded in the continuous spectrum for σ^2.

The example just given is instructive in showing that free-surface waves are not necessarily faster than internal waves. In fact, even if the depth is finite, free-surface waves or interfacial waves (corresponding to discontinuous density changes) are not necessarily faster than internal waves that owe their existence to continuous stratifications. They are faster only if the gradients of the continuous density stratifications are small.

If the top of the fluid is covered with a rigid boundary, no solution is possible for $gb \leqslant \sigma^2$. The continuous spectrum is given by

$$\frac{gb}{\sigma^2} > 1, \quad \text{or} \quad \sigma^2 < gb.$$

These values of σ^2 all correspond to internal waves. The free-surface mode is removed with the removal of the free surface, as expected.

7. Calculation of phase velocities

The phase velocities of waves propagating in a stratified fluid can be calculated rapidly by the method of Ritz. The differential system determining $\lambda = gd/c^2$ for a given density variation and a given wave-number consists of equations (15) and (16) for the case of fixed boundaries. Equation (15) is a special case of the general equation

$$L(f) = \lambda G(\eta) f, \tag{39}$$

in which L is a linear operator. According to the Ritz method, a set of N linearly independent functions $\phi_r(\eta)$ satisfying the boundary conditions will be chosen. The quantities

$$A_{rs} = -\int_0^1 \phi_r(\eta)\, L[\phi_s(\eta)]\, d\eta \tag{40}$$

and

$$B_{rs} = -\int_0^1 G(\eta)\, \phi_r(\eta)\, \phi_s(\eta)\, d\eta \tag{41}$$

are symmetric in the sense that their values are unaffected as r and s are interchanged. This is obvious with B_{rs}. With A_{rs} symmetry is immediately clear upon integration by parts and utilization of the boundary conditions. The integrals in equations (40) and (41) are in the Stieltjes sense when applied to wave propagation in a stratified fluid with density jumps. (For a similar application, see Courant & Hilbert (1931, Vol. I. pp. 349–50). In fact, in case a free surface exists, it is not necessary to assume that there is a layer of light fluid with non-zero density over it. The choice of $\phi(\eta)$ can therefore be less restricted, see Courant (1926).) The eigenfunction is now approximated by a linear combination of the chosen functions

$$F(\eta) = \sum_{r=1}^{N} c_r \phi_r(\eta). \tag{42}$$

With f in equation (39) replaced by F, that equation is multiplied by F and integrated to yield

$$\int_0^1 FL(F)\, d\eta + \mu \int_0^1 \bar{\rho}' F^2\, d\eta = \sum_{r,s=1}^{N} (A_{rs} - \mu B_{rs})\, c_r c_s.$$

The right-hand side of this equation depends only on the c's. If the condition is imposed that it be stationary in value for variations in the c's, the N equations are obtained

$$\sum_{r=1}^{N} (A_{rs} - \mu B_{rs}) c_r = 0, \quad (s = 1, 2, \ldots, N).$$

Since the c's must not all vanish, it is necessary that

$$\begin{vmatrix} A_{11}-\mu B_{11} & A_{12}-\mu B_{12} & \ldots & A_{1N}-\mu B_{1N} \\ A_{21}-\mu B_{21} & A_{22}-\mu B_{22} & \ldots & A_{2N}-\mu B_{2N} \\ \ldots & \ldots & \ldots & \ldots \\ A_{N1}-\mu B_{N1} & A_{N2}-\mu B_{N2} & \ldots & A_{NN}-\mu B_{NN} \end{vmatrix} = 0. \tag{43}$$

Ritz has proved that the N roots (for μ) of this equation are near and slightly larger than the first N eigenvalues of λ. In general, if $N+M$ terms are taken for F in equation (42) the first N roots of the enlarged determinantal equation are nearer and nearer the first N eigenvalues as M becomes larger and larger. Thus, if only N terms are taken, the accuracy of the roots as eigenvalues increases in general from the Nth to the first root.

Two examples (for continuous density distribution) will be given to demonstrate the accuracy of the Ritz method. For the first, the density variation is assumed to be

$$\bar{\rho} = \rho_0 e^{-\beta\eta}.$$

Equation (15) can then be reduced to the form

$$f'' - \beta f' - \left(m^2 - \frac{\beta g d}{c^2}\right) f = 0. \tag{44}$$

With $$(\alpha_1, \alpha_2) = \frac{1}{2}\left[\beta \pm \sqrt{\left\{\beta^2 - 4\left(\frac{\beta g d}{c^2} - m^2\right)\right\}}\right],$$

the solution satisfying the boundary condition at $\eta = 0$ is

$$f = A(e^{\alpha_1 \eta} - e^{\alpha_2 \eta}).$$

The condition $f(1) = 0$ then demands that

$$e^{\alpha_1} - e^{\alpha_2} = 0,$$

or $$\alpha_1 - \alpha_2 = \sqrt{\{\beta^2 - 4(\beta\lambda - m^2)\}} = 2n\pi i \quad (n = 1, 2, \ldots).$$

Hence $$4\beta\lambda = 4n^2\pi^2 + \beta^2 + 4m^2,$$

or, with $$\lambda' = \beta\lambda,$$

$$\lambda' = n^2\pi^2 + m^2 + \tfrac{1}{4}\beta^2. \tag{45}$$

To use the Ritz method, it is better to write equation (44) in its original form, before the exponential factor was cancelled out

$$(e^{-\beta\eta} f')' - m^2 e^{-\beta\eta} f = -\lambda e^{-\beta\eta} f.$$

If $\phi_r(\eta) = \sin r\pi\eta$ and the first element of the determinant in equation (43) is equated to zero, the result (after cancelling a common factor) is obtained

$$2\pi^4 + m^2(2\pi^2 - \beta^2) = \mu_1(2\pi^2 - \beta^2),$$

or, for small β, $$\mu_1 = \pi^2 + m^2 + \tfrac{1}{2}\beta^2.$$

This is greater than the first eigenvalue only by the amount $\frac{1}{4}\beta^2$. That roots of equation (43) are always greater than the first eigenvalue is well known, but it is important to remember that this is so only if the differential equation is written in the form of equation (15), i.e. in the self-adjoint form. Had equation (44) been used for the application of the Ritz method, the value π^2+m^2 would have been obtained for μ_1, which is *smaller* than the first eigenvalue.

Had the true eigenfunctions $e^{\frac{1}{2}\beta\eta}\sin r\pi\eta$ been chosen to be $\phi_r(\eta)$, the true eigenvalues would of course be obtained. However, the purpose of this example is to demonstrate the power of Ritz's method in the general case, in which the form of the eigenfunctions is not known and cannot be easily guessed.

A second example is provided by the density variation

$$\bar{\rho}(\eta) = \rho_0\sqrt{(1-\beta\eta)}.$$

An exact solution exists in this case for long waves. Equation (15) can be written, for zero wave-number,

$$[\sqrt{(1-\beta\eta)}f']' + \frac{\beta\lambda}{2\sqrt{(1-\beta\eta)}}f = 0,$$

or

$$\frac{d^2f}{d\xi^2} + \frac{2\lambda}{\beta}\{1-\sqrt{(1-\beta)}\}^2 f = 0,$$

with

$$\xi = \frac{1-\sqrt{(1-\beta\eta)}}{1-\sqrt{(1-\beta)}}.$$

The boundary conditions are

$$f(\xi) = 0 \quad \text{at} \quad \xi = 0 \quad \text{and} \quad \xi = 1.$$

The eigenvalues for long waves are exactly

$$\lambda' = \beta\lambda = \frac{1}{2}\left[\frac{\beta n\pi}{1-\sqrt{(1-\beta)}}\right]^2.$$

Here again, if $\sin r\pi\xi$ were chosen to be $\phi_r(\eta)$ in the application of Ritz's method, the true eigenvalues would be obtained. This will not be done, for the same reason as stated before. Instead, we choose

$$\phi_r(\eta) = (1-\beta\eta)^{\frac{1}{4}}\sin r\pi\eta.$$

Then

$$B_{11} = \tfrac{1}{4},$$

$$A_{11} = \int_0^1 \left[\pi^2(1-\beta\eta)\cos^2\pi\eta - \frac{\beta\pi}{2}\sin\pi\eta\cos\pi\eta + \frac{\beta^2}{16}\frac{\sin^2\pi\eta}{1-\beta\eta}\right]d\eta$$

$$= \frac{\pi^2}{2} - \frac{\beta\pi^2}{4} + \frac{\beta^2}{32}\int_0^1 \frac{1-\cos 2\pi\eta}{1-\beta\eta}\,d\eta$$

$$= \frac{\pi^2}{2} - \frac{\beta\pi^2}{4} - \frac{\beta}{32}\ln(1-\beta) + O(\beta^4).$$

Therefore

$$\mu_1 = 2\pi^2 - \beta\pi^2 + \frac{\beta^2}{8} - \frac{\beta^3}{16} + O(\beta^4),$$

whereas

$$\lambda_1' = 2\pi^2 - \beta\pi^2 - \frac{\beta^2\pi^2}{8} + \frac{3\pi^2}{32}\beta^3 + O(\beta^4),$$

showing that the error is again of the order of β^2. The two examples given demonstrate that the modified Froude number $c/\sqrt{(g'd)}$ (with g' equal to $(g/\bar{\rho})\,d\bar{\rho}/d\eta$) for a small and practically constant density gradient is approximately equal to π^{-1} for long waves—a fact of great importance for prediction of the existence of lee waves in the wake of a body advancing in a stratified fluid. The number π^{-1}, however, cannot be applied to fluids whose density gradient is not practically constant.

It has been shown that for n continuously stratified layers with $n-1$ or n surfaces of density discontinuity there are $n-1$ or n modes of motion corresponding to interfacial (or free-surface) waves. If the density gradient in each layer is small, approximations to the first $n-1$ or n eigenvalues corresponding to these modes can be found by Greenhill's formula on the assumption that the density in each layer is constant and equal to the mean of the actual density in that layer. Since it has been shown that for higher modes the surfaces of density discontinuity behave like solid barriers, the subsequent eigenvalues can be found without appreciable error by considering each layer to be bounded by solid planes, and by arranging the eigenvalues λ found separately for all the layers in ascending order of magnitude.

To test the validity of this statement, one may consider the case of two layers of depth d_1 and d_2, and with density variations given by

$$\bar{\rho}_1(\eta_1) = C_1 e^{-\beta_1 \eta_1}, \quad \bar{\rho}_2(\eta_2) = C_2 e^{-\beta_2 \eta_2},$$

in which

$$\eta_1 = \frac{z}{d_1}, \quad \eta_2 = \frac{z}{d_2},$$

the subscript 1 is for the upper layer, and the origin of z is taken at the interface. The differential equation governing the motion in each layer is equation (44), and the solutions satisfying the boundary conditions $f_1(1) = 0$ and $f_2(-1) = 0$ are

$$f_1(\eta_1) = A(e^{\alpha_1 \eta_1} - e^{(\alpha_2-\alpha_1)+\alpha_2 \eta}),$$

$$f_2(\eta_2) = B(e^{\gamma_1 \eta_2} - e^{(\gamma_2-\gamma_1)+\gamma_2 \eta}),$$

with

$$(\alpha_1, \alpha_2) = \frac{1}{2}\left[\beta_1 \pm \sqrt{\left(\beta_1^2 - 4\left(\frac{\beta_1 g d_1}{c^2} - m^2\right)\right)}\right],$$

$$(\gamma_1, \gamma_2) = \frac{1}{2}\left[\beta_2 \pm \sqrt{\left(\beta_2^2 - 4\left(\frac{\beta_2 g d}{c^2} - m^2\right)\right)}\right].$$

Imposing the interfacial conditions

$$f_1(0) = f_2(0) \quad \text{and} \quad \frac{C_1}{d_1} f_1'(0) - \frac{C_2}{d_2} f_2'(0) + (C_2 - C_1)\frac{g}{c^2} f_1(0) = 0,$$

one has

$$\frac{C_1}{d_1}(\alpha_1 - \alpha_2 e^{\alpha_2-\alpha_1}) - \frac{C_2}{d_2}\frac{1-e^{\alpha_2-\alpha_1}}{1-e^{\gamma_2-\gamma_1}}(\gamma_1 - \gamma_2 e^{\gamma_2-\gamma_1}) + (C_2 - C_1)\frac{g}{c^2}(1 - e^{\alpha_2-\alpha_1}) = 0, \quad (46a)$$

or, alternatively,

$$\frac{C_1}{d_1}\frac{1-e^{\gamma_2-\gamma_1}}{1-e^{\alpha_2-\alpha_1}}(\alpha_1 - \alpha_2 e^{\alpha_2-\alpha_1}) - \frac{C_2}{d_2}(\gamma_1 - \gamma_2 e^{\gamma_2-\gamma_1}) + (C_2 - C_1)\frac{g}{c^2}(1 - e^{\gamma_2-\gamma_1}) = 0. \quad (46b)$$

The question is now asked: what error will be committed if g/c^2 is calculated from equation (45) for each layer, on the assumption that the interface is rigid? For the upper layer

$$\frac{g}{c^2} = \frac{1}{\beta_1 d_1}(n^2\pi^2 + m^2 + \tfrac{1}{4}\beta_1^2) \tag{45a}$$

according to equation (45), which is large* for small β_1. The dominant term in equation (46) is therefore the last term, and one sequence of phase velocities is given approximately by $1 - e^{\alpha_2 - \alpha_1} = 0$,

which is the condition that would be obtained for the upper layer if the interface were rigid. The error committed is the first term, and is of the magnitude $2n\pi C_1/d_1$ which can be annihilated by changing c^2 slightly (and therefore also making $1 - e^{\alpha_2 - \alpha_1}$ slightly different from zero). One may, in fact, multiply equation (46*a*) by $c^2/(C_2 - C_1)g$ and note that the error committed in calculating c^2/g by (45*a*) is of the order of $[2n\pi C_1/(C_2 - C_1)][\beta_1/(n^2\pi^2 + m^2)]$, which is small if β_1 is small or if n or m is large. For the lower layer, equation (46*b*) can be used for proving that little error is committed if equation (45) is used to calculate c, provided β_2 is small or n or m large. Thus the entire phase-velocity spectrum of internal waves (i.e. with the interfacial one excepted) is obtained by superimposing the phase-velocity spectrum of one layer on that of the other, both obtained on the supposition that the interfaces were rigid. Although the example is a specific one, the conclusion reached is evidently valid in general, in virtue of the results obtained in § 4.

If, however, the density difference in each layer is not small compared with the mean density, phase velocities can only be obtained by solving the entire eigenvalue problem. This can be done either approximately, by the use of the Ritz method, or analytically, by solving the differential equation for the bottom layer with the restriction that $f(0) = 0$ and with $f'(0)$ arbitrary. In the analytical solution, when the first interface is reached the starting f for the next layer is made to be the same as the terminal f for the bottom layer, and the starting f' for the new layer is found from the first interfacial boundary condition. This procedure is continued until the upper boundary, free or rigid, is reached. The final boundary condition is imposed and the eigenvalues for λ are found from the final equation obtained.

8. Waves generated by a plane wave-maker

The motion generated in a stratified fluid contained between two rigid boundaries by an oscillating plane normal to these boundaries and extending all the way between them can be found by solving

$$(\bar{\rho}f')' - m^2\left(\bar{\rho} + \frac{g}{\sigma^2 d}\bar{\rho}'\right)f = 0, \tag{15a}$$

with σ now equal to 2π times the oscillation frequency of the wave-maker. The eigenvalues are now those of m^2 consistent with equations (16). If σ is sufficiently large, the quantity in the second parenthesis of equation (15*a*) is positive, and the

* Since interval waves are being discussed, c^2 is very small even according to the exact equations (46), as can be asserted by virtue of the inequalities (22). Therefore the statement that g/c^2 is large for small β_1 is not based on a circular argument.

eigenvalues will be negative. These correspond to imaginary m's and exponential (instead of sinusoidal) dependence of the disturbance on x. If σ is very small, the quantity referred to above is negative, and the eigenvalues for m^2 are positive. The m will be real and waves will propagate from the oscillating plane. For the intermediate case of medium σ, the quantity in the second parenthesis in equation (15a) is positive for certain levels, and negative at others. In this case the eigenvalues of m^2 go from negative infinity (through discrete values) to positive infinity.

If the oscillating plane is situated at $x = 0$ and oscillates as $a\cos\sigma t$, and the fluid extends from there to $x = \infty$, the solution for the motion in general consists of a parallel-flow part, a part corresponding to the local disturbance, and a part corresponding to wave motion. The parallel-flow part is necessary in order to satisfy the demand of continuity and is given by

$$-a^2\sigma\left(\int_0^1 \frac{d\eta}{\overline{\rho}}\right)^{-1}\int_0^\eta \frac{d\eta}{\overline{\rho}},$$

which obviously satisfies equation (15a), with m equal to zero (not an eigenvalue). The solution for the stream function is then, with Sommerfeld's radiation condition at infinity,

$$\frac{\psi}{a^2\sigma} = -\cos\sigma t\left(\int_0^1 \frac{d\eta}{\overline{\rho}}\right)^{-1}\int_0^\eta \frac{d\eta}{\overline{\rho}} + \sum_{n=-\infty}^{n_1-1} A_n f_n(\eta)\, e^{-|m_n|x}\cos\sigma t + \sum_{n=n_1}^{\infty} A_n f_n(\eta)\cos(m_n x - \sigma t), \tag{47}$$

in which n_1 is the index of the first positive eigenvalue for m^2, and the coefficients A are determined by the condition at the oscillating plane

$$-\eta = -\left(\int_0^1 \frac{d\eta}{\overline{\rho}}\right)^{-1}\int_0^\eta \frac{d\eta}{\overline{\rho}} + \sum_{n=-\infty}^{\infty} A_n f_n(\eta),$$

by the usual method, since the eigenfunctions f_n are orthogonal. Since the f's are eigenfunctions of a Sturm–Liouville system, and since the latter are known to be complete, the completeness of the f's is not in question. A similar solution can be obtained if density jumps are present, and if the wave-maker has any shape and any specified motion whatever.

The mean energy flux at infinity can be calculated either directly or by means of the group velocity for each wave component. (The formula for calculating group velocity from phase velocity is the usual one.) The mean rate of work done by the wave-maker is equal to this mean energy flux. If all the m's are imaginary, there is no wave motion and no mean energy flux at infinity. Hence the mean rate of work done by the oscillating plane is zero.

The sign of the second parenthesis, which decides whether the eigenvalues of m^2 are positive or negative, or partly positive and partly negative, is directly connected with the type of the partial differential equation governing the motion. For incompressible fluids in two-dimensional motion with a time dependence described by $e^{-i\sigma t}$, equation (8) assumes the form

$$(\sigma^2\overline{\rho} + g\overline{\rho}')\frac{\partial^2 w}{\partial x^2} + \sigma^2\frac{\partial^2}{\partial z^2}\left(\overline{\rho}\frac{\partial w}{\partial z}\right) = 0.$$

If this is multiplied by $\bar{\rho}$ and the new variable

$$\xi = \int_0^z \frac{dz}{\bar{\rho}}$$

is used, the equation

$$\left(\sigma^2\bar{\rho}^2 + g\bar{\rho}\frac{d\bar{\rho}}{dz}\right)\frac{\partial^2 w}{\partial x^2} + \sigma^2\frac{\partial^2 w}{\partial \xi^2} = 0 \tag{48}$$

is obtained, which is elliptic or hyperbolic according as (Görtler 1954)

$$\sigma^2\bar{\rho} + g\frac{d\bar{\rho}}{dz}$$

is positive or negative. But this quantity is proportional to

$$\bar{\rho} + \frac{g}{\sigma^2 d}\frac{d\bar{\rho}}{d\eta}.$$

Consequently the sign of the second parenthesis in equation (15*a*) determines the type of equation (48). However, the type of the partial differential equation governing the motion of a stratified fluid, though of course relevant to the type of solution obtained (as shown in this section), does not play as significant a role as the type of the partial differential equation governing the homentropic flow of a compressible fluid. The reason is simply that for a given mode of wave motion corresponding to a $[\bar{\rho} + (g/\sigma^2 d)(d\bar{\rho}/d\eta)]$ with alternating signs, the particle velocities being small, the velocity in the steady flow relative to the waves is simply c everywhere, and the elliptic and hyperbolic regions do not in any sense correspond to subsonic and supersonic flows.

When equation (48) is hyperbolic, real characteristics exist, with slopes given by

$$\tan\gamma' = \frac{\sigma}{[-g\bar{\rho}(d\bar{\rho}/dz) - \sigma^2\bar{\rho}^2]^{\frac{1}{2}}}.$$

For very small σ, the characteristics are horizontal. This is in agreement with the finding (Yih 1959*a*) that steady, two-dimensional flows of an inviscid stratified fluid become one-dimensional when the motion is weak—a phenomenon that has been experimentally demonstrated (Yih 1959*b*).

9. Stability of stratified liquid under vertical vibration

The stability of a homogeneous liquid with a free surface when the container is accelerated periodically has been considered by Benjamin & Ursell (1954). The cause of instability is a kind of resonance, though not in the usual sense of a forced harmonic oscillation, and the frequency of free oscillation plays a role in the determination of stability or instability. For a stratified liquid the frequencies of free oscillation are infinite in number, and it can be expected that the resonance phenomenon has to be investigated for each mode of free oscillation, i.e. for each of the eigen-frequencies in the absence of the imposed vibration. That this is indeed the case can be seen from the following analysis.

The equations of motion *relative to the vibrating container* are

$$\bar{\rho}\frac{\partial}{\partial t}(u, v, w) = -\left(\frac{\partial}{\partial x}, \frac{\partial}{\partial y}, \frac{\partial}{\partial z}\right)p - \rho(0, 0, g - F\cos\omega t), \tag{49}$$

in which $F\cos\omega t$ is the acceleration of the container. Cross-differentiation of the first two of equations (49) again produces an equation which shows that $\bar{\rho}u$ and $\bar{\rho}v$ possess a potential ϕ, so that

$$\bar{\rho}(u,v) = -\left(\frac{\partial}{\partial x}, \frac{\partial}{\partial y}\right)\phi.$$

By the same procedure as that employed in § 2, an equation similar to equation (6) is obtained

$$\frac{\partial}{\partial t}\left(\frac{\partial\phi}{\partial z} + \bar{\rho}w\right) + (g - F\cos\omega t)\rho = 0. \tag{50}$$

The equation of continuity now has the form

$$\bar{\rho}\frac{\partial w}{\partial z} = \nabla^2\phi,$$

and the equation of incompressibility is

$$\frac{\partial\rho}{\partial t} = -w\bar{\rho}',$$

with the prime indicating differentiation with respect to z. These equations are applicable even to gases if the effect of compressibility is small. Applying the Laplacian operator in x and y to equation (50), dividing throughout by $g - F\cos\omega t$, differentiating the result with respect to t, and utilizing the equations of continuity and of incompressibility, one has

$$\frac{\partial}{\partial t}\frac{\dfrac{\partial}{\partial t}\left[\dfrac{\partial}{\partial z}\left(\bar{\rho}\dfrac{\partial w}{\partial z}\right) + \bar{\rho}\nabla^2 w\right]}{g - F\cos\omega t} = \bar{\rho}'\nabla^2 w. \tag{51}$$

With equation (7) and

$$w = A(t)\,S(x,y)\,w(z),$$

equation (51) can be written, with w denoting $w(z)$ for simplicity,

$$\frac{\partial}{\partial t}\frac{(\partial/\partial t)\,A[(\bar{\rho}w')' - \alpha^2\bar{\rho}w]}{g - F\cos\omega t} = -\alpha^2\bar{\rho}'wA. \tag{52}$$

This shows that

$$(\bar{\rho}w')' - \alpha^2\bar{\rho}w = C\bar{\rho}'w \tag{53}$$

and

$$\frac{d}{dt}\left(\frac{dA/dt}{g - F\cos\omega t}\right) = -\frac{\alpha^2}{C}A. \tag{54}$$

For a continuously stratified fluid bounded by two horizontal planes of the container (at distance d apart), C must be $g\alpha^2/\sigma^2$ in which σ^2 is exactly the eigenvalue in equation (15a), which is simply the dimensionless form (with w changed to f and for the special case of two-dimensional flow) of

$$(\bar{\rho}w')' - \alpha^2\left(\bar{\rho} + \frac{g\bar{\rho}'}{\sigma^2}\right)w = 0, \tag{55}$$

for only when C assumes such a value can the boundary conditions $w(0) = w(d) = 0$ be satisfied. Since surfaces of density discontinuity can be considered as limiting cases of regions of large density gradients, C must be equal to

$g\alpha^2/\sigma^2$ even in the presence of density discontinuities, so long as σ^2 is understood to be the eigenvalue of (55) for the given stratification, and so long as the effect of surface tension is neglected. Consequently, in the absence of surface tension, equation (54) has the form

$$\frac{d}{dt}\left(\frac{dA/dt}{g - F\cos\omega t}\right) = -\frac{\sigma^2}{g}A. \tag{56}$$

A more convenient equation than equation (56) for investigation of stability is the equation for the amplitude function $a(t)$ of the deflexion ζ of any material particle from its mean position. Since $w = \partial\zeta/\partial t$, we have $A = da/dt$, and integration of equation (56) yields

$$\frac{d^2a}{dt^2} = -\frac{\sigma^2}{g}(g - F\cos\omega t)\,a + C'. \tag{57}$$

Initially, u, v, w, p, ρ and ζ are all zero, so that a is zero and, from equation (49),

$$\frac{\partial w}{\partial t} = \frac{\partial^2\zeta}{\partial t^2} = 0$$

or

$$\frac{d^2a}{dt^2} = 0.$$

Consequently $C' = 0$, and, with $T = \frac{1}{2}\omega t$, equation (57) becomes

$$\frac{d^2a}{dT^2} + (p - 2q\cos 2T)\,a = 0, \tag{58}$$

in which (p not indicating pressure)

$$p = \frac{4\sigma^2}{\omega^2}, \quad q = \frac{2\sigma^2 F}{\omega^2 g}. \tag{59}$$

Equation (58) is Mathieu's equation in its standard form. If q vanishes, equation (58) shows that the frequency of oscillation is $\sigma/2\pi$, as expected. The quantity F/ω^2 is the linear amplitude of the vibration of the container. Hence $q = (2\sigma^2/g) \times$ (amplitude of vibration) (compare with Benjamin & Ursell 1954).

Whether the fluid is stable or not depends on whether $a(T)$ remains bounded as $T \to \infty$, and this in turn depends on p and q. The regions of stability and instability are shown in figure 1. Only the first quadrant of the diagram is shown because both p and q are positive. In fact, the complete diagram in McLachlan's book (1947, p. 41) shows that the diagram is symmetric about the p-axes. The unshaded regions are stable regions and the shaded ones unstable regions. Apart from an exponential factor $e^{\mu T}$ (μ depending on p and q) indicating the rate of growth, the solution for the unstable cases also possesses exact periodicities (see McLachlan 1947, pp. 40, 41, 77, 78). In the lowest shaded part of figure 1, the period for T is 2π, so that the period for ωt is 4π. This means that the frequency of fluid oscillation is only half the frequency of the container. In the next shaded region, the period for T is π, so that the oscillation of the fluid and that of the container are isochronous. The third shaded region is a region of half-frequency, etc. The stable regions would be regions of half-frequency or isochronous regions

but for a factor $e^{i\beta T}$, with β dependent on p and q. If β is irrational, the solution is not periodic at all.

Since

$$\frac{p}{q} = \frac{2g}{F},$$

the points in the p–q plane to be considered in each case are all on a straight line radiating from the origin. For *each** α there are infinitely many σ, and therefore infinitely many points on that straight line. Whereas some points may lie in regions of instability, others may lie in regions of stability. Since σ decreases

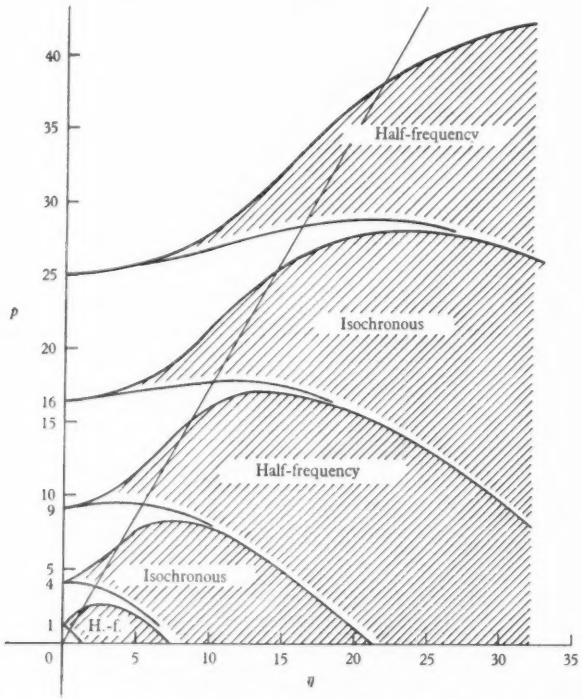

FIGURE 1. Chart for stability of fluid under vertical vibration. The acceleration of the container is $F\cos\omega t$, σ is the frequency (radians per second) of free oscillation, and $p = 4\sigma^2/\omega^2$, $q = 2\sigma^2 F/\omega^3 g$. The points for different modes lie on the line $p/q = 2g/F$.

toward zero as the index of the mode is higher and higher, the origin is a limit point of the (infinitely many) points in the p–q plane whose locations determine stability or instability. From figure 1 it is clear that there is a small region of stability around the origin, so that the fluid is stable for sufficiently high driving frequency, and against resonance with sufficiently high modes of free oscillation. Significant is the fact that no matter how small F is, there is always a region of instability, though the region is smaller and smaller as F becomes smaller and smaller.

* In the case treated by Benjamin & Ursell for each α there is only one σ.

So far surface tension has been omitted from the discussion. If the amount of density discontinuity ($\Delta\rho$) is constant, and if the fluid in each layer is homogeneous, the effect of surface tension can be taken into account in a very simple manner. The differential equation governing the flow in each layer is the Laplace equation, satisfied by the potential function $\phi(x, y, z)$. The boundary conditions at the interfaces are (compare with equation (20*a*))

$$\left(\rho\frac{\partial\phi}{\partial t}\right)_l - \left(\rho\frac{\partial\phi}{\partial t}\right)_u - (g - F\cos\omega t)\,\Delta\rho\zeta + \Gamma\nabla^2\zeta = 0. \tag{60}$$

Since $\nabla^2\zeta = -\alpha^2\zeta$, this is enough to show that in the absence of continuous stratification, and if $\Delta\rho$ is constant, the effect of Γ is to increase g by the amount $\alpha^2\Gamma/\Delta\rho$. Thus, under the stated restrictions, the stability of superposed layers of homogeneous fluids can be studied by changing g to $g+(\alpha^2\Gamma/\Delta\rho)$, and subsequently applying the results obtained for the case of no surface tension. In particular, if there is only one layer of fluid with a free surface (with $\Delta\rho = \rho$)

$$\sigma^2 = \alpha\tanh\alpha d\left(g+\frac{\alpha^2\Gamma}{\rho}\right),$$

so that

$$p = \frac{4\alpha\tanh\alpha d}{\omega^2}\left(g+\frac{\alpha^2\Gamma}{\rho}\right), \quad q = \frac{2\alpha F\tanh\alpha d}{\omega^2},$$

in agreement with the results of Benjamin & Ursell. The case of two homogeneous fluids bounded by two rigid barriers and having an interface can be treated similarly. If the thickness of each layer is $\frac{1}{2}d$

$$\sigma^2 = \frac{\Delta\rho}{\rho_1+\rho_2}\alpha\tanh\frac{\alpha d}{2}\left(g+\frac{\alpha^2\Gamma}{\Delta\rho}\right),$$

and p and q are again given by equation (59).

If there is continuous density change as well as discontinuous ones, or if each layer is homogeneous but the density discontinuities ($\Delta\rho$) are not constant, the effect of surface tension becomes rather difficult to determine—especially in the former case. However, it seems unlikely, in view of the behaviour of surfaces of density discontinuity when the fluid is undergoing free oscillation with *small* frequencies, that surface tension will have an appreciable effect on the 'resonance' of the imposed acceleration with these free oscillations. In other words, for very small σ's, it is reasonable to expect that the stability or instability can be decided by ignoring surface tension entirely. Additional research in this direction is necessary before more definite and more general conclusions can be drawn as to the effect of surface tension on the kind of stability under discussion.

This work has been done during the tenure of a Senior Post-Doctoral Fellowship of the National Science Foundation, while the author has been at the Department of Applied Mathematics and Theoretical Physics, University of Cambridge. The author wishes to express his appreciation to the Foundation for the opportunity to pursue uninterrupted research. He is indebted to Dr G. K. Batchelor for stimulation, criticism, and several useful discussions, and to Dr. F. Ursell for a discussion that has led to an improvement of this paper. It is also a

pleasure to acknowledge the support of fundamental research on stratified flows by the Office of Ordnance Research in the past several years, without which the present work would have taken much longer to accomplish.

REFERENCES

BENJAMIN, T. B. & URSELL, F. 1954 The stability of the plane free surface of a liquid in vertical periodic motion. *Proc. Roy. Soc.* A, **225**, 505–15.

BENTON, G. S. 1953 *A General Solution for the Celerity of Long Gravitational Waves in a Stratified Fluid*, pp. 149–62. Fluid Models in Geophysics, U.S. Government Printing Office.

COURANT, R. 1926 Über die Anwendung der Variationsrechnung.... *Acta Math.* vol. 49.

COURANT, R. & HILBERT, D. 1931 *Methoden der Mathematischen Physik*, Vol. I. Berlin: Julius Springer.

FJELDSTAD, J. E. 1933 Interne Wellen. *Geof. Publ.* Vol. X, no. 6, Oslo.

FJELDSTAD, J. E. 1952 Article in *Gravity Waves*, National Bureau of Standards Circular, **521**, 39–45.

GÖRTLER, H. 1954 Neuere Anwendungen der Charakteristikentheorie in der Hydrodynamik, Colloque Julius Massau des Mémoires des Sciences, Tom XXVIII.

GREENHILL, A. G. 1887 Wave motion in hydrodynamics. *J. Math.* **9**, 62–112.

INCE, E. L. 1944 *Ordinary Differential Equations.* New York: Dover Publications.

LAMB, H. 1945 *Hydrodynamics.* New York: Dover Publications.

MCLACHLAN, N. W. 1947 *Theory and Applications of Mathieu Functions.* Oxford.

SQUIRE, H. B. 1933 On the stability for three-dimensional disturbances of viscous fluid flow between parallel walls. *Proc. Roy. Soc.* A, **142**, 621–8.

SZ.-NAGY, B. 1947 Vibrations d'une corde non homogène. *Bull. Soc. Math. France*, vol. 75, pp. 193–208. See also, Riesz, F and Sz.-Nagy, B. 1956 *Functional Analysis*, §99. London and Glasgow: Blackie and Son.

WEBB, R. R. 1884. Math. Tripos Papers, Cambridge.

YIH, C.-S. 1959*a* Effects of gravitational or electromagnetic fields on fluid motion. *Quart. Appl. Math.* **16**, 409–15.

YIH, C.-S. 1959*b* Effects of density variation on fluid flow. *J. Geophys. Res.* **64**, 2219–23.

Piston theory applied to strong shocks and unsteady flow

By JOSEPH L. RAYMOND
Aero-Astronautics Department, The RAND Corporation, Santa Monica, California

(Received 7 January 1960)

The utility of piston theory as a means of solving isentropic two-dimensional aerodynamic problems has been aptly demonstrated by many writers in recent years. The present treatment removes the restriction of isentropic flows, extending the applicability of piston theory to flows with strong shocks. Sample calculations for a thin biconvex airfoil are carried out in which the local flow is assumed to be isentropic and non-isentropic. Comparison of the result is made with that of the shock expansion theory of Cole, Gazley & Williams (1956).

1. Introduction

Several papers have been published in recent years which deal with various problems of isentropic shock-free flows; for example, Lighthill (1953), Ashley & Zartarian (1956), Landahl (1957), and Chawla (1958). The condition of isentropy in essence defines a reasonable upper limit for the piston speed of the order of the speed of sound, i.e. $w/a_\infty \leqslant 1$, where w is the local velocity normal to the main undisturbed flow and a_∞ is the undisturbed speed of sound. However, according to Hayes (1947, 1957) this is a restriction which does not seem always justifiable.

In the development of the piston analogy there is no effect of the piston speed which limits its validity. The local Mach number, M, must be large, and since Hayes (1947) shows that $M = O(\delta^{-1})$, where δ is local slope, it is only necessary that δ be sufficiently small. In general, the error in pressure coefficients or other parameters of interest are of the order δ^2 for all Mach numbers, as pointed out by Van Dyke (1954). This again requires that the local slopes be small in order to limit errors in the pressure coefficient, but does not necessarily limit the piston speed, $K_\infty \equiv M_\infty \delta$.

Assuming that the piston theory is valid for all speeds including those corresponding with strong shock flow, where $K_\infty > 1$, then there is an extension of the works on piston theory to flows with strong steady and unsteady shocks. Hence, we seek a relationship between the local piston speed, w, and the local pressure, p, for strong shock flows, since the corresponding pressure relationship for isentropic flows is well known.

2. The strong-shock pressure function

Previously, Raymond & Williams (1957) found an empirical relationship for the reduced pressure coefficients, C_p/δ^2, based on the hypersonic small-disturbance theory of Van Dyke (1954) or the piston theory of Cole *et al.* (1956). It is

$$\bar{C}_{p_c} + \bar{C}_{p_e} = \gamma + 1, \tag{1}$$

where the coefficients on the left-hand side refer to compression and expansion respectively. The isentropic expression for the reduced expansion pressure coefficient is

$$\bar{C}_{p_e} = \frac{2}{\gamma K_\infty^2}\left[\left(1-\frac{\gamma-1}{2}K_\infty\right)^{2\gamma/\gamma-1}-1\right]. \tag{2a}$$

For $K_\infty \geqslant 1{\cdot}4$, this comes within 4 % of the value given by

$$\bar{C}_{p_e} = -\frac{2}{\gamma K_\infty^2}. \tag{2b}$$

Using equation (2*b*) for the sake of simplicity, equation (1) becomes

$$\bar{C}_{p_c} = \gamma + 1 + \frac{2}{\gamma K_\infty^2}. \tag{3}$$

Hypersonic flows over small local slopes are typified by the head shock lying close to and almost parallel to the body. In the case of a two-dimensional body, a component of flow, u_n, is generated normal to the local surface and is related to the shock-induced normal flow component u_s, by

$$u_s = \frac{u_n}{\cos(\theta_w - \delta)}. \tag{4}$$

For $\theta_w = O(\delta) \ll 1$, we find, from equation (4), that $u_s \cong u_n$, and $u_n \cong U_\infty \delta$ from the usual small-angle approximations applied to the body surface.

We now proceed to some of the inferences that can be made with the use of the small-angle approximations. Recalling the previous remarks on the limitation of piston speed, $w \leqslant a_\infty$, we seek now the relationship between w and p.

From equation (3) we get

$$\frac{p_c}{p_\infty} = \frac{\gamma K_\infty^2}{2}(\gamma+1)+2, \tag{5a}$$

but we see that $K_\infty = U_\infty \delta / a_\infty \cong w/a_\infty$ within the small-angle approximation, hence

$$\frac{p_c}{p_\infty} = \frac{\gamma(\gamma+1)}{2}\left(\frac{w}{a_\infty}\right)^2 + 2. \tag{5b}$$

Equation (5*b*) was predicted theoretically by the piston analysis of Cole *et al.*, except that they were only able to show that the second term on the right-hand side was $O(1)$.

3. Application to a biconvex airfoil

It is relatively simple to calculate w/a_∞ as a function of the time (or the x-co-ordinate) and then use the appropriate piston equation for pressure coefficient depending upon whether the flow is isentropic or not. The following developments were considered by Lighthill (1953), and to a large extent we shall make use of his nomenclature.

Let y be the co-ordinate normal to the body and positive away from the centre line, then

$$y = Y_s(x) \pm Y_i(x,t) \text{ on the } \begin{Bmatrix}\text{lower}\\ \text{upper}\end{Bmatrix} \text{ surface}, \tag{6}$$

where Y_s is the equation of the profile shape and Y_i is the unsteady y-displacement. Differentiating equation (6), we get

$$w = w_s(x) \pm w_i(x,t) \text{ on the } \begin{Bmatrix}\text{lower}\\ \text{upper}\end{Bmatrix} \text{ surface.} \tag{7}$$

In general, for one-dimensional flow

$$w = \frac{\partial Y}{\partial t} + U_\infty \frac{\partial Y}{\partial x}, \tag{8}$$

so that if we take a thin biconvex airfoil as an example, we get

$$Y_s = 2\tau[x - (x^2/c)], \tag{9}$$

where $\tau = t/c$ is the thickness-to-chord ratio. Then from equations (8) and (9),

$$w_s = 2U_\infty \tau[1 - (2x/c)]. \tag{10}$$

Let
$$Y_i = \alpha(t)\,(x - x_0), \tag{11}$$

then from equation (8)

$$w_i = \dot{\alpha}(x - x_0) + U_\infty \alpha. \tag{11a}$$

Let $\alpha = \alpha_0 e^{i\omega t}$, then equation (11$a$) becomes

$$w_i = \alpha_0 e^{i\omega t}\{i\omega(x - x_0) + U_\infty\}, \tag{12}$$

and adding equations (10) and (12) results in

$$\frac{w}{a_\infty} = \frac{w_s + w_i}{a_\infty} = 2M_\infty \tau\left[1 - \frac{2x}{c}\right] \pm \alpha_0 e^{i\omega t}\left[\frac{i\omega(x - x_0)}{a_\infty} + M_\infty\right]. \tag{13}$$

Taking the real parts, we obtain

$$\frac{w}{a_\infty} = 2M_\infty \tau\left[1 - \frac{2x}{c}\right] \pm \alpha_0\left[M_\infty \cos\omega t - \frac{\omega(x - x_0)}{a_\infty}\sin\omega t\right]. \tag{14}$$

The last equation is not in its most convenient form from the conventional point of view. Letting $k = \omega c/2U_\infty$, equation (14) becomes

$$\frac{w}{a_\infty} = 2M_\infty \tau\left[1 - \frac{2x}{c}\right] \pm \alpha_0 M_\infty\left[\cos\frac{2kx}{c} + \frac{2k}{c}(x_0 - x)\sin\frac{2kx}{c}\right], \tag{15}$$

where $t = x/U_\infty$. This is essentially a statement of Hayes's piston transformation.

4. Force and moment calculation

For the biconvex airfoil thus selected, we calculate the force and moment coefficients:

$$C_N = \frac{2}{\gamma M_\infty^2}\int_0^1 \frac{(p_l - p_u)}{p_\infty}\frac{dx}{c}, \tag{16}$$

and
$$-C_M = \frac{2}{\gamma M_\infty^2}\int_0^1 \frac{(p_l - p_u)}{p_\infty}\frac{(x - x_0)}{c}\frac{dx}{c}, \tag{17}$$

where p_l and p_u are the local pressures on the lower and supper surfaces, respectively.

The pressure relationship for isentropic flow is

$$\frac{p}{p_\infty} = \left(1 + \frac{\gamma - 1}{2}\frac{w}{a_\infty}\right)^{2\gamma/\gamma - 1}. \tag{18}$$

Now it is clear that some rules must be formulated for the use of equations (5*b*) and (18) in terms of piston Mach number. To help resolve this question in the range of piston Mach numbers $1{\cdot}0 \leqslant w/a_\infty \leqslant 1{\cdot}4$, the compression-pressure ratio was calculated based on both (5*b*) (valid for $w/a_\infty \geqslant 1{\cdot}4$ in the present approximation) and the corresponding equation valid in the range $1{\cdot}0 \leqslant w/a_\infty \leqslant 1{\cdot}4$,

$$\frac{p_c}{p_\infty} = \frac{\gamma(\gamma+1)}{2}\left(\frac{w}{a_\infty}\right)^2 + 2 - \left(1 - \frac{\gamma-1}{2}\frac{w}{a_\infty}\right)^{2\gamma/\gamma-1}. \tag{19}$$

(Equation (19) is based on equations (1) and (2*a*).) Both pressure ratios were compared with the isentropic value given by equation (18) for $w/a_\infty = 1{\cdot}0$. It was found that equations (5*b*) and (19) result in pressure ratios which are 3 % high and 3 % low, respectively, compared to equation (18). Consequently, since there appears to be no serious error in using equation (5*b*) over equation (19), the former was used because of simplicity in the example which follows. Clearly, some idealization is embraced here since aerodynamic flows do not transform abruptly from isentropic to strong shock flows as the above usage implies.

Suggested rules based on piston Mach numbers are

$\dfrac{w}{a_\infty} \leqslant \dfrac{-2}{\gamma-1}$,	$\dfrac{p}{p_\infty} = 0$	Isentropic flow
$\dfrac{-2}{\gamma-1} < \dfrac{w}{a_\infty} \leqslant 1$,	Equation (18)	Isentropic flow
$\dfrac{w}{a_\infty} > 1$,	Equation (5*b*)	Strong-shock flow

5. Results

The biconvex airfoil of equation (9) with $\tau = 0{\cdot}025$, $\alpha_0 = 0{\cdot}1047$, $M_\infty = 10$, and $x_0/c = 0{\cdot}50$ was selected as an example calculation. The results are:

k	C_N	C_M
0	0·0521	0·00438
0·01	0·0521	0·00438
0·10	0·0516	0·00445
$\pi/4$	0·0339	0·00996
$\pi/2$	0·0252	0·01661
π	0·0699	0·00749

It will be noted that $M_\infty\tau$ and $M_\infty\alpha_0$ appear only in combination in equation (15); hence the calculations apply over a wide range of M_∞, τ and α_0.

A point of comparison was made for C_N at $k = 0$, with the results of the shock-expansion theory by Cole *et al.*, and the present value was found to be high by about 4·5 %.

REFERENCES

Ashley, H. & Zartarian, G. 1956 Piston theory—a new aerodynamic tool for the aeroelastician. *J. Aero. Sci.* **23**, 1109–18.

Chawla, J. P. 1958 Aeroelastic instability at high Mach number. *J. Aero. Sci.* **25**, 246–58.

Cole, J. D., Gazley, C., Jr. & Williams, E. P. 1956 Class notes for a hypersonic aerodynamics course, 1956 and 1957. University of California, Los Angeles. (To be published.)

HAYES, W. D. 1947 On hypersonic similitude. *Quart. Appl. Math.* **5**, 105–6.

HAYES, W. D. 1957 Private communication.

LANDAHL, MARTIN T. 1957 Unsteady flow around thin wings at high Mach numbers. *J. Aero. Sci.* **24**, 33–8.

LIGHTHILL, M. J. 1953 Oscillating airfoils at high Mach number. *J. Aero. Sci.* **20**, 402–6.

RAYMOND, J. L. & WILLIAMS, E. P. 1957 A simple relation between the shock and expansion pressure coefficients for two-dimensional hypersonic flow. *J. Aero. Sci.* **24**, 389–90.

VAN DYKE, M. D. 1954 A study of small-disturbance theory. *Nat. Adv. Comm. Aero. Tech. Report* 1194.

Mixing of dense fluid in a turbulent pipe flow

Part 1. Overall description of the flow

By T. H. ELLISON AND J. S. TURNER
Department of the Mechanics of Fluids, University of Manchester

(Received 17 December 1959)

This paper concerns an investigation into the behaviour of a layer of dense salt solution on the floor of a sloping rectangular pipe in which there is a turbulent flow. The various phenomena which are observed are described qualitatively and by the presentation of typical concentration profiles.

Numerical values are obtained experimentally for the rates of spread of the edge of the layer in the case where the salt is moving entirely in the direction of the main stream. The rate of spread is found to depend mainly on the slope α and on the pipe Richardson number, defined by $\mathrm{Ri}_p = D\Delta_d \cos\alpha / V^2$, where D is the depth of the pipe, $\Delta_d = g(\rho_d - \rho_a)/\rho_a$, ρ_d is the density of the fully mixed discharge and ρ_a is the density of the ambient flow. In the range of Ri_p from 0 to 0·005 the rate of spread of the layer decreases by a factor of about 3 at small slopes.

Some discussion is given of the factors determining the initial rate of spread just after the layer leaves the slit. Finally, it is shown how the depth measurements can be related to the determination of the concentration at the floor.

1. Introduction

In an earlier paper (Ellison & Turner 1959, hereafter called I) we have discussed the turbulent flow down a slope of a layer of fluid which is heavier than its surroundings. Such flows occur commonly in nature, examples being katabatic winds and turbidity currents in the oceans. We were able to characterize the mixing of these layers by the entrainment E, defined as the ratio of the velocity of inflow of the still or smoothly flowing ambient fluid into the turbulent layer to the relative velocity between the layer and its surroundings. Provided the Reynolds number was large, E was found to depend mainly on the overall Richardson number of the layer $\mathrm{Ri} = g(\rho - \rho_a)h\cos\alpha/\rho_a V^2$, where h is the depth of the layer and V its velocity relative to the ambient fluid. Once the function $E(\mathrm{Ri})$ had been determined empirically, it was possible to make certain theoretical predictions about, for example, how great a flow in the ambient fluid in the direction opposing gravity would be needed to cause the flow in the layer to be reversed.

Our previous calculations were, however, necessarily restricted to the case where the ambient fluid was deep and in laminar motion. There are many practical problems where the ambient fluid is contained in a pipe or channel and is turbulent for which analogous information is required. The situation is then much more complicated, since more variables are involved, and it is clear that the state of turbulence in both parts of the flow will be important. In this

paper we report a series of experiments in a rectangular pipe which demonstrate qualitatively the various phenomena which can occur and provide quantitative information on the rate of mixing in such a channel as a function of a suitable stability parameter. The dependence on stability should have a similar form in other situations, but for reasons which will be discussed later, the numerical values which we find do not have the universal validity which is to be expected for the function $E(\mathrm{Ri})$ used in I. Great caution should be used in applying them to pipes of different shapes from ours or to cases where the ambient flow has a very different Reynolds number.

This investigation forms part of a more general study of the process of mixing in a turbulent fluid when there is a density gradient present. The information given here on the rate of spread of the layer is of direct practical interest and also indicates the values of the Richardson number at which the stabilizing effect of the density gradient becomes important, but in order to get to the heart of the problem it is necessary to consider the mechanism of the flow in more detail. In the second part of this paper simultaneous measurements of velocity and density will be present which can be used to interpret the mixing phenomena in terms of the dependence of the turbulent transfer coefficients on *local* stability parameters.

2. The apparatus

The discussion of the various observed phenomena will be simplified if we first describe the apparatus which was used. The experiments were carried out in a Perspex pipe of 10 by 5 cm rectangular section and $2\frac{1}{2}$ m long, mounted with

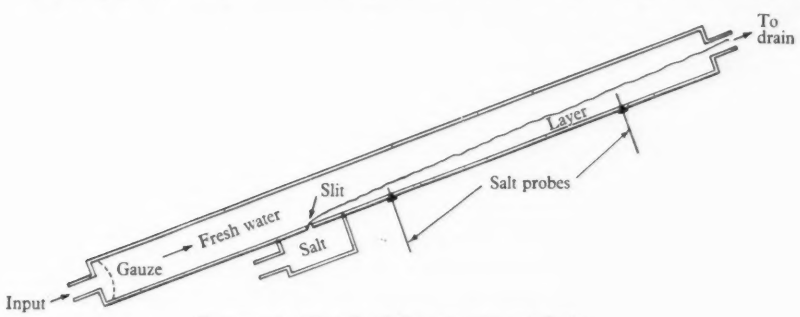

FIGURE 1. Sketch of the experimental pipe.

the 5 cm sides vertical (in order to have stratified flows as nearly two-dimensional as possible) on a tiltable Dexion frame. Water for the ambient or ventilating flow was supplied through a gauze screen at one end of the pipe from a constant head tank in the roof of the laboratory and flowed to waste at the other end. The drain pipe was raised to such a level that the static pressure in the experimental pipe was slightly positive as this facilitated the withdrawal of samples. Mean velocities of up to 15 cm s^{-1} could be maintained and were measured either by recording the time needed to fill a container of known volume or by timing the passage of patches of dye between fixed marks.

Salt solution was used to form the layer of denser fluid, and this was led from a roof tank to a Perspex box mounted against the lower face of the pipe. From this it flowed slowly through a slit 5 mm wide cut right across the face of the pipe about 1 m from one end (in the majority of the experiments the input end). The general arrangement is shown in figure 1. The rate of flow of salt solution was controlled by a series of nozzles, any one of which could be inserted in the supply pipe.

The techniques for determining the density profiles have been described in I. Provision was made at 10 cm intervals along the centre of the bottom face of the pipe for the insertion of fine stainless-steel tubes which could be traversed across the flow and through which samples of fluid could be obtained from any desired level; the density was measured by passing the samples continuously through a simple conductivity cell.

3. The types of flow observed

The various types of flow can be established depending on the slope of the pipe, the salt flux and the amount of ventilating water flow. We shall now describe these in turn, illustrating where appropriate with some quantitative measurements.

(i) *Ventilation with gravity (negative slopes)*

When the ventilating stream is in the same direction as the free flow of the layer with no ventilation, it is found that its turbulence has little effect on the qualitative behaviour of the system and the predictions of I for a laminar ventilating stream apply. As the ventilating velocity is increased, with slope and salt flux constant, mixing decreases until over an appreciable range of speed there is so little difference in velocity between the ventilating flow and the layer that the buoyancy forces become dominant and almost completely inhibit mixing. At very large ventilating velocities, when the layer is being dragged forward by the main stream, mixing again increases.

The dependence of mixing on slope is not very dramatic. One might expect it to decrease with increasing negative slope until at very steep slopes the $\cos\alpha$ term causes an appreciable reduction in the Richardson number (whose precise definition will be discussed in the next section) and an increase in the mixing. However, we found that at $-20°$ the mixing was greater than at $-10°$ and that breaking waves appeared on the top of the layer. It is unlikely that the layer is properly turbulent in either of these conditions (at the Reynolds numbers attainable in our pipe), and the effect is outside the scope of this paper though it deserves further study.

(ii) *Ventilation against gravity (positive slopes)*

When the water is flowing uphill, the picture is very different. Two cases may be distinguished according as the ventilating velocity is great enough to reverse the layer when it leaves the slit or not.

The simplest situation arises when the ventilating velocity is large, for then all the salt solution is carried uphill, forming a layer whose thickness increases with distance as it mixes across the channel. The rate of mixing depends quite strongly

on the slope, since at steep slopes a greater turbulent shear stress is required to counteract the weight of the layer and drag it uphill: mixing is then increased both because the level of turbulence is increased and also because the local Richardson number is smaller and a given level of turbulence is likely to be associated with a larger diffusivity. This case of large ventilating flow when the layer is *fully reversed* is the one we have studied in most detail in §§4 and 5.

At rather lower rates of ventilation, part at least of the salt solution flows downhill against the water flow, gradually mixing as it does so. Thus in the part of the pipe downhill of the slit three regions of flow may be distinguished. First, there is a thin layer near the floor flowing downhill, whose depth decreases with distance from the slit as fluid is mixed out of it, but in which the concentration is

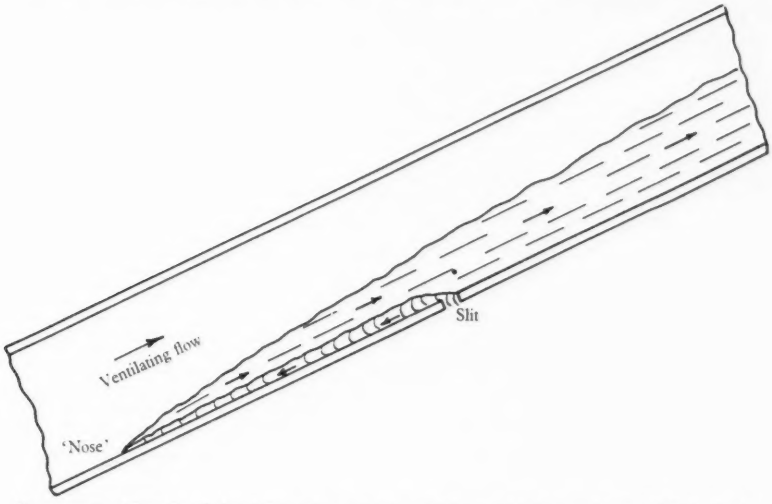

FIGURE 2. Sketch of the 'three-layer' type of flow which can be established at low ventilation velocities.

falling, showing that there is mixing in both directions across its boundary. This layer ultimately disappears, but in practice our channel was not always long enough to include the termination of the layer, and in these cases the part of the layer reaching the bottom end of the pipe was forcibly mixed near the fresh-water inlet. Above this downflowing layer is an intermediate region of mixed fluid flowing uphill and growing in thickness as it is swept up the channel; and above that, at the top of the pipe, is the pure ventilating stream. On the uphill side of the slit there is, of course, no layer flowing downwards and that part of the salt solution which moves uphill immediately it leaves the slit soon becomes part of the mixing intermediate region. The situation is shown diagrammatically in figure 2.

The great difference between the rates of mixing in a horizontal pipe and one tilted so that the three-layer flow is established is shown in figure 3. The two density profiles were obtained at the same station 20 cm uphill of the slit, and with identical flow rates for the fresh water and for the salt solution: the only difference lay in the slopes, which were respectively 0° and 13°.

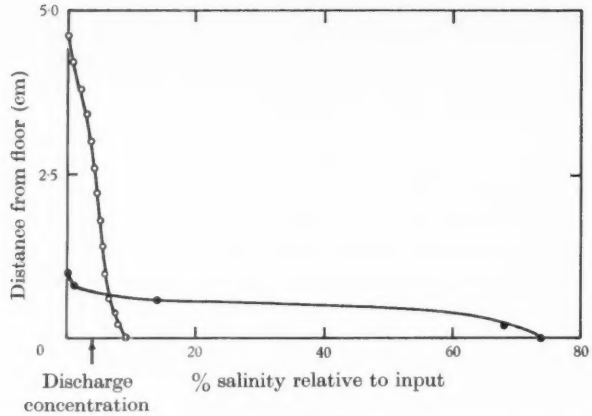

FIGURE 3. Density profiles at 20 cm uphill of the slit, showing the great differences between the mixing in a horizontal and an inclined pipe. $A/V^3 = 0{\cdot}017$. ○, Tilted at 13°; ●, horizontal.

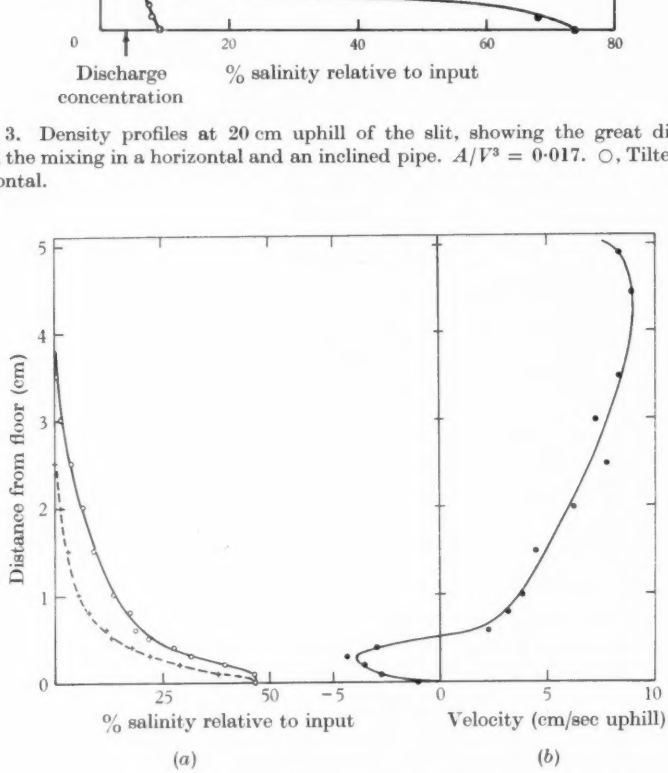

FIGURE 4. (*a*) Density profiles at 30 and 50 cm downhill in a 'three-layer' flow with the channel tilted at 23°. $\mathrm{Ri}_p = 0{\cdot}015$. (*b*) Velocity profile in the same flow, at 40 cm downhill. ○, salinity 30 cm from slit. +, Salinity 30 cm from slit. ●, Velocity 40 cm from slit.

The characteristic shapes of the density profiles downhill from the slit in the three-layer flow are shown in figure 4*a*. The two profiles are at 30 and 50 cm downhill from the slit with the channel tilted at 23°. The velocity profile at 40 cm is shown in figure 4*b*. This was obtained with thermistors and may not be very accurate, but it clearly shows the most important features. The greatest velocity

downhill occurs near the top of the region of concentrated salt (where we would place the edge of the layer visually or from inspection of the density profiles alone). At a small distance above this is a region of very high velocity gradient, but even where there is only sufficient salt to change the density by a few parts in ten thousand the velocity profile is still distorted.

4. Fully reversed flows: basic ideas

When the whole of the salt solution is moving in the same direction there is hope that the dominant properties of the flow can be characterized simply by one or two quantities and a description of its development given in terms of overall parameters of the flow. Thus if h is a length specifying the depth of the layer (a precise definition will be discussed later) one would expect from dimensional reasoning that in a two-dimensional pipe of depth D, h/D would be a function of x/D, Re_p, Ri_p, α and Δ_0/Δ_d, where x is the distance from the slit, Re_p is the Reynolds number defined by $\mathrm{Re}_p = VD/\nu$, Ri_p is the 'pipe Richardson number' defined by $\mathrm{Ri}_p = D\Delta_d \cos\alpha/V^2 = A\cos\alpha/V^3$, α is the slope, and Δ_d and Δ_0 are related to ρ_d the discharge density (i.e. the density when the salt solution is fully mixed with the ventilating flow) and the density ρ_0 with which it is emitted by $\Delta_d = (\rho_d - \rho_a)\, g/\rho_a$ and $\Delta_0 = (\rho_0 - \rho_a)\, g/\rho_a$, V is the discharge velocity, A the rate of output of excess weight, which is constant in a given experiment, and ρ_a the density of the ambient flow. In attempting to apply this relation in practice, the dependence on Δ_0/Δ_d presents a special difficulty. There is inevitably a region of rapid mixing close to the slit, where the salt solution is being accelerated and one might expect that even if the rate of output of salt solution was always kept constant the effective Δ_0/Δ_d might depend critically on the details of the design of the slit. If this were so and h/D depended appreciably on Δ_0/Δ_d, measurements of the depth as a function of the other variables might have rather little value.

In order to avoid this difficulty, one might suggest that except very near the slit the flow would be in local equilibrium at each section with properties independent of its history. In that case one would have

$$\frac{\partial h}{\partial x} = f\left(\frac{h}{D}, \mathrm{Re}_p, \mathrm{Ri}_p, \alpha\right). \tag{1}$$

We did attempt to interpet our measurements, for which Re_p was constant = 6500, in terms of this formula, but we found inconsistencies suggesting that history did matter. If, however, instead of attempting to plot $\partial h/\partial x$ as a function of Ri_p and α, choosing the position x at which h/D has a particular value, we plot the difference between the values of h at two fixed positions, taken in our case to be at $x/D = 4$ and $x/D = 24$, we find much greater consistency. It is possible in practice to ignore variations in h/D except where this attains values comparable with $\frac{1}{2}$, and to obtain the rate of increase of depth as a function of Ri_p or A/V^3 and α alone. We shall therefore present our measurements in this way, discussing separately the manner in which h/D at $x/D = 4$ is determined by the initial conditions.

The definition of h

In I we were able to define the depth of a sloping plume from integrals of the velocity profile, but such a definition is clearly impossible here. So far as the dimensional argument is concerned, any dimensionally correct definition may be used and the choice is entirely one of convenience in measurement and practical application; if a detailed theory were available it might well influence the choice, but at present there is none. There are several possibilities. For example, one might define h as the height where the concentration is 1/10 or 1/100 the value it has at the floor at the same station. This definition would have several disadvantages: it would require two measurements to determine h since the way the floor concentration varies with x is not known *a priori* (indeed, the floor concentration is rather an unsatisfactory quantity, since it depends critically on the behaviour of any thin viscous sublayer which may be otherwise negligible) and it also breaks down at whatever value of x the flow becomes so mixed that the variation of concentration across the channel is less than the selected standard ratio.

We decided therefore to define h as the height where the concentration equals the discharge concentration Δ_d. This height can readily be determined since Δ_d is independent of x; it certainly always exists, and as will be shown later it is readily related empirically to quantities of direct practical importance. It does, however, suffer from its own disadvantages. The most serious of these is that the measurement of $\partial h/\partial x$ is sensitive to the accuracy of the determination of Δ_d, and in our channel, owing to its rectangular shape, the actual discharge value of Δ_d, which is what we used in the experiments, is not exactly the same as that for an ideal two-dimensional channel having the same flow as exists on the centre line of our pipe. One must also note that although h always exists, its value has little significance after it first reaches a value of $\frac{1}{2}D$. In most cases the layer is then for practical purposes mixed, but if it is of interest to study the final stages a different specification will be required.

In the next section our measurements will be presented in detail, indicating how the salt profiles and h change between $x/D = 4$ and 24. In the following section some discussion of the factors determining h at $x/D = 4$ will be given and then finally a few comments will be made on the relation between h and the other quantities of interest.

It must be emphasized that whatever criticisms may be made of our particular definition of h, the measurements of $\partial h/\partial x$ as a function of Ri_p and α do clearly indicate the values of these quantities which produce significant changes in the rate of mixing. These were not previously known even approximately: and they should be little changed by changes in the scale and shape of the channel, which will probably alter the numerical values for $\partial h/\partial x$.

5. Measurements on fully reversed flows against gravity and on flows in the same direction as gravity

All the measurements reported in this section have been obtained using the same rate of ventilating flow; this was the maximum which could be conveniently maintained with the available water supply and corresponded to a pipe Reynolds

number based on depth and discharge velocity of about 6500. We have not studied the variation of mixing with Re_p as we thought it best to concentrate on obtaining a broad picture of the phenomenon by operating the highest possible Reynolds number. However, except in certain cases at high values of Ri_p when the

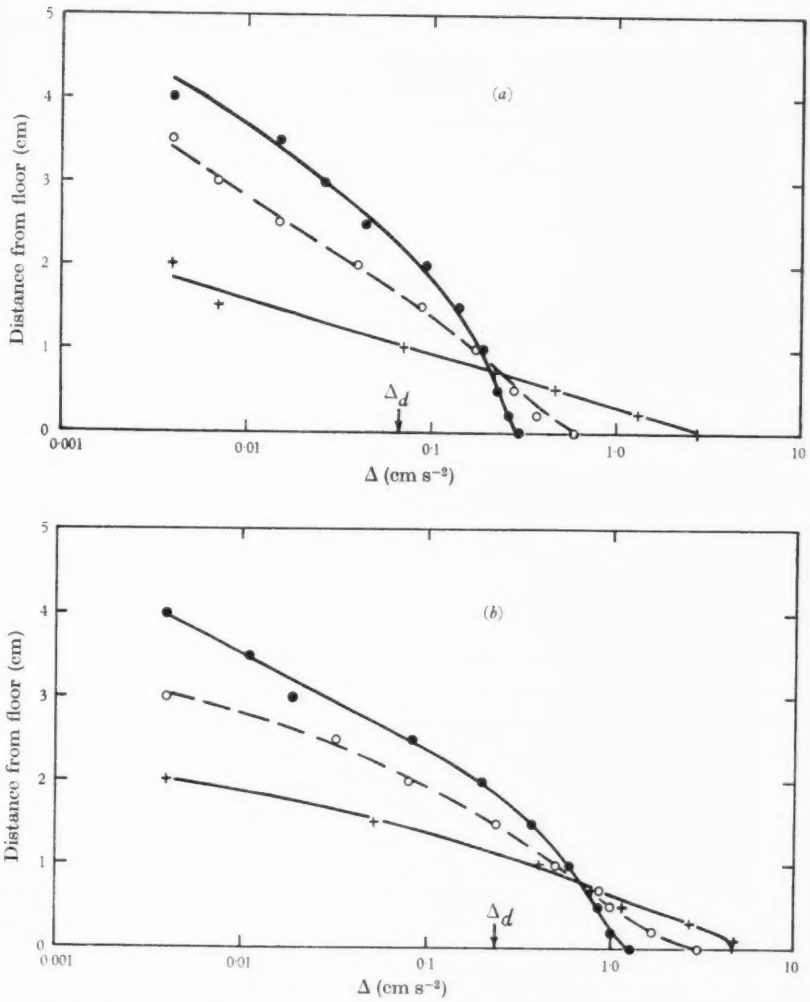

FIGURE 5. Density profiles in fully reversed flow, slope + 10°. +, 20 cm uphill; ○, 70 cm uphill; ●, 120 cm uphill. (*a*) $\mathrm{Ri}_p = 0{\cdot}0018$. (*b*) $\mathrm{Ri}_p = 0{\cdot}0068$.

mixing is very small and complicated problems of stability arise, it seems plausible to suggest that the mixing in a given distance will be proportional to the turbulent intensity which is roughly proportional to $C_D^{\frac{1}{2}}$; hence since C_D, the drag coefficient of the pipe, is a slow function of Re, the mixing will only depend on Re weakly.

The differences between laboratory measurements in smooth pipes and large scale phenomena in rough pipes (e.g. mine galleries) should also be small since C_D is not very different in the two cases.

(i) *Profile measurements*

For comparison with the measurements recorded in §3 we first present some density profiles which illustrate in outline the effects we have been discussing. In figures 5*a* and *b* are shown density profiles taken at 20, 70 and 120 cm uphill from the slit with the pipe sloping at 10°. A logarithmic scale is used for Δ in

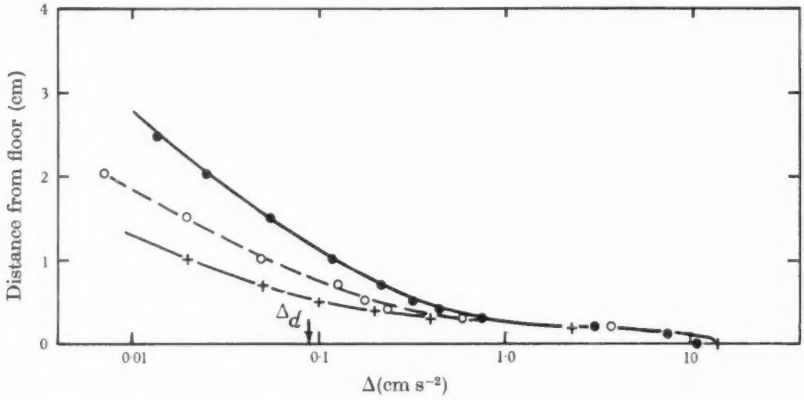

FIGURE 6. Density profiles in fully reversed flow, slope + 5°, Ri_p = 0·0025. +, 20 cm uphill; ○, 70 cm uphill; ●, 120 cm uphill.

order to cover the wide range observed, and the measured discharge values are shown; they correspond to Ri_p = 0·0018 in figure 5*a* and 0·0068 in figure 5*b*. It is apparent that the layer with the higher Richardson number spreads less rapidly than the other; the absolute depths are not very different in the two cases.

In figure 6 are shown profiles at the same stations as before for an experiment with Ri_p = 0·0025, much the same as that in figure 5*a*, but with the slope 5°. The rate of spread is much less at the lower slope. Note that there is also a very thin region near the wall containing rather concentrated salt which is almost certainly governed by viscosity. Viscous layers such as this are unlikely to carry an appreciable fraction of the salt flux except where the mixing is extremely small, so the behaviour of the outer edge of the layer should be little changed, but we should remember that the dependence on Reynolds number is likely to be more serious at low slopes.

The measurement of full profiles is tedious, so frequently we have determined h alone by first measuring the discharge concentration and then finding by trial and error two points at each cross-section having mean concentrations straddling this value and between which we could interpolate. This technique has enabled us to conduct an extensive series of experiments at different slopes and Richardson numbers, and the results are shown in the next section.

(ii) *The dependence of the growth of the layer on stability and slope*

All our measurements of the difference between h/D at $x/D = 4$ and $x/D = 24$ with the pipe at the fixed slope of $+10°$ are plotted in figure 7 as a function of A/V^3. The mean absolute values of h/D are shown. It should be noted that although we chose not to measure the rates of spread at a fixed height, our results cover a fairly narrow range of mean layer depths with h/D between 0·2 and 0·4; within this range there is no systematic variation of the rate of spread with h/D.

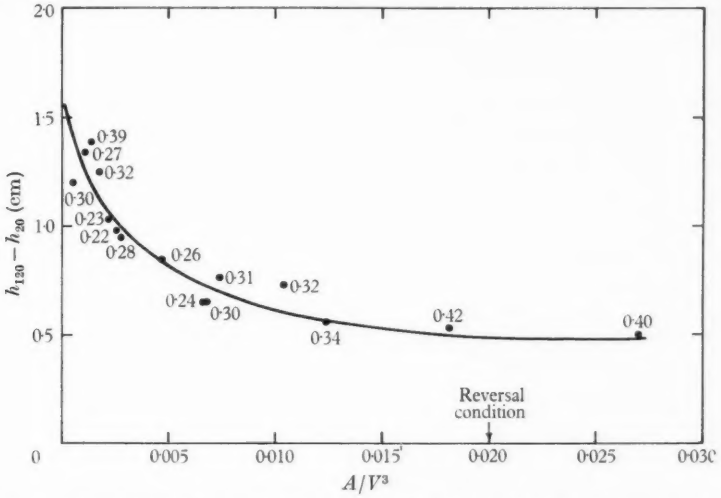

FIGURE 7. Experimental values for the increase in depth of the layer between $x/D = 4$ and $x/D = 24$ at a fixed slope of $+10°$, as a function of A/V^3. The mean values of h/D are marked against the points.

Also marked on figure 7 is the reversal condition taken from our measurements which were previously published in I; points to the right of this correspond to layers which had some nose extending downhill.

We did also attempt to measure the spread of unstable layers by inverting the channel so that the slit was in the top, but as might be expected the layer disintegrated in all cases well before $x/D = 24$ was reached. All that can be said is that over the range $x/D = 4$ to $x/D = 8$ the rate of spread was much greater than it is in the stable case.

Graphs similar to figure 7 have been prepared for other slopes, but no useful purpose would be served by presenting all the experimental points in detail here. Instead, smooth curves have been drawn through each set of points; these are combined in figures 8*a* and *b*, and constitute the main results of this paper. The general trend of these curves and the variation with slope is much as expected from the previous discussion. Note, however, that as we mentioned briefly in §3, the mixing at the downhill slopes of $-20°$ and $-30°$ is greater than it is at $-10°$. Such an increase would be expected at very steep slopes where the layers would be pulled forward by gravity at a velocity greater than the stream above,

but in this case a different mechanism is thought to operate. Breaking waves, rather like roll waves, were observed on the interface and these probably were responsible for transferring the salt solution upwards.

At very low Richardson numbers all the curves come together (within the experimental error), as, of course, they must when density differences are negligible. The value of the rate of spread in neutral conditions has to be found by

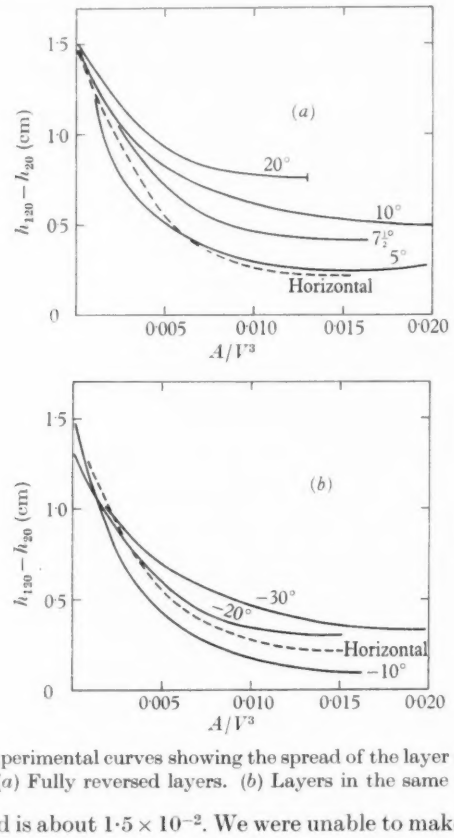

FIGURE 8. Mean experimental curves showing the spread of the layer as a function of A/V^3 at various slopes. (*a*) Fully reversed layers. (*b*) Layers in the same direction as gravity.

extrapolation, and is about $1{\cdot}5 \times 10^{-2}$. We were unable to make measurements at Richardson numbers lower than about 0·0005 because the discharge concentration was then only about twice that in the fresh-water supply. In an attempt to obtain more accurate results in neutral conditions we made a conducting solution of neutral buoyancy by mixing salt solution with methylated spirits, but we were unable to use such a mixture, since its density does not remain equal to that of water when it is diluted by further mixture with the ventilating flow the rates of mixing in normal and inverted experiments were quite different.

In neutral conditions the diffusing solution ought not to affect the flow in the pipe and if one made the usual assumption that the *Austausch* coefficients for momentum and salinity are equal (Reynolds analogy) or in a known ratio, there is no reason why a theoretical calculation of the concentration profiles in neutral

conditions could not be carried out, since K_M is sufficiently known. We have not been able to find such a calculation in the literature, although Calder (1949) has given a theory of diffusion from a line source in a constant stress boundary layer in which he approximates to the logarithmic velocity profile by a power law. This theory can only be applied to flow in a pipe when none of the pollutant has reached half way across and this restriction prevents us from using it in our case except at small values of x/D. Here Calder's theory gives profiles in broad agreement with our measurements, but seems to predict a rate of spread greater than we observed.

6. The initial mixing

As we have mentioned earlier, the rapid mixing near the source is very important in determining the depth of the layer at $x/D = 4$; and indeed this depth is often much greater than the increase in depth between $x/D = 4$ and $x/D = 24$. Detailed attempts to explain quantitatively our results for this region have not been successful, but a discussion of some factors which must be involved in any full theory may perhaps stimulate someone to clarify the position. This leads us away from our main theme, but since we are in this paper aiming to present results in a form in which they can usefully be applied, it seems undesirable to ignore the initial mixing and so to imply that measurements of the steady state mixing solve the whole problem.

The initial mixing takes place while the layer is accelerating to its quasi-equilibrium velocity, and in order to determine its depth at the end of this process we must consider not only the acceleration itself, but also the way in which the depth and velocity of the unmixed layer are determined when it leaves the slit.

While the layer is thin and the velocity difference between it and the ambient stream is large, the turbulence in the ambient stream is unlikely to have much influence and the methods of I may be used subject to some reservation concerning the ability of the turbulence to adjust itself quickly enough to maintain a state of changing equilibrium. A calculation based on this idea shows that the layer accelerates rapidly, at first becoming thinner and then after a very short distance beginning to thicken again. When the channel is sloping a calculation of the final depth requires a detailed knowledge of the dependence of entrainment on 'layer Richardson number'; but, for a horizontal channel, if we neglect friction and any change in the velocity of the ambient stream which may be produced if the layer is not thin enough, it is easily seen that one relation between the velocity and depth of the layer before and after mixing may be obtained from consideration of momentum alone. In fact for rectangular (top-hat) velocity profiles

$$V_0(V_a - V_0)\,h_0 = V_1(V_a - V_1)\,h_1, \tag{2}$$

where V_0 and V_1 are respectively the velocities of the layer before and after the acceleration and V_a is that of the ambient stream. A second relation is to be found from the condition that the acceleration will have ceased when the Richardson number approaches its critical value (which we may take from I to be about 0·8).

There remains the difficulty that in order to find the final depth, the initial depth and velocity have to be specified. The manner in which they are determined is very complicated and we can envisage at least three different mechanisms which can operate.

First, one may consider a layer flowing downhill with only a low ventilating velocity. In this case the velocity and depth very near the slit are determined by the condition that long gravity waves on the interface should be stationary, just as in the case of the flow of water over a weir. The expression for the wave velocity on the interface between two moving streams of finite depth is well known (Lamb 1932, §234) and it shows that stationary waves can only exist provided that

$$\Delta_0 > V_d^2/D\cos\alpha, \tag{3}$$

and that if h_0 is small compared with D, it is given by

$$\left(\frac{h_0}{D}\right)^3 = \frac{(\Delta_d/\Delta_0)^2}{[(\Delta_0/\Delta_d)\,\mathrm{Ri}_p - 1]}. \tag{4}$$

Once h_0 is known, the value of V_0 can be found from the given values of A and Δ_0.

At high values of the ventilating velocity or low values of the initial density, the condition (3) is not satisfied and a second mechanism must operate. In this the saline water issuing from the slit is initially bent forwards by the pressure of the oncoming stream on the interface. One may make a very crude theory of this by assuming that the initial depth is determined in a distance so short that the component of the weight of this part of the layer along the slope, mixing across the interface and bottom friction can all be neglected. If this is so, one can apply the law of conservation of momentum to the whole flow in the pipe before and after the slit and also Bernouilli's equation to the flow of fresh water. These equations lead to

$$\left(\frac{h_0}{D}\right)^3 = \frac{2(\Delta_d/\Delta_0)^2}{[1-(\Delta_0/\Delta_d)\,\mathrm{Ri}_p]}. \tag{5}$$

Unfortunately not even (4) and (5) are sufficient to cover all situations; when the flow is uphill the weight of the layer may have serious consequences which invalidate the two theories. The turbulence on the interface takes a short distance to develop and the weight of the layer over this distance is unbalanced and causes the layer to flow back over the slit forming an embryonic version of the three-layer flow described in §3(ii), with a nose a centimetre or so downhill. In this situation (which is the rule rather than the exception) there are obviously many complications—for example, the nose may be so thin that viscosity is important—and we have not found any simple description of it.

However, this last difficulty does not arise when the channel is horizontal, and we have calculated the values of h_0 for that case using (4) and (5) and taking $\Delta_d/\Delta_0 = 5\times10^{-3}$, and then h_1 using (2) and the assumption that the acceleration is complete when the layer Richardson number is 0·8. The results are plotted in figure 9 and may be compared with a curve representing the average of a series of measurements in our channel. The theoretical values are very sensitive to the assumptions which have been made, but the theory at least gives the right form

of variation. At high uphill slopes the measured h_1/D are found to increase with increasing Ri_p, an effect which must be associated with the complications discussed in the last paragraph.

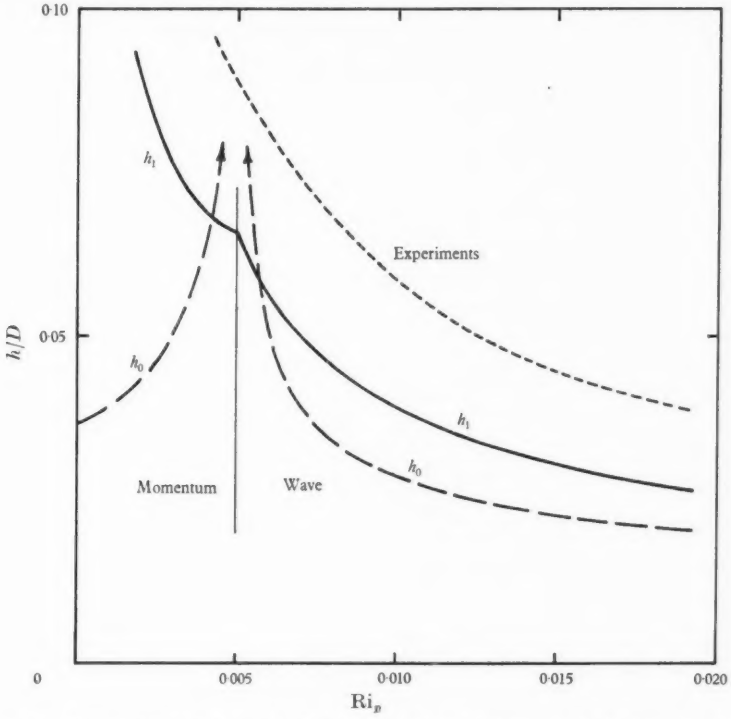

FIGURE 9. Comparison of theoretical estimates of the thickness of the layer at the slit and immediately after the initial mixing in a horizontal channel with measurements near the slit.

7. The relation between h and the floor concentration in dilute layers

The maximum concentration in the layer, which occurs at the floor, is often of practical interest. We decided against the floor concentration as an adequate parameter to describe the whole development of the layer, because of the possibility of a thin concentrated viscous region at the wall, but this sublayer disappears as the salt spreads out. After the layer has become diluted the concentration profiles do not depend much on other properties of the flow and it is thus possible to determine experimentally a unique relation between the maximum concentration Δ_s expressed as a multiple of the discharge concentration, and h. This is presented in figure 10, where we have taken mean values from a dozen experiments for which concentration profiles were available and which covered a wide range of Ri_p and slopes of from 5° to 40°. The experimental relation can be represented with good accuracy over the range of the measurements by

$$\log_{10}(\Delta_s/\Delta_d) = 3{\cdot}60 - 7{\cdot}1\,h/D. \tag{6}$$

This result enables us to predict the rate of decrease of the floor concentration in dilute layers as a function of A/V^3 and slope. Further, if we are given the depth of a layer somewhere before it has become dilute we can estimate the distance it must travel before the floor concentration falls below some specified multiple of the discharge concentration.

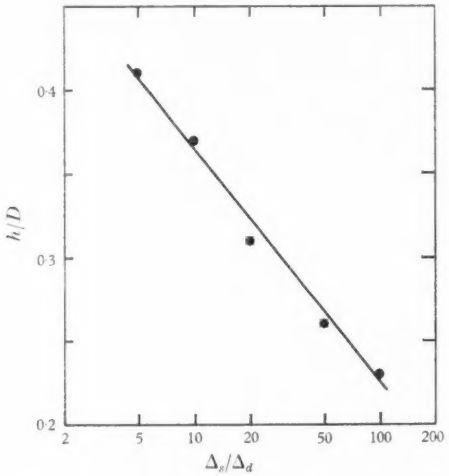

FIGURE 10. The experimental relation between the depth of dilute layers and the floor concentration.

To make the example specific, let us assume that $A/V^3 = 0{\cdot}01$ and that the slope is 10°. Suppose that at a known position $h/D = 0{\cdot}1$ and that we require to find how far from this the maximum concentration will be only 10 times the discharge concentration. From figure 7 the steady state dh/dx is seen to be $6{\cdot}0 \times 10^{-3}$, and from equation (6) we find that the final h/D is 0·365. Hence the required length is about $44D$.

The curves of figure 8 could have been drawn with this application in mind, and in special situations, where the conditions of emission of the layer are well defined, it would also be possible to include the effect of initial mixing and present results for the distance from the point of emission to points where the maximum concentration had certain standard values, as functions of Ri_p. However, because of the difficulties referred to in the last section we prefer to leave the results in their present form, which contains all the information which ought to be applied directly.

One of us (J.S.T.) wishes to acknowledge the financial support of the Ministry of Power.

REFERENCES

CALDER, K. L. 1949 *Quart. J. Mech. Appl. Math.* **2**, 153–76.
ELLISON, T. H. & TURNER, J. S. 1959 *J. Fluid Mech.* **6**, 423–48.
LAMB, H. 1932 *Hydrodynamics*, 6th ed. Cambridge University Press.

Mixing of dense fluid in a turbulent pipe flow

Part 2. Dependence of transfer coefficients on local stability

By T. H. ELLISON AND J. S. TURNER
Department of the Mechanics of Fluids, University of Manchester

(Received 5 January 1960)

This paper continues an investigation into the mixing of a dense layer of salt solution in a turbulent pipe flow in order to obtain a more detailed understanding of the underlying physical processes. The effect of the density difference on the velocity profile in a sloping pipe is calculated using a simplified model, and the results compared with direct measurements obtained by timing streaks of dye at various levels in the pipe. These velocity profiles are also used in conjunction with density profiles to estimate the dependence of the transfer coefficients for salt and momentum, K_S and K_M, on stability.

It is found that K_S is much more greatly affected by the density gradient than K_M, and that the ratio K_S/K_M may be represented, to the accuracy of the experiments, as a function of the local Richardson Number Ri. The results agree with what is known of K_S/K_M in neutral and very stable conditions, and they confirm an earlier prediction by Ellison that the critical flux Richardson number, at which K_S becomes zero, is much less than unity.

Finally, a crude semi-empirical method is outlined which indicates how the new measurements of the transfer coefficients may be related to the overall properties of the flow discussed in the first part of the paper.

1. Introduction

The first part of this paper (Ellison & Turner 1960) presented the results of measurements of the mixing of dense fluid in a turbulent stream in terms of density profiles alone. Although this is adequate for the application of the results, and may indeed be more directly useful than a more fundamental approach, a real understanding of the underlying physical phenomena can only be achieved by studying the mechanism of the flow in more detail. As the next step, this paper discusses the flow using concepts which also require a knowledge of the velocity gradients and the manner in which they are changed by the presence of a dense layer in the pipe. Simultaneous measurements of velocity and density profiles are recorded, and those for occasions when the condition of the flow was especially simple are analysed to give the turbulent transfer coefficients for salt and momentum, K_S and K_M, in terms of the local Richardson number.

2. The velocity profile

The density gradients can affect the velocity in several ways. In a tilted pipe with the flow uphill, even if K_M is not affected directly, the component of the weight of a layer of heavy fluid along the pipe will reduce the velocity near the floor and increase it near the roof. This distortion will itself lead to a change in the stress distribution and hence lead to a change in K_M, although the effect may not be great. Thirdly, there is the direct stabilizing effect of the density gradient which may modify the relation between K_M and the stress distribution. Since the heavy fluid spreads as it becomes mixed, the magnitudes of these effects change with distance producing accelerations which further complicate the flow.

It is difficult to separate the various modes of action of the density gradient experimentally, but for a given density profile the first, which depends solely on the weight of the layer, can be calculated. After setting down the equations of motion in full for future reference, we shall describe such a calculation and consider how far it explains the observed velocity profiles.

Equations of motion

Let the x-axis be along the pipe which slopes upwards at an angle α, and the z-axis across the pipe perpendicular to its floor. Then on the usual assumption that the variation of density may be neglected in the inertia terms, the x-component of the equations of motion may be written as

$$U\frac{\partial U}{\partial x}+W\frac{\partial U}{\partial z}+\frac{\partial p}{\partial x}+\Delta\sin\alpha-\frac{\partial}{\partial z}\left[(K_M+\nu)\frac{\partial U}{\partial z}\right]=0, \tag{1}$$

where p is the pressure divided by the density of the ambient fluid, ρ_a, and $\Delta=g(\rho-\rho_a)/\rho_a$. If we neglect the turbulent pressures, we may relate p at any height to its value at the roof p_r through the hydrostatic equation; so

$$p=p_r+\int_z^D \Delta\cos\alpha\,dz'. \tag{2}$$

We also have the continuity equation

$$\frac{\partial U}{\partial x}+\frac{\partial W}{\partial z}=0. \tag{3}$$

If we make use of these and integrate (1) from z to D, we obtain

$$\int_z^D\frac{\partial U^2}{\partial x}dz'-UW+(D-z)\frac{dp_r}{\partial x}+\frac{\partial}{\partial x}\int_z^D(z'-z)\Delta(z')\cos\alpha\,dz' + \int_z^D\Delta\sin\alpha\,dz'+(K_M+\nu)\frac{\partial U}{\partial z}=-\frac{\tau_r}{\rho_a}, \tag{4}$$

where τ_r is the stress at the roof. In the particular case when U and Δ are independent of x, this simplifies to

$$(M-z)\frac{dp_r}{dx}+\int_z^D\Delta\sin\alpha\,dz'+(K_M+\nu)\frac{\partial U}{\partial z}=0, \tag{5}$$

where M is defined by $(D-M)\,dp_r/dx=-\tau_r/\rho_a$.

The theoretical modification of velocity due to weight alone

We shall now use a simple theoretical model in which K_M is held fixed at its neutral value and approximated by a parabola to investigate how much the weight of the layer modifies the velocity profile. The density profile will be taken to have a triangular form, falling linearly with height from a surface value Δ_s to zero at a height h_A. This form is quite close to the observed density profile in all but very concentrated layers except in small regions near the floor and near h_A; since only an integral of the density profile enters the calculation, these regions may be neglected and it is not difficult to represent observed profiles by equivalent triangles.

Thus, our assumptions are

$$K_M = K_0 \frac{z}{D}\left(1-\frac{z}{D}\right); \tag{6}$$

$$\begin{aligned} \Delta &= \Delta_s\left(1-\frac{z}{h_A}\right) && \text{for } z \text{ less than } h_A, \\ &= 0 && \text{for } z \text{ greater than } h_A. \end{aligned} \tag{7}$$

We also assume that U is zero at the same distance z_0 from the roof and the floor, and that z_0 may be considered constant; we take $z_0/D = 2\times 10^{-4}$, which is the value appropriate to smooth flow at the Reynolds number of our experiments.

For convenience we introduce the following dimensionless variables:

$$\Pi = D^2 K_0^{-1} U_d^{-1} dp_r/dx; \quad \mu = M/D; \quad \delta = D^2 K_0^{-1} U_d^{-1} \Delta_s \sin\alpha;$$

$$\sigma = D^{-1} U_d^{-1} \Delta_s^{-1} \int_0^D \Delta U\, dz; \quad \xi = h_A/D; \quad \zeta = z/D; \quad v = DU_d^{-1} dU/dz;$$

where $U_d = D^{-1}\int_0^D U\, dz$. Then we see that the pipe Richardson number, which was introduced in the first part of this paper, is given by

$$\mathrm{Ri}_p = U_d^{-3} \int_0^D \Delta U \cos\alpha\, dz = \sigma\delta K_0 D^{-1} U_d^{-1} \cot\alpha.$$

If molecular viscosity is neglected, it follows from (5) that

$$\begin{aligned} v &= \frac{(\zeta-\mu)\,\Pi - \delta\xi[\tfrac{1}{2}-\xi^{-1}\zeta+\tfrac{1}{2}\xi^{-2}\zeta^2]}{\zeta(1-\zeta)} && \text{for} \quad \zeta \leqslant \xi, \\ &= \frac{(\zeta-\mu)\,\Pi}{\zeta(1-\zeta)} && \text{for} \quad \zeta > \xi. \end{aligned} \tag{8}$$

Hence after integration,

$$\begin{aligned} \frac{U}{U_d} &= \tfrac{1}{2}\xi^{-1}\zeta\delta - (\mu\Pi + \tfrac{1}{2}\delta\xi)\ln\zeta/\zeta_0 \\ &\qquad - [(1-\mu)\,\Pi + \delta(1-\tfrac{1}{2}\xi^{-1}-\tfrac{1}{2}\xi)]\ln(1-\zeta) \quad \text{for} \quad \zeta \leqslant \xi, \\ &= -\mu\Pi\ln\zeta - (1-\mu)\,\Pi\ln\frac{1-\zeta}{\zeta_0} \quad \text{for} \quad \zeta > \xi. \end{aligned} \tag{9}$$

μ and Π may now be found from the conditions that U is continuous at $\zeta = \xi$ and that $\int_0^1 \frac{U}{U_d}\, d\zeta = 1$. We obtain

$$\Pi = \frac{-2+\delta[-\frac{1}{2}+\frac{3}{2}\xi-\frac{1}{2}\xi\ln\xi/\zeta_0+(1-\frac{1}{2}\xi^{-1}-\frac{1}{2}\xi)\ln(1-\xi)]}{\ln\zeta_0^{-1}-2}, \tag{10}$$

and

$$(2\mu-1)\,\Pi = \frac{\delta[\frac{1}{2}-\frac{1}{2}\xi\ln\xi/\zeta_0-(1-\frac{1}{2}\xi^{-1}-\frac{1}{2}\xi)\ln(1-\xi)]}{\ln\zeta_0^{-1}}. \tag{11}$$

The dimensionless salt flux σ can be evaluated in an elementary manner using (7) and (9), and is given by

$$\begin{aligned}\sigma = {} & \mu\Pi[\tfrac{1}{2}-\tfrac{1}{2}\xi\ln\xi/\zeta_0-a\ln(1-\xi)] \\ & +\Pi[a\ln(1-\xi)-\tfrac{1}{2}+\tfrac{3}{4}\xi] \\ & +\delta[a^2\ln(1-\xi)-\tfrac{1}{4}\xi^2\ln\xi/\zeta_0+\tfrac{1}{4}\xi^{-1}+\tfrac{13}{12}\xi-\tfrac{7}{8}],\end{aligned} \tag{12}$$

where a has been written for $(1-\frac{1}{2}\xi-\frac{1}{2}\xi^{-1})$.

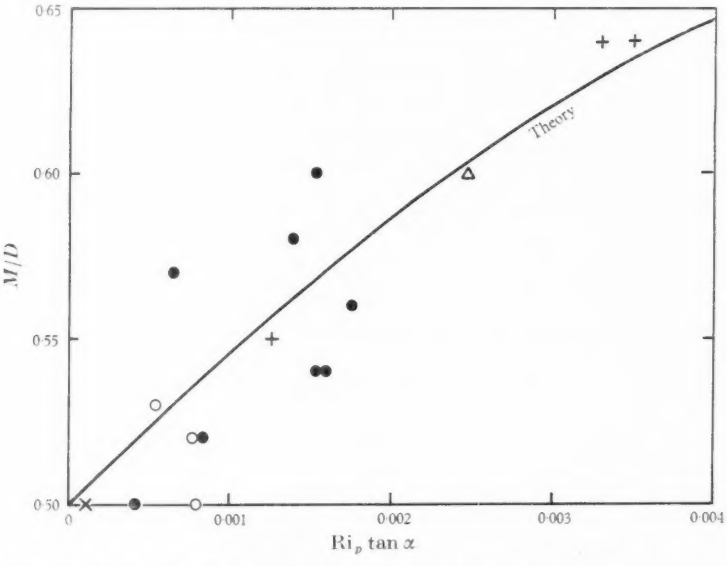

FIGURE 1. The height of the velocity maximum in an inclined pipe containing heavy salt solution as a function of $\mathrm{Ri}_p \tan\alpha$. The curve drawn is theoretical, and individual experimental points are shown. ○, 6°; +, 20°; ×, 7½°; △, 30°; ●, 10°.

With a knowledge of σ it is simple to calculate Ri_p. Since in each of our experiments Ri_p is independent of x it is convenient to make it the independent variable and to regard the profiles as functions of Ri_p and ξ. The dependence of μ on ξ for a fixed value of $\mathrm{Ri}_p \tan\alpha$ turns out to be so weak that μ can be represented adequately as a function of $\mathrm{Ri}_p \tan\alpha$ alone; this is plotted in figure 1 together with our observations of the height of the velocity maximum. which are further discussed below. Π also depends very little on ξ, and it is

clear that the distortion of the profile is much more closely governed by the channel Richardson number than by the depth of the layer, and we should not expect much change in velocity as the layer spreads. This provides some justification for the use of the simplified form of the equation of motion in which U and Δ are assumed to be independent of x. A comparison between a typical theoretical profile and observation will be discussed after the techniques of measurement have been described.

The measurement of velocity

Several methods were tried before consistent measurements of velocity were obtained. The low velocities made it impossible to use Pitot tubes, and at first an attempt was made to use thermistors as in an earlier investigation (Ellison & Turner 1959). They proved to be too inaccurate owing to the sensitivity of the system to ambient temperature, to the non-linearity of the calibration which caused difficulty in averaging the highly fluctuating velocity, and to the obstruction to the flow which became important when the thermistor was traversed more than half way across the pipe.

Later, a twisting wire device was tried, in which the deflexion of a fine steel wire set across the flow was observed with a microscope. This also failed to give the required accuracy, possibly because the drag of a cylinder depends on the level of turbulence in the stream.

The useful measurements were taken using the most direct method of all, that of timing streaks of dye released into the stream. Moveable opaque guides were placed on each side of the pipe so that they could be set at any given height and the motion of the dye along their open edge followed; the measurements were made between fixed marks drawn 30 cm apart at the positions of the salt probes. It was possible to time to the nearest $\frac{1}{20}$ sec in about 2 sec, and the variations greater than this were due to real variations in velocity from one realization of the flow to another; the average of ten readings was taken at each height and the standard deviation of this was about 3 %. In order to achieve this accuracy it was necessary to have an adequate length of pipe between the point of introduction of the dye and the first mark, so that the general appearance of the dye did not change appreciably between the stations. Systematic errors are likely to be small except near the roof or floor where the velocity gradient is high and one can unconsciously follow material at the wrong level.

Our estimates of the velocity gradients are, of course, much less accurate than those of velocity itself, and may be in error by 10 %; this means that our estimates of the local Richardson number may be out by 20 % due to the uncertainties of velocity alone.

We also attempted to measure velocity variations in the direction of flow by timing over overlapping intervals at the same height; we found that, except with very concentrated salt layers, the variations were less than the experimental errors in accordance with the theoretical prediction mentioned above.

The experiments were conducted using two standard discharge velocities, 13·5 and 10·6 cm s^{-1}, the majority being at the higher speed which is that used for the measurements reported in the first part of this paper.

Comparison with simple theory

Examples of measured velocity profiles are shown in figures 2 and 3. In figure 2 the experimental points (crosses) are compared with the theoretical curve calculated by the method outlined above; the measured density profiles and the 'equivalent triangle' assumed for the purpose of the calculation are also shown.

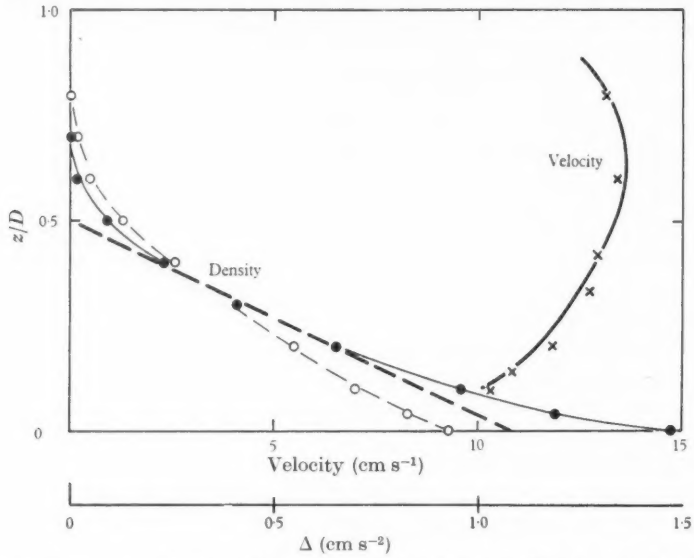

FIGURE 2. Comparison of observed and calculated velocity profiles in a pipe inclined at 20°; $\mathrm{Ri}_p = 0{\cdot}0090$. The density profiles 30 cm apart and the 'equivalent triangle' used in the calculation are also shown.

The general shape of the velocity profile is adequately represented by the theory, although the slopes of the theoretical curve are somewhat greater than those corresponding to the measured points in this instance. The height of the velocity maximum is well predicted; the more extensive measurements of this quantity shown in figure 1 also confirm that in spite of considerable scatter there is no systematic difference between the theory and the measurements. Thus it appears that the assumption that K_M is unchanged by the presence of the dense fluid is a fair first approximation and that the direct action of the weight of the layer is the most important factor distorting the velocity profile.

This suggests the possibility of using the theory in order to estimate the velocity gradients entering into the expression for the local Richardson number. For the determination of the dependence of K_S and K_M on Ri, we have preferred to use directly measured velocity profiles; but in §6 below we do develop an empirical extension of the theory in order to relate the eddy transport coefficients to the rate of increase of the depth of the layer described in detail in Part 1.

The theory is, of course, at its weakest when one considers thin concentrated layers at low slopes, since in these the effect of stability in reducing K_M is relatively more important.

3. The momentum transfer

From the measurements of velocity described in the last section and the density profiles obtained by the method described in Ellison & Turner (1959), it is possible to estimate the eddy viscosity K_M. The analysis was confined to occasions when the layer was not too thin and the velocity changed little in the x-direction. Then, since the only term in (4) depending on $\partial\Delta/\partial x$, namely

$$\frac{\partial}{\partial x}\int_z^D (z'-z)\,\Delta(z')\cos\alpha\,dz',$$

is quite negligible, it is permissible to use (5).

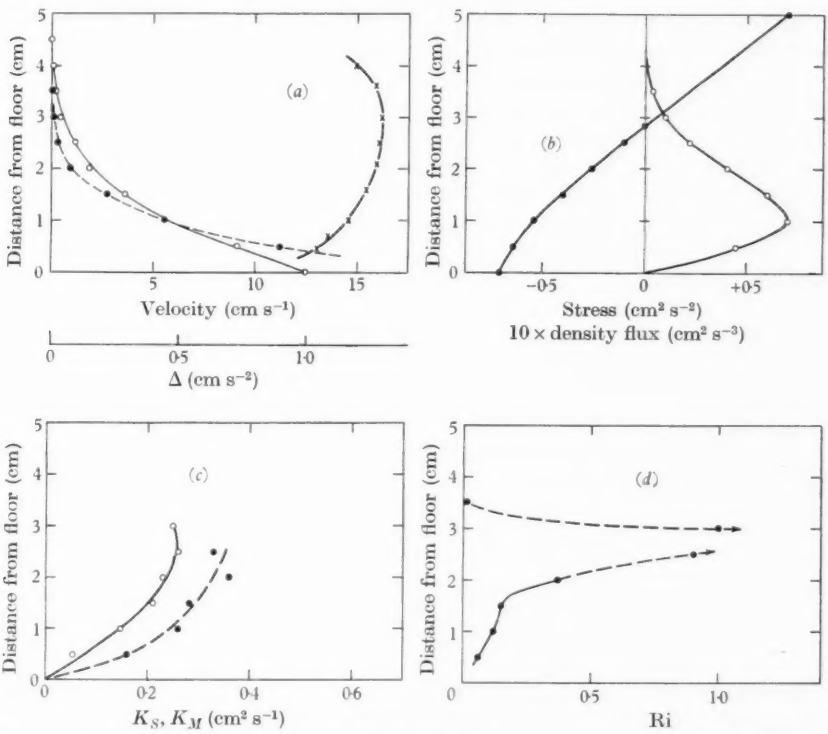

FIGURE 3. Turbulent transfer in a pipe inclined at 10°; $\mathrm{Ri}_p = 0{\cdot}0037$. (*a*) Measured velocity and density profiles. ●, Density at 40 cm; ○, density at 70 cm; ×, velocity. (*b*) Distributions of stress and density flux. ●, $-(K_M+\nu)\,dU/dz$; ○, $-K_S(d\Delta/dz)$. (*c*) Transfer coefficients for salt (K_S) and momentum (K_M). ●, K_M; ○, K_S. (*d*) Local Richardson number, Ri.

However, (5) contains two unknown quantities, dp_r/dx and M. In order to measure the pressure gradient directly a much more uniform pipe than ours would be required, even if the considerable difficulties of devising and using a sufficiently sensitive manometer could be overcome. We therefore had to make two assumptions to fix dp_r/dx and M:

(*a*) the friction coefficient relating the stress on the roof to the discharge velocity is the same as at the same Reynolds number without any salt flow;

(*b*) the total stress is zero at the height of the velocity maximum.

The first of these assumptions is unlikely to be far wrong, since there is never sufficient density gradient in the top half of the channel to give rise to any significant stability effects. The second assumption is not so satisfactory either theoretically or in practice. Although the idea behind the use of an eddy viscosity implies that the stress vanishes when the velocity gradient does, there is no theoretical reason for believing that this happens exactly; and in practice the measured velocity maxima are broad, making the determination of the position of no stress difficult and thus introducing another considerable source of error.

If these assumptions are accepted, K_M can be found from (5). However, reasonably consistent results could not be obtained either in the centre of the pipe where the velocity gradients are small and K_M is the ratio of two small quantities, or near the floor where the velocity gradients are too high to be determined by our technique. Our most accurate results are therefore restricted to the two heights 1·0 and 1·5 cm. Measurements at these positions have the additional advantage that usually the density flux and Richardson number are changing less rapidly with height in this region than elsewhere (see figures 3*b* and *d*).

In figures 3*a*, *b* and *c* are shown typical velocity and density profiles and the variation with height of the stress and eddy viscosity derived from them. We shall return to discuss the results of all the experiments analysed in this way after describing the calculation of the eddy diffusivity.

4. The salt transfer

In the steady state, with the neglect of turbulent transfer in the direction of the flow and of the minute contribution of molecular diffusion, the equation for the transfer of salt may be written

$$U\frac{\partial\Delta}{\partial x}+W\frac{\partial\Delta}{\partial z}-\frac{\partial}{\partial z}\left(K_S\frac{\partial\Delta}{\partial z}\right)=0. \tag{13}$$

When the velocity is independent of x, so that $W = 0$, this simplifies to

$$K_S\frac{\partial\Delta}{\partial z}=-\int_z^D U\frac{\partial\Delta}{\partial x}dz'. \tag{14}$$

The salt flux is zero at the top and bottom of the channel so the integral taken from 0 to D should be zero if U is in fact independent of x; and, in the absence of measurements of $\partial U/\partial x$ on every occasion, this has been used as a check in selecting runs for analysis. Values of the salt flux and of K_S calculated from (14) are included in figures 3*b*, and *c*.

5. The dependence of K_M and K_S on the local Richardson number

It is clear that K_M and K_S must depend on the stability, but since the scale of turbulence is such that any eddy covers a considerable height range, it is by no means obvious that there should be a simple dependence on a strictly local parameter such as

$$\mathrm{Ri}=-\frac{\partial\Delta}{\partial z}\Big/\left(\frac{\partial U}{\partial z}\right)^2$$

which changes with height as is shown for a typical occasion in figure 3*d*. Nevertheless, the curve obtained when the results are analysed in this way is very encouraging.

The eddy viscosity

The dependence of the eddy viscosity on the Richardson number has been discussed in the meteorological literature (see Charnock 1958 for a recent review). It is usual (Deacon 1955) to consider the dimensionless quantity $K_M^* = K_M/u_* z$,

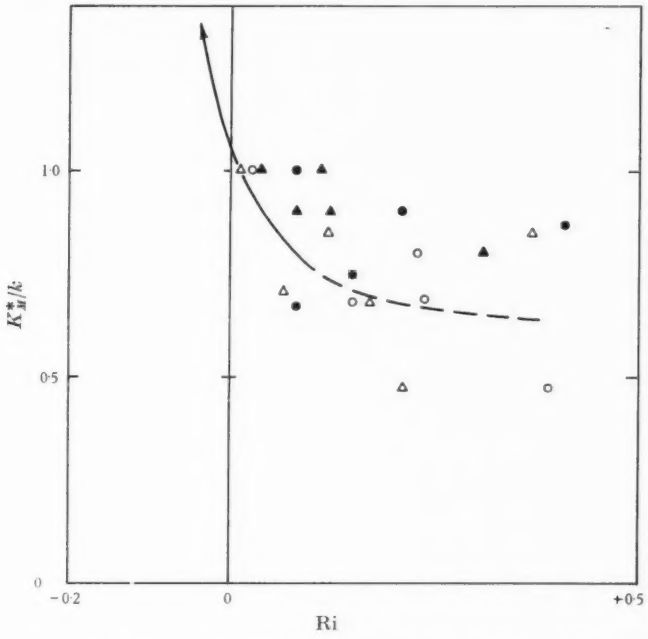

FIGURE 4. Measurements of the non-dimensional eddy viscosity K_M^*/k as a function of local Richardson number. ▲ △, 1·0 cm; ● ○, 1·5 cm. The curve drawn represents an average of the atmospheric measurements reported by Rider (1954).

where u_* is the friction velocity defined by $u_* = |K_M \partial U/\partial z|^{\frac{1}{2}}$. In figure 4 K_M^*/k, where k is von Karman's constant, is plotted as a function of Ri together with a curve which represents an average of Rider's (1954) widely scattered atmospheric measurements. Rider was mainly concerned with unstable conditions and took only a few measurements in the range of Richardson numbers for which we have dotted the curve.

Our measurements are also scattered, but they confirm the trend for K_M^* to fall below its neutral value, k, as Ri is increased. These results and those shown later for K_S have been grouped according to the accuracy with which $\int_0^D U \dfrac{\partial \Delta}{\partial x}\, dz'$ is zero. In the first group (indicated in the figures by solid symbols) are experiments for which the integral is zero to within the experimental accuracy; in the

second group (indicated by open symbols) are those for which the negative part of the integral at the bottom of the pipe is up to 50 % higher than the top part, indicating a small but probably negligible vertical velocity near the bottom of the pipe. Lastly, there are the experiments shown by crosses in some of the figures in which the criterion is clearly not satisfied. These correspond to cases when there was a very concentrated layer near the floor, and for which even from visual observation we should expect W to be important.

The ratio K_S/K_M

When we come to compare the ratio K_S to K_M, the scatter is less important since the dependence on Ri is more dramatic. In figure 5 are shown all the results at the two heights of 1·0 and 1·5 cm. The points for which significant values of W have been ignored lie low in the left-hand corner of the diagrams, which is to

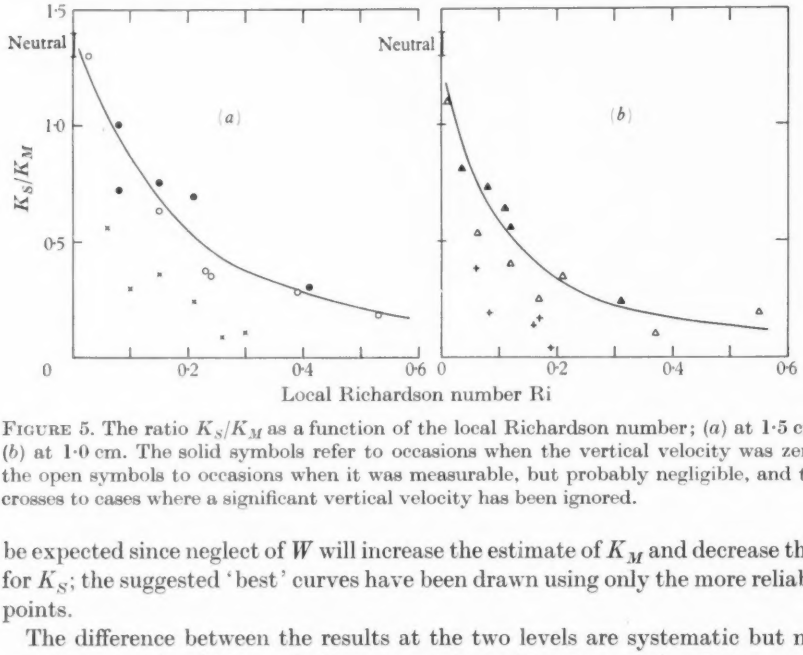

FIGURE 5. The ratio K_S/K_M as a function of the local Richardson number; (*a*) at 1·5 cm; (*b*) at 1·0 cm. The solid symbols refer to occasions when the vertical velocity was zero; the open symbols to occasions when it was measurable, but probably negligible, and the crosses to cases where a significant vertical velocity has been ignored.

be expected since neglect of W will increase the estimate of K_M and decrease that for K_S; the suggested 'best' curves have been drawn using only the more reliable points.

The difference between the results at the two levels are systematic but not very large; it is hard to say whether or not it is significant or on what factors, such as Reynolds number, it depends. The striking feature of the results is the sharp fall of K_S/K_M at quite small Ri, and this will now be discussed further in relation to previous measurements and theories.

Previous measurements of K_S/K_M

The possibility of a dependence of K_S/K_M on Ri has been discussed in the meteorological literature (e.g. Pasquill 1949; Rider 1954; Swinbank 1955), but the difficulties of measurement are great and accuracy has not been good, largely, we would suggest, because of the neglect of advection terms (cf. the neglect of

$\partial U/\partial x$ in our problem). A tendency for K_S/K_M to decrease with increasing Ri has been found, but there is not even agreement about the value of the ratio in neutral conditions: Rider gets 1·3 and Swinbank about 0·8.

Fortunately, there are more precise measurements in controlled laboratory conditions from which the neutral value can be found. Sherwood & Woertz (1939) made measurements in a nearly two-dimensional vertical duct one wall of which was covered with water and the other with strong calcium chloride solution, so that a humidity gradient was set up. They found that in the central region of the duct the eddy diffusivity for water vapour was around 1·5 times the eddy viscosity at a Reynolds number of 10^5.

Forstall & Shapiro (1950) measured profiles of velocity and helium concentration in a turbulent jet and also surveyed previous experimental results for the turbulent diffusion of heat (or matter) and momentum in both liquids and gases. They concluded that all the measurements led to a value for K_S/K_M within 10 % of 1·40.

In 1952 Page, Schlinger, Breaux & Sage reported an experiment in a small two-dimensional duct with the floor and roof maintained at different temperatures and through which air was flowing so rapidly in relation to the temperature gradients that Ri was negligible. They measured the ratio of the transfer coefficients as a function of position and Reynolds number, and found a value of 1·30 at the Reynolds number used in our pipe. Later Schlinger, Berry, Mason & Sage using the same apparatus gave a value appropriate to our case of 1·35 and suggested that it decreased to about 1·1 at very high Reynolds numbers. More recent reports from the same laboratory (Hsu, Sato & Sage 1956) disagree about the detailed dependence on Re, but this does not have much effect on the values we have taken. We can assert with some confidence that in neutral conditions and at the Reynolds number we used, K_S/K_M lies between 1·3 and 1·4; these limits have been marked in figures 5 and 6.

Our previous experimental results for wall plumes (Ellison & Turner 1959) can be reanalysed to give K_S and K_M. The calculation is tedious since W can certainly not be neglected and all the terms in the equations of motion must be determined, but we have carried it through for one case. At the height at which Ri was changing least and had a value of 0·23, we obtained $K_S/K_M = 0{\cdot}23$. This is not inconsistent with the present series of measurements and is marked with them on figure 6.

At the extreme of very high Richardson numbers, there are the frequently quoted measurements made in the Kattegat under conditions of very great stability, which have often been used to verify that the flux Richardson number, $\mathrm{Rf} = \mathrm{Ri}\, K_S/K_M$, is always less than unity. The analysis of Proudman (1953) shows that K_S/K_M is between 0·05 and 0·03 when Ri is in the range from 4 to 10. It is likely that the difference in Reynolds number between our experiments and the oceanographic observations is important; and, moreover, there is a strong probability that at very high Richardson numbers the transfer mechanism may be more closely associated with the breaking of internal waves than with turbulence in the ordinary sense (Stewart 1959). Nevertheless, Proudman's estimates are quite consistent with an extrapolation of our results and are shown together with them in figure 6.

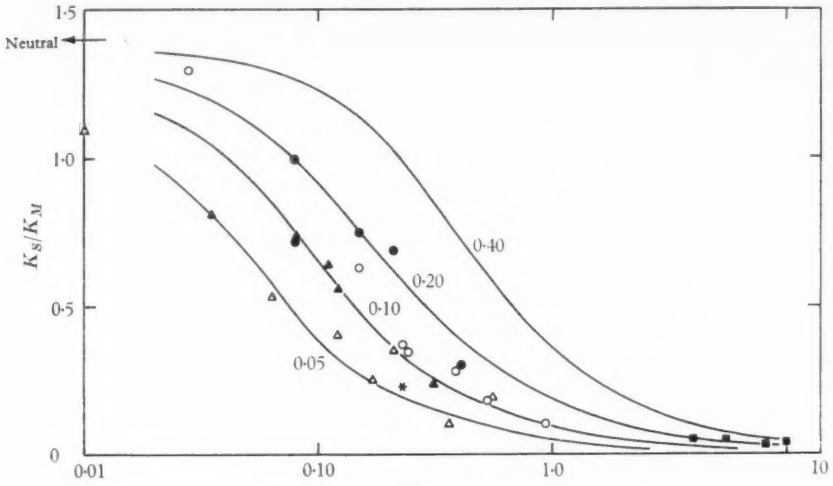

FIGURE 6. The comparison of our experimental results and other available data with the theory of Ellison (1957). The values of the parameter Rf_c are marked on the theoretical curves. ● ○, 1·5 cm; ▲ △, 1·0 cm; ∗, Wall plume; ■, Kattegat.

Comparison with the theory of Ellison (1957)

In 1957 Ellison presented a speculative theory which predicts dependence of K_S/K_M on Ri. Using the equations of motion, continuity and diffusion together with some assumptions concerning the rates at which the velocity and density fluctuations and their covariance would decay in the absence of the terms in the equations describing their production, Ellison arrived at an equation (numbered 20 in his paper) of the form

$$\frac{K_S}{K_M} = \frac{b(1-\mathrm{Rf}/\mathrm{Rf}_c)}{(1-\mathrm{Rf})^2}, \tag{15}$$

where b and Rf_c are constants or very slowly varying functions which depend on the structure of the turbulence. Clearly b is the value of K_S/K_M in neutral conditions and Rf_c is the critical value of Rf at which K_S vanishes. In order to evaluate the constants, Ellison made further numerical assumptions, but we can do this directly from our experimental results. With K_S/K_M in neutral conditions fixed at 1·4, say, (15) gives a family of curves connecting K_S/K_M to Rf (or Ri) with Rf_c as parameter, and these are drawn in figure 6. Our results at 1·5 cm are seen to be fitted best by the curve corresponding to $\mathrm{Rf}_c = 0{\cdot}15$, but if we include our measurements at 1·0 cm, the best estimate of Rf_c will be nearer to 0·10.

Note that even at higher Ri the theoretical curves are broadly in agreement with the Kattegat measurements. In this range, however, the assumption that b and Rf_c are constants independent of stability is less likely to be accurate, and in any case the comparison between theory and experiment is less reliable in this range. By using the range where K_S/K_M depends strongly on stability, we have obtained a more sensitive comparison with theory.

Ellison's original estimate for Rf_c was 0·15, and our results are in surprisingly close agreement with this, confirming his conclusion that Rf_c is much less than unity. This is a remarkable result, since it implies that the term representing the rate of working against buoyancy forces in the turbulent energy equation, which is commonly invoked at the beginning of discussions of turbulence in a stratified fluid, is never dominant; the rate of transfer of dense fluid is drastically affected before the direct effects of the reduction of turbulent energy could make themselves felt. Further clues about the operative mechanism may be obtained from Ellison's paper. The expression for the correlation coefficient between density and vertical velocity given by him leads to

$$\frac{(\overline{w'\Delta'})^2}{\overline{w'^2}\,\overline{\Delta'^2}} \propto \frac{1-\mathrm{Rf}/\mathrm{Rf}_c}{1-\mathrm{Rf}}. \tag{16}$$

Thus as Rf approaches Rf_c the correlation between velocity and density is destroyed more rapidly than the fluctuations themselves. This suggests the simple physical picture that in stable conditions a displaced fluid particle tends to return to its equilibrium level before it has mixed with its surroundings. A particle can transfer momentum during a brief excursion without mixing, but in order to transfer matter or heat it must mix.

6. Conclusions

The work we have described in this paper forms an intermediate link in the chain of knowledge leading from the detailed equations of motion to the magnitudes of the spread of salt solution, the measurements of which were recorded in Part 1. On the one side it is connected to the theory, as yet very imperfect, relating the transfer coefficients to the local Richardson number as has been described in §5; and it must be possible to link it on the other side with some calculation of the development of the density profiles yielding values of dh/dx from those of K_S and K_M. We shall outline such a calculation in an appendix.

We may now summarize our main conclusions as follows:

(1) In tilted pipes the weight of the dense fluid is the dominant factor modifying the velocity profile; the changes in K_M due to stability and to the alteration in the stress distribution are less important.

(2) Our results are consistent with, but do not establish, a reduction of K_M^* with increasing Richardson number of the magnitude suggested by the meteorological observations.

(3) Our measurements show that K_S/K_M is strongly dependent on the Richardson number. The form found for this dependence (figures 5 and 6) is likely to have wide validity, but the numerical values may be in error by 30–50 %. It must also be stressed that strictly they apply only to one particular region in the pipe and may be affected somewhat by the shape of the pipe and the Reynolds number.

The investigation described was made in the course of work carried out for the Ministry of Power on problems relating to the movement of firedamp in the roadways of coal mines. One of us (J.S.T.) wishes to acknowledge the financial support of the Ministry of Power.

REFERENCES

CHARNOCK, H. 1958 *Sci. Progr.* **46**, 470–87.

DEACON, E. L. 1955 *Comm. Sci. Ind. Res. Org., Div. Met. Phys.* (*Melbourne*), *Tech. Pap.* no. 4.

ELLISON, T. H. 1957 *J. Fluid Mech.* **2**, 456–66.

ELLISON, T. H. & TURNER, J. S. 1959 *J. Fluid Mech.* **6**, 423–48.

ELLISON, T. H. & TURNER, J. S. 1960 *J. Fluid Mech.* **8**, 514–28.

FORSTALL, W. & SHAPIRO, A. H. 1950 *J. Appl. Mech.* **17**, 399–407.

HSU, N. T., KAZUHIKO SATO & SAGE, B. H. 1956 *Industr. Engng Chem.* **48**, 2219–23.

PAGE, F., SCHLINGER, W. G., BREAUX, D. K. & SAGE, B. H. 1952 *Industr. Engng Chem.* **44**, 424–30.

PASQUILL, F. 1949 *Proc. Roy. Soc.* A, **198**, 116–40.

PROUDMAN, J. 1953 *Dynamical Oceanography*. London: Methuen.

RIDER, N. E. 1954. *Phil. Trans.* A, **246**, 481–501.

SCHLINGER, W. G., BERRY, V. J., MASON, J. L. & SAGE, B. H. 1953 *Industr. Engng Chem.* **45**, 662–6.

SHERWOOD, T. K. & WOERTZ, B. B. 1939 *Trans. Amer. Inst. Chem. Engrs*, **35**, 517–40.

STEWART, R. W. 1959 *Advances in Geophysics*, Vol. 6, *Proceedings of Symposium on Atmospheric Diffusion and Air Pollution* (Oxford, August 1958), pp. 303–10. New York and London: Academic Press.

SWINBANK, W. C. 1955 *Comm. Sci. Ind. Res. Org., Div. Met. Phys.* (*Melbourne*), *Tech. Pap.* no. 2.

Appendix

The relation between the measurements of K_S/K_M and dh/dx

If we had shown that K_M^* and K_S/K_M were everywhere exactly determined by the local value of Ri and had found the form of the dependence, a complete set of equations would be available and in principle it would be possible to start with an arbitrary distribution of concentration and calculate its development; but our measurements were much too limited for that. In any case, such a calculation would be highly complex and we must beware of doing elaborate calculations on the basis of inadequate information. Nevertheless, it seems desirable to make some attempt to relate our new knowledge of the transfer coefficients to the rate of spread of the layer, and we shall therefore present a brief description of a very crude semi-empirical approach to the problem, which doubtless can be refined as understanding increases.

For this purpose we shall again use the simple model proposed in §2 in which the density profile is assumed to be triangular. Although this form is adequate for calculating the distortion of the velocity profile, the actual density profiles do depart considerably from it in some circumstances, especially near $z = h$. We have tried several more elaborate models which take this into account, but the improvement in accuracy is only moderate, and we have chosen to present only the simplest here.

It is convenient to divide the calculation into stages as follows.

(*a*) The determination of the local Ri at a standard height, which we have chosen to be $\frac{1}{2}\xi$, as a function of Ri_p, ξ, and α.

(*b*) The use of our empirical relation between K_S/K_M and Ri, together with the assumption that K_M is given by (6), to obtain K_S at the height $\frac{1}{2}\xi$ as a function of Ri_p, ξ, and α.

(*c*) The relation of K_S to $\partial\xi/\partial x$ at this height.

(*d*) The relation of h to ξ and so the determination of dh/dx as a function of Ri_p, ξ, and α.

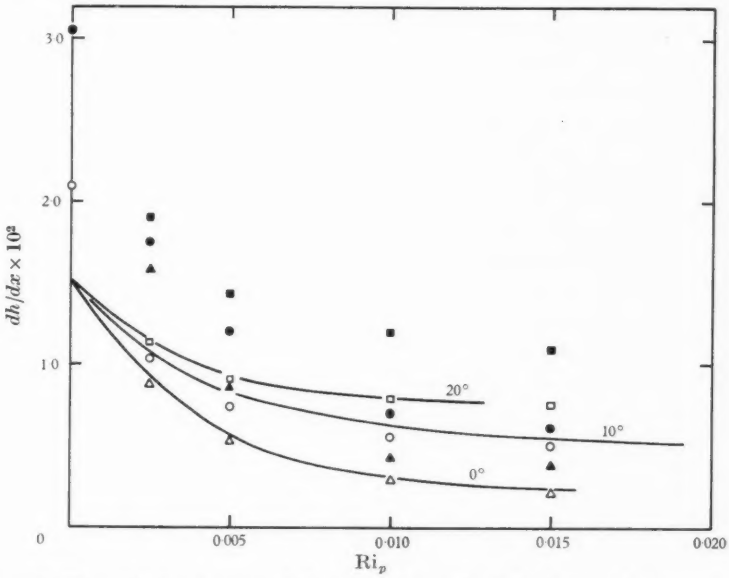

FIGURE 7. Theoretical estimates of the rate of spread of the layer using experimental values of K_S/K_M. The curves represent the measured values of this quantity which were reported in Part 1.

	$\xi = 0{\cdot}4$	$\xi = 0{\cdot}6$
0°	▲	△
10°	●	○
20°	■	□

The first stage is simple since it follows from the definitions in §2 that $\mathrm{Ri} = \sigma^{-1}\xi^{-1}\upsilon^{-1}\mathrm{Ri}_p$; σ and υ are known functions of ξ and δ (for $\zeta = \frac{1}{2}\xi$) and δ depends on ξ and $\mathrm{Ri}_p \tan\alpha$. This means that $\mathrm{Ri}\tan\alpha$ is a function of $\mathrm{Ri}_p \tan\alpha$ and ξ. The numerical dependence has been computed for two values of ξ, 0·4 and 0·6, because for these $\frac{1}{2}\xi$ corresponds to the two heights 1·0 and 1·5 cm at which we measured K_S/K_M. It is found that in both cases $\mathrm{Ri}\tan\alpha$ is proportional to $\mathrm{Ri}_p \tan\alpha$ when the quantities are small, but changes only slowly when $\mathrm{Ri}_p \tan\alpha$ is large. This explains an effect which proved troublesome during our experiments: it was impossible to obtain large local Richardson numbers except at small slopes.

The second stage of the calculation follows quite directly. For the third stage we use equation (14) and assume that we may replace U in it by U_d. Then, since Δ is given by (7),

$$\frac{K_S\Delta_s}{U_d h_A} = \frac{h_A}{8}\frac{d\Delta_s}{dx} + \tfrac{3}{8}\Delta_s\frac{dh_A}{dx} = \frac{\Delta_s}{8}\left[\frac{h_A}{\Delta_s}\left(\frac{\partial\Delta_s}{\partial h_A}\right)_{\mathrm{Ri}_p} + 3\right]\frac{dh_A}{dx}. \tag{17}$$

Now, the numerical value of $h_A \Delta_s^{-1} (\partial \Delta_s / \partial h_A)_{\mathrm{Ri}_p}$ varies little with $\mathrm{Ri}_p \tan \alpha$ and ξ and is around $-1{\cdot}2$, so

$$\frac{K_S}{U_d h_A} = 0{\cdot}22 \frac{dh_A}{dx}. \tag{18}$$

This equation and equation (6) gives K_S/K_M.

For the last stage it is necessary only to observe that, by definition, $\sigma = \Delta_d/\Delta_s$, and so

$$h = h_A(1-\sigma). \tag{19}$$

The final results are shown in figure 7. The points represent the theoretical values of dh/dx as a function of Ri_p for the slopes 0°, 10° and 20°, at the two values of ξ 0·4 and 0·6, corresponding roughly to $h = 1{\cdot}7$ cm. and 2·2 cm, and they are compared with our earlier experimental curves given in Part 1. It will be seen that this semi-empirical theory explains the general shape of the curves and the dependence on slope, and shows clearly the range of pipe Richardson number where stability becomes important. It is, however, less good at small values of Ri_p and predicts a dependence of dh/dx on ξ which was not observed (but which may, of course, be detected in more refined experiments). In view of the very crude approximations that were made and the experimental difficulties at small Ri_p, these discrepancies are not surprising and the qualitative success of the theory suggests that further progress will be made as increasing experimental information enables it to be refined.

The effect of turbulence and magnetic field on electron density fluctuations in the ionosphere

By I. D. HOWELLS
Trinity College, Cambridge

(Received 6 January 1960)

Dungey (1956) has shown that the number densities of electrons and positive ions, under the action of turbulence and the magnetic field in the ionosphere, are closely equal—in other words the only fluctuations in electron density are those controlled electrostatically by the ions—and he has estimated the magnitude of the fluctuations. The present paper uses Dungey's model and results, reduces his equations to a single equation for electron density, in each of several cases, and then investigates the possible spectra of fluctuations. It is concluded that, in the circumstances that commonly arise, the spectrum on this model should be nearly isotropic, though exceptionally there could be a strong elongation of irregularities at right angles to the magnetic field. Thus some other mechanism is required to account for the elongation that is observed, parallel to the field.

Below 110 km, where the magnetic effect on the ions' motion is small, and at wave-numbers in the inertial subrange of the turbulence, dimensional argument shows that the spectrum function (integrated over all directions) is proportional partly to κ^{-1} and partly to $\kappa^{-\frac{5}{3}}$. Above 120 km the magnetic effect is large; a more detailed study shows that when turbulence is present, which probably is not often, the spectrum function in the inertial subrange is proportional to $\kappa^{\frac{2}{3}}$, with considerable anisotropy.

1. Introduction

Radio waves are scattered in the ionosphere by irregularities of electron density, which are believed to owe their form, in the E region at least, largely to atmospheric turbulence. Most theoretical studies of the irregularities' formation have used a model in which the electrons and ions are subject only to convection by the turbulent motion, and (because electrostatic attraction keeps the number densities closely equal) to diffusion with one effective diffusivity which is about twice the kinematic viscosity. In fact, since compressibility and recombination effects are generally agreed to be insignificant (Batchelor 1955, p. 10; Villars & Weisskopf 1955; Wheelon 1957), the model is simply that of turbulent convection of heat, with Prandtl number of about $\frac{1}{2}$. The quantity of greatest interest in scattering theory is the spectrum function of electron density; an account of the present state of knowledge about the spectrum function of a conserved scalar, subject only to turbulent convection and to diffusion, can be found in Batchelor (1959).

But the suggestion of Booker (1956), that the elongated irregularities that are observed in some places can be explained by taking into account the earth's magnetic field, makes it desirable to study the effect of turbulence on an ionized gas, in the presence of a magnetic field. A suitable model for this purpose has been put forward by Dungey (1956).

Dungey considered a gas lightly ionized into electrons and N_2^+ ions, in turbulent motion in a uniform magnetic field. He ignored the processes of formation and recombination of ions, and supposed all constituents of the gas to have the same temperature. He showed that for the eddy sizes that are of most interest (up to a few kilometres) the motion of the neutral gas is not appreciably influenced by the magnetic field and collisions with charged particles. Thus he could suppose this gas to have a known turbulent motion, and write equations of motion for the charged particles regarded as gaseous constituents, taking into account their collisions with neutral molecules but not with one another.

For these equations, giving the parameters typical values for the ionosphere, Dungey obtained the results that the inertia terms can be omitted, that electromagnetic effects (other than the magnetic force on charged particles) are negligible for eddy sizes up to several kilometres, and that the number densities of electrons and ions are everywhere equal, to a very good approximation, although their velocities are not necessarily equal. (These results can also be confirmed by a linearized calculation, in which a single Fourier component $\mathbf{C}\, e^{i(\boldsymbol{\kappa}.\mathbf{x}+\omega t)}$ is used for the neutral gas velocity, so that the number densities are found by solving a set of algebraic equations.)

So we have to reject one of Booker's ideas: that it would be possible to have irregularities of electron density controlled by the magnetic field and collisions between electrons and neutral molecules, co-existing with those controlled electrostatically by the ions. This would violate the result that the number densities of electrons and ions are everywhere equal.

The present paper starts with the same model as Dungey's, and makes use of these results of his to study in more detail the irregularities of electron density (and it takes into account diffusion due to electron and ion partial pressures, which he neglected). Recent results that the principal ion present at most heights is NO^+ instead of N_2^+ will not appreciably affect the conclusions.

We can describe some of the effects of the magnetic field in simple physical terms. The motion of charged particles across the field tends to be reduced, and changed in direction. Thus irregularities of number density do not move with the air. Further, irregularities can be produced even when the air is uniformly ionized at first, and the motion involves no appreciable fluctuations in air density. There are two mechanisms which produce this effect, the first being that described by Dungey (1956):

(*a*) If the air has a motion involving compression along the magnetic field, and expansion perpendicular to it, then, because the charged particles have their motion perpendicular to the field inhibited to some extent, they suffer a net compression (or, in the converse case, an expansion).

(*b*) If the air has a rotational motion, with a component of vorticity in the direction of the magnetic field, the charged particles tend to spiral outwards or

inwards, depending on the charge and the direction of rotation. Because the air exerts a greater drag on ions than on electrons, the motion of the ions dominates and a net compression or expansion results. (But this mechanism does not operate when the motion is two-dimensional in planes perpendicular to the field, because opposing electrostatic fields are then set up.)

In addition to these magnetic effects, there will be the ordinary turbulent mixing of ionization gradients giving rise to irregularities. All of these mechanisms are correlated over roughly the same distance in all directions, and will not of themselves produce irregularities strongly elongated along the magnetic field. The only possible effect of this kind would arise if the ions had a large-scale drift relative to the air, and hence to the eddies. For irregularities of ion density produced by eddies moving through the ionization will tend to have the form of wakes behind the eddies, and so to be elongated in the direction of the drift. Such a large-scale drift cannot have a strong component parallel to the magnetic field, because there is no force which could maintain it (an electrostatic field would be mostly neutralized because electrons are conducted much better than ions along the magnetic field), and hence a strong elongation of irregularities of this type must be at right angles to the magnetic field. This is referred to again at various points in the paper.

2. Notation, and equations of motion

We use the following notation:

$\mathbf{u}(\mathbf{x}, t)$ = gas velocity, supposed known,
$\mathbf{E}(\mathbf{x}, t)$ = electrostatic field,
$\mathbf{B}$ = magnetic induction,
T = absolute temperature,
k = Boltzmann's constant,
e = electronic charge.

For the charged particles we use the following symbols, with suffixes + and − where appropriate:

$m_\pm$ = mass,
$\Omega_\pm$ = $eB/m_\pm$ = gyrofrequency,
$f_\pm$ = collision frequency with molecules (defined in terms of momentum transfer—see (iii) below),
γ = $2kT(m_+f_+ + \mathrm{m}_-f_-)^{-1}$ = coefficient of ambipolar diffusion—see (vi) below,
$\lambda_\pm$ = $\Omega_\pm/f_\pm$,
$\mathbf{u}_\pm(\mathbf{x}, t)$ = velocity,
$n_\pm(\mathbf{x}, t)$ = number density,
$p_\pm(\mathbf{x}, t) = kTn_\pm$ = partial pressure.

In the specification of the last three quantities, electrons and ions are regarded as two gaseous constituents of the atmosphere.

For the spectra of number density we use the notation of Batchelor (1959): $\Gamma(\kappa)$, the spectrum function, is the density of contributions to $\overline{n^2}$ on the wave-

number magnitude axis (the overbar denotes average over all realizations), and $\Delta(\boldsymbol{\kappa})$ is the density of contributions to $\overline{n^2}$ in wave-number space. (Strictly these should be contributions to $\overline{(n-n_0)^2}$, since we do not include a δ-function at zero wave-number to take account of the mean value n_0.)

We make some simplifications, of which the first five are taken from Dungey (1956).

(i) Electromagnetic effects are negligible; thus $\mathbf{B}$ is constant, and $\mathbf{E} = -\nabla\phi$.

(ii) The inertia of the charged particles is negligible.

(iii) The effects of collisions with neutral molecules are included as a drag term in each equation of motion: $m_+f_+(\mathbf{u}-\mathbf{u}_+)$ per ion, and $m_-f_-(\mathbf{u}-\mathbf{u}_-)$ per electron. These can be taken as defining $f_\pm$, since if the ordinary collision frequencies were used we should expect a factor of $\frac{1}{2}$ in the expression for the drag on ions. Collisions between electrons and ions are ignored.

(iv) The motion of the neutral gas is incompressible: $\operatorname{div}\mathbf{u} = 0$.

(v) The number densities of electrons and ions are everywhere equal: $n(\mathbf{x}, t)$. (This is a good approximation because in the region of interest $|n_+ - n_-|$ is small compared with the magnitude of fluctuations in n, as can be checked using Dungey's results. But we cannot infer that $\operatorname{div}\mathbf{E} = 0$; $\mathbf{E}$ is determined by the equations of motion, together with the fact that it is derived from a potential.) The mean value of n over the region of interest is called n_0.

(vi) The temperature T is the same for all constituents of the gas, and constant in time and space. Hence the partial pressures of electrons and ions are the same: $p(\mathbf{x}, t)$. The terms in ∇p in the equations represent diffusion of charged particles; the effective diffusivity is $\gamma = 2kT(m_+f_+ + m_-f_-)^{-1}$, which is about twice the kinematic viscosity, in practice.

We take for the gyrofrequencies of electrons and N_2^+ ions the values

$$\Omega_- = 7\times10^6\,\mathrm{sec}^{-1}, \quad \Omega_+ = 140\,\mathrm{sec}^{-1}.$$

The collision frequencies vary greatly with height, and figure 1 shows graphs of the ratios $\lambda_\pm = \Omega_\pm/f_\pm$ against height. In those calculations, collision frequencies for electrons were taken from Nicolet (1959); they were multiplied by $\frac{1}{2}\times4\sqrt{2}\times(m_-/m_+)^{\frac{1}{2}}$ to obtain those for ions, where the factor $\frac{1}{2}$ takes account of our definition in terms of drag. Thus the ratio λ_+/λ_- is constant at 0·00156.

The equations of motion are

$$\left.\begin{aligned} m_+f_+(\mathbf{u}_+-\mathbf{u}) &= -e\nabla\phi + \mathbf{u}_+\wedge e\mathbf{B} - n^{-1}\nabla p,\\ m_-f_-(\mathbf{u}_--\mathbf{u}) &= e\nabla\phi - \mathbf{u}_-\wedge e\mathbf{B} - n^{-1}\nabla p,\\ \text{and}\qquad \frac{\partial n}{\partial t} + \nabla.(n\mathbf{u}_+) &= \frac{\partial n}{\partial t} + \nabla.(n\mathbf{u}_-) = 0,\\ \text{which implies}\qquad \nabla.(n\mathbf{u}_+ - n\mathbf{u}_-) &= 0. \end{aligned}\right\} \tag{1}$$

Now $p = kTn = \frac{1}{2}(m_+f_+ + m_-f_-)\gamma n$, and we obtain some simplification by introducing a function $g(\mathbf{x}, t)$ such that

$$e\phi = \tfrac{1}{2}\gamma(m_+f_+ - m_-f_-)\log(n/n_0) + eBg(\mathbf{x}, t).$$

With **b** as the unit vector in the direction of **B**, the first two equations become

$$n\mathbf{u}_+ - \lambda_+ n\mathbf{u}_+ \wedge \mathbf{b} = n\mathbf{u} - \gamma\nabla n - \lambda_+ n\nabla g,$$

$$n\mathbf{u}_- + \lambda_- n\mathbf{u}_- \wedge \mathbf{b} = n\mathbf{u} - \gamma\nabla n + \lambda_- n\nabla g.$$

These can be solved for the velocities $\mathbf{u}_\pm$, in terms of $\mathbf{u}$, n, g:

$$nu_{i+} = S_{ij+}\left(nu_j - \gamma\frac{\partial n}{\partial x_j} - \lambda_+ n\frac{\partial g}{\partial x_j}\right),$$

$$nu_{i-} = S_{ij-}\left(nu_j - \gamma\frac{\partial n}{\partial x_j} + \lambda_- n\frac{\partial g}{\partial x_j}\right),$$

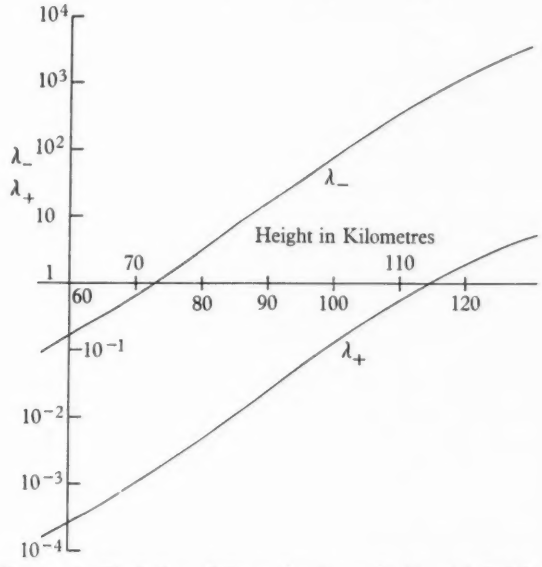

FIGURE 1. Variation of the ratios $\lambda_\pm = \Omega_\pm/f_\pm$ with height.

where

$$S_{ij+} = \frac{1}{1+\lambda_+^2}\begin{pmatrix} 1 & \lambda_+ & 0 \\ -\lambda_+ & 1 & 0 \\ 0 & 0 & 1+\lambda_+^2 \end{pmatrix}, \quad S_{ij-} = \frac{1}{1+\lambda_-^2}\begin{pmatrix} 1 & -\lambda_- & 0 \\ \lambda_- & 1 & 0 \\ 0 & 0 & 1+\lambda_-^2 \end{pmatrix},$$

and the 3-axis is in the direction of **B**.

Substitution into the last of (1) gives an equation for g in terms of n and **u**

$$(\lambda_+ S_{ij+} + \lambda_- S_{ij-})\frac{\partial}{\partial x_i}\left(n\frac{\partial g}{\partial x_j}\right) = (S_{ij+} - S_{ij-})\left(\frac{\partial(nu_j)}{\partial x_i} - \gamma\frac{\partial^2 n}{\partial x_i \partial x_j}\right); \qquad (2)$$

this must be combined with the equation for n obtained from the third of (1)

$$\frac{\partial n}{\partial t} + S_{ij+}\left\{\frac{\partial}{\partial x_i}\left(nu_j - \lambda_+ n\frac{\partial g}{\partial x_j}\right) - \gamma\frac{\partial^2 n}{\partial x_i \partial x_j}\right\} = 0. \qquad (3)$$

3. Small magnetic effect on ions' motion

When $\lambda_+ \ll 1$, which holds below about 110 km (see figure 1), the magnetic effect is small for the ions' motion but not necessarily for the electrons' motion. Irregularities of number density have a motion which is nearly that of the ions, attracted only a little towards that of the electrons. Hence the distortion and rotation suffered by existing irregularities is such as to destroy rapidly any tendency to a preferred orientation. If the mechanism of production itself led to a strong elongation in one direction, this feature would show in the resulting spectrum, but, as mentioned in the introduction, none of the mechanisms (magnetic effects and mixing of a gradient) available on the present model can do this. The spectrum of number density must therefore be nearly isotropic in wave-number space.

Further, only small fractional fluctuations in number density can be produced by the magnetic effects. (More detailed arguments for this are given by Dungey 1956, and in § 4.) And fluctuations produced by the mixing of a gradient must also be small, unless the mean number density changes by an appreciable fraction over the length scale of the large eddies. Observations of radio scattering in the *E* region show that the fluctuations there are small, except in aurorae and in meteor trails, where it is evident that mechanisms other than those considered here are operating. So in the more detailed work on the case $\lambda_+ \ll 1$ we shall suppose that the fractional fluctuations in n are small.

We write

$$\mathbf{u}_+ = \mathbf{u} - \gamma n^{-1} \nabla n + \mathbf{v},$$

where $\mathbf{v}(\mathbf{x}, t)$ is a random velocity field. The energy spectrum function of $\mathbf{v}$ is small compared with that of $\mathbf{u}$, except possibly at large wave-numbers, near the spectral cut-off. The equation for n is

$$\frac{\partial n}{\partial t} + \mathbf{u} \,.\, \nabla n + \nabla \,.\, (n\mathbf{v}) = \gamma \nabla^2 n, \tag{4}$$

and the entire magnetic effect is represented by $\nabla \,.\, (n\,\mathbf{v})$. From equations (2) and (3)

$$\nabla \,.\, (n\,\mathbf{v}) = (S_{ij+} - \delta_{ij}) \left(\frac{\partial (n u_j)}{\partial x_i} - \gamma \frac{\partial^2 n}{\partial x_i \partial x_j} \right) - \lambda_+ S_{ij+} \frac{\partial}{\partial x_i} \left(n \frac{\partial g}{\partial x_j} \right), \tag{5}$$

and g satisfies

$$(\lambda_+ + \lambda_-) \left\{ \frac{1 + \lambda_+ \lambda_-}{(1 + \lambda_+^2)(1 + \lambda_-^2)} \left(\frac{\partial^2 g}{\partial x_1^2} + \frac{\partial^2 g}{\partial x_2^2} \right) + \frac{\partial^2 g}{\partial x_3^2} \right| = (S_{ij+} - S_{ij-}) \frac{1}{n} \left(\frac{\partial (n u_j)}{\partial x_i} - \gamma \frac{\partial^2 n}{\partial x_i \partial x_j} \right)$$
$$- (\lambda_+ S_{ij+} + \lambda_- S_{ij-}) \frac{1}{n} \frac{\partial n}{\partial x_i} \frac{\partial g}{\partial x_j}. \tag{6}$$

In order to calculate g, and hence $\nabla \,.\, (n\mathbf{v})$, we wish to neglect products of gradients of g and gradients of n in equation (6), so as to use the first or second approximation in an iteration process as the solution for g. For a finite region of irregularities, this will be justified if the fluctuations in n are sufficiently small. Reasons have been given for supposing that they are small; we now have to make the hypothesis that they are small enough for the approximation to be valid. But it can at least be said that if the term in g on the right-hand side of (6) were important, it would tend to indicate the presence of strong electric fields, and hence

of large drift velocities. Drift velocities larger than the wind velocities have been observed in the aurorae (Booker 1956), where in any case the approximation breaks down because the fractional fluctuations in n are of order unity, but not elsewhere in the E region. Further comments on this point will be made after the approximate solution has been obtained.

In the two limiting cases, $\lambda_- \ll 1$ and $\lambda_- \gg 1 \gg \lambda_+$, we can use a different approximation procedure, expanding in powers of λ_- and of λ_+/λ_-, respectively. The requirement of small fluctuations in n is no longer necessary, but it is not any easier to see what condition should be imposed. However, in the limiting cases to which they apply, the equations obtained give the same results as those obtained by the more general approximation. Provided there is no significant large-scale drift of irregularities relative to the air, the equations are

$$\left.\begin{aligned} \frac{\partial n}{\partial t} + \mathbf{u}.\nabla n + \lambda_+\lambda_- \frac{\partial (n u_3)}{\partial x_3} = \gamma \nabla^2 n \quad \text{if} \quad \lambda_- \ll 1, \\ \frac{\partial n}{\partial t} + \mathbf{u}.\nabla n + \lambda_+ \left(\frac{\partial (n u_2)}{\partial x_1} - \frac{\partial (n u_1)}{\partial x_2} \right) = \gamma \nabla^2 n \quad \text{if} \quad \lambda_- \gg 1 \gg \lambda_+. \end{aligned}\right\} \tag{7}$$

A large-scale drift could be included by adding the drift velocity to $\mathbf{u}$ in the term $\mathbf{u}.\nabla n$.

For the more general treatment, we write the equations in terms of Fourier transforms (following Dougherty 1960). $N(\boldsymbol{\kappa}, t)$, $\mathbf{U}(\boldsymbol{\kappa}, t)$ and $G(\boldsymbol{\kappa}, t)$ are used for the Fourier transforms of $(n - n_0)$, $\mathbf{u}$, and g. Any large-scale gradient of n can be considered as a low-wave-number component, and so included in $N(\boldsymbol{\kappa}, t)$.

We also write

$$P_{ij} = S_{ij+} - S_{ij-}, \quad Q_{ij} = \lambda_+ S_{ij+} + \lambda_- S_{ij-},$$

$$\delta_{ij} - L_{ij}(\theta) = \frac{(\lambda_- S_{kl-} S_{ij+} + \lambda_+ S_{kl+} S_{ij-}) \kappa_k \kappa_l}{Q_{mn} \kappa_m \kappa_n},$$

$$M_{ij}(\theta) = \frac{\lambda_+ \lambda_- (S_{kl-} S_{ij+} - S_{kl+} S_{ij-}) \kappa_k \kappa_l}{Q_{mn} \kappa_m \kappa_n},$$

where $\kappa_3 = \kappa \cos\theta$. The last two matrices are functions of the angle θ between $\boldsymbol{\kappa}$ and $\mathbf{B}$, but not of the magnitude of $\boldsymbol{\kappa}$. Equation (6) becomes

$$Q_{jk} \kappa_j \kappa_k n_0 G(\boldsymbol{\kappa}) = -P_{jk} \left\{ i n_0 \kappa_j U_k(\boldsymbol{\kappa}) + i \kappa_j \int U_k(\boldsymbol{\kappa}') N(\boldsymbol{\kappa} - \boldsymbol{\kappa}') \, d\boldsymbol{\kappa}' + \gamma \kappa_j \kappa_k N(\boldsymbol{\kappa}) \right\}$$
$$- Q_{jk} \kappa_j \int \kappa'_k G(\boldsymbol{\kappa}') N(\boldsymbol{\kappa} - \boldsymbol{\kappa}') \, d\boldsymbol{\kappa}', \tag{8}$$

where the time-dependence has not been shown explicitly. We approximate as suggested, solving (8) for G by iteration and omitting terms of 2nd and higher degree in N. Substitution into the Fourier transforms of (4) and (5) gives

$$\frac{\partial N(\boldsymbol{\kappa})}{\partial t} + i \kappa_k \int \{ U_k(\boldsymbol{\kappa}') - W_k(\theta, \boldsymbol{\kappa}') \} N(\boldsymbol{\kappa} - \boldsymbol{\kappa}') \, d\boldsymbol{\kappa}' - i \kappa_j L_{jk}(\theta) n_0 U_k(\boldsymbol{\kappa})$$
$$= -\gamma \{ \kappa^2 - L_{jk}(\theta) \kappa_j \kappa_k \} N(\boldsymbol{\kappa}), \tag{9}$$

where $$W_k(\theta, \boldsymbol{\kappa}') = L_{kl}(\theta) U_l(\boldsymbol{\kappa}') + (Q_{ij} \kappa'_i \kappa'_j)^{-1} M_{kl}(\theta) \kappa'_l P_{mn} \kappa'_m U_n(\boldsymbol{\kappa}').$$

The term $L_{jk}(\theta) \kappa_j \kappa_k \gamma N(\boldsymbol{\kappa})$, representing an effect of the magnetic field on diffusion, can be omitted. When $\lambda_+ \ll 1$, $\kappa^{-2} L_{jk} \kappa_j \kappa_k$ is small except for a small range of angles θ, about 90°, in which it may be of order unity. And its average

value over all directions is small, so that we are justified in neglecting it entirely, considering the rapid rotation and distortion of irregularities. (It may be noted that the effect of this term *tends* to elongate irregularities along the magnetic field, but that it cannot achieve this to a significant extent in the presence of turbulence, unless there is a mechanism for producing irregularities on a scale small compared with the smallest eddies. And in the present model there is no such mechanism.)

The term $i\kappa_j L_{jk}(\theta)\, n_0 U_k(\boldsymbol{\kappa})$ represents the production of fluctuations in n. Some production is also represented by the term in W_k, but this can be shown to be relatively small.

The drift velocity $W_k(\theta, \boldsymbol{\kappa}')$ of irregularities relative to the air represents a further interaction, due to the magnetic effects, between Fourier components of velocity and number density. Fuller treatment of these drifts has been carried out by Dougherty (1960), but if we average this velocity over all angles θ, the result is of the order of λ_+ times the magnitude of $U(\boldsymbol{\kappa}')$, and so its direct distorting effect should be unimportant, when $\lambda_+ \ll 1$.

It is possible, however, that the drift velocity associated with large-scale motions could be greater than the air velocity on much smaller scales, and thus there could be an indirect effect due to the motion of irregularities relative to the eddies which are acting on them. The result would be roughly a decrease in the effective time constant of the smaller eddies. The influence that this might have on the spectrum of number density is discussed in the next section. For it to happen, the large-scale velocities must be more than λ_+^{-1} times the velocities characteristic of the smallest eddies.

External electrostatic fields are not included here, although it is known that such fields are present in the E region, generated by winds blowing horizontally across the magnetic field. These winds can be represented as Fourier components with wave-numbers directed vertically and small in magnitude, and it appears that the electrostatic fields are accounted for by equation (9) if we include such components in $\mathbf{U}(\boldsymbol{\kappa}, t)$.

We conclude this section with a comment on the approximation by which the equations were linearized in $N(\boldsymbol{\kappa})$. The principal effect of the magnetic field is the production of fluctuations, and the integral involving W_k is really a second approximation to the leading term $i\kappa_j L_{jk}(\theta)\, n_0 U_k(\boldsymbol{\kappa})$. Since the integral can be shown to be small compared with the leading term, there is thus some confirmation of the validity of the approximation, irrespective of the size of the region.

4. Spectrum of electron density when the magnetic effect is small

Let us now see if the idea of a universal equilibrium, which has been applied to the spectra of turbulent energy and of a convected scalar, can be used to obtain some results about the spectrum of electron density at large wave-numbers, under the conditions assumed in the preceding section. Certainly, if a statistical equilibrium exists for that part of the velocity field with length scales less than a certain value, it should also exist for the same part of the field of number density. But it is not true that the second equilibrium is determined simply by the supply of contributions to $\overline{n^2}$ at small wave-numbers and their destruction at the same rate

by diffusion at large wave-numbers, for the dependence of the term $\nabla.(n\mathbf{v})$ on velocity derivatives means that an important part of the supply occurs in the equilibrium range itself.

At first we shall suppose that there is no significant large-scale drift of irregularities relative to the air, so that the reduction of the eddies' effective time constant, referred to at the end of last section, does not occur. Thus the only effect of the magnetic field is the production of the irregularities. Now we consider the parameters on which the equilibrium depends.

The term in (9) that represents the drift can be neglected (together with the magnetic effect on diffusion), and the equation becomes

$$\frac{\partial N(\boldsymbol{\kappa})}{\partial t}+i\kappa_j\int N(\boldsymbol{\kappa}')\,U_j(\boldsymbol{\kappa}-\boldsymbol{\kappa}')\,d\boldsymbol{\kappa}'-i\kappa_j\,n_0L_{jk}(\theta)\,U_k(\boldsymbol{\kappa})=-\gamma\kappa^2N(\boldsymbol{\kappa}). \tag{10}$$

The parameters ϵ (energy dissipation) and ν (kinematic viscosity) determine the turbulent energy equilibrium; in addition we need the diffusivity, γ, a rate of supply of contributions to $\overline{n^2}$ from the small wave-numbers, χ, and one or more parameters specifying the production in the equilibrium range.

Now two types of irregularity can be distinguished: those due to the mixing of a gradient of ionization density, and those produced in the first place by magnetic effects; it can be seen that these types are not correlated (on the supposition of small fractional fluctuation in n), although they are subject to the same convection and diffusion processes once they are formed. And the convection is practically independent of the magnetic field. Thus the spectrum of number density fluctuations is the sum of two parts, of which one depends on the gradient of mean number density, but not on the magnetic field, and the other depends on the rate of production of contributions to $\overline{n^2}$ by the magnetic effect, but not on the gradient. In the equilibrium range the first part is proportional to χ, and the second part to this rate of production, because of the linearity of equation (10).

If we seek merely the spectrum function $\Gamma(\kappa)$, which gives the density of contributions to $\overline{n^2}$ on the wave-number magnitude axis, then it can be seen from the isotropy of the equilibrium part of the velocity field that only the rate of production of $\overline{n^2}$ per unit interval of wave-number magnitude is needed. And since the $\mathbf{U}(\boldsymbol{\kappa})$ at different wave-numbers are uncorrelated, this rate of production at a given wave-number magnitude should be proportional, in its dependence on the magnetic effect, to the integral of $|n_0\kappa_jL_{jk}(\theta)\,U_k(\boldsymbol{\kappa})|^2$ over all directions, that is to

$$\begin{aligned}
&2\pi n_0^2\int_0^\pi \kappa_j\kappa_l\,\Phi_{km}(\boldsymbol{\kappa})\,L_{jk}(\theta)\,L_{lm}(\theta)\sin\theta\,d\theta\\
&\quad=\tfrac{1}{2}n_0^2\kappa^{-4}E(\kappa)\int_0^\pi \kappa_j\kappa_l(\delta_{km}\kappa^2-\kappa_k\kappa_m)\,L_{jk}L_{lm}\sin\theta\,d\theta\\
&\quad=\tfrac{1}{2}n_0^2E(\kappa)\,\frac{\lambda_+^2\lambda_-^2}{(1+\lambda_+^2)(1+\lambda_-^2)}\\
&\qquad\times\int_0^\pi\sin^3\theta\left[1+\frac{(\lambda_--\lambda_+)^2\sin^4\theta-(1+\lambda_+^2)(1+\lambda_-^2)(1+\lambda_+\lambda_-\cos^2\theta)^2\sin^2\theta}{\{(1+\lambda_+^2)(1+\lambda_-^2)\cos^2\theta+(1+\lambda_+\lambda_-)\sin^2\theta\}^2}\right]d\theta\\
&\quad=E(\kappa)\,n_0^2\eta^2.
\end{aligned} \tag{11}$$

η, which is defined by (11), depends principally on height above ground (figure 2), but also to some extent on latitude and atmospheric conditions. $\Phi_{km}(\boldsymbol{\kappa})$, $E(\kappa)$ are the kinetic energy spectrum tensor and function, respectively, in the usual notation, and the relation between them is a consequence of isotropy (Batchelor 1953, §3.4). The factor of proportionality between the rate of production and (11) depends only on ϵ, κ, ν and γ, and so does the factor $E(\kappa)$. These can therefore be omitted, and we obtain the single additional parameter $(n_0\eta)^2$, which occurs linearly in the expression for Γ.

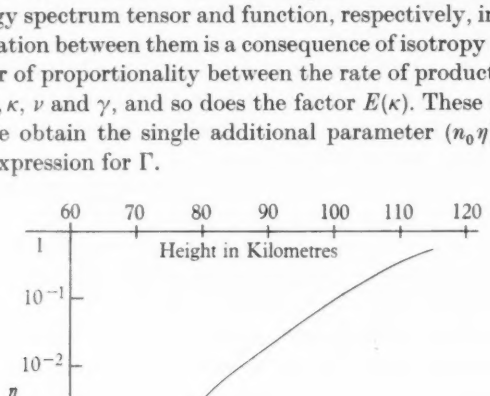

FIGURE 2. Variation of η with height.

Thus, in the equilibrium range,

$$\Gamma(\kappa) = \chi f_1(\kappa, \epsilon, \nu, \gamma) + (n_0\eta)^2 f_2(\kappa, \epsilon, \nu, \gamma),$$

and the first term is the same as the spectrum function of a conserved scalar subject to convection and diffusion.

Precise expressions for f_1 and f_2 can be given if there exists a range of wave-numbers, corresponding to an inertial subrange in the kinetic energy spectrum, in which $\Gamma(\kappa)$ is independent of ν and γ. Dimensional argument then shows that $f_1 \propto \epsilon^{-\frac{1}{3}}\kappa^{-\frac{5}{3}}$, the usual form, and that $f_2 \propto \kappa^{-1}$. Making use of the fact that $\gamma \approx 2\nu$, we have

$$\Gamma(\kappa) = C_1\chi\epsilon^{-\frac{1}{3}}\kappa^{-\frac{5}{3}} + C_2(n_0\eta)^2\kappa^{-1}, \quad \text{in} \quad l^{-1} \ll \kappa \ll \epsilon^{\frac{1}{4}}\nu^{-\frac{3}{4}}, \tag{12}$$

where l is a length-scale of the energy-containing eddies, provided there are values of κ satisfying the two inequalities.

Beyond the cut-off, the spectrum would be expected to fall off in much the same way as the kinetic energy spectrum, owing to the combined effects of viscosity and diffusivity.

The three-dimensional spectrum function $\Delta(\boldsymbol{\kappa})$, which gives the density of contributions to $\overline{n^2}$ in wave-number space, is also a sum of two terms, proportional to χ and $(n_0\eta)^2$, respectively. The first should be isotropic in the equilibrium range, but the second will not be strictly isotropic, its form depending on the variation of L_{jk} with θ. Dimensional argument is of no use, but it is possible to estimate the θ-dependence by a calculation which assumes a simplified

mechanism of transfer, replacing the effect of the smaller eddies by an eddy diffusivity, and that of the larger eddies by a uniform shearing and rotating action. We find that

$$\Delta(\boldsymbol{\kappa}) = (4\pi\kappa^2)^{-1}\{C_1\chi\epsilon^{-\frac{1}{3}}\kappa^{-\frac{8}{3}} + (n_0\eta)^2\kappa^{-1}j(\theta)\},$$

where $j(\theta)$ satisfies a certain integral equation. It has been evaluated in the two limiting cases $\lambda_- \ll 1$ and $\lambda_- \gg 1 \gg \lambda_+$, for the simplified equations (7), and in each case it does not depart from its mean value C_2 by more than 10%. Hence the departure from isotropy is not important, and presumably the same is true when λ_- is of order unity. The same calculation gives a value of 3·1 for C_2.

The quantity χ would be expected to depend principally on the gradient of mean number density. If we assume a gradient $d\bar{n}/dh$, r.m.s. turbulent velocity u ($u^2 = \frac{1}{3}\overline{\mathbf{u}^2}$), and a length scale l for the large eddies, the best estimate of χ is $(d\bar{n}/dh)^2 ul$. But to check the completeness of expression (12) we may add to χ a contribution from the magnetic effect on the large eddies: of order $(n_0\eta)^2 u/l$. Then estimating ϵ as u^3/l, we have

$$\Gamma(\kappa) = B_1(d\bar{n}/dh)^2 l^{\frac{4}{3}}\kappa^{-\frac{8}{3}} + B_2(n_0\eta)^2 l^{-\frac{2}{3}}\kappa^{-\frac{8}{3}} + C_2(n_0\eta)^2\kappa^{-1}, \quad \text{in} \quad l^{-1} \ll \kappa \ll \epsilon^{\frac{1}{4}}\nu^{-\frac{3}{4}},$$

and since κl is large the second term is negligible compared with the third. So χ may be taken to be completely independent of the magnetic effects.

As for the relative importance of the two principal terms, the ratio of the term depending on the gradient to that depending on the magnetic effect is (omitting a factor of order unity)

$$\left(\frac{l}{n_0}\frac{d\bar{n}}{dh}\right)^2 \frac{1}{\eta^2}(l\kappa)^{-\frac{2}{3}}, \quad \text{in} \quad l^{-1} \ll \kappa \ll \epsilon^{\frac{1}{4}}\nu^{-\frac{3}{4}}.$$

The first factor is small, as we have supposed a uniform gradient extending a distance many times l. The last factor is also small, but the second factor is large. The variation of η with height is shown in figure 2. So it seems possible that the part of the spectrum due to the magnetic effect may be dominant at the larger wave-numbers above (say) 90 km.

The total contribution to $\overline{n^2}$ from magnetic effects is approximately $C_2(n_0\eta)^2 \log(l\epsilon^{\frac{1}{4}}\nu^{-\frac{3}{4}})$, and in practice the log factor should not exceed 7. Thus the fractional fluctuation arising from this cause is small below 110 km (where $\lambda_+ \ll 1$).

So far in this section we have ignored the possibility of significant drift velocities of irregularities relative to the air, which would cause the eddies' effective time constant to be decreased. If such drifts exist, the r.m.s. velocity w relative to the air must be included in the parameters determining the statistical equilibrium for irregularities of number density, and the problem cannot be solved by dimensional argument alone, even in the inertial subrange.

It can be argued, however, that if w is large compared with the turbulent velocities associated with larger wave-numbers, then only a single combination of ϵ and w will occur in the expression for the spectrum at these wave-numbers. For the effective time constant is then simply $(w\kappa)^{-1}$. The production of irregularities, the process of eddy diffusivity, and the straining and rotating action of the large eddies, can all be calculated, in a rather idealized way, so that only the products of mean square velocity or vorticity with the effective time constant

are involved. The expressions $\epsilon^{\frac{3}{4}}\kappa^{-\frac{3}{4}}(w\kappa)^{-1}$ and $\epsilon^{\frac{1}{4}}\kappa^{\frac{1}{4}}(w\kappa)^{-1}$, which are obtained below the viscous cut-off, involve ϵ and w only in the combination $(\epsilon^2 w^{-3})$, which is of dimensions LT^{-3}.

Dimensional arguments give

$$\Gamma(\kappa) = C_3\chi\epsilon^{-\frac{3}{4}}w\kappa^{-\frac{4}{3}} + C_4(n_0\eta)^2\kappa^{-1},$$

in any range of wave-numbers where the above argument holds, and where molecular diffusivity is not important. But this is not the same as the inertial subrange, for molecular diffusivity now becomes comparable with eddy diffusivity $(\epsilon^{\frac{3}{4}}w^{-1}\kappa^{-\frac{4}{3}})$ at a wave-number below the viscous cut-off, and the point where w is comparable with the eddy velocities may also occur in the equilibrium range. Further, the calculations mentioned show that the anistropy is increased, with irregularities becoming elongated, not parallel to the magnetic field but at right angles to it.

There appears to be no observational evidence for such anisotropy. Perhaps below 110 km w does not take large enough values to have a serious effect, especially as the Reynolds numbers of turbulence may not be very large. So it is not worth while to study the complexities of the situation any further here. But the same type of anisotropy is predicted in the case which occurs above 120 km. and in § 5 (*b* and *c*) it is described more fully.

5. Large magnetic effect on the ions' motion

When $\lambda_+ \gg 1$, say above 120 km, both electrons and ions are practically stopped from moving across the magnetic lines of force. (We ignore large-scale electric fields, since their only effect on the number density spectrum is the same as that of large-scale winds.) One result is that eddies move relative to the ionization at velocities at least comparable with those of the turbulence, and hence the reduction of effective time-constant, which was mentioned in §§ 3 and 4 as a possibility below 110 km, must occur at these greater heights, and will certainly be important if the Reynolds number of turbulence is reasonably high.

We expect the irregularities to behave as if they were simply convected along lines of force. And since the tendency of the magnetic field to separate electrons and ions is not great, there is no need for strong electric fields to restrain this tendency, and so the motion of irregularities along the lines of force should be close to the component of the air velocity in that direction. This is all confirmed by a calculation using an iteration process as in § 3 (but expanding in inverse powers of λ_+). Here the Fourier transform is not needed, and the leading terms in the equation for n are

$$\frac{\partial n}{\partial t} + \frac{\partial(nu_3)}{\partial x_3} = \gamma\frac{\partial^2 n}{\partial x_3^2}. \tag{13}$$

Because the three processes of production, distortion, and destruction of irregularities are described by this equation, the second-approximation terms should not be significant, unless the gradients of n perpendicular to the magnetic field are λ_+^{-1} times those parallel to it. If such a highly anisotropic distribution should occur, the second approximation terms would tend to limit the degree of

anisotropy; hence it is legitimate to neglect those terms provided that we check afterwards that solutions of (13) are not strongly anisotropic in this way.

As Dungey (1956) stated, the magnetic effect must now give rise to large fluctuations in n, since the divergence of the large-scale part of the ions' velocity, multiplied by the time constant of the corresponding eddies, is of order unity. But this is not so if there is a steady wind, much stronger than the turbulent winds, since the effective time constant is then greatly reduced. In any case, however, the fluctuations produced by mixing of a gradient should always be insignificant.

(*a*) *Growth of irregularities in the absence of diffusion*

We omit the diffusion term, and do not show explicitly dependence on (x_1, x_2). Then $n(x_3, t)$ satisfies

$$\frac{dn}{dt} = \frac{\partial n}{\partial t} + u_3 \frac{\partial n}{\partial x_3} = -n \frac{\partial u_3}{\partial x_3}, \tag{14}$$

and

$$n(x_3, 0) = n_0.$$

The characteristics of this equation are the solutions $x_3(t)$ of

$$\frac{dx_3}{dt} = u_3(x_3, t).$$

Writing $q = \log(n/n_0)$, we find

$$\frac{dq}{dt} = -\frac{\partial u_3}{\partial x_3},$$

and

$$q(x_3, t) = -\int_0^t \frac{\partial u_3}{\partial x_3'}(x_3', t')\, dt',$$

where the integration is along a characteristic.

Now the statistical properties of a variable such as $\partial u_3/\partial x_3'$, on a characteristic through a fixed point (x_3, t), depend on the interval $(t - t')$. In particular, the average value of $\partial u_3/\partial x_3'$ has the same sign as $(t - t')$, and vanishes when $t' = t$. But it can be reasonably claimed that as this interval becomes large the statistical properties tend to a constant form. Thus by the same plausible extension of the Central Limit Theorem as is used in showing that, for example, salt concentration in a turbulent liquid flowing along a pipe acquires a normal distribution, it follows that the value of q at a fixed point (x_3, t) should have a probability distribution which tends to the normal form as t becomes large.

Let us first suppose that the probability distribution is exactly normal. Then

$$p(q, t) = \frac{1}{\sqrt{(2\pi)}\,\sigma(t)} \exp -\frac{1}{2}\left\{\frac{q - \mu(t)}{\sigma(t)}\right\}^2,$$

and the fact that the mean of n is always n_0, so that

$$1 = \int_{-\infty}^{\infty} e^q p(q, t)\, dq,$$

leads to the relation

$$\mu = -\tfrac{1}{2}\sigma^2.$$

We also find that

$$\overline{n^2} = n_0^2 \int_{-\infty}^{\infty} e^{2q} p(q,t)\, dq$$
$$= n_0^2 \exp \sigma^2. \tag{15}$$

Then σ^2 can be calculated as follows, making use of the fact that the averages of $\partial u_3/\partial x_3, \partial(q u_3)/\partial x_3$, evaluated at a fixed point (x_3, t) are zero.

$$\frac{d}{dt}(\tfrac{1}{2}\sigma^2) = -\frac{d\mu}{dt} = -\overline{\frac{\partial q(x_3,t)}{\partial t}}$$
$$= \overline{u_3(x_3,t)\frac{\partial q(x_3,t)}{\partial x_3}} + \overline{\frac{\partial u_3(x_3,t)}{\partial x_3}}$$
$$= -\overline{q(x_3,t)\frac{\partial u_3(x_3,t)}{\partial x_3}}$$
$$= \int_0^t \overline{\frac{\partial u_3}{\partial x_3}(x_3,t)\frac{\partial u_3}{\partial x_3'}(x_3',t')}\, dt',$$

where (x_3', t') lies on the characteristic through (x_3, t). As $t \to \infty$, $d\sigma^2/dt$ approaches a constant value

$$\zeta = 2\int_{-\infty}^{t} \overline{\frac{\partial u_3}{\partial x_3}(x_3,t)\frac{\partial u_3}{\partial x_3'}(x_3',t')}\, dt', \tag{16}$$

and

$$\sigma^2 = \zeta t + O(1), \tag{17}$$

provided the necessary convergence holds. Then, from (15),

$$\frac{d\overline{n^2}}{dt} \sim \zeta \overline{n^2} \quad \text{as} \quad t \to \infty. \tag{18}$$

But the Central Limit Theorem does not ensure sufficiently uniform convergence of $p(q,t)$ to the normal form to justify the use of the normal distribution in evaluating $\overline{n}$ and $\overline{n^2}$ (because of the strong weighting factors e^q and e^{2q} in the integrals). It seems clear that equation (18) must be correct in form, but that the value (16) for ζ will be accurate only in special cases, one of which would be if the values of $\partial u_3/\partial x_3$ on a characteristic had a joint normal probability distribution. In general, the accurate value of ζ must be obtained from the ratio of

$$\frac{d\overline{n^2}}{dt} = -2\overline{n\frac{\partial(n u_3)}{\partial x_3}}$$
$$= -\overline{n^2\frac{\partial u_3}{\partial x_3}}$$
$$= -n_0^2 \overline{\frac{\partial u_3}{\partial x_3}\exp\left[-2\int_0^t \frac{\partial u_3}{\partial x_3'}(x_3',t')\, dt'\right]}$$

to

$$\overline{n^2} = n_0^2 \overline{\exp\left[-2\int_0^t \frac{\partial u_3}{\partial x_3'}(x_3',t')\, dt'\right]}.$$

Consideration of the integral in these expressions as the sum of a number of weakly dependent random variables makes it intuitively clear that the ratio

tends to a finite limit as $t \to \infty$, and that this limit should be practically achieved when t is not much greater than the correlation time of $\partial u_3/\partial x_3$ on the characteristic. Now if at such a value of t the integral is small, then the exponential can be expanded in series, and the first-order approximation to ζ is found to be given by (16). At first sight it may seem that this case could not arise, since the correlation time should be approximately the reciprocal of the r.m.s. value of $\partial u_3/\partial x_3$. But in the problem we are concerned with, the correlation time is considerably shortened because of the convection of eddies relative to the ionization (especially the convection of small eddies by large-scale air motions), so that (16) is a good approximation, and all the results which were obtained for the distribution of q should be reasonably accurate.

Another result, which is more straightforward, involves the integral of n with respect to x_3. Let $Z(x_3, t)$ be the position at $t = 0$ of the characteristic through (x_3, t), so that

$$n = n_0 \frac{\partial Z}{\partial x_3}. \tag{19}$$

Now
$$Z(x_3, t) - x_3 = -\int_0^t u_3(x_3', t')\, dt',$$

and a standard argument shows that, as $t \to \infty$,

$$\begin{aligned} \frac{d}{dt}\overline{(Z - x_3)^2} &\to 2\int_{-\infty}^{t} \overline{u_3(x_3, t)\, u_3(x_3', t')}\, dt \\ &= \rho. \end{aligned} \tag{20}$$

When there is a sufficiently strong uniform wind, we can calculate ζ and ρ as if a static distribution of velocity were convected by a velocity V at right angles to the lines of force. A motion parallel to the lines of force carries the irregularities as well as the eddies with it, and so is not relevant. The results are, for isotropic turbulence,

$$\left.\begin{aligned} \zeta &= \frac{\pi}{8V}\int_0^\infty \kappa E(\kappa)\, d\kappa, \\ \rho &= \frac{\pi}{2V}\int_0^\infty \kappa^{-1} E(\kappa)\, d\kappa, \\ &= \frac{u^2 L_p}{V}, \end{aligned}\right\} \tag{21}$$

where L_p is the longitudinal integral scale, and $u^2 = \frac{1}{3}\overline{\mathbf{u}^2}$.

When the only velocities are those of the turbulence, the effect on the smaller eddies is the same, since the bulk of the kinetic energy is contained in large eddies, except that the convecting velocity takes random values. We average the expressions for ρ and ζ over all such values, assuming a normal distribution of velocity at a point, and find that V is to be replaced by $u\sqrt{(2/\pi)}$. Of course it cannot be expected that an accurate estimate of ρ will be obtained in this case, but the estimate of ζ may still be good, since ζ depends to a greater extent on the smaller eddies.

(b) Spectrum at large wave-numbers for small diffusivity

Next, we consider the behaviour of a fluctuation which is initially a single Fourier component, of wave-number κ_{0i} large compared with the cut-off wave-number of the turbulence, at first in the absence of diffusion. After some time, the fluctuation will be nearly sinusoidal but with a wave-number κ_i which varies slowly in space. The variation of κ_i along a characteristic of equation (14) is given by

$$\left.\begin{aligned} \frac{d\kappa_1}{dt} &= -a(t)\,\kappa_3, \\ \frac{d\kappa_2}{dt} &= -b(t)\,\kappa_3, \\ \frac{d\kappa_3}{dt} &= -c(t)\,\kappa_3, \end{aligned}\right\} \tag{22}$$

where $(a, b, c) = (\partial u_3/\partial x_1, \partial u_3/\partial x_2, \partial u_3/\partial x_3)$, evaluated on the characteristic. Now since n satisfies the same equation as κ_3, the amplitude of the fluctuation is everywhere proportional to κ_3, and $\log(\kappa_3/\kappa_{03})$, has the same probability distribution as has been found for $q = \log(n/n_0)$ in (*a*). The density on the κ_3-axis of contributions to $\overline{n^2}$ from this fluctuation is obtained by weighting this probability distribution with the square of the amplitude, and transforming from a base of q to one of $\kappa_3 = \kappa_{03}\exp q$. It is

$$\begin{aligned} \int_{-\infty}^{\infty}\int_{-\infty}^{\infty} \Delta(\boldsymbol{\kappa})\,d\kappa_1 d\kappa_2 = \Psi(\kappa_3) &\propto \frac{1}{\sqrt{(2\pi)}\,\sigma}\left(\frac{\kappa_3}{\kappa_{03}}\right)^2 \exp\left\{-\frac{(q+\frac{1}{2}\sigma^2)^2}{2\sigma^2}\right\}\frac{dq}{d\kappa_3} \\ &= \frac{1}{\sqrt{(2\pi)}\,\sigma\kappa_{03}}\exp\left\{q-\frac{(q+\frac{1}{2}\sigma^2)^2}{2\sigma^2}\right\}. \end{aligned}$$

Using the result (17), $\sigma^2 = \zeta t + 0(1)$, we find that, at large times, Ψ satisfies the equation

$$\frac{\partial\Psi}{\partial t} = \tfrac{1}{2}\zeta\kappa_3^2\frac{\partial^2\Psi}{\partial\kappa_3^2}, \tag{23}$$

and this will hold in general, whatever the initial form of Ψ.

It does not appear possible to obtain a differential equation for $\Delta(\boldsymbol{\kappa})$ by a continuation of this argument. But the fact that Ψ satisfies this equation of the diffusion type makes it reasonable to seek to generalize it for $\Delta(\boldsymbol{\kappa})$. We can do this by regarding $\boldsymbol{\kappa}$ as a sum of random, weakly dependent terms, each small compared with κ, and without correlation between the 1, 2 and 3 components, by symmetry. Then, making use of (23), we obtain the equation,

$$\frac{\partial\Delta}{\partial t} = \tfrac{1}{2}\zeta_n\kappa_3^2\left(\frac{\partial^2}{\partial\kappa_1^2}+\frac{\partial^2}{\partial\kappa_2^2}\right)\Delta + \tfrac{1}{2}\zeta\kappa_3^2\frac{\partial^2\Delta}{\partial\kappa_3^2}. \tag{24}$$

By analogy with the expression for ζ, ζ_n should be given by

$$\zeta_n = 2\int_{-\infty}^{t}\overline{\frac{\partial u_3}{\partial x_1}(x_1, x_2, x_3, t)\frac{\partial u_3}{\partial x_1}(x_1, x_2, x_3', t')}\,dt'.$$

A small diffusivity will not influence the mechanism of transfer of $\overline{n^2}$ that is involved here, and we can include it by subtracting $2\gamma\kappa_3^2\Delta$ from the right-hand side of (24). The condition for equilibrium is then

$$\left(\frac{\partial^2}{\partial\kappa_1^2}+\frac{\partial^2}{\partial\kappa_2^2}+\frac{\zeta}{\zeta_n}\frac{\partial^2}{\partial\kappa_3^2}-\frac{4\gamma}{\zeta_n}\right)\Delta=0,$$

of which the appropriate solution is

$$\Delta(\boldsymbol{\kappa})\propto\left(\kappa_1^2+\kappa_2^2+\frac{\zeta_n}{\zeta}\kappa_3^2\right)^{-\frac{1}{2}}\exp\left\{-2\left(\frac{\gamma}{\zeta_n}\right)^{\frac{1}{2}}\left(\kappa_1^2+\kappa_2^2+\frac{\zeta_n}{\zeta}\kappa_3^2\right)^{\frac{1}{2}}\right\}.$$

The surfaces of constant Δ are the ellipsoids

$$\kappa_1^2+\kappa_2^2+\frac{\zeta_n}{\zeta}\kappa_3^2=\text{constant},$$

so that no pronounced anisotropy is obtained beyond the viscous cut-off, if the diffusivity is small, because ζ_n will not differ greatly from ζ. This could have been inferred from equations (22), which show that the rates at which contributions to $\overline{n^2}$ spread out in different directions are about the same.

But this depends on the presence of axial symmetry about the magnetic lines of force. If there is a sufficiently strong uniform wind for ζ and ζ_n to be calculated as in (*a*), as if a static velocity distribution is carried past the lines of force, it is not consistent to assume such symmetry. Taking the uniform velocity V along the 2-axis, we find that the derivatives with respect to κ_1 and κ_2 in (24) have different coefficients, ζ_1 and ζ_2, of which $\zeta_1=3\zeta$, while ζ_2 is zero. Thus the spectrum can spread out at right angles to the convecting velocity but not parallel to it. And it follows that irregularities are elongated in some direction at right angles to the magnetic field.

(*c*) *General form of spectrum*

When it comes to the general question of the transfer of $\overline{n^2}$ in $\boldsymbol{\kappa}$-space, the rates of strain are not the only determining factors; the interaction of Fourier components of velocity and number density must be considered. Further, these interactions do not occur in isolation; their effectiveness in transferring $\overline{n^2}$ depends on all the velocity components, and on molecular diffusion. But we have here a rather special case, since, at least for small diffusivity, and for wave-numbers corresponding to the equilibrium range, the smallest time-constant relevant to a given velocity component is in general that determined by the sweeping action of the large-scale motion, rather than by diffusion, or some eddy diffusivity, or an inherent time constant of the turbulence. Hence we may with some reason suppose that the transfer of $\overline{n^2}$ is determined essentially by the two interacting Fourier components, since this time constant depends entirely on one of them.

Further, the action of a single velocity Fourier component $\boldsymbol{\kappa}'$, being convected at a fixed speed, on a number density Fourier component $\boldsymbol{\kappa}$ may be easily calculated. The resulting wave-numbers are $\boldsymbol{\kappa}+m\boldsymbol{\kappa}'$, where $m=\pm1,\pm2$, etc., and an approximate Fourier analysis, valid when the convecting velocity is much larger

than the amplitude of the velocity Fourier component, may be obtained. So we assume a sufficiently strong convecting velocity, in the 2-direction, for this to be valid for all significant Fourier components. To determine the transfer of $\overline{n^2}$, an effective time constant is needed, but this can be obtained if we require that equation (18) shall be satisfied, with the expression (16) for ζ. Calculating in this way, and including the effect of diffusion as before, we find

$$\frac{\partial \Delta(\boldsymbol{\kappa})}{\partial t} = \kappa_3^2 \int \{\Delta(\boldsymbol{\kappa}-\boldsymbol{\lambda}) - \Delta(\boldsymbol{\kappa})\} K(\boldsymbol{\lambda})\, d\boldsymbol{\lambda} + \kappa_3^2 n_0^2 K(\boldsymbol{\kappa}) - 2\gamma\kappa_3^2 \Delta(\boldsymbol{\kappa}), \tag{25}$$

where $K(\boldsymbol{\kappa}) = 2\pi V^{-1}\delta(\kappa_2)\,\Phi_{33}(\boldsymbol{\kappa})$, and the integration is over $\boldsymbol{\lambda}$-space. The δ-function, which actually has a finite width depending on the length scales and the ratio of V to the turbulent velocities, implies that the spectrum is confined close to the plane $\kappa_2 = 0$, so that the irregularities are strongly elongated in the 2-direction. Physically the elongation could be described as a streakiness in the ionization, left behind as the eddies are carried through it.

We can apply some checks to the equation when $\gamma = 0$. If κ is large we obtain equation (24) without the κ_2-derivative, in accordance with the remarks at the end of §5(*b*). The equation was formed in such a way that equation (18) could be obtained from it by integration over all $\boldsymbol{\kappa}$, but we can also divide by κ_3^2 and integrate. Making use of (19) and (21) we find

$$\begin{aligned} n_0^2 \frac{d}{dt}\overline{(Z-x_3)^2} &= \frac{d}{dt}\int \frac{1}{\kappa_3^2}\,\Delta(\boldsymbol{\kappa})\, d\boldsymbol{\kappa} = n_0^2 \int K(\boldsymbol{\kappa})\, d\boldsymbol{\kappa} \\ &= n_0^2 \rho, \end{aligned}$$

in agreement with (20).

We take the Fourier transform of (25) and write $S(\mathbf{r})$, $T(\mathbf{r})$ for the transforms of Δ, K, respectively. $S(\mathbf{r})$ is the correlation function of $(n-n_0)$, and

$$T(\mathbf{r}) = \frac{1}{V}\int_{-\infty}^{\infty} R_{33}(r_1, r_2+y, r_3)\, dy.$$

Then at equilibrium $$S(\mathbf{r}) = \frac{n_0^2 T(\mathbf{r})}{T(0) - T(\mathbf{r}) + 2\gamma}.$$

Now $T(0) = u^2 L_p V^{-1}$ and, in the inertial subrange of the turbulence,

$$T(0) - T(\mathbf{r}) \propto \epsilon^{\frac{2}{3}} V^{-1} (r_1^2 + r_3^2)^{-\frac{1}{6}} (8r_1^2 + 3r_3^2),$$

and, provided γ is not too large,

$$\Delta(\boldsymbol{\kappa}) \propto n_0^2 u^2 L_p \epsilon^{-\frac{2}{3}} \kappa^{-\frac{1}{3}} \delta(\kappa_2)\,(1 - 0{\cdot}097\cos 2\theta + \ldots),$$

where θ is the angle between $\boldsymbol{\kappa}$ and the 3-axis (magnetic field).

When there is no steady wind, the turbulent velocities will produce much the same result, but the effective convecting velocity will take all directions in the plane at right angles to the magnetic field. It may then be reasonable to use the spectrum just obtained, broaden the δ-function to a width of about L_p^{-1}, rotate the whole distribution about the 3-axis, and take the average. We still obtain a strongly anisotropic spectrum, with a rate of decrease of $\kappa^{-\frac{1}{3}}$ along the 3-axis and $\kappa^{-\frac{4}{3}}$ in other directions.

The function $\Gamma(\kappa)$ actually increases in the inertial subrange, like $\kappa^{\frac{3}{3}}$.

Once again, the situation is very complex. It can at least be claimed that the neglect of second-approximation terms in (13) is justified by the conclusion that no marked elongation of irregularities in the direction of the magnetic field occurs. For although the calculations given are rather tentative, they do make it clear that the action of the turbulence, even with the constraint of the magnetic field, does not increase the components κ_3 (parallel to the field) of the wave-numbers of fluctuations much less rapidly than the other components.

6. Conclusion

The point that emerges most strongly is that atmospheric turbulence, in the presence of the earth's magnetic field, cannot account for the sort of anisotropy which is observed experimentally (though it need not prevent its formation). The theory shows that irregularities of electron density which are produced by this means could possibly be strongly elongated in directions at right angles to the field, but never parallel to it, whereas in all observations, when strong anisotropy occurs it takes the form of elongation along the field. So it appears that the circumstances in which the theoretically predicted sort of anisotropy can occur are not often present, and it is necessary to find some other explanation for the anisotropy that is observed—for example, trails of ionization behind charged particles entering the atmosphere along lines of force.

The spectral forms which are given by the theory do not seem to be much help, either, in the interpretation of experimental results. Below 110 km it is predicted that a term proportional to κ^{-1} should be added to the usual term in $\kappa^{-\frac{5}{3}}$, in the 'convection subrange' of the spectrum function $\Gamma(\kappa)$, whereas observations mostly indicate a function with a higher power law, κ^{-2} to κ^{-4}. There is considerable evidence pointing to the presence of turbulence at these heights, and, provided the Reynolds number is high enough, the prediction should be correct over some range of wave-numbers. It may be, of course, that the observations refer to a part of the spectrum about or beyond the cut-off.

Above 120 km the predicted form is of a rather unusual type, which is not altogether surprising in view of the constraints imposed on the particles' motion. It is probable that at these heights turbulence exists only occasionally, and that when it does the Reynolds number is not high, so that this type of spectrum is not of immediate practical interest.

Another matter that remains uncertain is the validity of the approximate solution given in § 3 for the electric field, and the possibility that in some circumstances the correct solution could be much larger. This is especially so in the aurora, where large fractional fluctuations of number density occur, together with strong electric fields. But this would not be likely to lead to an explanation of the elongated irregularities there—the argument against their being produced by turbulence is valid even if the detailed calculation in §§ 3 and 4 is not correct.

I should like to thank Mr John Dougherty for several helpful discussions, and for letting me see his own work on a related subject. A brief preliminary account

of this work is contained in the December 1959 issue of the *Journal of Geophysical Research*, as part of the proceedings of a Symposium on Fluid Mechanics in the Ionosphere held at Cornell University in July 1959. The height above which the magnetic effect is large, there given as 140 km, has been reduced to 120 km here by the use of lower values for the collision frequency of ions.

REFERENCES

Batchelor, G. K. 1953 *The Theory of Homogeneous Turbulence*. Cambridge University Press.

Batchelor, G. K. 1955 *Tech. Rep.* no. 26, School of Electrical Engineering, Cornell University.

Batchelor, G. K. 1959 *J. Fluid Mech.* **5**, 113.

Booker, H. G. 1956 *J. Geophys. Res.* **61**, 675.

Dougherty, J. 1960 *Phil. Mag.* (in the Press).

Dungey, J. W. 1956 *J. Atmos. Terr. Phys.* **8**, 39.

Nicolet, M. 1959 *Phys. Fluids*, **2**, 95.

Villars, F. & Weisskopf, V. F. 1955 *Proc. Inst. Radio Engrs, N.Y.*, **43**, 1232.

Wheelon, A. D. 1957 *Phys. Rev.* **105**, 1706.

Changes in the form of short gravity waves on long waves and tidal currents

By M. S. LONGUET-HIGGINS
National Institute of Oceanography, Surrey

AND R. W. STEWART
University of British Columbia

(Received 2 January 1960)

Short gravity waves, when superposed on much longer waves of the same type, have a tendency to become both shorter and steeper at the crests of the longer waves, and correspondingly longer and lower in the troughs. In the present paper, by taking into account the non-linear interactions between the two wave trains, the changes in wavelength and amplitude of the shorter wave train are rigorously calculated. The results differ in some essentials from previous estimates by Unna. The variation in energy of the short waves is shown to correspond to work done by the longer waves against the *radiation stress* of the short waves, which has previously been overlooked. The concept of the radiation stress is likely to be valuable in other problems.

1. Introduction

It is well known that when gravity waves of fairly short wavelength ride upon the surface of much longer waves such as ocean swell or tidal currents then the wavelength of the short waves is diminished at the crests of the long waves and increased in the troughs. The phenomenon was pointed out by Unna in a series of papers (1941, 1942, 1947). The relative shrinking of the short wavelength L' compared to its mean value L was expressed by Unna (1947) as

$$\frac{L'}{L} = 1 - a_2 k_2 \coth k_2 h \tag{1.1}$$

at the crests of the long waves, where a_2 denotes the amplitude and $2\pi/k_2$ the wavelength of the long waves; h denotes the total mean depth.

Besides this contraction of the wavelength on the long-wave crests, the amplitude of the short waves can be expected to be correspondingly increased. On intuitive grounds Unna (1947) suggested the formula

$$\frac{a'}{a_1} = 1 + a_2 k_2 \coth k_2 h, \tag{1.2}$$

where a_1 is the mean value of a'.

Being unconvinced by Unna's reasoning, we carried out a systematic evaluation of the wave motion by Stokes's method of approximation, as far as the second order. This method allows one to calculate rigorously the change in

wavelength and amplitude arising from non-linear interactions between the two wave trains. The results are given in § 2 of the present paper. Equation (1.1) is verified, but in place of (1.2) we find

$$\frac{a'}{a_1} = 1 + a_2 k_2 (\tfrac{3}{4} \coth k_2 h + \tfrac{1}{4} \tanh k_2 h). \tag{1.3}$$

In deep water (when $k_2 h \to \infty$) both (1.2) and (1.3) tend to the same result

$$\frac{a'}{a_1} = 1 + a_2 k_2. \tag{1.4}$$

An interesting physical interpretation of (1.3) can be given. In § 3 of this paper it is shown that when a train of gravity waves of amplitude a ride upon a steady current U, the transfer of energy across any vertical plane normal to the motion is the sum of four terms

$$Ec_g + EU + S_x U + \tfrac{1}{2}\rho h U'^3, \tag{1.5}$$

where E denotes the mean energy density, c_g denotes the group velocity and U' is a modified stream velocity. S_x is defined below. The first two terms of (1.5) represent simply the bodily transport of energy by the group velocity c_g and by the stream velocity U. The last term in (1.5) represents the transport by the stream U' of its own kinetic energy. All these terms are to be expected. However, the third term $S_x U$ represents the work done by the current U against the *radiation stress* of the waves. S_x is given by

$$S_x = E\left(\frac{2c_g}{c} - \frac{1}{2}\right), \tag{1.6}$$

which for short waves reduces to $\frac{1}{2}E$. The quantity S_x is one component of a two-dimensional *stress tensor* defined in § 3. The presence of this term does not seem to have been pointed out previously.

If the short waves are riding not upon a uniform current but upon much longer waves, then the alternate contraction and expansion at the surface of the longer waves results in work being done against the radiation stress of the short waves. In § 5 it is shown that if this work is assumed to appear as additional energy in the short waves, then there must be a change in the amplitude of the short waves precisely by (1.3) This confirms the conclusions of § 2.

By the same method we are also able to calculate the change in the form of short waves riding on very long waves such as tidal currents. Setting $k_2 h \ll 1$ in equation (1.3) gives

$$\frac{a'}{a} \doteq 1 + \frac{3a_2}{4h}. \tag{1.7}$$

This, however, is valid only when the ratio of the wave frequencies σ_2/σ_1 is still small compared with $k_2 h$. If both σ_2/σ_1 and $k_2 h$ are small but of the same order of magnitude we find, on the crests of the long waves,

$$\frac{a'}{a} = 1 + a_2 k_2 \frac{3k_2 h - 2\sigma_2/\sigma_1}{(2k_2 h - \sigma_2/\sigma_1)^2}. \tag{1.8}$$

This reduces to (1.7) when $\sigma_2/\sigma_1 \ll k_2 h$.

The results of the present paper may be extended without difficulty to systems of waves crossing at an arbitrary angle, and to wavelengths short enough to be influenced by capillarity. In the latter case, however, viscosity probably plays a predominant role.

2. Determination of the wave profile

In this section we shall give a rigorous evaluation of the wave motion by the method of Stokes (1847) as far as the second approximation.

It is well known that in a real fluid the motion does not remain irrotational for long after it is generated from rest, and that a second-order vorticity ultimately penetrates the interior (Longuet-Higgins 1953). However, except in the boundary layers, which are very thin, the vorticity is quasi-steady and produces only second-order currents which, to the second approximation, are simply superposed upon the oscillatory motion. Since we shall be concerned only with the oscillatory part of the motion, it is therefore sufficient to assume the existence of a velocity potential ϕ; any steady second-order currents may be added afterwards.

Infinite depth

Take rectangular axes with the x-axis horizontal in the mean surface and the z-axis vertically upwards. Let $\mathbf{u}$, p, ρ, ζ denote the velocity, pressure, density and surface elevation respectively. Within the fluid we have the following relations

$$\left.\begin{aligned} \mathbf{u} &= \nabla\phi, \\ \nabla^2\phi &= 0, \\ \frac{p}{\rho} + gz + \tfrac{1}{2}\mathbf{u}^2 + \frac{\partial\phi}{\partial t} &= 0, \end{aligned}\right\} \tag{2.1}$$

the second equation being the equation of continuity and the third being Bernoulli's integral with the arbitrary function of t absorbed into ϕ. The boundary conditions are

$$\left.\begin{aligned} \left(\frac{p_0}{\rho} + gz + \tfrac{1}{2}\mathbf{u}^2 + \frac{\partial\phi}{\partial t}\right)_{z=\zeta} &= 0, \\ \left(\frac{\partial\zeta}{\partial t} + \frac{\partial\phi}{\partial x}\frac{\partial\zeta}{\partial x} - \frac{\partial\phi}{\partial z}\right)_{z=\zeta} &= 0, \end{aligned}\right\} \tag{2.2}$$

and

$$\lim_{z\to-\infty} \nabla\phi = 0, \tag{2.3}$$

where p_0 denotes the pressure at the free surface (hereafter assumed to be zero). The surface conditions (2.2) may be replaced by conditions to be satisfied at $z = 0$ by assuming the left-hand sides to be expansible in a power series in z

$$\left.\begin{aligned} g\zeta + \left(\tfrac{1}{2}\mathbf{u}^2 + \frac{\partial\phi}{\partial t}\right)_{z=0} + \zeta\left[\frac{\partial}{\partial z}\left(\tfrac{1}{2}\mathbf{u}^2 + \frac{\partial\phi}{\partial t}\right)\right]_{z=0} + \ldots &= 0, \\ \frac{\partial\zeta}{\partial t} + \left(\frac{\partial\phi}{\partial x}\frac{\partial\zeta}{\partial x} - \frac{\partial\phi}{\partial z}\right)_{z=0} + \zeta\left[\frac{\partial}{\partial z}\left(\frac{\partial\phi}{\partial x}\frac{\partial\zeta}{\partial x} - \frac{\partial\phi}{\partial z}\right)\right]_{z=0} + \ldots &= 0. \end{aligned}\right\} \tag{2.4}$$

Now let us assume expansions of the form

$$\left.\begin{aligned} \mathbf{u} &= \epsilon\mathbf{u}^{(1)}+\epsilon^2\mathbf{u}^{(2)}+\ldots,\\ \phi &= \epsilon\phi^{(1)}+\epsilon^2\phi^{(2)}+\ldots,\\ \zeta &= \epsilon\zeta^{(1)}+\epsilon^2\zeta^{(2)}+\ldots,\\ \frac{p}{\rho}+gz &= \epsilon p^{(1)}+\epsilon^2 p^{(2)}+\ldots, \end{aligned}\right\} \tag{2.5}$$

where ϵ is a small quantity.* On substituting in equations (2.1), (2.3), (2.4), we have

$$\left.\begin{aligned} \mathbf{u}^{(1)} &= \nabla\phi^{(1)},\\ \frac{p^{(1)}}{\rho}+\frac{\partial\phi^{(1)}}{\partial t} &= 0, \end{aligned}\right\} \tag{2.6}$$

$$\left.\begin{aligned} \nabla^2\phi^{(1)} &= 0,\\ \lim_{z\to-\infty}\nabla\phi^{(1)} &= 0, \end{aligned}\right\} \tag{2.7}$$

and

$$\left.\begin{aligned} g\zeta^{(1)}+\left(\frac{\partial\phi^{(1)}}{\partial t}\right)_{z=0} &= 0,\\ \frac{\partial\zeta^{(1)}}{\partial t}-\left(\frac{\partial\phi^{(1)}}{\partial z}\right)_{z=0} &= 0. \end{aligned}\right\} \tag{2.8}$$

Elimination of $\zeta^{(1)}$ from the last two equations gives

$$\left(\frac{\partial^2\phi^{(1)}}{\partial t^2}+g\frac{\partial\phi^{(1)}}{\partial z}\right)_{z=0} = 0. \tag{2.9}$$

Equations (2.7) and (2.9) are equations for $\phi^{(1)}$ alone, while the remaining equations give $\mathbf{u}^{(1)}$, $p^{(1)}$ and $\zeta^{(1)}$ in terms of $\phi^{(1)}$.

As a solution of these equations we select the first-order motion corresponding to two progressive surface waves of wave-numbers k_1 and k_2; that is

$$\phi^{(1)} = A_1 e^{k_1 z}\cos(k_1 x-\sigma_1 t+\theta_1)+A_2 e^{k_2 z}\cos(k_2 x-\sigma_2 t+\theta_2), \tag{2.10}$$

where $A_1, A_2, \sigma_1, \sigma_2, k_1, k_2$ are constants and

$$\sigma_1^2 = gk_1, \quad \sigma_2^2 = gk_2. \tag{2.11}$$

The corresponding free surface is given by

$$\zeta^{(1)} = a_1\sin(k_1 x-\sigma_1 t+\theta_1)+a_2\sin(k_2 x+\sigma_2 t+\theta_2), \tag{2.12}$$

where

$$a_1 = -\frac{A_1 k_1}{\sigma_1}, \quad a_2 = -\frac{A_2 k_2}{\sigma_2}. \tag{2.13}$$

* ϵ is proportional roughly to the surface slope; here, however, ϵ will be used only as an ordering parameter.

Proceeding now to the second approximation, we have to satisfy

$$\left.\begin{aligned} \mathbf{u}^{(2)} &= \nabla\phi^{(2)}, \\ \frac{p^{(2)}}{\rho} + \tfrac{1}{2}\mathbf{u}^{(1)2} + \frac{\partial\phi^{(2)}}{\partial t} &= 0, \\ \nabla^2\phi^{(2)} &= 0, \\ \lim_{z\to-\infty} \nabla\phi^{(2)} &= 0, \\ g\zeta^{(2)} + \left(\tfrac{1}{2}\mathbf{u}^{(1)2} + \frac{\partial\phi^{(2)}}{\partial t} + \zeta^{(1)}\frac{\partial^2\phi^{(1)}}{\partial z\,\partial t}\right)_{z=0} &= 0, \\ \frac{\partial\zeta^{(2)}}{\partial t} + \left(\frac{\partial\phi^{(1)}}{\partial x}\frac{\partial\zeta^{(1)}}{\partial x} - \frac{\partial\phi^{(2)}}{\partial z} + \zeta^{(1)}\frac{\partial^2\phi^{(1)}}{\partial z^2}\right)_{z=0} &= 0. \end{aligned}\right\} \tag{2.14}$$

Elimination of $\zeta^{(2)}$ from the last two equations gives

$$\left(\frac{\partial^2\phi^{(2)}}{\partial t^2} + g\frac{\partial\phi^{(2)}}{\partial z}\right)_{z=0} = -\left[\frac{\partial}{\partial t}(\mathbf{u}^{(1)2}) + \zeta^{(1)}\frac{\partial}{\partial z}\left(\frac{\partial^2\phi^{(1)}}{\partial t^2} + g\frac{\partial\phi^{(1)}}{\partial z}\right)\right]_{z=0}. \tag{2.15}$$

On substituting the special solution (2.10) in the right-hand side, we see that the last group of terms vanishes identically, and we have

$$\begin{aligned} \frac{\partial^2\phi^{(2)}}{\partial t^2} + g\frac{\partial\phi^{(2)}}{\partial z} &= -\frac{\partial}{\partial t}(\mathbf{u}^{(1)2}) \\ &= 2A_1A_2k_1k_2(\sigma_1-\sigma_2)\cos\{(k_1-k_2)x - (\sigma_1-\sigma_2)t + (\theta_1-\theta_2) + \tfrac{1}{2}\pi\}. \end{aligned} \tag{2.16}$$

This and the above equations for $\phi^{(2)}$ are satisfied by

$$\phi^{(2)} = (A_1A_2k_1k_2/\sigma_2)\,e^{(k_1-k_2)z}\cos\{(k_1-k_2)x - (\sigma_1-\sigma_2)t + (\theta_1-\theta_2-\tfrac{1}{2}\pi)\} + Ct, \tag{2.17}$$

where C is an arbitrary constant to be determined by the condition that the origin is in the mean surface level. In fact $\zeta^{(2)}$ may be found from (2.14):

$$g\zeta^{(2)} = -\left(\frac{\partial\phi^{(2)}}{\partial t} + \tfrac{1}{2}\mathbf{u}^{(1)2} + \zeta^{(1)}\frac{\partial^2\phi^{(1)}}{\partial z\,\partial t}\right)_{z=0}. \tag{2.18}$$

On making the substitutions and writing for short

$$k_1x - \sigma_1t + \theta_1 = \psi_1, \quad k_2x - \sigma_2t + \theta_2 = \psi_2, \tag{2.19}$$

we find

$$\zeta^{(2)} = -\tfrac{1}{2}a_1^2k_1\sin 2\psi_1 - \tfrac{1}{2}a_2^2k_2\sin 2\psi_2, \quad -a_1a_2(k_1\cos\psi_1\cos\psi_2 - k_2\sin\psi_1\sin\psi_2). \tag{2.20}$$

Thus if the small parameter ϵ is absorbed into a_1, a_2 by writing $\epsilon = 1$, we have

$$\begin{aligned} \zeta = {} & (a_1\sin\psi_1 - \tfrac{1}{2}a_1^2k_1\sin 2\psi_1) + (a_2\sin\psi_2 - \tfrac{1}{2}a_2^2k_2\sin 2\psi_2) \\ & - a_1a_2(k_1\cos\psi_1\cos\psi_2 - k_2\sin\psi_1\sin\psi_2) + \ldots. \end{aligned} \tag{2.21}$$

It is supposed that one of the waves is short compared with the other, say $k_1 \gg k_2$, and we wish to examine the influence of the second wave upon the first. For this purpose the terms in a_1^2, a_2, a_2^2 are irrelevant, and the remaining terms in (2.21) may be written

$$a_1\sin\psi_1(1 + a_2k_2\sin\psi_2) - a_1\cos\psi_1(a_2k_1\cos\psi_2). \tag{2.22}$$

Now if P, Q are any small quantities (varying slowly compared to ψ_1), the expression

$$\zeta = a_1(1+P)\sin\psi_1 + a_1 Q\cos\psi_1 \tag{2.23}$$

represents a wave of slightly modified amplitude

$$a' = a_1(1+P), \tag{2.24}$$

and of slightly modified wave-number

$$k' = k_1\left(1+\frac{1}{k_1}\frac{\partial Q}{\partial x}\right). \tag{2.25}$$

Writing

$$P = a_2 k_2 \sin\psi_2, \quad Q = -a_2 k_1 \cos\psi_2, \tag{2.26}$$

we see that the amplitude of the small waves is increased by a factor

$$\frac{a'}{a_1} = 1+P = 1+a_2 k_2 \sin\psi_2, \tag{2.27}$$

and the wave-number is increased by the same factor; the wavelength is therefore correspondingly reduced. This factor varies between $(1+a_2k_2)$ on the crests of the long wave and $(1-a_2k_2)$ in the troughs.

Finite depth

We now suppose that the water is of uniform finite depth h and that k_1h, k_2h are not necessarily large. The boundary condition at the bottom ($z=-h$) is that the vertical velocity vanishes

$$\left(\frac{\partial\phi}{\partial z}\right)_{z=-h} = 0, \tag{2.28}$$

and so

$$\left(\frac{\partial\phi^{(1)}}{\partial z}\right)_{z=-h} = \left(\frac{\partial\phi^{(2)}}{\partial z}\right)_{z=-h} = 0. \tag{2.29}$$

In order that the elevation of the free surface may be given by

$$\zeta^{(1)} = a_1\sin\psi_1 + a_2\sin\psi_2 \tag{2.30}$$

in the first approximation, we must have

$$\phi^{(1)} = -\frac{a_1\sigma_1}{k_1\sinh k_1h}\cosh k_1(z+h)\cos\psi_1 - \frac{a_2\sigma_2}{k_2\sinh k_2h}\cosh k_2(z+h)\cos\psi_2, \tag{2.31}$$

where

$$\sigma_1^2 = gk_1\tanh k_1h, \quad \sigma_2^2 = gk_2\tanh k_2h. \tag{2.32}$$

The evaluation of the second approximation now proceeds exactly as before. The algebra is somewhat longer, but may be simplified by omitting all terms except those involving the product a_1a_2 in which alone we are interested. This being understood we have for the surface condition

$$\left(\frac{\partial^2\phi^{(2)}}{\partial t^2}+g\frac{\partial\phi^{(2)}}{\partial z}\right)_{z=0} = A\sin(\psi_1-\psi_2)+B\sin(\psi_1+\psi_2), \tag{2.33}$$

where

$$\left.\begin{aligned} A &= -\tfrac{1}{2}a_1a_2[2\sigma_1\sigma_2(\sigma_1-\sigma_2)(1+\alpha_1\alpha_2)+\sigma_1^3(\alpha_1^2-1)-\sigma_2^3(\alpha_2^2-1)],\\ B &= -\tfrac{1}{2}a_1a_2[2\sigma_1\sigma_2(\sigma_1+\sigma_2)(1-\alpha_1\alpha_2)-\sigma_1^3(\alpha_1^2-1)-\sigma_2^3(\alpha_2^2-1)],\end{aligned}\right\} \tag{2.34}$$

and where we have written

$$\alpha_1 = \coth k_1 h, \quad \alpha_2 = \coth k_2 h \tag{2.35}$$

for brevity. The solution of this equation satisfying Laplace's equation and equation (2.29) is

$$\phi^{(2)} = \frac{A\cosh(k_1-k_2)(z+h)\sin(\psi_1-\psi_2)]}{-(\sigma_1-\sigma_2)^2\cosh(k_1-k_2)h+g(k_1-k_2)\sinh(k_1-k_2)h} + \frac{B\cosh(k_1+k_2)(z+h)\sin(\psi_1+\psi_2)}{-(\sigma_1+\sigma_2)^2\cosh(k_1+k_2)h+g(k_1+k_2)\sinh(k_1+k_2)h}. \tag{2.36}$$

On substituting this expression in (2.18) and using the period equations (2.32), we find

$$g\zeta^{(2)} = \tfrac{1}{2}a_1a_2[C\cos(\psi_1-\psi_2) - D\cos(\psi_1+\psi_2)], \tag{2.37}$$

where

$$C = \frac{[2\sigma_1\sigma_2(\sigma_1-\sigma_2)(1+\alpha_1\alpha_2)+\sigma_1^3(\alpha_1^2-1)-\sigma_2^3(\alpha_2^2-1)](\sigma_1-\sigma_2)(\alpha_1\alpha_2-1)}{\sigma_1^2(\alpha_1^2-1)-2\sigma_1\sigma_2(\alpha_1\alpha_2-1)+\sigma_2^2(\alpha_2^2-1)} + (\sigma_1^2+\sigma_2^2)-\sigma_1\sigma_2(\alpha_1\alpha_2+1), \tag{2.38}$$

and D is given by a similar expression with the signs of α_2, σ_2 reversed. A more convenient form for $\zeta^{(2)}$, equivalent to the above, is

$$\zeta^{(2)} = a_1a_2k_1/\alpha_1[E\cos\psi_1\cos\psi_2 + F\sin\psi_1\sin\psi_2], \tag{2.39}$$

where

$$E = \frac{\alpha_1\alpha_2[(\alpha_1^2-1)^2-\lambda^2(3\alpha_1^2+1)(\alpha_2^2-1)-\lambda^4(3\alpha_2^2+1)(\alpha_1^2-1)+\lambda^6(\alpha_2^2-1)^2] + 2\lambda^3(\alpha_1^2\alpha_2^2-1)(\alpha_1^2+\alpha_2^2)}{[(\alpha_1^2-1)-2\lambda\alpha_1\alpha_2+\lambda^2(\alpha_2^2-1)]^2-4\lambda^2}, \tag{2.40}$$

$$F = \frac{-2\alpha_1\alpha_2[\lambda(\alpha_1^4-1)+\lambda^5(\alpha_2^4-1)]+(\alpha_1^2+\alpha_2^2+2\alpha_1^2\alpha_2^2)[\lambda^2(\alpha_1^2-1)+\lambda^4(\alpha_2^2-1)]}{[(\alpha_1^2-1)-2\lambda\alpha_1\alpha_2+\lambda^2(\alpha_2^2-1)]^2-4\lambda^2}, \tag{2.41}$$

and where we have written

$$\sigma_2/\sigma_1 = \lambda. \tag{2.42}$$

The quantities P, Q of equation (2.23) are now given by

$$\left.\begin{aligned} P &= (a_2k_1/\alpha_1)F\sin\psi_2, \\ Q &= (a_2k_1/\alpha_1)E\cos\psi_2. \end{aligned}\right\} \tag{2.43}$$

The case of deep water is easily retrieved from the above expressions by letting

$$\alpha_1 \to 1, \quad \alpha_2 \to 1 \tag{2.44}$$

(in that order, since $\sigma_1 > \sigma_2$). We then find

$$E \to -1, \quad F \to \lambda^2 = k_2/k_1, \tag{2.45}$$

and the equations (2.43) for P and Q reduce to (2.26).

Let us now suppose that the shorter waves are effectively in deep water (e^{-k_1h} is negligible) but that the depth h is not necessarily great compared with

the wavelength of the long waves. Under these conditions α_1 tends to 1 and $\lambda^2(\alpha_2^2-1)$ becomes a factor in both numerator and denominator of E and F. Hence

$$\left.\begin{aligned} E &= \frac{-2\alpha_2(2-\lambda\alpha_2)+2\lambda-\lambda^4\alpha_2(\alpha_2^2-1)}{(2-\lambda\alpha_2)^2-\lambda^2}, \\ F &= \frac{-2\alpha_2\lambda^3(1+\alpha_2^2)+\lambda^2(1+3\alpha_2^2)}{(2-\lambda\alpha_2)^2-\lambda^2}. \end{aligned}\right\} \tag{2.46}$$

Of particular interest to us is the case when λ is very small. Then

$$E = -\alpha_2, \quad F = \lambda^2\frac{1+3\alpha_2^2}{4}, \tag{2.47}$$

and so

$$\left.\begin{aligned} P &= a_2k_2\frac{1+3\alpha_2^2}{4\alpha_2}\sin\psi_2, \\ Q &= -a_2k_2\alpha_2\cos\psi_2. \end{aligned}\right\} \tag{2.48}$$

Hence the wave amplitude is increased by a factor

$$\frac{a'}{a_1} = 1+a_2k_2(\tfrac{1}{4}\tanh k_2h+\tfrac{3}{4}\coth k_2h)\sin\psi_2 \tag{2.49}$$

and the wave-number is increased by a factor

$$\frac{k'}{k_1} = 1+a_2k_2\coth k_2h\sin\psi_2. \tag{2.50}$$

This is always assuming that k_2h is not very small also.

The case when the longer waves are effectively in shallow water, that is

$$\tanh k_2h = \frac{1}{\alpha_1} \equiv \mu \ll 1 \tag{2.51}$$

may also be studied. Such a situation may occur, for example, with waves riding on a tidal current. But the small quantities λ, μ may be of the same order of magnitude. In a typical situation we might have waves of period $T_1 = 10$ seconds riding on a tidal stream of period $T_2 = 12{\cdot}4$ hours, in 50 fathoms of water. Then

$$\lambda = \frac{\sigma_2}{\sigma_1} = \frac{T_1}{T_2} = 2{\cdot}2\times10^{-4} \tag{2.52}$$

and

$$\mu \doteqdot k_2h = \frac{2\pi h}{T_2\sqrt{(gh)}} = 4{\cdot}4\times10^{-4}. \tag{2.53}$$

Retaining the terms of lowest order in both λ and μ, we find from (2.46)

$$\left.\begin{aligned} E &= -\frac{2}{2\mu-\lambda}+\frac{\lambda^4}{\mu(2\mu-\lambda)^2}, \\ F &= \frac{\lambda^2(3\mu-2\lambda)}{\mu(2\mu-\lambda)^2}, \end{aligned}\right\} \tag{2.54}$$

and so from (2.43)

$$\left.\begin{aligned} P &= a_2k_2\frac{3\mu-2\lambda}{(2\mu-\lambda)^2}\sin\psi_2, \\ Q &= -a_2k_1\left\{\frac{2}{2\mu-\lambda}-\frac{\lambda^4}{\mu(2\mu-\lambda)^2}\right\}\cos\psi_2. \end{aligned}\right\} \tag{2.55}$$

The changes in wave amplitude and wave-number are therefore given by

$$\frac{a'}{a_1} = 1 + a_2 k_2 \frac{3\mu - 2\lambda}{(2\mu - \lambda)^2} \sin \psi_2, \tag{2.56}$$

and

$$\frac{k'}{k_1} = 1 + a_2 k_2 \left(\frac{2}{2\mu - \lambda} - \frac{\lambda^4}{\mu (2\mu - \lambda)^2} \right) \sin \psi_2. \tag{2.57}$$

When λ/μ is small these equations reduce to

$$\frac{a'}{a_1} = 1 + \frac{3a_2}{4h} \sin \psi_2, \tag{2.58}$$

and

$$\frac{k'}{k} = 1 + \frac{a_2}{h} \sin \psi_2, \tag{2.59}$$

respectively.

The above results for shallow water may also be deduced directly starting from a velocity potential

$$\phi^{(1)} = -\frac{a_1 \sigma_1}{k_1} e^{k_1 z} \cos \psi_1 - \frac{a_2 \sigma_2}{k_2^2 h} [1 + \tfrac{1}{2} k_2^2 (z + h)^2] \cos \psi_2. \tag{2.60}$$

The only other special cases of interest are when the longer waves are shallow-water waves and the shorter waves are either shallow-water or deep-water waves. However, the results are all contained in equation (2.41), and the appropriate simplifications may be left to the reader.

Standing waves

So far we have considered only waves of progressive type riding on longer waves, also of progressive type, travelling in the same direction.

It is evident, however, that when λ is very small ($\lambda \ll \mu$) the expressions for the shortening or the steepening of the waves are unaffected if λ is reversed in sign, that is if the direction of one of the waves is reversed. Hence the shortening and steepening of the waves are the same whether the second system of waves is travelling in the same or opposite direction to the first.

Further, the interaction terms, on which these effects depend, are evidently linear in the two wave amplitudes a_1, a_2 separately. It follows that, if two of the longer waves are superposed to give a standing wave, and if the short progressive waves ride on top of these, the relative shortening and steepening will be similar. More precisely if

$$\begin{aligned} \zeta^{(1)} &= a_1 \sin (k_1 x - \sigma_1 t + \theta_1) + a_2 \sin (k_2 x - \sigma_2 t + \theta_2) + a_2 \sin (k_2 x + \sigma_2 t + \theta_2) \\ &= a_1 \sin (k_1 x - \sigma_1 t + \theta_1) + 2a_2 \sin k_2 x \cos (\sigma_2 t + \theta_2), \end{aligned} \tag{2.61}$$

then on the crests of the longer waves the amplitude of the shorter waves is found to increase by a factor

$$1 + a_2 k_2 (\tfrac{1}{2} \tanh k_2 h + \tfrac{3}{2} \coth kh), \tag{2.62}$$

and the wavelength is diminished by a factor

$$1 + 2a_2 k_2 \coth k_2 h. \tag{2.63}$$

If a_2 is written for $2a_2$ these formulae are similar to (2.49) and (2.50).

Similarly, if two *short* waves are added to produce a short standing wave, then by the linearity of the interaction terms it follows that the changes in amplitude and wavelength of the combined wave are given by identical expressions, both when the longer waves are progressive and when they are standing waves.

On the other hand, in shallow water when λ is not much less than μ, the change of form of short progressive waves depends upon their direction relative to the longer waves. Hence different formulae for standing waves result, which may be deduced without difficulty from equations (2.56) and (2.57).

3. The radiation stresses

In order to interpret physically the conclusions of § 2, we first consider from a general point of view the transfer of energy by surface waves on a steady, uniform current.

In a non-viscous fluid, the rate of transfer of energy across a surface fixed in space is given by

$$R = \iint_S (p + \tfrac{1}{2}\rho\mathbf{u}^2 + \rho g z)\,\mathbf{u}.\mathbf{n}\,dS, \tag{3.1}$$

where $\mathbf{n}$ denotes the unit normal to the surface, and z is measured vertically upwards. Hence the mean rate of transfer across a vertical plane $x = \text{const.}$, per unit distance in the y-direction, is

$$R_x = \overline{\int_{-h}^{\zeta} (p + \tfrac{1}{2}\rho\mathbf{u}^2 + \rho g z)\,u\,dz}, \tag{3.2}$$

where $z = \zeta(t)$ denotes the free surface, and the mean value with respect to time, indicated by a bar, is taken *after* performing the integration. We now express the velocity as the sum of two parts

$$\mathbf{u} = \mathbf{U} + \mathbf{u}', \tag{3.3}$$

where $\mathbf{U} = (U, 0, 0)$ denotes the mean stream velocity and $\mathbf{u}'$ is the additional velocity due to the wave motion. It may be assumed that the mean value of $\mathbf{u}'$ at any point in the *interior* is zero

$$\overline{\mathbf{u}'} = 0 \tag{3.4}$$

and further that U is independent of z.* On substituting (3.3) into (3.2) and taking mean values, we have identically

$$R_x = R_0 + R_1 + R_2 + R_3, \tag{3.5}$$

where

$$\left.\begin{aligned} R_0 &= \overline{\int_{-h}^{\zeta} (p + \tfrac{1}{2}\rho\mathbf{u}'^2 + \rho g z)\,u'\,dz}, \\ R_1 &= \overline{\int_{-h}^{\zeta} (p + \tfrac{1}{2}\rho\mathbf{u}'^2 + \rho g z + \rho u'^2)\,dz}\ U, \\ R_2 &= \overline{\int_{-h}^{\zeta} \tfrac{3}{2}\rho u'\,dz}\ U^2, \\ R_3 &= \overline{\int_{-h}^{\zeta} \tfrac{1}{2}\rho\,dz}\ U^3. \end{aligned}\right\} \tag{3.6}$$

* These assumptions taken together are valid only for irrotational flow; vorticity may be taken into account by supposing U to depend upon z.

Let us consider these terms separately. The first term R_0 is simply equal to the energy transfer by the waves in the absence of a steady stream. Adapting the notation of § 2, we have

$$\left.\begin{aligned}\zeta &= a\cos(kx-\sigma t+\theta)+O(a^2k),\\ \phi &= \frac{a\sigma}{k\sinh kh}\cosh k(z+h)\sin(kx-\sigma t+\theta)+O(a^2\sigma),\end{aligned}\right\} \tag{3.7}$$

where
$$\sigma^2 = gk\tanh kh, \quad \sigma/k = c. \tag{3.8}$$

Hence it is easily found that, to second order,

$$R_0 = \tfrac{1}{4}\rho g a^2 c\left(1+\frac{2kh}{\sinh 2kh}\right) = Ec_g, \tag{3.9}$$

where
$$E = \tfrac{1}{2}\rho g a^2 \tag{3.10}$$

denotes the mean energy density per unit horizontal area and

$$c_g = \frac{d\sigma}{dk} = \tfrac{1}{2}c\left(1+\frac{2kh}{\sinh 2kh}\right) \tag{3.11}$$

denotes the group velocity (cf. Lamb 1932, § 237).

The second term in (3.6) may be separated into two parts

$$R_1 = R_{11}+R_{12}, \tag{3.12}$$

where
$$\left.\begin{aligned}R_{11} &= \overline{\int_{-h}^{\zeta}(\tfrac{1}{2}\rho\mathbf{u}'^2+\rho gz)\,dz}\;\; U+\tfrac{1}{2}\rho gh^2U = EU,\\ R_{12} &= \overline{\int_{-h}^{\zeta}(p+\rho u'^2)\,dz}\;\; U-\tfrac{1}{2}\rho gh^2U = S_xU.\end{aligned}\right\} \tag{3.13}$$

The term R_{11} is self-explanatory; it is the bodily transport of kinetic and gravitational energy by the mean velocity U. The term R_{12} is more interesting and its presence does not seem to have been previously noticed. It represents the work done by the mean velocity U against the *radiation stress* defined by

$$S_x = \overline{\int_{-h}^{\zeta}(p+\rho u'^2)\,dz}-\tfrac{1}{2}\rho gh^2. \tag{3.14}$$

To interpret this expression we divide it again into two parts: first take the integral with respect to z up to a fixed point, say the mean level $z = 0$. (If $\zeta < 0$ then p and $\mathbf{u}$ may be extended analytically.) Thus we have

$$T_x = \int_{-h}^{0}\overline{(p+\rho u'^2)\,dz}-\tfrac{1}{2}\rho gh^2, \tag{3.15}$$

say. In this expression the quantity $\rho\overline{u'^2}$ represents the well-known Reynolds stress, which arises because the excess velocity u' transfers horizontal momentum $\rho u'$ at a rate $\rho u'^2$; even when u' is negative the contribution to the Reynolds stress is positive.

To obtain S_x we have only to add to T_x the quantity

$$Z_x = \overline{\int_0^{\zeta}(p+\rho u'^2)\,dz} \tag{3.16}$$

(the integral being interpreted in the usual way when $\zeta < 0$). In this expression the term $\rho u'^2$ contributes only a small quantity of the third order. The remaining term p gives a positive contribution to Z_x since when ζ is positive (the surface is above the mean level) so also is the pressure, and when ζ is negative so also is p; in fact near the mean level p is given almost by the hydrostatic pressure term $\rho g(\zeta - z)$; hence

$$Z_x \doteq \overline{\int_0^\zeta \rho g(\zeta - z)\, dz} = \tfrac{1}{2}\rho g \overline{\zeta^2}. \tag{3.17}$$

It will be seen that this term arises essentially from the deformation of the free surface.

On the other hand, to evaluate T_x we must express $\overline{p}$ to the second order in the wave amplitude a: assuming $\overline{\zeta} = 0$, we find

$$\overline{p} = -\rho g z - \frac{\rho g a^2 k}{\sinh 2kh} \cosh^2 k(z+h). \tag{3.18}$$

It will be seen that the second term on the right is negative, so that the mean pressure at a point is actually reduced by the presence of the waves. On substituting in (3.15) and (3.17) we have, to order a^2,

$$\left.\begin{aligned} T_x &= \tfrac{1}{2}\rho g a^2 \frac{2kh}{\sinh 2kh}, \\ Z_x &= \tfrac{1}{4}\rho g a^2. \end{aligned}\right\} \tag{3.19}$$

Combining these, we have

$$S_x = \tfrac{1}{2}\rho g a^2 \left(\frac{2kh}{\sinh 2kh} + \frac{1}{2}\right) = E\left(\frac{2c_g}{c} - \frac{1}{2}\right). \tag{3.20}$$

Thus S_x is an additional stress, due to the wave motion, per unit length across a plane normal to the direction of wave propagation. It is composed of the integrated Reynolds stress, plus the stress due to the correlation between surface elevation and pressure, less the effect of the reduction in the average pressure in the body of the fluid due to the presence of the waves. Altogether

$$R_1 = (E + S_x)\, U = E\left(\frac{2c_g}{c} + \frac{1}{2}\right) U. \tag{3.21}$$

The last two terms in (3.6) are easily evaluated. Since $\overline{u'}$ vanishes everywhere in the interior of the fluid, and $\overline{\zeta} = 0$, we have

$$R_2 = \tfrac{3}{2} E U^2/c, \quad R_3 = \tfrac{1}{2}\rho h U^3. \tag{3.22}$$

But since the motion is irrotational there is, owing to the mass-transport velocity, a net momentum E/c in the direction of wave propagation (Stokes 1847), that is, a mean velocity $E/c\rho h$. Writing

$$U + E/c\rho h = U' \tag{3.23}$$

and substituting in (3.22) we have, to the present order of approximation,

$$R_2 + R_3 = \tfrac{1}{2}\rho h U'^3 \tag{3.24}$$

which represents the transport of the kinetic energy of the current by itself.

Collecting together the various terms, we find

$$R_x = Ec_g + EU + S_x U + \tfrac{1}{2}\rho h U'^3, \tag{3.25}$$

where S_x and U' are given by (3.20) and (3.23).

In an exactly similar way we may calculate the flow of energy in the y-direction in the presence of a steady transverse current $\mathbf{U} = (0, V, 0)$. This is given by the integral

$$R_y = \overline{\int_{-h}^{\zeta} (p + \tfrac{1}{2}\rho \mathbf{u}'^2 + \rho g z + V^2)\, V\, dz}, \tag{3.26}$$

which is easily found to be

$$R_y = EV + S_y V + \tfrac{1}{2}\rho h V^3, \tag{3.27}$$

where

$$S_y = \tfrac{1}{4}\rho g a^2 \frac{2kh}{\sinh 2kh} = E\left(\frac{c_g}{c} - \frac{1}{2}\right). \tag{3.28}$$

In the general case of a mean stream velocity $\mathbf{U} = (U, V, 0)$ the transfer of energy across a vertical plane in direction $\mathbf{n} = (l, m, 0)$ is

$$\bar{R} = \overline{\int_{-h}^{\zeta} (p + \tfrac{1}{2}\rho \mathbf{u}'^2 + \rho g z + \rho \mathbf{u}' . \mathbf{U} + \tfrac{1}{2}\rho \mathbf{U}^2)\, (\mathbf{u}' + \mathbf{U}) . \mathbf{n}\, dz}, \tag{3.29}$$

which by exactly similar analysis is found to be

$$\bar{R} = E\mathbf{c}_g . \mathbf{n} + E\mathbf{U} . \mathbf{n} + \mathbf{U} . \mathbf{S} . \mathbf{n} + \tfrac{1}{2}\rho h \mathbf{U}'^2 (\mathbf{U}' . \mathbf{n}), \tag{3.30}$$

where

$$\mathbf{c}_g = (c_g, 0, 0) \tag{3.31}$$

denotes the vector group velocity,

$$\mathbf{U}' = (U + E/\rho c h, V, 0) \tag{3.32}$$

denotes the modified stream velocity, and where $\mathbf{S}$ denotes the tensor

$$\mathbf{S} = \begin{pmatrix} S_x & 0 \\ 0 & S_y \end{pmatrix}. \tag{3.33}$$

$\mathbf{S}$ may be called the *stress tensor* of the wave motion. In full it is

$$\mathbf{S} = \begin{pmatrix} E\left(\dfrac{2c_g}{c} - \dfrac{1}{2}\right) & 0 \\ 0 & E\left(\dfrac{c_g}{c} - \dfrac{1}{2}\right) \end{pmatrix}. \tag{3.34}$$

In very deep water ($c_g = \frac{1}{2}c$) it becomes

$$\mathbf{S} = \begin{pmatrix} \frac{1}{2}E & 0 \\ 0 & 0 \end{pmatrix}, \tag{3.35}$$

and in shallow water ($c_g = c$) it becomes

$$\mathbf{S} = \begin{pmatrix} \frac{3}{2}E & 0 \\ 0 & \frac{1}{2}E \end{pmatrix}. \tag{3.36}$$

It is interesting to note that there is also a transport of energy corresponding to a vertical component of velocity W across the horizontal plane $z =$ constant. In fact the mean energy transport per unit horizontal area is

$$\overline{(p + \tfrac{1}{2}\rho \mathbf{u}'^2 + \rho g z + \rho w' W + \tfrac{1}{2}\rho W^2)\, (w' + W)}. \tag{3.37}$$

The terms independent of W together vanish identically (there is no upwards transport of energy in an ordinary surface wave). The terms proportional to W are

$$(p+\tfrac{1}{2}\rho\mathbf{u}'^2+\rho gz+\rho w'^2)\,W=\frac{\rho ga^2k}{2\sinh 2kh}\cosh 2k(z+h)\,W. \tag{3.38}$$

In deep water ($kh \gg 1$) this becomes

$$\tfrac{1}{2}W\rho ga^2k\,e^{-2kz}, \tag{3.39}$$

which is negligible below about half a wavelength.

4. The relation between wave amplitude and energy in an accelerated wave

In the preceding section we have calculated the transfer of energy horizontally when surface waves are superposed upon a steady, uniform current. We propose in the following to investigate the case when the surface waves ride not upon a steady current but upon a much longer wave, as in § 2, that is to say in place of the steady current U of § 3 we have instead the orbital velocity of the long waves. (This latter velocity is however supposed small compared with the phase velocity of the short waves.)

If the wavelength of the longer waves is sufficiently great compared with that of the shorter waves, then it is permissible to regard the orbital velocity U as being approximately constant and uniform over a period and wavelength, respectively, of the shorter waves. To a certain extent therefore we may make use of the formulae of § 3. However, a significant factor is introduced by the presence of a vertical acceleration in the longer waves; this alters the relation between the amplitude and the energy of the short waves, as will now be shown.

We shall consider from a general point of view the relation between the potential and the kinetic energy of a system undergoing vertical movements.

The discussion of energy relations in frames of reference not moving with constant acceleration leads generally to complications. Therefore we shall agree from the start to refer all energies to a stationary frame of reference.

In the stationary frame of reference, a progressive wave train of amplitude a' will have a gravitational potential energy

$$\text{P.E.} = \tfrac{1}{4}\rho ga'^2 \tag{4.1}$$

per unit horizontal distance (apart from terms independent of the wave amplitude a' and terms of higher order than the second).

Consider on the other hand the kinetic energy, measured in the same frame of reference. A very general theorem in dynamics states that the kinetic energy of a system of particles of mass m_i and velocity $\mathbf{v}_i$ is given by

$$\text{K.E.} = \tfrac{1}{2}M\mathbf{V}^2+\sum_i \tfrac{1}{2}m_i(\mathbf{v}_i-\mathbf{V})^2, \tag{4.2}$$

where M is the total mass and $\mathbf{V}$ the velocity of the centre of mass. Now the vertical co-ordinate Z of the centre of mass of a wave train differs from the vertical co-ordinate Z_S of the mean free surface by an amount

$$Z-Z_S = \tfrac{1}{4}\rho a'^2/M \quad + \text{constant} \tag{4.3}$$

(neglecting terms of higher order). Hence the vertical velocity of the centre of mass differs from that of the free surface by an amount

$$\mathbf{V}-\mathbf{V}_S=\left[0,0,\frac{\partial}{\partial t}(\tfrac{1}{4}\rho a'^2/M)\right]. \tag{4.4}$$

The first term on the right of (4.2) can therefore be written

$$\tfrac{1}{2}M\mathbf{V}_S^2+W_S\frac{\partial}{\partial t}(\tfrac{1}{4}\rho a'^2). \tag{4.5}$$

The last term in (4.2) represents simply the kinetic energy calculated with reference to a frame moving (nearly) with the free surface and is therefore given by

$$\tfrac{1}{4}\rho a'^2\sigma'^2/k', \tag{4.6}$$

where $2\pi/\sigma'$ and $2\pi/k'$ are the period and wavelength of the waves in the moving frame. But since this frame is accelerated these are related by the equations

$$\sigma'^2=g'k', \tag{4.7}$$

where g' is the apparent value* of gravity

$$g'=g+\frac{\partial W_S}{\partial t}. \tag{4.8}$$

Altogether then we have

$$\text{K.E.}=\tfrac{1}{2}M\mathbf{V}_S^2+\tfrac{1}{4}\rho g a'^2+\frac{\partial}{\partial t}(\tfrac{1}{4}\rho a'^2W_S). \tag{4.9}$$

The total wave energy E' may be defined as those parts of the kinetic-plus-potential energy which depend on the wave amplitude only, i.e.

$$E'=\tfrac{1}{2}\rho g a'^2+\frac{\partial}{\partial t}(\tfrac{1}{4}\rho a'^2W_S). \tag{4.10}$$

When $\partial a'^2/\partial t$ and W_S are both small quantities this expression becomes

$$E'=\tfrac{1}{2}\rho g a'^2\left(1+\frac{1}{2g}\frac{\partial W_S}{\partial t}\right). \tag{4.11}$$

5. A physical interpretation of the results of §2

In the situation described in §2 we may regard the shorter waves as being superposed upon the longer waves, whose orbital velocity near the free surface has the components

$$\left.\begin{aligned}U&=a_2\sigma_2\coth k_2h\,\sin\psi_2,\\ W&=-a_2\sigma_2\cos\psi_2.\end{aligned}\right\} \tag{5.1}$$

Consider first the changes in wavelength of the shorter waves. We make the physical assumption that *the wavelength of the short waves expands in proportion to the stretching of the surface by the long waves.*

* It is assumed that $(1/g')\,\partial g'/\partial t$ is small compared with σ'.

Now two particles in the surface which initially are separated by a distance dx have a small relative velocity $(\partial U/\partial x)\,dx$. The separation of these particles after time t is therefore given by

$$dx+\int_0^t \frac{\partial U}{\partial x}\,dx\,dt = dx\left[1+\int_0^t \frac{\partial U}{\partial x}\,dt\right], \tag{5.2}$$

where to a first approximation $\partial U/\partial x$ may be evaluated at the original position x. The relative stretching of the surface is therefore given by

$$1+\int_0^t \frac{\partial U}{\partial x}\,dt = 1-a_2k_2\coth k_2h\,\sin\psi_2. \tag{5.3}$$

The relative increase in wave-number of the short waves is the reciprocal of this expression, or

$$1+a_2k_2\coth k_2h\,\sin\psi_2, \tag{5.4}$$

in agreement with (2.50).

Now to account for the change in the wave amplitude we shall make the following assumptions.

(*a*) *The energy density of the short waves is given by* (4.11) (despite the distortion caused by stretching of the surface).

(*b*) *The rate of transfer of short-wave energy is given by*

$$E'(c_g+U)+S_xU \tag{5.5}$$

as in § 3.

(*c*) *The short-wave energy is conserved* (and in particular that work done against the radiation stress appears as short-wave energy).

With these assumptions the equation for the budget of short-wave energy becomes

$$\frac{\partial E'}{\partial t} = -\frac{\partial}{\partial x}[E'(c_g+U)+S_xU]. \tag{5.6}$$

To the order of approximation with which we are concerned we may take on the right-hand side of (5.6)

$$E' = \text{const.} = \tfrac{1}{2}\rho g a_1^2 = E_1, \tag{5.7}$$

and similarly $S_x = \text{const.}$, so that (5.6) reduces to

$$\frac{\partial E'}{\partial t} = -E_1\frac{\partial}{\partial x}(c_g+U)-S_x\frac{\partial U}{\partial x}. \tag{5.8}$$

The physical interpretation of this last equation is that the rate of change of the short-wave content between x and $x+dx$ is determined by the divergence of the energy transport due to the group velocity c_g and the ambient flow U, plus the rate at which the convergence of the ambient flow, $(\partial U/\partial x)$, does work against the radiation stress S_x. Our assumption is that in this case the work done against the radiation stress appears as additional wave energy (although it is not possible to assert that such would be the case in other circumstances).

The term $S_x\partial U/\partial x$ appearing in (5.8) is closely analogous to the term $\overline{u_iu_j}\partial U_1/\partial x_j$ which appears in the equations for turbulent energy and the term $p\nabla.\mathbf{V}$ which occurs in the energy expression for turbulent flows.

Now, on relacing S_x by (3.19) and E by E_1, we have

$$\frac{\partial E'}{\partial t} = -E_1 \frac{\partial}{\partial x}\left[(c_g + U) + \left(\frac{2c_g}{c_1} - \frac{1}{2}\right) U\right], \tag{5.9}$$

or, since $\partial c_g/\partial x \ll \partial U/\partial x$,

$$\frac{\partial E'}{\partial t} = -E_1\left(\frac{2c_g}{c_1} + \frac{1}{2}\right)\frac{\partial U}{\partial x}. \tag{5.10}$$

Since U represents a progressive wave motion, the operation $\partial/\partial x$ may be replaced by $-(1/c_2)\,\partial/\partial t$, giving

$$\frac{\partial E'}{\partial t} = E_1\left(\frac{2c_g}{c_1} + \frac{1}{2}\right)\frac{1}{c_2}\frac{\partial U}{\partial t}. \tag{5.11}$$

Integration with respect to t (from an instant when the surface crosses the mean level and $U = 0$, $E = E_1$) gives

$$E' - E_1 = E_1\left(\frac{2c_g}{c} + \frac{1}{2}\right)\frac{U}{c_2}, \tag{5.12}$$

or

$$\frac{E'}{E_1} = 1 + \left(\frac{2c_g}{c_1} + \frac{1}{2}\right)\frac{U}{c_2}. \tag{5.13}$$

Substituting for E' from (4.11), we obtain

$$\frac{a'^2}{a_1^2} = 1 + \left(\frac{2c_g}{c_1} + \frac{1}{2}\right)\frac{U}{c_2} - \frac{1}{2g}\frac{\partial W}{\partial t}, \tag{5.14}$$

and so, since U and W are both of order $a_2\sigma_2$,

$$\frac{a'}{a_1} = 1 + \left(\frac{c_g}{c_1} + \frac{1}{4}\right)\frac{U}{c_2} - \frac{1}{4g}\frac{\partial W}{\partial t}. \tag{5.15}$$

In the case when the shorter waves are in deep water, $c_g/c_1 = \frac{1}{2}$ and hence

$$\frac{a'}{a_1} = 1 + \frac{3}{4}\frac{U}{c_2} - \frac{1}{4g}\frac{\partial W}{\partial t}. \tag{5.16}$$

Since, from (5.1) and (2.32),

$$\left.\begin{aligned} \frac{U}{c_2} &= a_2 k_2 \coth k_2 h \sin\psi_2, \\ -\frac{1}{g}\frac{\partial W}{\partial t} &= \frac{a_2\sigma_2^2}{g}\sin\psi_2 = a_2 k_2 \tanh k_2 h \sin\psi_2, \end{aligned}\right\} \tag{5.17}$$

equation (5.16) is equivalent to (2.49). Thus we have verified both equations (2.49) and (2.50) by alternative reasoning.

It will be seen that in shallow water, when the term $(1/g)\,\partial W/\partial t$ proportional to the vertical acceleration, is negligible, we have from (5.15) and (5.16)

$$\frac{a'}{a_1} = 1 + \left(\frac{c_g}{c} + \frac{1}{4}\right)\frac{U}{c_2} \tag{5.18}$$

and

$$\frac{a'}{a_1} = 1 + \frac{3}{4}\frac{U}{c_2}, \tag{5.19}$$

respectively, the last equation being equivalent to (2.58).

The derivation of (5.16), (5.18) and (5.19) does not depend upon the sinusoidal character of the longer waves but only upon their being progressive. These formulae can therefore be expected to remain valid for short waves riding on cnoidal or solitary waves, or any other kind of progressive disturbance, provided it is sufficiently long.

Equation (5.16) can be further generalized to any disturbance consisting of the sum of a number of wave motions in which the velocities $c_2^{(i)}$ may be positive or negative. Thus we have

$$\frac{a'}{a_1} = 1 + (\Sigma^{(+)} - \Sigma^{(-)}) \left(\frac{3}{4} \frac{U^{(i)}}{c_2^{(i)}} - \frac{1}{4g} \frac{\partial W^{(i)}}{\partial t} \right), \tag{5.20}$$

where $\Sigma^{(+)}$ denotes the sum over all values of i for which $c_2^{(i)}$ is positive, and $\Sigma^{(-)}$ the corresponding sum for $c_2^{(i)}$ negative. In shallow water, when $c_2^{(i)} = \pm\sqrt{(gh)}$ we have

$$\frac{a'}{a_1} = 1 + \frac{3}{4\sqrt{(gh)}} (\Sigma^{(+)} U^{(i)} - \Sigma^{(-)} U^{(i)}). \tag{5.21}$$

It should be noted that the present method is not capable of yielding in a simple way the more refined formulae (2.56) and (2.57) which are applicable when the ratio of the wave frequencies is no longer small compared with $k_2 h$. For deriving these, the longer but more rigorous method of § 2 is to be preferred.

6. On a result of Unna

As mentioned in § 1, a formula for the change in amplitude essentially different from that which we have found was suggested by Unna (1941, 1947); his result is stated in equation (1.2).

Unna apparently did not work out the wave interactions exactly but relied on a physical argument. His reasoning differs from ours in two respects. First, he neglects entirely the work done by the longer waves against the radiation stress S_x, which we have taken into account. Secondly, he calculates the potential energy of the waves in the accelerated frame of reference, replacing g by $g + \partial W_S/\partial t$ in equation (4.1). He then assumes that kinetic and potential energy are conserved in the *accelerated* system.

It is not difficult to show that the kinetic-plus-potential energy is not generally conserved in an accelerated frame of reference, even when the acceleration is slow compared to the natural period of oscillation of the system. As examples we may quote a simple pendulum hinged at a point which is accelerated vertically, or the oscillations of water in a U-tube likewise accelerated.

The argument from conservation of energy therefore fails unless it is applied in a fixed or inertial frame of reference, as in §§ 4 and 5. If an accelerated frame of reference is used it must be supposed that there is some kind of interaction between the dynamical system and the accelerating forces.

In the case of deep water ($k_2 h \gg 1$) it happens that Unna's two mistakes—neglect of the radiation stress and assumption of energy conservation in the accelerated system—exactly cancel. But that they do not generally cancel is shown by the difference between equations (1.2) and (1.3).

7. Conclusions

The change in wavelength of short waves on the crests of longer waves can be interpreted as being due simply to the contraction of the particles in the longer wave.

However, to account for the increase in the amplitude of the short waves it is necessary to allow for the work done by the longer waves against the *radiation stress* of the short waves. This work is converted into short-wave energy, and produces a steepening of the short waves beyond what was previously expected.

The radiation stress is likely to play an important part in other situations, for example in waves riding on steady but non-uniform currents. Without close examination it cannot be assumed that work done against the radiation stress must necessarily appear as additional wave energy. But we have shown that in the present situation at least this assumption proves correct.

REFERENCES

LAMB, H. 1932 *Hydrodynamics*, 6th ed. Cambridge University Press.

LONGUET-HIGGINS, M. S. 1953 Mass-transport in water waves. *Phil. Trans.* A, **245**, 535–81.

STOKES, G. G. 1847 On the theory of oscillatory waves. *Trans. Camb. Phil. Soc.* **8**, 441–55. (Reprinted in *Math. and Phys. Papers*, **1**, 314–26.)

UNNA, P. J. 1941 White horses. *Nature, Lond.*, **148**, 226–7.

UNNA, P. J. 1942 Waves and tidal streams. *Nature, Lond.*, **149**, 219–20.

UNNA, P. J. 1947 Sea waves. *Nature, Lond.*, **159**, 239–42.

Hypersonic flow over axially symmetric spiked bodies

By D. J. MAULL
Department of Aeronautics, Imperial College, London University*

(Received 6 January 1960)

An investigation has been made of the flow over axisymmetric spiked bodies at a Mach number of 6·8. For some ranges of the ratio of spike length to body diameter the flow was found to be unsteady. The effect of the shape of the body nose on this unsteadiness was investigated and an explanation of the mechanism of the oscillation is given.

1. Introduction

The supersonic flow around axially symmetric blunt bodies is characterized by the presence of a strong bow shock wave standing away from the nose of the body. The presence of this shock wave results in a high drag coefficient compared with that of a pointed body with an attached nose shock wave.

It has been shown by Eggers & Allen (1958) that for a body re-entering the earth's atmosphere at a high supersonic speed, it is advisable, to minimize heating effects, to have a body whose nose radius and drag coefficient are high. However, for motion through the earth's atmosphere at take off, it is necessary to have a body with a low drag coefficient to make the best use of the thrust of the propulsive system. It would therefore be an advantage for a body such as a re-entry missile to be equipped with some form of variable drag device.

The object of this investigation has been to study the flow over such a device, namely a blunt body equipped with a nose spike (figure 1). The tests were carried out in the Imperial College hypersonic gun tunnel at a Mach number of 6·8 and a Reynolds number of $0{\cdot}17 \times 10^6$/in.

2. Experimental facility and models

The Imperial College hypersonic gun tunnel has been described by Stollery, Belcher & Maull (1960). For this series of experiments the driving gas was air at approximately 600 p.s.i. and the working gas was air at initially room temperature and pressure. The nozzle used gave a Mach number of approximately 6·8 and the total running time of the steady flow was approximately 300 msec.

Five different model configurations were used. These were a plain flat-ended cylinder and four models having rounded nose shoulders with radii one-eighth, one-quarter, three-eighths and one-half of the cylindrical body diameter (figure 1).

The models were made of brass, the cylindrical portion being $\frac{1}{2}$ in. in diameter. The spike was a commercial sewing needle 0·030 in. in diameter which screwed

* Now at Engineering Laboratory, University of Cambridge.

into the nose of the body. The models were mounted at zero angle of incidence on a support in the working section.

Both schlieren and shadow photographs were taken of the flow, the schlieren arrangement being of the double pass type. A single-spark light source of duration approximately $1\,\mu s$ was used for most studies although for some configurations a multiple spark source (Cranz-Schardin) was used. This gave a series

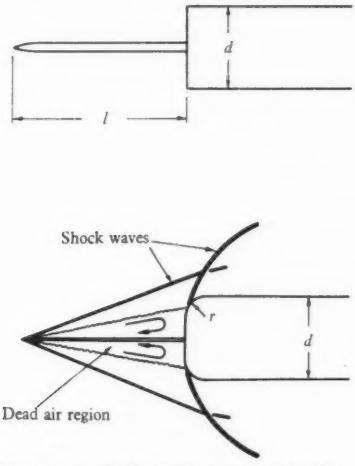

FIGURE 1. Spiked blunt-nosed bodies.

of eight sparks, which, by suitable optical arrangements, could be photographed on one half plate. The time interval between the sparks was variable down to $5\,\mu s$.

A high-speed ciné camera was also used to investigate the flow using a constant intensity mercury-vapour light source. The cameras and the spark sources were triggered electronically by picking up the noise of the tunnel start on a microphone, and passing this pulse via a delay circuit to the apparatus.

3. Results

3.1 *Test programme*

For each body, schlieren photographs of the flow were taken as the ratio of the spike length l to the body diameter d was varied over the range $0 \leqslant l/d \leqslant 4$. It was found that for $l/d > 4$ the spike vibrated and investigations at these spike lengths were not carried out. When unsteady flow was suspected a series of spark photographs was taken. Initially a high-speed ciné picture of some of the oscillations was taken but the oscillations were of too high a frequency to be picked up by the ciné camera.

3.2. *The oscillatory flow*

It was found that there was an oscillation of the flow around the flat-nosed body with spike lengths in the range $0{\cdot}25 < l/d \leqslant 2{\cdot}5$. The lower limit of this range was difficult to determine, but it appears that oscillation began when the spike

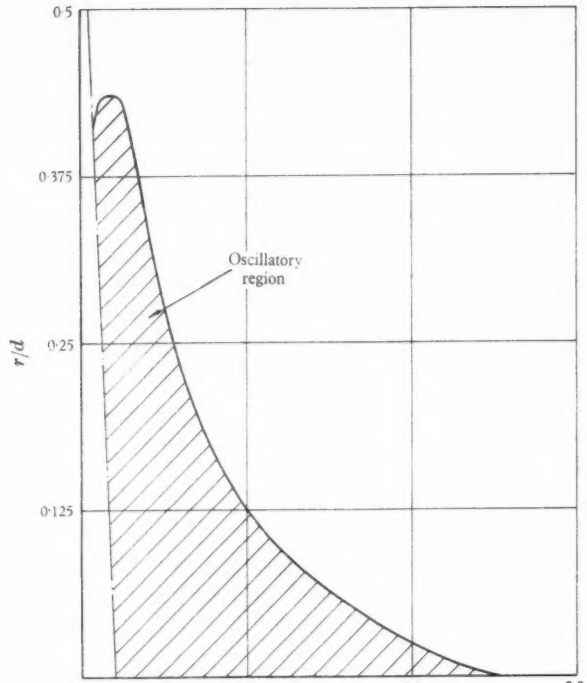

FIGURE 3. The effect of shoulder radius on the oscillatory region.

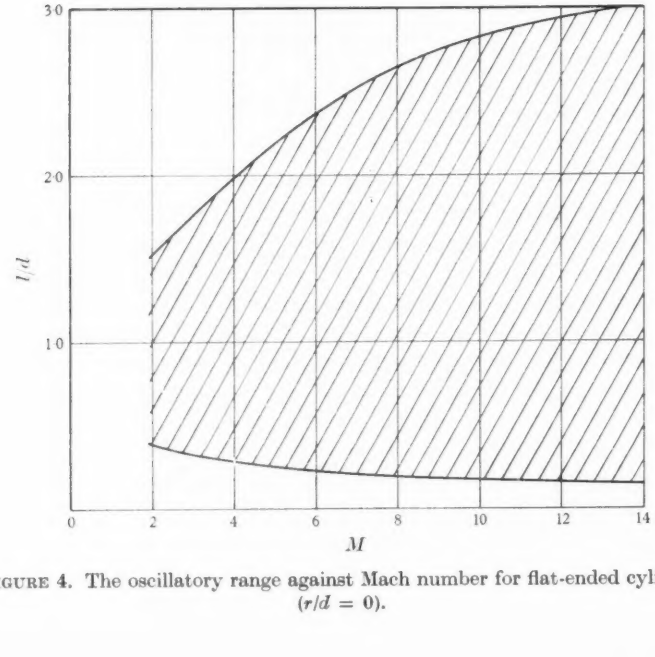

FIGURE 4. The oscillatory range against Mach number for flat-ended cylinders ($r/d = 0$).

protruded through the bow shock wave of the body. A typical spark shadowgraph photograph of the unsteady flow is shown in figure 2 (plate 1). By using the Cranz-Schardin spark source it was possible to determine the spike length required for oscillation to cease. By comparing a series of photographs taken with the Cranz-Schardin camera with the sparks set at 10 μs intervals the frequency of the oscillation was found to be approximately 2×10^4 c/s.

The flow around the spiked hemispherically nosed body was steady for all spike lengths, but all the bodies whose shoulder radius was less than half the diameter of the cylindrical portion of the body had ranges of spike lengths for which oscillation occurred. It is thus possible to draw the range of spike length for which oscillation occurred against shoulder radius (figure 3).

The investigations of Mair (1952) and Bogdonoff & Vas (1959) showed oscillation of the flow pattern for the flat-nosed cylinder with a spike at different Mach numbers and hence a graph of the oscillatory range against Mach number may be drawn for this configuration (figure 4). It should be noted that the experiments of Bogdonoff & Vas were performed in helium.

4. Discussion

A thorough investigation of separated flows has been reported by Chapman, Kuehn & Larson (1957) for the two-dimensional case of flow up and down steps. The only theoretical investigation of the problem of flow separation caused by a spike on a blunt body is by Moeckel (1951*a*), who used a simple theoretical model in which the separated shear layer re-attaches tangentially to the nose of the body. The assumption of tangential re-attachment is found to be in error in both this investigation and subsequent work by Moeckel (1951*b*). The three-dimensional problem may be subdivided into two parts, the separation of the boundary layer on the spike and the re-attachment of the separated shear layer.

4.1. *Shock-induced separation*

A boundary layer will be separated by a sufficiently strong shock wave which is either generated externally by another body in the flow field or by some influence of the body itself. Thus the boundary layer on the nose spike of a blunt body will separate initially under the influence of the nearly normal bow shock wave of the body if the spike protrudes through this shock wave. This separated layer will re-attach on the face of the body enclosing an approximately conical region between itself and the face. This region which will contain some circulatory flow will, in the text, be called the 'dead air region'. A conical shock wave will be required to turn the main flow past this dead air region. This conical shock wave may still be stronger than is required to separate the boundary layer at this point on the spike and will influence the boundary layer upstream causing further separation. If the separated layer still re-attaches on the face of the body the resulting conical shock wave will have a smaller half-cone angle and its strength, as measured by the pressure ratio across it, will decrease.

The pressure ratio, which the boundary layer can withstand without separation, increases as the distance from the nose of the spike decreases, and since the

pressure ratio across the conical shock wave decreases as the distance from the spike nose decreases an equilibrium position must be reached where the boundary layer will just separate.

The pressure ratio that will just cause separation is thus a function of Mach number and Reynolds number based on the distance of the separation point from the spike nose. Thus the angle that the separated layer makes with the spike axis is also a function of these two parameters.

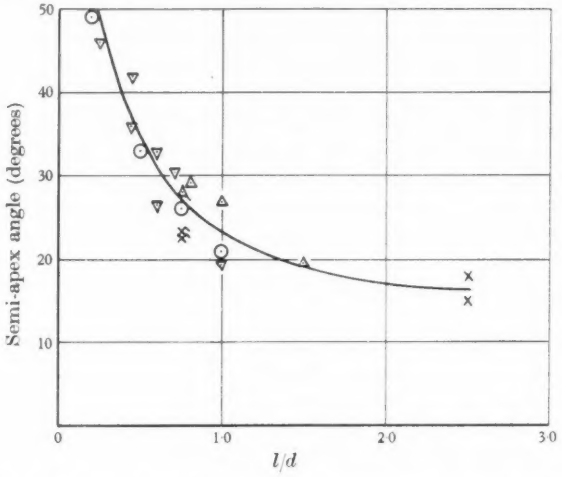

FIGURE 5. The semi-apex angle of the conical shock wave about the dead air region against l/d. The symbols indicate the different shoulder radii. ×, $r/d = 0$; △, $r/d = \frac{1}{4}$; ▽, $r/d = \frac{3}{8}$; ⊙, $r/d = \frac{1}{2}$. The flagged symbols indicate unsteady flow.

At the beginning of a cycle of the oscillatory flow under consideration the separation point appears to be very close to the nose of the spike and it is not possible to measure accurately its position. A plot of the measured shock half-cone angle against spike length (figure 5) shows that the shock angle decreases with increased spike length, indicating a useful reduction in drag as found by Mair and by Bogdonoff & Vas. The majority of these measured angles are from flow photographs of the steady conditions, but some are from unsteady flow photographs where the oscillation cycle is just beginning and the dead air region is approximately conical with separation near the spike tip.

It is apparent from figure 5 that the shock angle, to a first approximation, is a function of the spike length rather than the shape of the nose of the body. In figure 6 the apex semi-angle of the separated layer as calculated from the shock angles of figure 5 is plotted against spike length.

4.2. *Re-attachment process*

The analysis of the re-attachemnt process by Chapman *et al.* assumes laminar two-dimensional flow. It is not possible to use their results for the three-dimensional re-attachment under consideration, but the basis of their analysis serves as a guide to the mechanism of re-attachment.

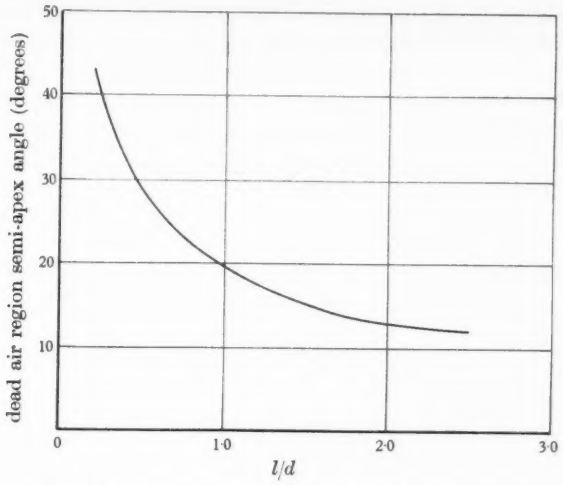

FIGURE 6. The semi-apex angle of the dead air region.

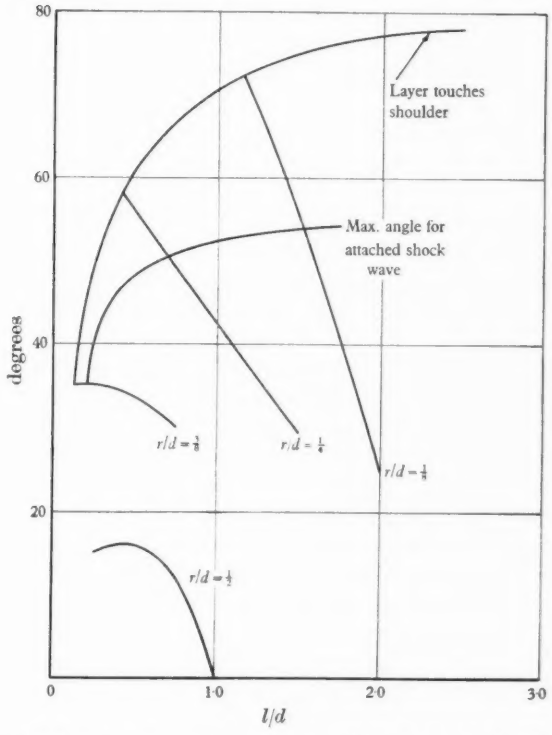

FIGURE 7. The angle between the separated layer and the body at the point of re-attachment against l/d. For $r/d = 0$ the separated layer touches the shoulder at the point shown.

The separated shear layer scavenges air from the dead air region and for equilibrium the mass of air scavenged must equal the mass reversed by a pressure gradient at the re-attachment point. From Chapman *et al.* the pressure at re-attachment that the separated layer can support under these equilibrium conditions is a function of the Mach number outside the shear layer. It is thus a function of the free-stream Mach number and the angle that the separated layer makes with the spike axis.

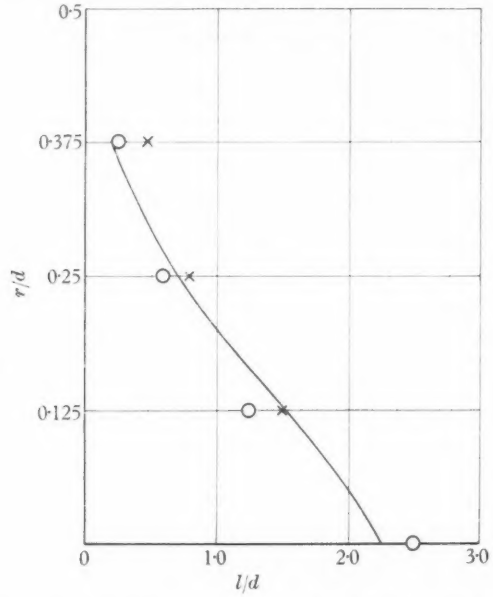

FIGURE 8. Comparison of the theoretical boundary of the oscillatory region with experimental results. ○, oscillatory flow; ×, steady flow.

If the separated layer re-attaches on the nose of the body non-tangentially, there must be an oblique shock at the re-attachment point to turn the supersonic flow just outside the layer up the nose of the body. If the pressure ratio across this oblique shock is such that the mass of air reversed at the re-attachment point balances the mass of air scavenged from the dead air region by the shear layer, then there will be steady flow.

From the measured angle between the separated layer and the spike axis (figure 6) it is possible to calculate, for the different configurations, the angle that the separated layer makes with the tangent to the body at the point of impingement (figure 7). It is also possible to calculate the maximum conical flow deflexion angle for the local Mach number prevailing on the conical surface of the separated region. If the angle through which the flow must be turned is greater than this, a detached shock wave is required, standing off from the point of impingement.

It is very unlikely that the separated layer can support this detached shock wave without the majority of the shear layer being reversed back into the dead

air region, and this shock pattern is certainly unstable. The lengths of spike to give this condition agree quite closely with the bounds of the observed oscillatory range (figure 8).

It should be noted that the maximum turning angle used in this analysis is that given by conical flow graphs whereas the maximum angle through which flow on the surface of a cone may be turned is theoretically given by the two-dimensional shock equations.

4.3. *Mechanism of the oscillation*

Figure 9 (plate 2) shows five spark shadowgraph photographs of the oscillatory flow about the flat-ended cylinder at a spike length three-quarters of the body diameter. The cycle starts with the boundary layer on the spike separating near the nose forming an approximately conical dead air region, which if continued to the face of the body would strike it well below the shoulder (figure 9*a*). To turn the flow just outside the separated layer up the nose of the body a detached shock wave is required. The pressure ratio across this shock and the area behind the shock through which air may be reversed into the dead air region are certainly too great for equilibrium to occur with the mass of air scavenged from the dead air region before the shock. Thus a non-equilibrium condition occurs with air flowing into the dead air region down the body nose. This enlarges the dead air region forming a nearly normal shock wave at the spike tip (figure 9*b*) which grows and replaces the conical shock wave. In figure 9*b* this growth has only just started.

The flow into the dead air region goes along the spike and the shock pattern should resemble the pattern produced by a jet of air from the body injected against the main stream. Figure 10 (plate 2) shows this flow pattern.

The strong shock wave grows from the spike tip as more air is fed into the dead air region. As it grows the intersection with the bow shock wave of the body moves out towards the shoulder of the body (figure 9*c*). The dead air region by this time is not conical but blunt in shape, with the re-attachment region moving up the face of the body. As the dead air region broadens, the angle through which the external flow must be turned at the end of it to pass round the nose decreases and the presssure ratio across the shock which turns it decreases. Thus the feeding of air into the dead air region stops. Air is now fed from the region out past the shoulder; the dead air region collapses and the shock wave which was at the spike tip moves towards the body (figure 9*d*) and grows weaker (compare figure 9*c* and *d*). As this shock wave moves downstream along the spike, separation again occurs at the spike tip with a conical shock wave formed (figure 9*e*). When the excess air in the dead air region has escaped and the strong shock wave originally at the spike tip has become the bow shock wave of the body the cycle begins again.

An interesting feature of figure 9*b* are the vortex sheets at the intersection of the conical shock wave and the bow shock wave. They are shown by Mair to be quite tightly closed. The strong shock wave near the body on figure 9*e* only appeared on one photograph in twenty of this configuration and occurs at the end of the period of the dead air region collapsing. This strong shock wave is probably

moving slowly upstream, and will merge with the bow shock wave originally at the spike tip to form the initial bow shock wave for the main body.

Lengthening the spike has the effect of moving the point of re-attachment of the separated layer up the nose of the body towards the shoulder. When the re-attachment point is at the shoulder of the flat-faced cylinder the supersonic flow just outside the separated layer can turn the corner through an expansion, and there will be no feed-back of air into the dead air region and no oscillation.

For bodies with rounded shoulders it is possible for the flow just outside the separated layer to be turned up by the nose by an oblique shock wave when the re-attachment point is far enough out on the rounded part of the nose. There will be a re-attachment point where the pressure ratio across the oblique shock wave is just sufficient for equilibrium of the dead air region and no oscillation occurs. This condition is shown in figure 11 (plate 1).

4.4. *Frequency of the oscillation*

The frequency of the oscillation as measured from the Cranz–Schardin photographs was about 2×10^4 c/s. A non-dimensional frequency may be defined as fd/u, where f is the measured frequency, d the body diameter and u the free-stream velocity. For the results in this report, this gives a non-dimensional frequency of 0·23. The results of Mair give a non-dimensional frequency of 0·15 at a Mach number of 1·96.

5. Conclusions

The investigation has shown that while fitting a spike to the nose of a blunt body may reduce the drag coefficient, it may in some cases cause a rapid fluctuation of the flow pattern and thus produce an unsteady drag coefficient.

The practical use of such a device must therefore be limited to bodies which do not exhibit these changes in flow pattern. The length of the spike will be determined by structural considerations and the shorter the spike the more the nose shape must tend towards a hemisphere for steady flow. It is also thought that bodies whose noses are not so blunt as hemispheres, i.e. ellipsoids of revolution, would also be stable with nose spikes.

REFERENCES

Bogdonoff, S. M. & Vas, E. 1959 *J. Aero./Space Sci.* **26**, 65.

Chapman, D. R., Kuehn, D. M., & Larson, H. K. 1957 *NACA TN* 3869.

Eggers, A. J. & Allen, M. J. 1958 *NACA Rep.* 1381.

Mair, W. A. 1952 *Phil. Mag.* **43**, 695.

Moeckel, W. E. 1951*a* *NACA TN* 2418.

Moeckel, W. E. 1951*b* *NACA RM* E51I25.

Stollery, J., Belcher, B. & Maull, D. J. 1960 *J. R. Aero. Soc.* **64**, 24.

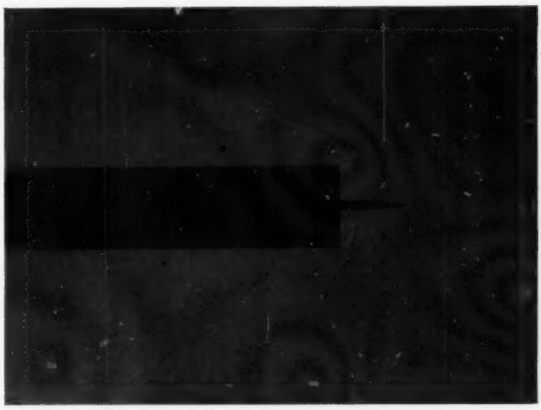

FIGURE 2 (plate 1). A typical photograph of the unsteady flow.

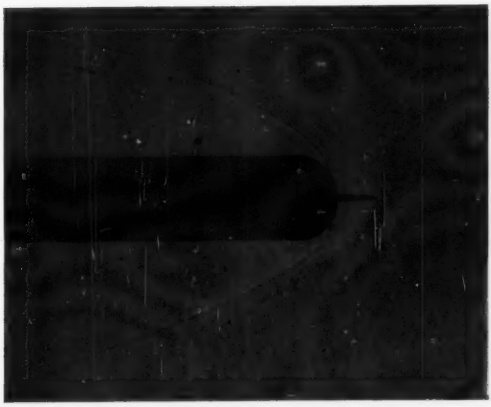

FIGURE 11 (plate 1). Steady conical separation from a spike on a hemispherically nosed body.

(*Facing p.* 592)

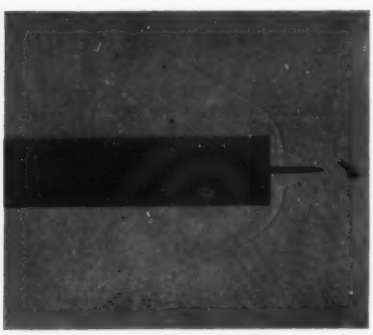

a

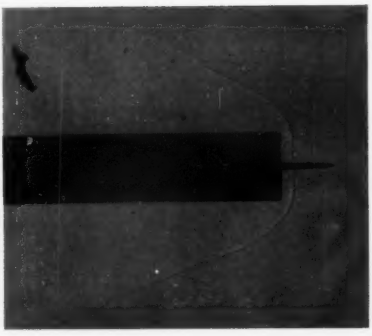

b

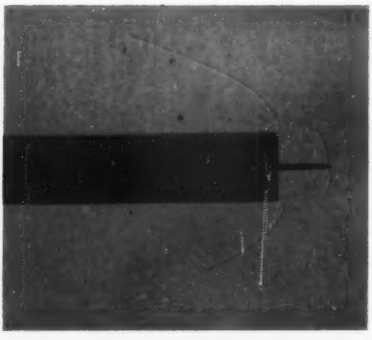

c

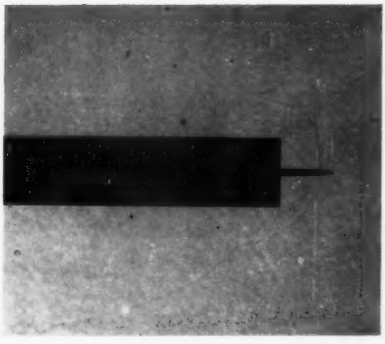

d

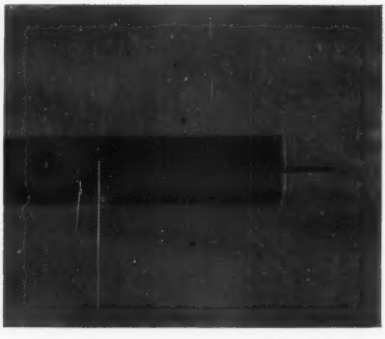

e

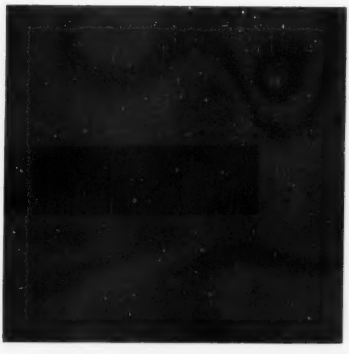

FIGURE 10

FIGURE 9 (plate 2). Phases of the oscillation for the spiked body with $l/d = 0{\cdot}75$, $r/d = 0$.

FIGURE 10 (plate 2). The shock pattern produced by air blowing out of the front of a flat-ended cylinder.

The hydrodynamic stability of a thin film of liquid in uniform shearing motion

By JOHN W. MILES

Department of Engineering and Institute of Geophysics, University of California, Los Angeles and Space Technology Laboratories, Inc.

(Received 18 January 1960)

The stability problem for a thin film of liquid having a linear mean-velocity profile and bounded by a fixed wall and free surface is solved asymptotically for large values of the Reynolds number R. The analysis is similar to that for plane Couette flow, but instability occurs for sufficiently large values of R in accordance with Heisenberg's criterion that neutral disturbances having finite wave numbers and phase velocities for $R = \infty$ are necessarily unstable as $R \to \infty$. It is found that a sufficient condition for stability is $W < 3$, where W is the Weber number based on the mean speed at the free surface and the depth of the film. The minimum critical Reynolds number, also based on free surface speed and film depth, is found to be $R = 203$. This last figure is in order-of-magnitude agreement with observation, but there remains considerable uncertainty as to whether the observed instability corresponds to that considered here. Neutral stability curves are presented in an R *vs* α (= wave-number) plane with W as the family parameter. Brief consideration also is given to the time-rate-of-growth of unstable disturbances and to the lighter fluid that, in actual configurations, is responsible for the shear in the film. An appendix gives extended and more accurate results for the function $\mathscr{F}(z)$, introduced and calculated previously by Tietjens (1925) and Lin (1955).

1. Introduction

We present here an approximate determination of the conditions governing surface wave formation on a thin film of liquid that is bounded below by a wall and subjected to a prescribed shearing stress at its upper and otherwise free surface. This configuration approximates that arising in, for instance, film cooling and nose-cone ablation if we assume that the only significant role of the much lighter fluid flowing over the film is to produce the mean shear flow. Neglecting the effect of the lighter fluid on surface-wave formation obviously can be justified if its density is sufficiently small, but we must bear in mind that *sufficiently small* also implies that the kinematic viscosity of the film must be small compared with that of the lighter fluid (see § 8 below).

We also shall assume that the flow is incompressible, two-dimensional and laminar (so that the mean velocity profile is linear) and that only those waves for which the wave speed is equal to the mean flow speed at some point between

the wall and the free surface can absorb energy from the mean flow.† Letting U_1 denote the velocity of the mean flow at the free surface, δ the mean thickness of the film, ν the kinematic viscosity, ρ the density, σ the surface tension, g the acceleration of gravity, and λ the wavelength of the surface wave, the dimensionless parameters characterizing the problem are:

$$R = U_1\delta/\nu \qquad \text{(Reynolds number)}, \tag{1.1}$$

$$W = T^{-1} = \rho U_1^2\delta/\sigma \qquad \text{(Weber number)}, \tag{1.2}$$

$$F = G^{-1} = U_1^2/g\delta \qquad \text{(Froude number)} \tag{1.3}$$

and

$$\alpha = 2\pi\delta/\lambda \qquad \text{(wave-number)}. \tag{1.4}$$

We shall assume $R \gg 1$ and $G \ll 1$ and seek the corresponding approximations to the neutral-stability (or simply *neutral*) curves for R *vs* α with T as the family parameter, say $R = R_c(\alpha; T)$.

The foregoing problem has been studied by Feldman (1957), who included the lighter fluid in his stability analysis on the assumption that its mean velocity profile could be regarded as linear and semi-infinite in extent (a reasonable approximation if $\alpha\delta_1 \gg 1$, where δ_1 denotes the thickness of the laminar sublayer in this fluid). Feldman's configuration is characterized by R, W, F, α and, in addition, r, the ratio of density of the lighter fluid to that of the lower fluid, and $1/m$, the corresponding viscosity ratio. This configuration presumably should reduce to that of the preceding paragraph as $r \to 0$ with m fixed. Feldman found that there was stability for all α in this limit, that both gravity and surface tension were destabilizing for $r \ll 1$, and that the minimum value of R_c for air blowing over an 0·005 in. film of water was an order of magnitude larger than that inferred from observation.

A problem closely related to that of the penultimate paragraph is presented by a laminar film on an inclined plane, the stability of which has been studied by Benjamin (1957). The essential differences are that the velocity profile for the latter problem is parabolic rather than linear and that the Reynolds and Froude numbers are not independent parameters (for a fixed angle of inclination). Benjamin gave special consideration to a vertical film and found instability for all R and sufficiently small α. He also found that surface tension was stabilizing and calculated a wavelength for maximum instability that was in close agreement with observation.

It might be thought that the very striking disparity between the respective results of Feldman and Benjamin is analogous to the disparity between plane Couette and plane Poiseuille flow and could be traced to the important role of profile curvature. In fact, the analogy between the film with a free surface and plane Couette flow is not appropriate, for it overlooks Heisenberg's criterion (as formulated by Lin 1946) that 'if a velocity profile has an "inviscid" neutral disturbance with non-vanishing wave-number and phase velocity (equal to the velocity of the mean flow at some point in the profile), the disturbance with the same wave-number is unstable in the real fluid when the Reynolds number is sufficiently large'. Lin's proof of Heisenberg's criterion is not directly applicable to the present configuration, but it is readily extended. In Lin's words (L 4.5,

† See §8 below for an *a posteriori* justification of this last assumption.

where the prefix L, followed by the appropriate section or equation number, refers to Lin's 1955 monograph), 'The key mechanism is a shift in the phase of the two components of the velocity of the oscillation by the viscous forces at the solid boundary. This produces a Reynolds stress which converts energy from the basic flow to the disturbance'. This energy is $O(R^{-\frac{1}{2}})$ as $R \to \infty$, whereas the energy dissipated in the neighbourhood of the free surface is $O(R^{-1})$, while that dissipated elsewhere in the flow is $O(R^{-\frac{3}{2}})$. We also observe (see § 4 below) that the film under consideration can support inviscid surface waves with two permissible wave speeds for each wave-number, one upstream and the other downstream relative to U_1, and that the former must lie in $(0, U_1)$ relative to the wall if U_1 is sufficiently large. It follows that the flow must be unstable for sufficiently large values of R, W and F (W and F being the appropriate measures of U_1 for $R = \infty$). Conversely, if either W or F is sufficiently small (T or G sufficiently large) no wave speed exists in $(0, U_1)$ relative to the wall, and we therefore should expect sufficiently large surface tension and/or gravity to be stabilizing.

It appears likely that the primary reason for the conflict between the foregoing arguments and Feldman's conclusions lies in the inadequacy of his asymptotic (as $R \to \infty$) approximations for small wave speeds (cf. L 3.4 and 3.6). Even this would not account for his conclusion of stability for all α as $r \to 0$, however, so that either his analysis contained mathematical errors or he simply misinterpreted the significance of the result that, for *his* asymptotic approximation, $R_c \to \infty$ as $r \to 0$—namely, that disturbances having wave speeds in $(0, U_1)$ are unstable for sufficiently large, finite values of R.

The argument outlined in the penultimate paragraph requires three important qualifications if the presence of a *laminar* flow in the lighter fluid is recognized. First, there may be an energy dissipation of $O(rR_g^{-\frac{1}{2}}) = O(r^{\frac{1}{2}}m^{-\frac{1}{2}}R^{-\frac{1}{2}})$ in this fluid ($R_g = rmR$ being its Reynolds number). This is especially important for large α (short wavelength), where the energy supply from the wall actually is found to be $O(e^{-2\alpha}R^{-\frac{1}{2}})$ at the interface. Secondly, the film of denser fluid will act essentially as a wall with respect to the viscous forces in the lighter fluid, whence energy may be supplied to disturbances having wave speeds in excess of U_1 (cf. Benjamin 1959). Thirdly, and perhaps unexpectedly, the lighter fluid may significantly alter the wave speeds as $R \to \infty$ if its kinematic viscosity is of the same order as or *less* than that of the film. We shall carry (in § 8) the mathematical analysis of the two-fluid problem far enough to elucidate these three effects, but we shall not attempt to present numerical results for the neutral curves (except, of course, for $r = 0$). These doubtless would be exceedingly complex in consequence of the two, distinct classes of modes (finding their primary source of energy in one fluid or the other) and might be expected to resemble the neutral curves obtained by Lock (1954) for two semi-infinite fluids with *curved* velocity profiles.

It seems likely that, in the majority of practical applications, the flow in the lighter fluid would be turbulent and that the laminar sublayer would not be large compared with significant wavelengths (see § 8 below). Energy then could be transferred from the mean flow in this upper fluid to disturbances in the film both through the direct action of turbulent fluctuations (Phillips 1957),

and through the Reynolds stress associated with profile curvature (Miles 1957, 1959, 1960). Limited experimental data (Knuth 1954) indicate that disturbances of relatively short wavelength are present for all film speeds, while stronger disturbances of relatively long (compared with film thickness) wavelength appear only when a rather well-defined, critical Reynolds number is exceeded. It is at least plausible to associate the former disturbances with the direct action of turbulent fluctuations and the latter with hydrodynamic instability. Whether this hydrodynamic instability depends primarily on energy transfer from the mean flow in the film (as described herein) or that in the upper fluid depends decisively on whether the phase velocity of the disturbance is less or greater than the interfacial speed.

The minimum critical Reynolds number (approximately 200) determined in the following analysis is in order-of-magnitude agreement with that observed by Knuth (1954), but the corresponding wavelengths are much smaller than those observed by him (private communication). Knuth's observations of phase velocity are inconclusive, but it appears that at least some of the larger, unstable waves were travelling downstream relative to the interface and hence did not correspond to those considered here. Further experiments, with special emphasis on wave kinematics, evidently are desirable.

2. Equations of motion

Consider the flow configuration sketched in figure 1. We designate the horizontal and vertical components of velocity by u and v, the hydrodynamic pressure by p, and the shear stress by τ and refer all lengths, velocities and stresses to δ, U_1 and ρU_1^2. The equilibrium flow then is specified by

$$u = U(y) = y, \quad p = p_0, \quad \tau = \tau_0 = R^{-1}, \tag{2.1 a, b, c}$$

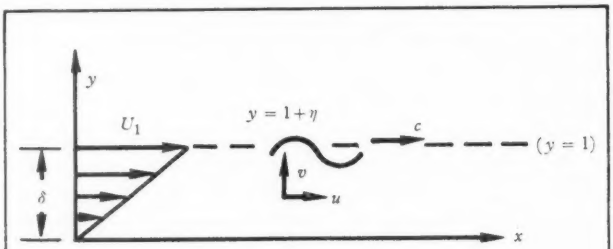

FIGURE 1. Sketch of the linear shear flow and surface-wave disturbance.

where p_0 denotes the static pressure. We superimpose on this equilibrium flow a small, travelling-wave disturbance having the (x, t)-dependence

$$E(x, t) = e^{i\alpha(x-ct)}, \tag{2.2}$$

where α denotes the wave-number (positive by definition) of (1.4) and c the wave speed, and we seek to determine those values of c, namely the eigenvalues, that are compatible with the equations of motion and the boundary conditions.

Requiring c to be real and in the interval $(0, 1)$ then yields the neutral curves, $R_c vs\, \alpha$.

We may satisfy the continuity equation by introducing a perturbation stream function

$$\psi(x, y, t) = \phi(y) E(x, t) \tag{2.3}$$

such that the perturbation velocity is given by

$$u = -\psi_y = -\phi' E, \quad v = \psi_x = i\alpha\phi E, \tag{2.4 a, b}$$

where the prime implies differentiation with respect to y. We also remark that the displacement η of any streamline—in particular the free surface or interface at $y \doteq 1$—is given by

$$\psi = (U - c)\,\eta. \tag{2.5}$$

Posing (2.4 a, b) in the equations of motion (cf. L 1.3), we obtain

$$(U - c)(\phi'' - \alpha^2\phi) = (i\alpha R)^{-1}(\phi^{\mathrm{iv}} - 2\alpha^2\phi'' + \alpha^4\phi), \tag{2.6}$$

$$p = [(U - c)\phi' - U'\phi - (i\alpha R)^{-1}(\phi''' - \alpha^2\phi')]\,E, \tag{2.7}$$

$$\tau = R^{-1}(u_y + v_x) = -R^{-1}(\phi'' + \alpha^2\phi)\,E, \tag{2.8}$$

for the determination of ϕ and the perturbation pressure and shear stress.

The boundary conditions are

$$u = v = 0, \quad y = 0, \tag{2.9 a, b}$$

$$-p + 2R^{-1}v_y = T\eta_{xx} - G\eta, \quad \tau = 0, \quad y = 1, \tag{2.9 c, d}$$

corresponding to the requirements that the velocity vanish at the wall, that the normal stress at the surface be in equilibrium with the capillary and gravitational forces resisting the displacement η, and that the shear stress vanish at the surface. Substituting (2.4 a, b), (2.5), (2.7) and (2.8) in (2.9 a, b, c, d), we obtain

$$\phi = \phi' = 0, \quad y = 0, \tag{2.10 a, b}$$

$$\varpi = (1 - c)\phi' - \phi - (i\alpha R)^{-1}(\phi''' - 3\alpha^2\phi') - (T\alpha^2 + G)(1 - c)^{-1}\phi = 0, \quad y = 1, \tag{2.10 c}$$

$$\phi'' + \alpha^2\phi = 0, \quad y = 1, \tag{2.10 d}$$

where we have introduced the abbreviation ϖ for convenience in the subsequent analysis.

3. Asymptotic solutions

We may determine four, linearly independent solutions to (2.6) with $U = y$ therein according to [see F (6)–(17) for details, where the prefix F denotes an equation in Feldman's paper]

$$\phi_1 = \cosh(\alpha y), \quad \phi_2 = \sinh(\alpha y), \tag{3.1 a, b}$$

$$\phi_{3,4} = \frac{1}{\alpha}\int_{\pm\infty}^{y} \sinh[\alpha(y - y')] f_{3,4}(\zeta')\, dy', \tag{3.2}$$

$$f_{3,4}(\zeta) = \zeta^{\frac{1}{2}} H_{\frac{1}{3}}^{(1,2)}[\tfrac{2}{3}(i\zeta)^{\frac{3}{2}}], \tag{3.3}$$

$$\zeta = (\alpha R)^{\frac{1}{3}}(y - c) - i\alpha^2(\alpha R)^{-\frac{2}{3}}, \tag{3.4}$$

where the upper and lower signs in (3.2) correspond to ϕ_3 and ϕ_4, respectively, and ζ' is given by (3.4) with y replaced by y' therein. We designate $\phi_{1,2}$ as the *inviscid* solutions and $\phi_{3,4}$ as the *viscous* solutions.

We require asymptotic approximations to $\phi_{3,4}$ as $\alpha R \to \infty$. The simplest such approximations are [cf. L (3.4.9)]

$$\phi_{3,4} \sim \text{const.} \times (y-c)^{-\frac{1}{4}} \exp\left[\mp \tfrac{2}{3}(i\alpha R)^{\frac{1}{2}}(y-c)^{\frac{3}{2}}\right], \quad \alpha R\,|y-c| \to \infty, \tag{3.5}$$

where $i^{\frac{1}{4}} = \exp(i\pi/4)$ and [cf. L (3.4.11)]

$$y-c = (c-y)\,e^{-i\pi} \quad (y < c). \tag{3.6}$$

We shall assume $0 < c < 1$ and (subject to *a posteriori* verification)

$$(\alpha R)^{\frac{1}{2}}(1-c)^{\frac{3}{2}} \gg 1, \tag{3.7}$$

so that (3.5) governs the behaviour of both ϕ_3 and ϕ_4 in the neighbourhood of the free surface; on the other hand, we cannot use (3.5) in the neighbourhood of the wall unless $(\alpha R)^{\frac{1}{2}} c^{\frac{3}{2}} \gg 1$. Irrespective of whether or not this last inequality is satisfied, however, (3.7) is sufficient to justify the neglect of ϕ_4 in the boundary conditions at $y = 0$ and ϕ_3 in the boundary conditions at $y = 1$, the error being $O\{\exp[-\frac{1}{3}(2\alpha R)^{\frac{1}{2}}(1-c)^{\frac{3}{2}}]\}$ relative to unity.

An asymptotic approximation to ϕ_3 that is uniformly valid with respect to c as $\alpha R \to \infty$ is [cf. L (3.6.4)]

$$\phi_3 \sim (\alpha R)^{-\frac{2}{3}} \int_{\infty}^{(\alpha R)^{1/3}(y-c)} [(\alpha R)^{\frac{1}{3}}(y-c) - \zeta] f_3(\zeta)\, d\zeta. \tag{3.8}$$

We shall base the subsequent analysis on this approximation, rather than (3.5), and it is primarily (but not only) in this that our analysis differs from that of Feldman.

4. Eigenvalue equation

We may obtain the eigenvalue equation for c by substituting a linear superposition of $\phi_{1,2,3,4}$ in the boundary conditions (2.10 a, b, c, d) and equating the determinant of the resulting algebraic equations (in the unknown coefficients of $\phi_{1,2,3,4}$) to zero. Invoking the approximation that ϕ_3 and ϕ_4 are exponentially small at the surface and at the wall, respectively, the result is

$$\begin{vmatrix} \phi_{10} & \phi_{20} & \phi_{30} & 0 \\ \phi'_{10} & \phi'_{20} & \phi'_{30} & 0 \\ \varpi_1 & \varpi_2 & 0 & \varpi_4 \\ 2\alpha^2\phi_{11} & 2\alpha^2\phi_{21} & 0 & \phi''_{41} + \alpha^2\phi_{41} \end{vmatrix} = 0, \tag{4.1}$$

where the first subscript $(1, 2, 3, 4)$ identifies the individual solution and the second the point of evaluation (0 or 1).

It is immediately evident from (4.1) that the eigenvalue equation depends on the viscous solutions only through ϕ_{30}/ϕ'_{30} and $\varpi_4/(\phi''_{41} + \alpha^2\phi_{41})$. The former quantity is given by (3.8) as

$$\frac{\phi_{30}}{\phi'_{30}} = -(\alpha R)^{-\frac{1}{3}} z F(z), \tag{4.2}$$

where

$$z = (\alpha R)^{\frac{1}{3}} c \tag{4.3}$$

and

$$F(z) = 1 + \frac{\displaystyle\int_{\infty}^{-z} \zeta f_3(\zeta)\, d\zeta}{z \displaystyle\int_{\infty}^{-z} f_3(\zeta)\, d\zeta} \tag{4.4}$$

is defined as in L 3.6 (although differing from Lin's form to the extent of integration by parts). The latter quantity is given by (2.10*c*) and (3.5) as

$$\frac{\varpi_4}{\phi_{41}''+\alpha^2\phi_{41}} = -\frac{(T\alpha^2+G)}{i\alpha R(1-c)^2}+O(R^{-\frac{3}{2}}). \tag{4.5}$$

Substituting (3.1 *a*, *b*), (4.2) and (4.5) in (4.1) and expanding the determinant, we may place the result in the form

$$[\alpha\coth\alpha+\alpha^2\operatorname{cosech}^2\alpha F(z)\,c](1-c-2i\alpha R^{-1})^2$$
$$-(1-c-2i\alpha R^{-1})-(T\alpha^2+G)+O(\alpha^2\operatorname{cosech}^2\alpha R^{-\frac{3}{2}}, R^{-\frac{3}{2}}) = 0. \tag{4.6}$$

We remark that the terms of $O(R^{-1})$ in (4.6) need be retained only if α is large; otherwise, they are of higher order than terms already neglected. If, on the other hand, α is large, the values of $c-1$ (the wave speed relative to the free surface) given by (4.6) reduce to those calculated by Stokes (1850; Lamb 1945, § 348) for surface waves on a slightly viscous, deep liquid. We also remark that neglecting the terms of $O(R^{-1})$ in (4.6) is tantamount to suppressing the boundary condition of zero shear at the free surface.

5. The inviscid problem

Letting $R = \infty$ in (4.6), we obtain

$$\alpha\coth\alpha(1-c)^2-(1-c)-(T\alpha^2+G) = 0 \tag{5.1}$$

as the eigenvalue equation governing the inviscid problem. The roots of (5.1), to which we find it convenient to assign the subscript zero, are

$$c_0 = 1-\left\{\frac{1\pm[1+4(T\alpha^2+G)\,\alpha\coth\alpha]^{\frac{1}{2}}}{2\alpha\coth\alpha}\right\}. \tag{5.2}$$

We note that the restoration of the original, physical parameters, in place of their dimensionless counterparts, yields

$$c_0-U_1 = \mp\left[\left(\frac{\sigma}{\rho}k+\frac{g}{k}\right)\tanh(k\delta)+\left(\frac{U_1\tanh k\delta}{2k\delta}\right)^2\right]^{\frac{1}{2}}-\left(\frac{U_1\tanh k\delta}{2k\delta}\right), \tag{5.3 a}$$

$$k = 2\pi/\lambda, \tag{5.3 b}$$

for the inviscid wave speeds relative to the free surface.

The eigenvalues given by (5.2) are real in consequence of the fact that there can be no energy transfer between an inviscid shear flow and a travelling wave disturbance in the absence of profile curvature (L 4.3). That eigenvalue corresponding to the negative radical lies in $c > 1$ and, by hypothesis, is not significant for our stability problem.† That root corresponding to the positive radical lies in (0, 1) if and only if

$$\alpha\coth\alpha-1-T\alpha^2-G > 0, \tag{5.4}$$

† Feldman discarded the root in $c > 1$ on the basis of the erroneous argument that it was algebraically extraneous. We also note that F(71) and F(72) are identical and not. as Feldman states, in disagreement. Cf. (8.7) below.

as will be true if $\alpha_0 < \alpha < \alpha_1$, where α_0 and α_1 are the roots of

$$f(\alpha) = T + G\alpha^{-2}, \tag{5.5}$$

and

$$f(\alpha) = \alpha^{-1}\coth\alpha - \alpha^{-2}. \tag{5.6}$$

The function $f(\alpha)$ is plotted in figure 3.

We can prove that (5.5) has either two or no real roots by noting that $f(\alpha)$ decreases monotonically from $\frac{1}{3}$ to 0 as α increases from 0 to α, while $T + G\alpha^{-2}$ decreases from ∞ to T. If $T < \frac{1}{3}$ and $G \ll 1$, α_0 and α_1 are determined by

$$\alpha_0^2 = (\tfrac{1}{3} - T)^{-1} G, \quad f(\alpha_1) = T. \tag{5.7a,b}$$

We infer that $T > \frac{1}{3}$ ($W < 3$) *is a sufficient condition for stability as* $R \to \infty$, since then no eigenvalue of c exists in (0, 1). We emphasize, however, that the presence of an upper fluid generally would alter this conclusion either by modifying the condition for $c < 1$ (see § 8 below) or by rendering unstable some modes for which $c > 1$.

6. The neutral curves

We may determine the neutral curves by assuming c to be real in (4.6) and equating the real and imaginary parts separately to zero to obtain

$$[\alpha\coth\alpha + \alpha^2\operatorname{cosech}^2\alpha\, F_r(z)\, c](1-c)^2 - (1-c) - (T\alpha^2 + G) = 0 \tag{6.1}$$

and

$$F_i(z)\,\alpha^2\operatorname{cosech}^2\alpha\, c(1-c)^2 - 2\alpha R^{-1}\{2(1-c)[\alpha\coth\alpha + \alpha^2\operatorname{cosech}^2\alpha\, F_r(z)\, c] - 1\} = 0, \tag{6.2}$$

where the subscripts r and i denote real and imaginary parts. Substituting

$$R = z^3 c^{-3}\alpha^{-1} \tag{6.3}$$

and rearranging, we obtain

$$z^3 F_i(z) = 2\left(\frac{c}{1-c}\right)^2 \{2(1-c)[\alpha\coth\alpha + \alpha^2\operatorname{cosech}^2\alpha\, F_r(z)\, c] - 1\}\sinh^2\alpha. \tag{6.4}$$

Now, within the approximations already invoked, we may neglect the term in $F_r c$ and replace c by the inviscid approximation c_0 on the right-hand side of (6.4) to obtain

$$z^3 F_i(z) = H(\alpha, T + G\alpha^{-2}), \tag{6.5}$$

where

$$H(\alpha, T) = 2\left[\frac{2\alpha\cosh\alpha}{1 + (1 + 4T\alpha^3\coth\alpha)^{\frac{1}{2}}} - \sinh\alpha\right]^2 (1 + 4T\alpha^3\coth\alpha)^{\frac{1}{2}}. \tag{6.6}$$

We emphasize that the retention of $F_r(z)$ in (6.1) is significant, even though we have neglected it in (6.5) and (6.6).

If α is small, (6.1) yields

$$c = \left(\frac{\frac{1}{3} - T}{1 - F_r}\right)(\alpha^2 - \alpha_0^2) \quad (\alpha_0 < \alpha \ll 1), \tag{6.7}$$

where α_0 is given by (5.7*a*). It follows that the right-hand side of (6.4) is $O(\alpha^6)$, whence we may approximate (6.5) by $F_i = 0$, which implies $z = 2{\cdot}294$ and $F_r = 0{\cdot}5637$. We then obtain

$$R = 27{\cdot}16(1 - 3T)^{-3}(\alpha^2 - \alpha_0^2)^{-3}\alpha^{-1} \tag{6.8}$$

from (6.3) and (6.7). We note that if $\alpha_0 = 0$ ($G = 0$), $R \sim \alpha^{-7}$ as $\alpha \to 0$, and the shape of the lower branch of the neutral curve then is similar to that for plane Poiseuille flow [L (3.6.12)]. We observe, however, that our neutral curves are single-valued as $\alpha \to 0$, the *upper* branch of the Poiseuille curve in this limit being determined by profile curvature [L (3.6.13)].

If $\alpha \gg \alpha_0$, we either may ignore G or may carry out our calculations for fixed values of T in (6.6) with the understanding that T may be replaced by $T + G\alpha^{-2}$ to account for G. To obtain a point on a neutral curve for fixed T, we may proceed as follows: (i) select α; (ii) determine H from (6.6); (iii) determine z from (6.5), the solution of which may not be single-valued (see below); (iv) determine c from (6.1), with $G = 0$ therein and $0 < c < 1$; (v) determine R from (6.3).

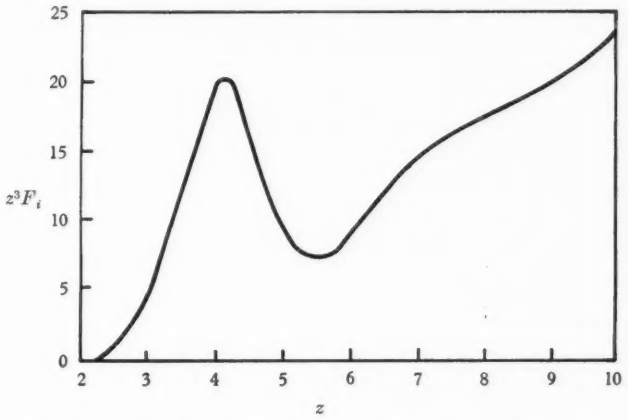

FIGURE 2. The function $z^3F_i(z)$, required for the solution of (6.5).

The left-hand side of (6.5), $z^3F_i(z)$, is plotted in figure 2 and is found to be positive for $z > 2{\cdot}294$, to rise to a maximum of 19·9 at $z = 4{\cdot}10$, to decrease to a minimum of 7·05 at $z = 5{\cdot}44$, and then to increase monotonically, being asymptotic to $2^{-\frac{1}{2}}z^{\frac{3}{2}}$.

The right-hand side of (6.5), $H(\alpha, T)$, vanishes at $\alpha = \alpha_0$ and $\alpha = \alpha_1$ and has a single maximum in (α_0, α_1) unless $T = 0$ ($\alpha_1 = \infty$) in which case it increases monotonically with α. It follows that the neutral curve will have either one or three branches and that we may determine the (α, T) regions in which these possibilities occur by plotting,

$$H(\alpha, T) = (z^3F_i)_{\min,\max}, \tag{6.9}$$

as shown in figure 3. If $0{\cdot}172 < T < 0{\cdot}184$ (approximate) a portion of the neutral curve will take the form of a closed loop, the interior of which forms an island of stability in an (α, R)-plane. If $T > 0{\cdot}184$ the neutral curves are single-valued.

Neutral curves were determined according to the foregoing procedure on a high-speed digital computer for $T = 0\,(0{\cdot}05)\,0{\cdot}15\,(0{\cdot}01)\,0{\cdot}20\,(0{\cdot}05)\,0{\cdot}30$. Neutral curves for $T = 0$, 0·10, 0·20, 0·25 and 0·30 are plotted in figure 4*a*, and that for

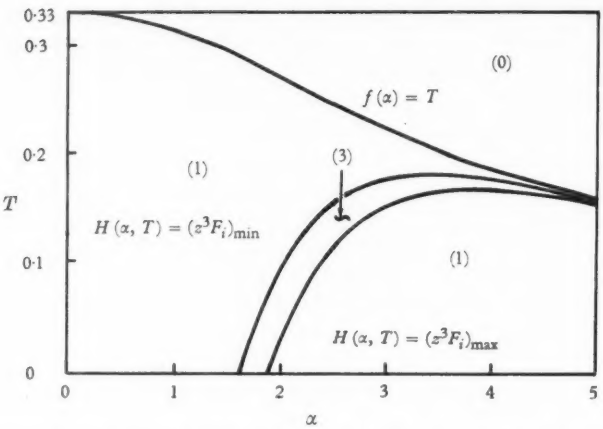

FIGURE 3. The number of branches of the neutral curves in the various α, T-regions is indicated in parentheses.

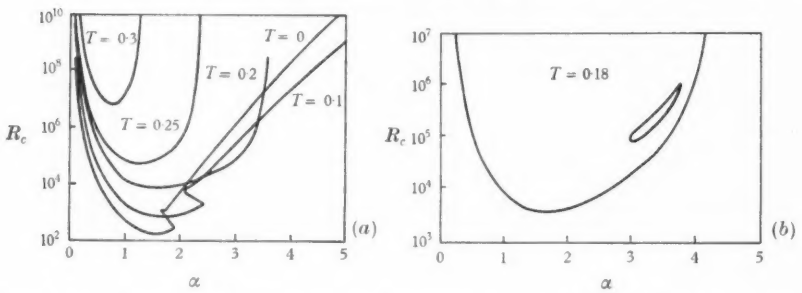

FIGURE 4*a*. The neutral stability curves determined by (6.1) and (6.5) for $G = 0$. If $G > 0$ the parameter labelled T may be replaced by $T + G\alpha^{-2}$.

FIGURE 4*b*. A neutral stability curve with an island of stability.

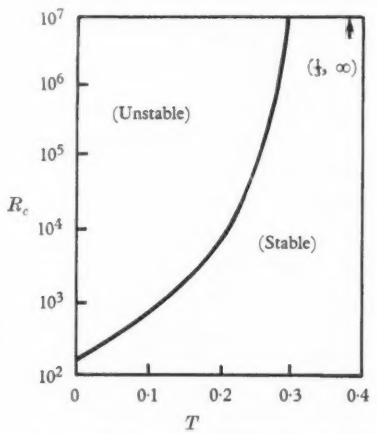

FIGURE 5. The (T, R)-locus of stability, as determined from the minima of the neutral curves.

$T = 0{\cdot}18$, illustrating an island of stability, in figure 4*b*.† The minimum values of the neutral curves are plotted versus T in figure 5. We remark that, although increasing T has a stabilizing effect for all α below α_c (where α_c indicates the location of R_c) and for sufficiently large α, there exist intermediate ranges of α for which increasing T is destabilizing.

7. Determination of most unstable mode

If $R > R_c$ the disturbance of (2.2) will grow like $\exp(\alpha c_i t)$, and the most unstable mode is that for which αc_i is a maximum.

We may obtain an approximation to αc_i that is at least qualitatively accurate by assuming $|c| \ll 1$ in (4.6) and letting $G = 0$, whence

$$c = \frac{\alpha \coth\alpha - 1 - T\alpha^2}{2\alpha\coth\alpha - 1 - \alpha^2 \operatorname{cosech}^2\alpha\, F(z)} - \frac{2i\alpha}{R} \tag{7.1a}$$

$$= \frac{[f(\alpha) - T]\mathscr{F}(z)\sinh^2\alpha}{1 + [1 - \alpha^2 f^2(\alpha)]\mathscr{F}(z)\sinh^2\alpha} - \frac{2i\alpha}{R}, \tag{7.1b}$$

where $f(\alpha)$ is defined by (4.4) and

$$\mathscr{F}(z) = [1 - F(z)]^{-1}. \tag{7.2}$$

Assuming $|c_i| \ll c_r$, approximating $\mathscr{F}$ according to

$$\mathscr{F}(z_r + iz_i) = \mathscr{F}_r(z_r) + i[\mathscr{F}_i(z_r) + z_i\mathscr{F}'_r(z_r)] + O(z_i^2\mathscr{F}''_r, z_i\mathscr{F}_i), \tag{7.3}$$

separating the real and imaginary parts of (7.1*b*), assuming $\alpha \gg 1$ in the resulting coefficient of R^{-1} (since it is only for $\alpha \gg 1$ that this term is significant), and eliminating c_r through

$$z_r = (\alpha R)^{\frac{1}{3}} c_r, \tag{7.4}$$

we obtain

$$z_r = \frac{R^{\frac{1}{3}}\alpha^{\frac{1}{3}}[f(\alpha) - T]\mathscr{F}_r\sinh^2\alpha}{1 + [1 - \alpha^2 f^2(\alpha)]\mathscr{F}_r\sinh^2\alpha} \tag{7.5a}$$

and

$$\alpha c_i = \frac{R^{-\frac{1}{3}}(z_r\mathscr{F}_i/\mathscr{F}_r)\alpha^{\frac{2}{3}}}{1 + [1 - \alpha^2 f^2(\alpha)]\mathscr{F}_r\sinh^2\alpha - (z_r\mathscr{F}'_r/\mathscr{F}_r)} - 2R^{-1}\alpha^2, \tag{7.5b}$$

where the argument of $\mathscr{F}_r$, $\mathscr{F}_i$, and $\mathscr{F}'_r$ is z_r. We remark that, since (see Appendix)

$$\mathscr{F}(z) \sim 1 + i(2\alpha R)^{-\frac{1}{2}} c_r^{-\frac{3}{2}}, \tag{7.6}$$

$c_i > 0$ (provided that $0 < c_r < 1$) as $R \to \infty$, in accordance with Heisenberg's criterion.

Some numerical results computed from (7.5*a*, *b*) are plotted in figure 6. The dashed portions of the curve are based on the asymptotic approximation (7.6) for $z > 5$ and are less accurate (see Appendix) than the solid portions, which were based on Lin's tabulated values for $\mathscr{F}(z)$ (and were computed prior to the recalculation of $\mathscr{F}$ described in the appendix). It appears that the maxima of the curves, where they are well defined, occur at values of α between 1 and 1·5, corresponding to wavelengths between 6 and 4 film thicknesses.

† The complete numerical results are tabulated in Table 2 of Report STL-TR-59-000-00892, Space Technology Laboratories, Inc., Los Angeles, California.

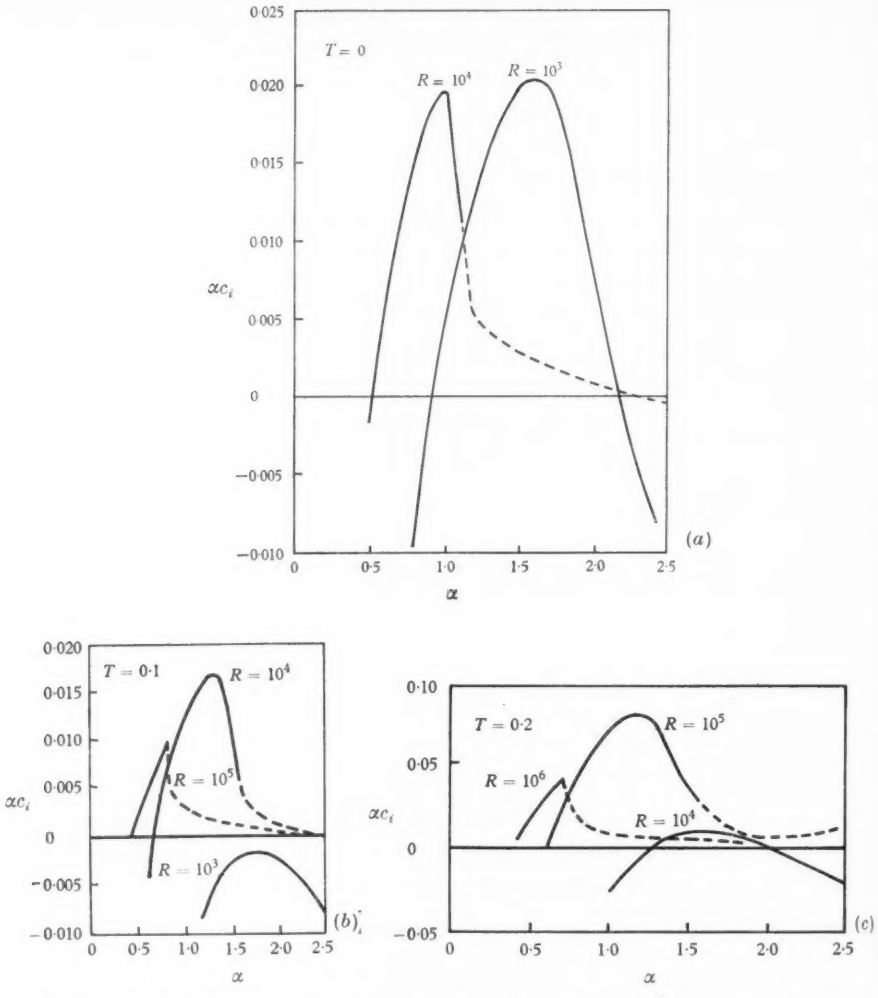

FIGURES 6*a*, *b*, *c*. The time-rate-of-growth of disturbances, as calculated from (7.5). The dashed portions of the curves are based on the asymptotic approximation (7.6).

8. Effect of upper fluid

We now consider quite briefly the dynamical effects of the upper fluid on the assumption that it too has a linear velocity profile. This consideration affords some clarification of the significance of the preceding analysis for small but finite values of the density ratio

$$r = \rho_g/\rho_l \tag{8.1}$$

and of the importance of the viscosity ratios

$$m = \mu_l/\mu_g, \quad n = rm = \nu_l/\nu_g. \tag{8.2\,a, b}$$

We emphasize that the assumption of a linear velocity profile in the upper fluid is likely to be valid only for very short wavelengths. Assuming aerodynamically smooth flow in the upper fluid, the thickness of the laminar sublayer is given approximately by

$$\delta_g = 5\nu_g/U_*, \tag{8.3}$$

where $\rho_g U_*^2$ is the shearing stress at the interface. Equating this stress to $\mu_l U_1/\delta$ and eliminating U_*, we obtain

$$\alpha_g = 2\pi\delta_g/\lambda = 5(rR)^{-\frac{1}{2}} m^{-1}\alpha. \tag{8.4}$$

Anticipating that the dynamical effects of the flow outside of the laminar sublayer would be $O[\exp(-2\alpha_g)]$, we conclude that $\alpha_g > 1$ might justify the assumption of a linear velocity profile in the upper fluid. This condition certainly was not satisfied in Knuth's experiments, and it seems unlikely that it would be satisfied in most configurations of practical interest.

Repeating Feldman's analysis except as regards the asymptotic approximation of the viscous solutions, and assuming $m \gg 1$, we obtain the asymptotic (as $R \to \infty$) eigenvalue equation

$$[(4.6)] + [n(1-c) - r(1-c)^2\alpha e^{\alpha}\operatorname{cosech}\alpha F(Z)][1 + O(m^{-1})] = 0, \tag{8.5}$$

where [(4.6)] stands for the left-hand side of equation (4.6), F is given by (4.4), and

$$Z = -\left(\frac{\alpha R r}{m}\right)^{\frac{1}{3}}(1-c) = -\left(\frac{r}{m}\right)^{\frac{1}{3}}\left(\frac{1-c}{c}\right)z. \tag{8.6 a, b}$$

Let us consider first the values of c for $R = \infty$, where (8.5) yields

$$\alpha\coth\alpha(1-c)^2 - (1-n)(1-c) - (T\alpha^2 + G) = 0 \tag{8.7}$$

in place of (5.1). If $n \ll 1$ its only significant effect is to reduce α_0^2, as may be seen by replacing G by $G-n$ in (5.7 *a*). If $n < 1$ but is not small it also raises the value of α_1 (the upper limit of α for which $c > 0$ is possible), but otherwise it does not affect the disposition of the roots relative to 0 and 1. If $n > 1$ the disposition of the roots is affected; for example, if $T\alpha^2 + G \ll n-1$ the roots to (8.7) are given approximately by

$$1 - c \doteq \frac{T\alpha^2 + G}{n-1}, \quad -(n-1)\frac{\tanh\alpha}{\alpha}. \tag{8.8 a, b}$$

Small, positive values of c then are impossible, and the primary instability may be associated with a mode for which $c > 1$, in which case the upper fluid no longer can be relegated to a subsidiary role, even though $r \ll 1$; moreover, the restriction (3.7) may break down if $|1-c| \ll 1$.

Turning now to the effect of the last term in (8.5), assuming c to be real and equating the imaginary part of the entire equation to zero yields

$$F_i(z) = [(6.4)]z^{-3} + r(\alpha c)^{-1}e^{\alpha}\sinh\alpha F_i(Z), \tag{8.9}$$

where [(6.4)] stands for the right-hand side of equation (6.4). We observe that the second term on the right-hand side of (8.9) will be of the same order of magni-

tude as the left-hand side if $(\alpha c)\, e^{-\alpha}\, \mathrm{cosech}\, \alpha$ is the of same order of magnitude as r; for example, if $r = 10^{-3}$ the coefficient of $F_i(Z)$ will exceed unity for $\alpha > 4{\cdot}6$. This term will represent an energy sink if $0 < c < 1$, since then $Z < 0$ and $F_i(Z) > 0$. If $c > 1$, $Z > 0$, and $F_i(Z) > (<) 0$ corresponds to an energy source (sink). We infer that the effect of the upper fluid cannot be neglected for sufficiently large α and that it will introduce a new class of modes having wave speeds in excess of the interfacial velocity. We then would expect far more complicated neutral curves, as in Lock's (1954) problem.

We again emphasize that the conclusions of the last two paragraphs are not likely to be valid if α_g is small.

9. Conclusions

We conclude that: (*a*) a thin film of liquid having a linear mean-velocity profile and bounded by a fixed wall and a free surface is unstable for sufficiently large values of both the Reynolds number R and the Weber number W; (*b*) a sufficient condition for stability of such a film with respect to small disturbances is either $R < 203$ or $W < 3$; (*c*) such a film constitutes an adequate model for a two-fluid configuration for sufficiently small values of the density ratio r, but the latter restriction may carry with it the requirement that the kinematic viscosity of the upper fluid be *large* compared with that of the film.

We have not established the conditions that determine whether the instability examined here, depending on energy transfer through the Reynolds stress in the wall layer, dominates that which could arise through energy transfer from the upper fluid, either through the Reynolds stress in the layer adjacent to the interface or through the Reynolds stress associated with profile curvature. An analysis comprising all of these models of energy transfer would be extremely involved, but it seems likely that their relative importance could be established by direct observations of wavelength and wave speed, the latter being decisive with respect to the role of Reynolds stress at the wall.

I am indebted to Mr David Giedt for programming and supervising the numerical calculations of §§ 6 and 7 and of $\mathscr{F}(z)$ in the appendix.

Appendix

The computation of $F(z)$

The function $F(z)$, as defined by (4.4) and (3.3), was introduced originally by Tietjens (1925), who computed it for $z = 0\,(0{\cdot}5)\,5$, while Lin (1945; see L 3.6) recomputed it for $z = 1\,(0{\cdot}2)\,5$; see also Holstein (1950). We have repeated the computation once again in order to obtain more accurate values of $z^3 F_i(z)$ and also to extend the results to larger values of z.

Following Lin, we find it more convenient to consider

$$\mathscr{F}(z) = [1 - F(z)]^{-1} = -z \int_{\infty}^{-z} f_3(\zeta)\, d\zeta \Big/ \int_{\infty}^{-z} \zeta f_3(\zeta)\, d\zeta, \tag{A 1}$$

where f_3 is given by (3.3) and satisfies

$$f''(\zeta) - i\zeta f(\zeta) = 0, \quad f(\infty) = 0. \tag{A 2 a, b}$$

Integrating (A 2 *a*) subject to (A 2 *b*), we obtain

$$\int_{\infty}^{\zeta} \zeta f_3(\zeta)\, d\zeta = -if_3'(\zeta), \tag{A 3}$$

whence (A 1) reduces to

$$\mathscr{F}(z) = \frac{z}{if_3'(-z)} \int_{\infty}^{-z} f_3(\zeta)\, d\zeta. \tag{A 4}$$

We may reduce the remaining integral to one more suitable for numerical evaluation with the aid of the result [W 13.21 (8), where W indicates Watson's treatise (1945)]

$$\int_0^{\infty} f_3(\zeta)\, d\zeta = \left(\frac{2}{\sqrt{3}}\right) e^{-11i\pi/12}. \tag{A 5}$$

We also find it convenient to introduce

$$g(z) = +\frac{e^{3i\pi/4}}{2\sqrt{3}} f_3(\zeta) = \mathrm{Ai}\,(z\, e^{-5i\pi/6}), \quad (z = \zeta\, e^{i\pi}), \tag{A 6 *a*, *b*}$$

where Ai denotes the Airy function of the first kind. Substituting (A 5) and (A 6 *a*, *b*) in (A 4) and (A 2 *a*), we obtain

$$\mathscr{F}(z) = \frac{z}{ig'(z)} \left[\tfrac{1}{3}\, e^{-i\pi/6} + \int_0^z g(z)\, dz\right] \tag{A 7}$$

and

$$g''(z) + izg(z) = 0. \tag{A 8}$$

We also note that

$$g(0) = [3^{\frac{2}{3}}\Gamma(2/3)]^{-1}, \quad g'(0) = [3^{\frac{1}{3}}\Gamma(1/3)]^{-1}\, e^{i\pi/6}. \tag{A 9 *a*, *b*}$$

The differential equation (A 8) was integrated numerically, with a z-interval of 0·01, to obtain $\mathscr{F}_r, \mathscr{F}_i, \mathscr{F}_r', \mathscr{F}_i', F_r$ and F_i for $z = 0{\cdot}1\,(0{\cdot}1)\,10$ and $-z = 0{\cdot}1\,(0{\cdot}1)6$. The results are presented in table 1.

We may obtain the asymptotic series for $\mathscr{F}(z)$ by carrying out the integration in (A 4) according to [W 10.74 (51)]

$$\zeta \int_{\infty}^{\zeta} f(\zeta)\, d\zeta = -i[wS_{0,\frac{1}{3}}(w) f'(\zeta) + w^2 S_{-1,-\frac{2}{3}}(w) f(\zeta)], \tag{A 10}$$

where $S_{\mu,\nu}$ denotes Lommel's function and

$$w = \tfrac{2}{3}\zeta^{\frac{3}{2}}\, e^{3i\pi/4}. \tag{A 11}$$

Introducing the known, asymptotic series for the Hankel and Lommel functions then yields

$$\mathscr{F}(z) \sim 1 + \frac{e^{i\pi/4}}{z^{\frac{3}{2}}} + \frac{9}{4}\frac{e^{i\pi/2}}{z^3} + \frac{263}{32}\frac{e^{3i\pi/4}}{z^{\frac{9}{2}}} + O(z^{-6}) \tag{A 12 *a*}$$

$$\sim 1 + \frac{e^{-5i\pi/4}}{\zeta^{\frac{3}{2}}} + \frac{9}{4}\frac{e^{-i\pi/2}}{\zeta^3} + \frac{263}{32}\frac{e^{i\pi/4}}{\zeta^{\frac{9}{2}}} + O(\zeta^{-6}). \tag{A 12 *b*}$$

We find that (A 12 *a*) is adequate only for very large z, say $z > 10$, and is still 5 % in error at $z = 8$. On the other hand, (A 12 *b*) gives better than 0·1 % accuracy for $\zeta = -z > 5$.

TABLE 1. $\mathscr{F}_r(z)$, $\mathscr{F}_i(z)$, $\mathscr{F}'_r(z)$, $\mathscr{F}'_i(z)$, $F_r(z)$, $F_i(z)$ and $z^3F_i(z)$ versus $z = 0{\cdot}1\,(0{\cdot}1)\,10{\cdot}0$ and $-0{\cdot}1\,(0{\cdot}1)-6{\cdot}0$. The position of the decimal point for the dependent variables is given by the last two digits, preceded by a space; for example,

$$0{\cdot}2901\quad 01 \equiv 2{\cdot}901, \qquad 0{\cdot}9302-02 \equiv 0{\cdot}009302.$$

The decimal point for the independent variable is placed in its natural position.

z	$\mathscr{F}_r$	$\mathscr{F}_i$	$\mathscr{F}'_r$	$\mathscr{F}'_i$	F_r	F_i	z^3F_i	z
0·1	−0·1183 00	−0·7778−01	−0·1249 01	−0·9281 00	0·6901 01	−0·3880 01	−0·3880−02	6·3
0·2	−0·2489 00	−0·1895 00	−0·1355 01	−0·1328 01	0·3544 01	−0·1936 01	−0·1549−01	6·4
0·3	−0·3867 00	−0·3485 00	−0·1380 01	−0·1879 01	0·2427 01	−0·1286 01	−0·3472−01	6·5
0·4	−0·5188 00	−0·5712 00	−0·1221 01	−0·2605 01	0·1871 01	−0·9593 00	−0·6139−01	6·6
0·5	−0·6194 00	−0·8741 00	−0·7156 00	−0·3467 01	0·1540 01	−0·7616 00	−0·9521−01	6·7
0·6	−0·6438 00	−0·1263 01	0·3311 00	−0·4283 01	0·1320 01	−0·6284 00	−0·1357 00	6·8
0·7	−0·5321 00	−0·1716 01	0·1995 01	−0·4641 01	0·1165 01	−0·5317 00	−0·1824 00	6·9
0·8	−0·2345 00	−0·2159 01	0·3949 01	−0·4029 01	0·1050 01	−0·4578 00	−0·2344 00	7·0
0·9	0·2409 00	−0·2484 01	0·5403 01	−0·2315 01	0·9613 00	−0·3989 00	−0·2908 00	7·1
1·0	0·8061 00	−0·2605 01	0·5689 01	−0·1210 00	0·8916 00	−0·3503 00	−0·3503 00	7·2
1·1	0·1342 01	−0·2522 01	0·4895 01	0·1672 01	0·8356 00	−0·3090 00	−0·4113 00	7·3
1·2	0·1770 01	−0·2298 01	0·3640 01	0·2662 01	0·7897 00	−0·2731 00	−0·4719 00	7·4
1·3	0·2072 01	−0·2012 01	0·2445 01	0·2973 01	0·7516 00	−0·2412 00	−0·5298 00	7·5
1·4	0·2268 01	−0·1717 01	0·1521 01	0·2897 01	0·7197 00	−0·2122 00	−0·5821 00	7·6
1·5	0·2386 01	−0·1438 01	0·8724 00	0·2659 01	0·6926 00	−0·1853 00	−0·6255 00	7·7
1·6	0·2450 01	−0·1186 01	0·4354 00	0·2385 01	0·6693 00	−0·1601 00	−0·6558 00	7·8
1·7	0·2478 01	−0·9606 00	0·1412 00	0·2129 01	0·6491 00	−0·1360 00	−0·6683 00	7·9
1·8	0·2481 01	−0·7590 00	−0·6314−01	0·1910 01	0·6314 00	−0·1128 00	−0·6576 00	8·0
1·9	0·2467 01	−0·5774 00	−0·2138 00	0·1727 01	0·6157 00	−0·8996−01	−0·6171 00	8·1
2·0	0·2439 01	−0·4126 00	−0·3339 00	0·1574 01	0·6014 00	−0·6742−01	−0·5393 00	8·2
2·1	0·2401 01	−0·2619 00	−0·4378 00	0·1443 01	0·5883 00	−0·4491−01	−0·4159 00	8·3
2·2	0·2352 01	−0·1235 00	−0·5334 00	0·1325 01	0·5760 00	−0·2227−01	−0·2371 00	8·4
2·3	0·2294 01	0·3379−02	−0·6242 00	0·1213 01	0·5641 00	0·6422−03	0·7814−02	8·5
2·4	0·2227 01	0·1191 00	−0·7107 00	0·1101 01	0·5523 00	0·2394−01	0·3310 00	8·6
2·5	0·2152 01	0·2234 00	−0·7912 00	0·9834 00	0·5403 00	0·4772−01	0·7456 00	8·7
2·6	0·2069 01	0·3155 00	−0·8625 00	0·8584 00	0·5277 00	0·7202−01	0·1266 01	8·8
2·7	0·1980 01	0·3948 00	−0·9208 00	0·7254 00	0·5143 00	0·9685−01	0·1906 01	8·9
2·8	0·1886 01	0·4604 00	−0·9625 00	0·5855 00	0·4995 00	0·1222 00	0·2682 01	9·0
2·9	0·1788 01	0·5118 00	−0·9845 00	0·4418 00	0·4831 00	0·1479 00	0·3608 01	9·1
3·0	0·1689 01	0·5487 00	−0·9851 00	0·2981 00	0·4646 00	0·1739 00	0·4695 01	9·2
3·1	0·1592 01	0·5715 00	−0·9640 00	0·1593 00	0·4435 00	0·1998 00	0·5952 01	9·3
3·2	0·1497 01	0·5809 00	−0·9225 00	0·2965−01	0·4195 00	0·2252 00	0·7379 01	9·4
3·3	0·1408 01	0·5779 00	−0·8632 00	−0·8679−01	0·3922 00	0·2495 00	0·8966 01	9·5
3·4	0·1325 01	0·5641 00	−0·7895 00	−0·1871 00	0·3611 00	0·2719 00	0·1069 02	9·6
3·5	0·1250 01	0·5411 00	−0·7055 00	−0·2695 00	0·3264 00	0·2915 00	0·1250 02	9·7
3·6	0·1184 01	0·5108 00	−0·6151 00	−0·3333 00	0·2881 00	0·3071 00	0·1433 02	9·8
3·7	0·1127 01	0·4751 00	−0·5223 00	−0·3787 00	0·2468 00	0·3174 00	0·1608 02	9·9
3·8	0·1080 01	0·4356 00	−0·4304 00	−0·4068 00	0·2036 00	0·3213 00	0·1763 02	10·0
3·9	0·1041 01	0·3942 00	−0·3424 00	−0·4194 00	0·1600 00	0·3180 00	0·1886 02	−0·1
4·0	0·1011 01	0·3522 00	−0·2603 00	−0·4183 00	0·1180 00	0·3072 00	0·1966 02	−0·2
4·1	0·9889 00	0·3109 00	−0·1859 00	−0·4058 00	0·7976−01	0·2893 00	0·1994 02	−0·3
4·2	0·9737 00	0·2714 00	−0·1203 00	−0·3842 00	0·4699−01	0·2656 00	0·1968 02	−0·4
4·3	0·9646 00	0·2343 00	−0·6392−01	−0·3556 00	0·2103−01	0·2378 00	0·1891 02	−0·5
4·4	0·9606 00	0·2004 00	−0·1708−01	−0·3222 00	0·2384−02	0·2081 00	0·1773 02	−0·6
4·5	0·9608 00	0·1700 00	0·2044−01	−0·2859 00	−0·9187−02	0·1785 00	0·1627 02	−0·7
4·6	0·9644 00	0·1433 00	0·4911−01	−0·2483 00	−0·1455−01	0·1507 00	0·1467 02	−0·8
4·7	0·9704 00	0·1203 00	0·6962−01	−0·2109 00	−0·1493−01	0·1258 00	0·1306 02	−0·9
4·8	0·9781 00	0·1010 00	0·8284−01	−0·1749 00	−0·1164−01	0·1045 00	0·1156 02	−1·0
4·9	0·9867 00	0·8524−01	0·8974−01	−0·1413 00	−0·5938−02	0·8690−01	0·1022 02	−1·1
5·0	0·9958 00	0·7267−01	0·9134−01	−0·1108 00	0·1128−02	0·7289−01	0·9111 01	−1·2
5·1	0·1005 01	0·6297−01	0·8867−01	−0·8371−01	0·8728−02	0·6212−01	0·8241 01	−1·3
5·2	0·1013 01	0·5580−01	0·8272−01	−0·6041−01	0·1625−01	0·5416−01	0·7616 01	−1·4
5·3	0·1021 01	0·5076−01	0·7444−01	−0·4092−01	0·2329−01	0·4855−01	0·7227 01	−1·5
5·4	0·1028 01	0·4749−01	0·6466−01	−0·2514−01	0·2958−01	0·4482−01	0·7057 01	−1·6
5·5	0·1034 01	0·4562−01	0·5411−01	−0·1285−01	0·3498−01	0·4257−01	0·7082 01	−1·7
5·6	0·1039 01	0·4482−01	0·4341−01	−0·3737−02	0·3942−01	0·4143−01	0·7276 01	−1·8
5·7	0·1043 01	0·4478−01	0·3305−01	0·2574−02	0·4292−01	0·4109−01	0·7610 01	−1·9
5·8	0·1046 01	0·4525−01	0·2339−01	0·6497−02	0·4553−01	0·4130−01	0·8059 01	−2·0
5·9	0·1048 01	0·4601−01	0·1471−01	0·8452−02	0·4731−01	0·4184−01	0·8594 01	−2·1
6·0	0·1049 01	0·4689−01	0·7167−02	0·8851−02	0·4836−01	0·4255−01	0·9191 01	−2·2
6·1	0·1049 01	0·4774−01	0·8349−03	0·8080−02	0·4878−01	0·4329−01	0·9826 01	−2·3
6·2	0·1049 01	0·4848−01	−0·4280−02	0·6487−02	0·4868−01	0·4397−01	0·1048 02	−2·9

TABLE 1 (*cont.*)

z	$\mathscr{F}_r$	$\mathscr{F}_i$	$\mathscr{F}_r'$	$\mathscr{F}_i'$	F_r	F_i	z^3F_i
6·3	0·1048 01	0·4902−01	−0·8229−02	0·4376−02	0·4815−01	0·4451−01	0·1113 02
6·4	0·1047 01	0·4935−01	−0·1111−01	0·2002−02	0·4729−01	0·4489−01	0·1177 02
6·5	0·1046 01	0·4942−01	−0·1303−01	−0·4284−03	0·4620−01	0·4506−01	0·1238 02
6·6	0·1045 01	0·4926−01	−0·1415−01	−0·2759−02	0·4495−01	0·4503−01	0·1295 02
6·7	0·1043 01	0·4888−01	−0·1459−01	−0·4876−02	0·4360−01	0·4481−01	0·1348 02
6·8	0·1042 01	0·4830−01	−0·1451−01	−0·6706−02	0·4222−01	0·4440−01	0·1396 02
6·9	0·1040 01	0·4755−01	−0·1403−01	−0·8210−02	0·4084−01	0·4384−01	0·1440 02
7·0	0·1039 01	0·4667−01	−0·1328−01	−0·9376−02	0·3951−01	0·4314−01	0·1480 02
7·1	0·1038 01	0·4568−01	−0·1236−01	−0·1021−01	0·3825−01	0·4234−01	0·1515 02
7·2	0·1037 01	0·4463−01	−0·1136−01	−0·1075−01	0·3706−01	0·4146−01	0·1548 02
7·3	0·1035 01	0·4354−01	−0·1034−01	−0·1101−01	0·3597−01	0·4054−01	0·1577 02
7·4	0·1035 01	0·4244−01	−0·9351−02	−0·1105−01	0·3497−01	0·3959−01	0·1604 02
7·5	0·1034 01	0·4134−01	−0·8436−02	−0·1091−01	0·3406−01	0·3863−01	0·1630 02
7·6	0·1033 01	0·4026−01	−0·7615−02	−0·1063−01	0·3324−01	0·3769−01	0·1654 02
7·7	0·1032 01	0·3922−01	−0·6901−02	−0·1024−01	0·3248−01	0·3676−01	0·1678 02
7·8	0·1031 01	0·3822−01	−0·6294−02	−0·9798−02	0·3180−01	0·3587−01	0·1702 02
7·9	0·1031 01	0·3726−01	−0·5793−02	−0·9317−02	0·3117−01	0·3502−01	0·1727 02
8·0	0·1030 01	0·3635−01	−0·5388−02	−0·8826−02	0·3058−01	0·3421−01	0·1751 02
8·1	0·1030 01	0·3549−01	−0·5067−02	−0·8344−02	0·3004−01	0·3343−01	0·1777 02
8·2	0·1029 01	0·3468−01	−0·4818−02	−0·7884−02	0·2952−01	0·3270−01	0·1803 02
8·3	0·1029 01	0·3392−01	−0·4627−02	−0·7455−02	0·2903−01	0·3201−01	0·1830 02
8·4	0·1028 01	0·3319−01	−0·4481−02	−0·7062−02	0·2855−01	0·3135−01	0·1858 02
8·5	0·1028 01	0·3250−01	−0·4368−02	−0·6708−02	0·2810−01	0·3073−01	0·1887 02
8·6	0·1027 01	0·3185−01	−0·4279−02	−0·6391−02	0·2765−01	0·3014−01	0·1917 02
8·7	0·1027 01	0·3122−01	−0·4206−02	−0·6109−02	0·2721−01	0·2957−01	0·1947 02
8·8	0·1027 01	0·3062−01	−0·4140−02	−0·5859−02	0·2678−01	0·2903−01	0·1978 02
8·9	0·1026 01	0·3005−01	−0·4079−02	−0·5638−02	0·2636−01	0·2851−01	0·2010 02
9·0	0·1026 01	0·2950−01	−0·4017−02	−0·5440−02	0·2595−01	0·2801−01	0·2042 02
9·1	0·1025 01	0·2896−01	−0·3953−02	−0·5262−02	0·2554−01	0·2752−01	0·2074 02
9·2	0·1025 01	0·2844−01	−0·3886−02	−0·5100−02	0·2514−01	0·2705−01	0·2107 02
9·3	0·1025 01	0·2794−01	−0·3815−02	−0·4951−02	0·2475−01	0·2659−01	0·2139 02
9·4	0·1024 01	0·2745−01	−0·3741−02	−0·4812−02	0·2436−01	0·2615−01	0·2172 02
9·5	0·1024 01	0·2698−01	−0·3664−02	−0·4681−02	0·2399−01	0·2572−01	0·2205 02
9·6	0·1024 01	0·2652−01	−0·3584−02	−0·4556−02	0·2362−01	0·2530−01	0·2238 02
9·7	0·1023 01	0·2607−01	−0·3503−02	−0·4436−02	0·2326−01	0·2488−01	0·2271 02
9·8	0·1023 01	0·2563−01	−0·3422−02	−0·4319−02	0·2291−01	0·2448−01	0·2304 02
9·9	0·1022 01	0·2520−01	−0·3341−02	−0·4206−02	0·2257−01	0·2409−01	0·2338 02
10·0	0·1022 01	0·2479−01	−0·3261−02	−0·4096−02	0·2223−01	0·2371−01	0·2371 02
-0·1	0·1047 00	0·5379−01	−0·9804 00	−0·4434 00	−0·6555 01	0·3880 01	−0·3880−02
-0·2	0·1964 00	0·9065−01	−0·8557 00	−0·3020 00	−0·3197 01	0·1937 01	−0·1549−01
-0·3	0·2763 00	0·1156 00	−0·7451 00	−0·2019 00	−0·2080 01	0·1288 01	−0·3477−01
-0·4	0·3459 00	0·1320 00	−0·6492 00	−0·1308 00	−0·1523 01	0·9627 00	−0·6162−01
-0·5	0·4066 00	0·1424 00	−0·5667 00	−0·8004−01	−0·1191 01	0·7671 00	−0·9588−01
-0·6	0·4597 00	0·1485 00	−0·4963 00	−0·4377−01	−0·9699 00	0·6363 00	−0·1374 00
-0·7	0·5062 00	0·1515 00	−0·4360 00	−0·1782−01	−0·8130 00	0·5425 00	−0·1861 00
-0·8	0·5472 00	0·1523 00	−0·3846 00	0·7189−03	−0·6961 00	0·4721 00	−0·2417 00
-0·9	0·5834 00	0·1515 00	−0·3404 00	0·1389−01	−0·6058 00	0·4171 00	−0·3040 00
-1·0	0·6155 00	0·1496 00	−0·3025 00	0·2314−01	−0·5341 00	0·3730 00	−0·3730 00
-1·1	0·6441 00	0·1470 00	−0·2698 00	0·2954−01	−0·4758 00	0·3368 00	−0·4483 00
-1·2	0·6696 00	0·1438 00	−0·2414 00	0·3383−01	−0·4276 00	0·3066 00	−0·5298 00
-1·3	0·6925 00	0·1403 00	−0·2168 00	0·3658−01	−0·3872 00	0·2810 00	−0·6174 00
-1·4	0·7131 00	0·1365 00	−0·1954 00	0·3819−01	−0·3528 00	0·2590 00	−0·7108 00
-1·5	0·7316 00	0·1327 00	−0·1766 00	0·3896−01	−0·3233 00	0·2399 00	−0·8098 00
-1·6	0·7484 00	0·1288 00	−0·1601 00	0·3911−01	−0·2977 00	0·2232 00	−0·9144 00
-1·7	0·7637 00	0·1249 00	−0·1455 00	0·3882−01	−0·2753 00	0·2085 00	−0·1024 01
-1·8	0·7776 00	0·1210 00	−0·1327 00	0·3821−01	−0·2556 00	0·1954 00	−0·1139 01
-1·9	0·7903 00	0·1172 00	−0·1212 00	0·3737−01	−0·2381 00	0·1836 00	−0·1260 01
-2·0	0·8019 00	0·1135 00	−0·1111 00	0·3637−01	−0·2225 00	0·1731 00	−0·1385 01
-2·1	0·8125 00	0·1099 00	−0·1020 00	0·3527−01	−0·2086 00	0·1635 00	−0·1515 01
-2·2	0·8223 00	0·1065 00	−0·9390−01	0·3411−01	−0·1960 00	0·1549 00	−0·1649 01
-2·3	0·8314 00	0·1031 00	−0·8662−01	0·3291−01	−0·1846 00	0·1470 00	−0·1788 01
-2·4	0·8397 00	0·9990−01	−0·8007−01	0·3170−01	−0·1743 00	0·1397 00	−0·1931 01
-2·5	0·8474 00	0·9679−01	−0·7415−01	0·3049−01	−0·1649 00	0·1331 00	−0·2079 01
-2·6	0·8545 00	0·9380−01	−0·6881−01	0·2931−01	−0·1563 00	0·1269 00	−0·2231 01
-2·7	0·8612 00	0·9093−01	−0·6396−01	0·2814−01	−0·1484 00	0·1213 00	−0·2387 01
-2·8	0·8673 00	0·8817−01	−0·5956−01	0·2702−01	−0·1412 00	0·1160 00	−0·2547 01
-2·9	0·8731 00	0·8552−01	−0·5555−01	0·2592−01	−0·1345 00	0·1111 00	−0·2710 01

TABLE 1 (*cont.*)

z	$\mathscr{F}_r$	$\mathscr{F}_i$	$\mathscr{F}_r'$	$\mathscr{F}_i'$	F_r	F_i	z^3F_i
−3·0	0·8785 00	0·8298−01	−0·5190−01	0·2487−01	−0·1283 00	0·1066 00	−0·2878 01
−3·1	0·8835 00	0·8055−01	−0·4856−01	0·2385−01	−0·1226 00	0·1023 00	−0·3049 01
−3·2	0·8882 00	0·7821−01	−0·4550−01	0·2288−01	−0·1172 00	0·9838−01	−0·3224 01
−3·3	0·8926 00	0·7597−01	−0·4269−01	0·2195−01	−0·1123 00	0·9467−01	−0·3402 01
−3·4	0·8967 00	0·7382−01	−0·4011−01	0·2106−01	−0·1077 00	0·9118−01	−0·3584 01
−3·5	0·9006 00	0·7176−01	−0·3774−01	0·2021−01	−0·1033 00	0·8791−01	−0·3769 01
−3·6	0·9043 00	0·6978−01	−0·3555−01	0·1939−01	−0·9931−01	0·8483−01	−0·3958 01
−3·7	0·9077 00	0·6788−01	−0·3353−01	0·1862−01	−0·9552−01	0·8192−01	−0·4149 01
−3·8	0·9110 00	0·6605−01	−0·3166−01	0·1788−01	−0·9197−01	0·7917−01	−0·4344 01
−3·9	0·9141 00	0·6430−01	−0·2993−01	0·1717−01	−0·8862−01	0·7658−01	−0·4543 01
−4·0	0·9170 00	0·6262−01	−0·2832−01	0·1650−01	−0·8547−01	0·7412−01	−0·4744 01
−4·1	0·9197 00	0·6100−01	−0·2683−01	0·1586−01	−0·8251−01	0·7179−01	−0·4948 01
−4·2	0·9224 00	0·5944−01	−0·2544−01	0·1525−01	−0·7970−01	0·6958−01	−0·5155 01
−4·3	0·9248 00	0·5795−01	−0·2414−01	0·1468−01	−0·7705−01	0·6748−01	−0·5365 01
−4·4	0·9272 00	0·5651−01	−0·2293−01	0·1413−01	−0·7455−01	0·6549−01	−0·5578 01
−4·5	0·9294 00	0·5512−01	−0·2180−01	0·1361−01	−0·7217−01	0·6359−01	−0·5794 01
−4·6	0·9315 00	0·5378−01	−0·2075−01	0·1312−01	−0·6992−01	0·6177−01	−0·6013 01
−4·7	0·9336 00	0·5249−01	−0·1976−01	0·1266−01	−0·6778−01	0·6004−01	−0·6234 01
−4·8	0·9355 00	0·5125−01	−0·1885−01	0·1224−01	−0·6575−01	0·5838−01	−0·6457 01
−4·9	0·9373 00	0·5005−01	−0·1801−01	0·1184−01	−0·6381−01	0·5680−01	−0·6682 01
−5·0	0·9391 00	0·4888−01	−0·1724−01	0·1146−01	−0·6197−01	0·5528−01	−0·6910 01
−5·1	0·9408 00	0·4775−01	−0·1656−01	0·1110−01	−0·6020−01	0·5381−01	−0·7138 01
−5·2	0·9424 00	0·4666−01	−0·1595−01	0·1075−01	−0·5851−01	0·5241−01	−0·7369 01
−5·3	0·9440 00	0·4560−01	−0·1544−01	0·1037−01	−0·5687−01	0·5106−01	−0·7601 01
−5·4	0·9455 00	0·4459−01	−0·1501−01	0·9932−02	−0·5528−01	0·4977−01	−0·7836 01
−5·5	0·9470 00	0·4362−01	−0·1465−01	0·9402−02	−0·5374−01	0·4854−01	−0·8076 01
−5·6	0·9484 00	0·4271−01	−0·1431−01	0·8725−02	−0·5223−01	0·4739−01	−0·8322 01
−5·7	0·9499 00	0·4188−01	−0·1392−01	0·7854−02	−0·5075−01	0·4633−01	−0·8580 01
−5·8	0·9512 00	0·4115−01	−0·1335−01	0·6758−02	−0·4932−01	0·4539−01	−0·8857 01
−5·9	0·9525 00	0·4054−01	−0·1245−01	0·5443−02	−0·4796−01	0·4460−01	−0·9160 01
−6·0	0·9537 00	0·4007−01	−0·1097−01	0·3999−02	−0·4671−01	0·4397−01	−0·9498 01

REFERENCES

BENJAMIN, T. B. 1957 *J. Fluid Mech.* **2**, 554.

BENJAMIN, T. B. 1959 *J. Fluid Mech.* **6**, 161.

FELDMAN, S. 1957 *J. Fluid Mech.* **2**, 343.

HOLSTEIN, H. 1950 *Z. angew Math. Mech.* **30**, 25.

KNUTH, E. L. 1954 *Jet Propulsion*, **24**, 359.

LAMB, H. 1945 *Hydrodynamics.* New York: Dover.

LIN, C. C. 1946 *Quart. Appl. Mech.* **3**, 277.

LIN, C. C. 1955 *The Theory of Hydrodynamic Stability.* Cambridge University Press.

LOCK, R. C. 1954 *Proc. Camb. Phil. Soc.* **50**, 105.

MILES, J. W. 1957 *J. Fluid Mech.* **3**, 185.

MILES, J. W. 1959 *J. Fluid Mech.* **6**, 568.

MILES, J. W. 1960 *J. Fluid Mech.* **7**, 469.

PHILLIPS, O. M. 1957 *J. Fluid Mech.* **2**, 417.

TIETJENS, O. 1925 *Z. angew Math. Mech.* **5**, 200.

WATSON, G. N. 1945 *A Treatise on the Theory of Bessel Functions.* Cambridge University Press.

Natural convection above fires

By M. P. MURGAI† AND H. W. EMMONS
Pierce Hall, Harvard University

(Received 26 January 1960)

The turbulent natural convection above fires in a dry calm atmosphere with a constant lapse rate has been the subject of several recent investigations (see references). The present paper presents solution curves from which the natural convection may be computed over a fire of arbitrary size in an atmosphere with arbitrary lapse-rate variation. The independent parameters of fire size, energy release rate (buoyancy), momentum release rate and atmospheric lapse rate are given over the expected range of values. The arbitrary variation of lapse rate is thus calculable as piecewise constant.

1. Introduction

The hot gasses produced by a fire, being lighter than the ambient air, experience an upward buoyant force. Thus a column of rising hot gas is formed. If the Reynolds number of this column is low enough, the flow will remain laminar and additional air will be mixed in and carried upward through molecular processes only. If the Reynolds number is high the gas column becomes turbulent and the mixing of additional air is greatly increased. Although the precise conditions required for a completely laminar convection column are not known (at least to the authors), recent experiments indicate that for open-pan fires the hot gas column is largely turbulent for all pan sizes larger than a few inches. The turbulent flow may take a distance of a pan diameter or two to become established but all further convection column flow is fully turbulent. For this reason the present work is confined to a treatment of the turbulent convection column.

As the column rises it cools due to both expansion and the mixing of atmospheric air. Thus in an atmosphere with a stable lapse rate, the column slows its rise, finally stops, and then falls back to an equilibrium level. For an atmosphere with an unstable lapse rate, any disturbance will grow to produce a large eddy. The rising column acts as such a disturbance, is augmented as it rises, and thus localizes one of the points of overturning. For an arbitrary lapse-rate variation, the solution to the convection problem would have to be carried out for each case from the beginning, since no sufficiently simple solution has yet been found. However, if the atmosphere is considered as of piecewise constant lapse rate, and the solution is given for arbitrary fire size b^0, velocity u^0 and buoyancy $\Delta\gamma^0$, then it is possible to compute the entire column by using the final b, u, $\Delta\gamma$ values from one section as the starting values of the next.

There are several methods of treatment of the turbulent flow in the rising

† On leave from the Defence Science Laboratory, Government of India, New Delhi.

column. Schmidt (1941), the first to examine this problem, neglected vertical diffusion and used both the Prandtl momentum transfer and Taylor vorticity theories. The mixing length was assumed equal to the plume width. Later Rouse, Yih & Humpheries (1952) independently made a similar investigation and showed close agreement with experimental results. Priestly & Ball (1955) gave a solution for the movement of smoke from chimneys. They assume that the plume spreads linearly with height from the virtual source. Indirectly this is equivalent to a mechanism of turbulence.

A simpler transfer mechanism was assumed by Morton, Taylor & Turner (1956). Their solutions also agree well with experiment, thus justifying their simpler assumption. Morton (1957) later included the effect of moisture on the rising column. He also more recently (1959) extended his previous work to the mathematical discussion of finite size, positive and negative buoyancy sources in a stable atmosphere.

The effect of moisture is worthy of note since its condensation is sometimes observed over fires and such condensation alters, considerably, the convection column rise.

In the present work, the convection problem is reduced to the smallest possible number of parameters that still permits calculation of a very general case. No assumption of virtual source is made. No additional assumptions are made, but a new set of dimensionless variables is required by the desire to compute a general atmosphere in a piecewise constant manner.

2. Fundamental equations

Consider a cylindrically symmetrical convection column. Take the $\bar{x}$-axis vertically upward, and r radial. The corresponding velocity components u, v, the density ρ, the pressure p and all other fluid properties are assumed to be local mean values. Thus turbulent components are averaged out or included in other terms as shear stress τ or heat flux q. Finally, we assume that the vertical pressure distribution is given by the usual hydrostatic approximation,

$$p = p_0 - \gamma_\infty \bar{x}, \tag{1}$$

γ_∞ being the specific weight of the fluid outside the plume at infinity, and p_0 the standard pressure. The equations of conservation of mass, momentum and energy are then

$$\frac{\partial \gamma r u}{\partial \bar{x}} + \frac{\partial \gamma r v}{\partial r} = 0, \tag{2}$$

$$ru\frac{\partial u}{\partial \bar{x}} + rv\frac{\partial u}{\partial r} = \frac{r(\gamma_\infty - \gamma)}{\rho} + \frac{1}{\rho}\frac{\partial r\tau}{\partial r}, \tag{3}$$

$$r\left(u\frac{\partial h}{\partial \bar{x}} + v\frac{\partial h}{\partial r} + ug\right) = -\frac{1}{\rho}\frac{\partial rq}{\partial r}, \tag{4}$$

in which γ is the specific weight of the fluid in the plume, h is the enthalpy per unit volume, g is the acceleration due to gravity, and τ and q are the vertical shear stress and radial component of heat flux, being given, for linear turbulence, by $r\tau = -\rho\overline{v'u'}$ and $rq = \rho c_p \overline{v'T'}$, respectively. u', v' and T' are the fluctuating

components of u, v and T, and c_p the average specific heat of air at constant pressure. While deriving the equation (4), the dissipation function and vertical heat flux have been neglected.

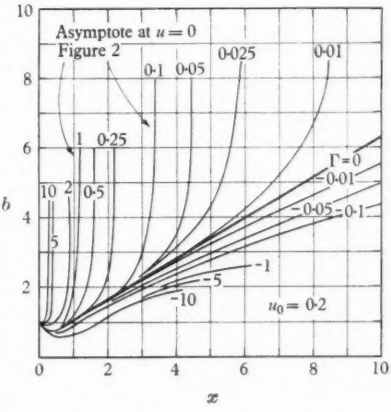

FIGURE 1. The variation of plume width b with height x and atmospheric lapse Γ. Parameter u_0 is initial plume velocity.

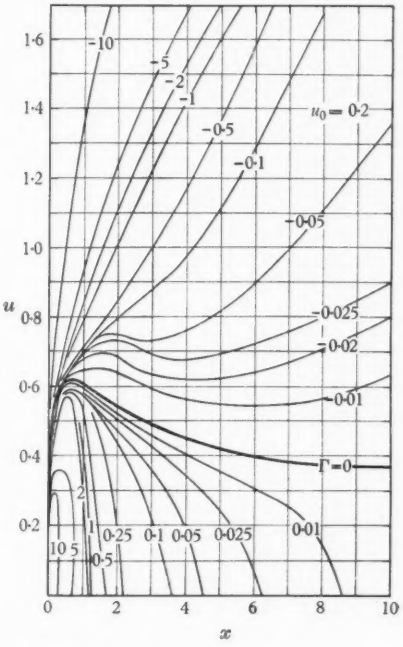

FIGURE 2. The variation of plume velocity u with height x and atmospheric lapse rate Γ. Parameter u_0 is initial plume velocity.

The major effects of the decrease of atmospheric pressure with height are taken into account in a simple way by introducing the potential temperature T_0 and specific weight γ_0 defined by

$$T_0 = \left(\frac{p_0}{p}\right)^{(k-1)/k} T, \quad \gamma_0 = \left(\frac{p_0}{p}\right)^{1/k} \gamma, \tag{5}$$

T being the absolute temperature and k the ratio of specific heats. After some manipulation the conservation equations become

$$\frac{\partial ru}{\partial \bar{x}} + \frac{\partial rv}{\partial r} = 0, \tag{6}$$

$$ru\frac{\partial u}{\partial \bar{x}} + rv\frac{\partial u}{\partial r} = \frac{rg\Delta\gamma_0}{\gamma_0} + \frac{1}{\rho_0}\frac{\partial r\tau_0}{\partial r}, \tag{7}$$

$$ru\frac{\partial}{\partial \bar{x}}\left(\frac{\Delta\gamma_0}{\gamma_0}\right) + rv\frac{\partial}{\partial r}\left(\frac{\Delta\gamma_0}{\gamma_0}\right) + ru\frac{d\ln T_{\infty 0}}{d\bar{x}} = \frac{1}{c_p T_0 \rho_0}\frac{\partial rq_0}{\partial r}, \tag{8}$$

where density variations are neglected in the continuity equation and a term involving variations of potential density is omitted from the energy equation

(see Appendix for details). The quantities with subscript 0 refer to the potential variables.

By integration of each of (6), (7), (8) from $r = 0$ to $r = \infty$, mean values of various quantities are defined. This is not a unique set of definitions but has some

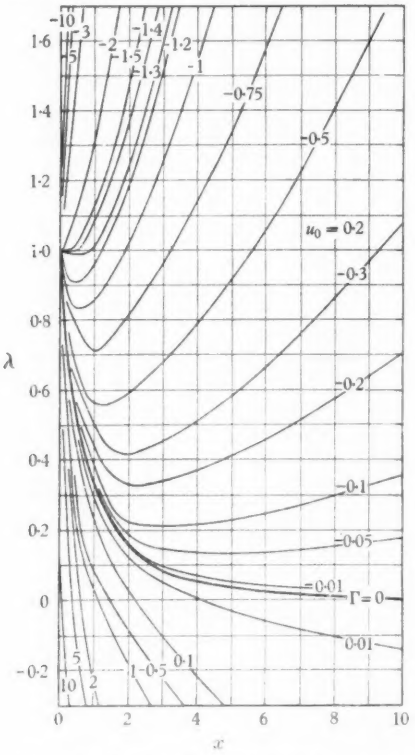

FIGURE 3. The variation of plume buoyancy λ with height x and atmospheric lapse rate Γ. Parameter u_0 is initial plume velocity.

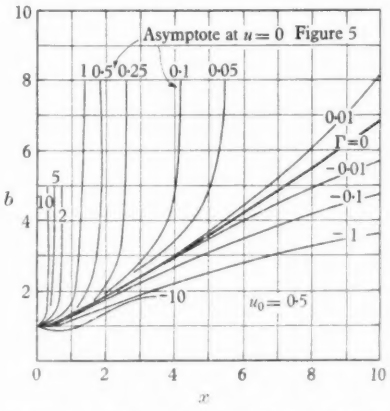

FIGURE 4. The variation of plume width b with height x and atmospheric lapse rate Γ. Parameter u_0 is initial plume velocity.

simple properties as noted below. The mean values may be looked upon as defining the equivalent top-hat profiles. Thus we obtain the mean velocity

$$\bar{u} = \frac{\int_0^\infty ru^2 dr}{\int_0^\infty ru\,dr}, \tag{9}$$

the mean width b, given by

$$b^2 = \frac{2\int_0^\infty ru\,dr}{\bar{u}}, \tag{10}$$

the mean specific gravity difference

$$\left(\overline{\frac{\Delta\gamma_0}{\gamma_0}}\right) = \frac{2}{b^2}\int_0^\infty r\frac{\Delta\gamma_0}{\gamma_0}dr, \tag{11}$$

and the shape factor

$$I = \frac{2\int_0^\infty ru\left(\frac{\Delta\gamma_0}{\gamma_0}\right)dr}{\bar{u}\left(\frac{\Delta\gamma_0}{\gamma_0}\right)b^2} = \frac{\int_0^\infty ru\left(\frac{\Delta\gamma_0}{\gamma_0}\right)dr\int_0^\infty rudr}{\int_0^\infty r\left(\frac{\Delta\gamma_0}{\gamma_0}\right)dr\int_0^\infty ru^2dr}. \tag{12}$$

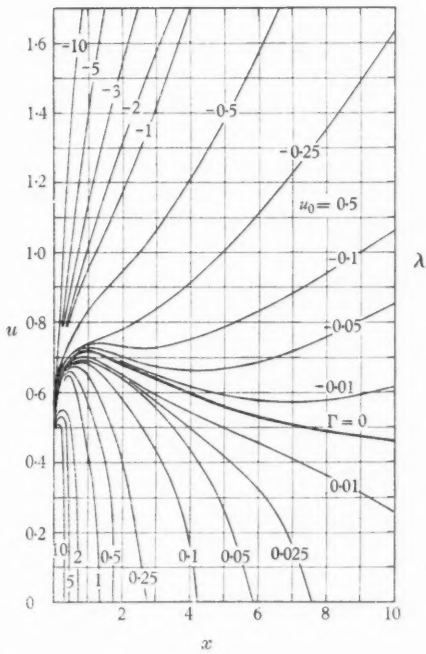

FIGURE 5. The variation of plume velocity u with height x and atmospheric lapse rate Γ. Parameter u_0 is initial plume velocity.

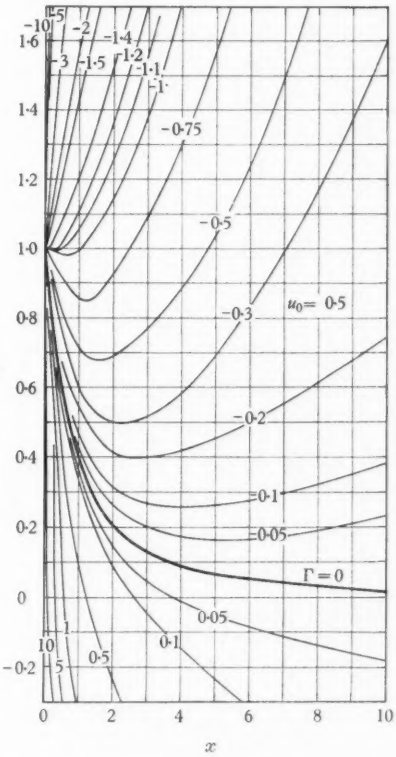

FIGURE 6. The variation of plume buoyancy λ with height x and atmospheric lapse rate Γ. Parameter u_0 is initial plume velocity.

The factor I depends upon the profile shapes as can be seen from the second form. In particular, if the velocity and specific gravity difference are of the same shape

$$u = Af(r), \quad \frac{\Delta\gamma_0}{\gamma_0} = Bf(r), \quad \text{and hence} \quad I = 1. \tag{13}$$

Furthermore, if

$$f(r) = e^{-r^2\beta^2},$$

as is sometimes assumed, then

$$\bar{u} = \tfrac{1}{2}\bar{u}_{\max.}, \quad \left(\frac{\Delta\gamma_0}{\gamma_0}\right) = \frac{1}{2}\left(\frac{\Delta\gamma_0}{\gamma_0}\right)_{\max.}, \quad b = \beta\sqrt{2}. \tag{14}$$

In the following neither (13) nor (14) will be assumed, but we will assume that I is independent of the height $\bar{x}$. If this is not so, then either a two- (or three-) dimensional theory is essential, or some assumption concerning the variation of I with $\bar{x}$ must be introduced.

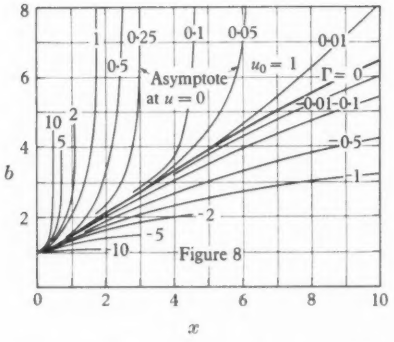

Figure 7. The variation of plume width b with height x and atmospheric lapse rate Γ. Parameter u_0 is initial plume velocity.

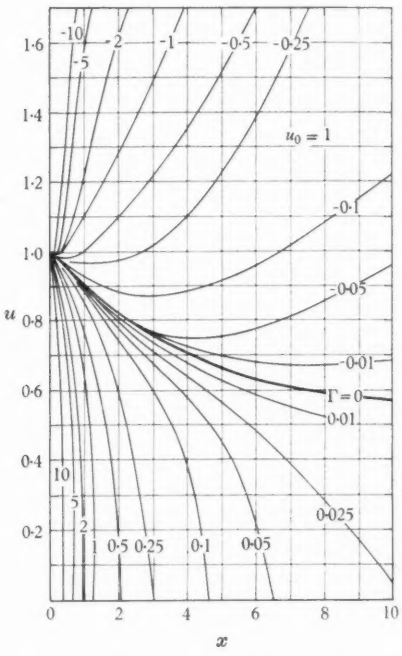

FIGURE 8. The variation of plume velocity u with height x and atmospheric lapse rate Γ. Parameter u_0 is initial plume velocity.

In terms of the above mean values, the three equations (6), (7), (8) become

$$\frac{d}{d\bar{x}}\bar{u}b^2 = \alpha\bar{u}b, \tag{15}$$

$$\frac{d}{d\bar{x}}\bar{u}^2b^2 = gb^2\frac{\overline{\Delta\gamma_0}}{\gamma_0}, \tag{16}$$

$$\frac{d}{d\bar{x}}\frac{\bar{u}\overline{\Delta\gamma_0}b^2}{\gamma_0} = -\frac{\bar{u}b^2}{I}\frac{d\ln T_{\infty 0}}{d\bar{x}}, \tag{17}$$

where $\alpha\bar{u}b = \lim_{r\to\infty}(-2rv)$ is the mass entrainment rate and α is supposed to be a constant. At the level of the ground (using the atmospheric pressure at the ground as p_0), the heat flux Q is given by

$$Q = 2\pi c_p T_\infty \int_0^\infty \frac{ru\Delta\gamma_0}{\gamma_0}dr = \pi c_p T_\infty \bar{u}\left(\frac{\overline{\Delta\gamma_0}}{\gamma_0}\right)b^2, \tag{18}$$

where the last expression assumes a top-hat distribution.

It has been customary to define dimensionless variables by use of Q. This has advantages when dealing with a point source of energy, but for the present general problem of arbitrary initial size, velocity and energy, the following is somewhat better since it simplifies the treatment of variable atmospheres. Let

$$\left.\begin{aligned} x &= \frac{\alpha \bar{x}}{\bar{b}_0}, \quad b = \frac{\bar{b}}{\bar{b}_0}, \quad u = \left(\frac{\alpha}{(\Delta\gamma_0/\gamma_0)_0}\right)^{\frac{1}{2}} \frac{\bar{u}}{(\bar{b}_0 g)^{\frac{1}{2}}}, \\ \lambda &= \frac{\Delta\gamma_0/\gamma_0}{(\Delta\gamma_0/\gamma_0)_0}, \quad \Gamma = \frac{\bar{b}_0}{\alpha I (\Delta\gamma_0/\gamma_0)_0} \frac{d \ln T_{\infty 0}}{d\bar{x}} \end{aligned}\right\} \tag{19}$$

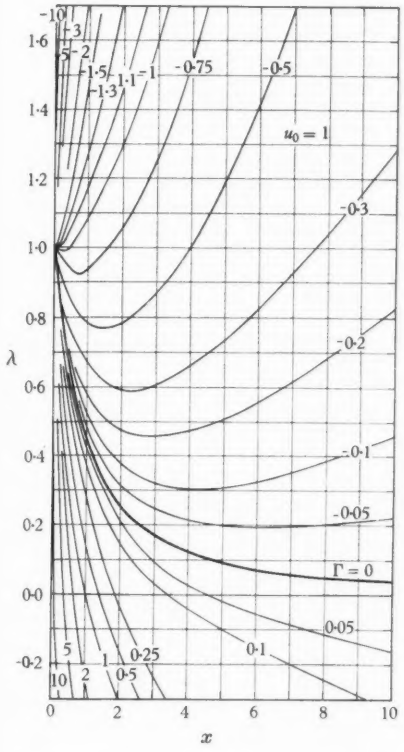

FIGURE 9. The variation of plume buoyancy λ with height x and atmospheric lapse rate Γ. Parameter u_0 is initial plume velocity.

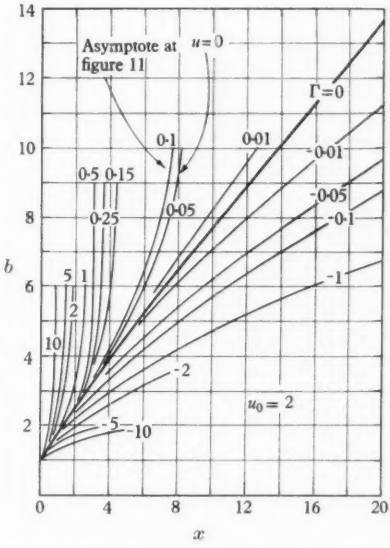

FIGURE 10. The variation of plume width b with height x and atmospheric lapse rate Γ. Parameter u_0 is initial plume velocity.

(Γ is the dimensionless lapse rate). The subscript 0 outside the brackets stand for the initial value of the potential variable. All quantities marked with an overbar have physical dimensions. (The defined quantities should not be confused with those of equations (1–11).) Note that u is the Froude number based upon buoyancy (except for α).

The final form of the conservation equations now is

$$\frac{d}{dx}ub^2 = ub, \tag{20}$$

$$\frac{d}{dx}u^2b^2 = \lambda b^2, \tag{21}$$

$$\frac{d}{dx}\lambda ub^2 = -\Gamma ub^2. \tag{22}$$

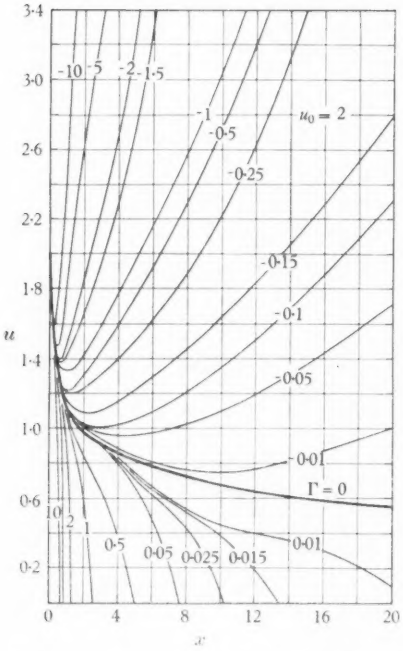

FIGURE 11. The variation of plume velocity u with height x and atmospheric lapse rate Γ. Parameter u_0 is initial plume velocity.

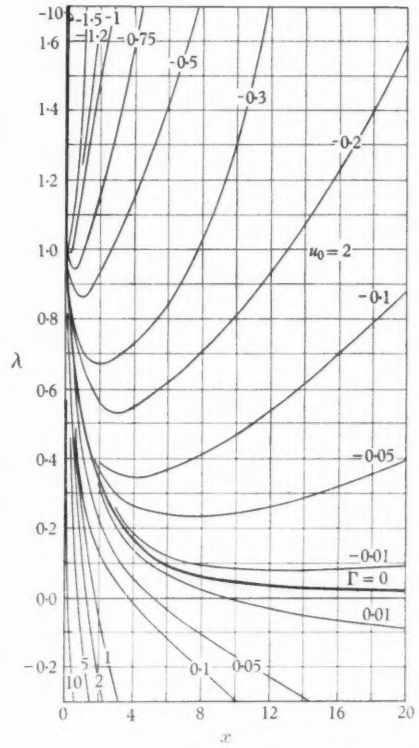

FIGURE 12. The variation of plume buoyancy λ with height x and atmospheric lapse rate Γ. Parameter u_0 is initial plume velocity.

If we are interested in an arbitrary atmosphere, the lapse rate is a function of height ($\Gamma = \Gamma(x)$). In view of the approximations already made it appears sufficiently accurate to take Γ as constant over ranges of x. Thus for any range (n) the boundary conditions at its lower edge ($x_n = 0$) are simply related to the solution at the top ($x_{n-1} = L_{n-1}$) of the next lower range ($n-1$). Thus for any range of height, the boundary conditions are

$$x_n = 0, \quad b_n = 1, \quad \lambda_n = 1,$$

$$u_n = u_0 \text{ for new range} = \left[\frac{u_{n-1}}{(\lambda_{n-1}b_{n-1})^{\frac{1}{2}}}\right]_{x_{n-1}=L_{n-1}}. \tag{23}$$

The solutions to equations (20), (21), (22), with boundary conditions (23) were drawn by a Pace computer for the following values of the two parameters

$$u_0 = 0{\cdot}2,\ 0{\cdot}5,\ 1,\ 2,\ 5, \quad -10 < \Gamma < 10.$$

These values were chosen to cover the range of fire convection columns. The value $u_0 = 0$ was omitted in spite of the fact that a hot plate appears to initiate such a rising column. The equations yield an unreal singular solution (see (24) below). This is as it should be, since our equations neglect vertical conduction.

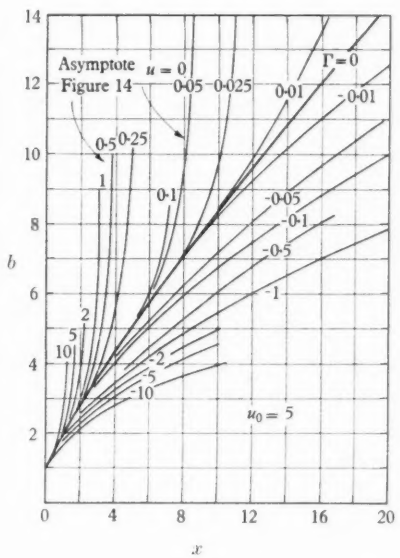

FIGURE 13. The variation of plume width b with height x and atmospheric lapse rate Γ. Parameter u_0 is initial plume velocity.

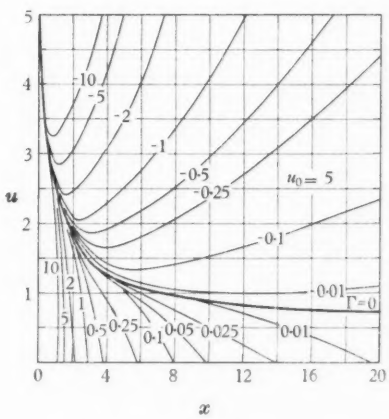

Figure 14. The variation of plume velocity u with height x at atmospheric lapse rate Γ. Parameter u_0 is initial plume velocity.

Figures 1 to 15 present velocity u, density defect λ and column width b as functions of x and the parameter Γ for each of the five chosen values of initial velocity u_0.

As mentioned before, the solution may be developed from these curves by interpolation in Γ at constant u_0 until such atmospheric height that the $d\,(\ln T_{\infty 0})/dx$ changes to a new constant value. At this height the computation must be started again using new values of u_0 and Γ (and, of course, a new elevation datum $x = 0$).

At the start of the computation, or when changing from one constant region to another, the value of u_0 may not fall on one of the values for which curves are presented in figures 1 to 15. One can sometimes with sufficient accuracy interpolate between available u_0 as well as Γ values. Such double interpolation

can be avoided by calculating a short range of altitude by the following approximate formulas:

$$\left.\begin{aligned} u &= u_0 + \left(\frac{1}{u_0} - u_0\right)x - \frac{x^2}{2u_0^3}\left(1 + \frac{2\Gamma+3}{2}u_0^2\right) + \ldots, \\ \lambda &= 1 - (\Gamma+1)x + \frac{x^2}{4}\left(2\Gamma - \frac{1}{2u_0^2}\right) + \ldots, \\ b &= 1 + \left(1 - \frac{1}{2u_0^2}\right)x + \frac{1}{8u_0^4}\{3 + 2u_0^2(\Gamma-2)\}x^2 + \ldots. \end{aligned}\right\} \tag{24}$$

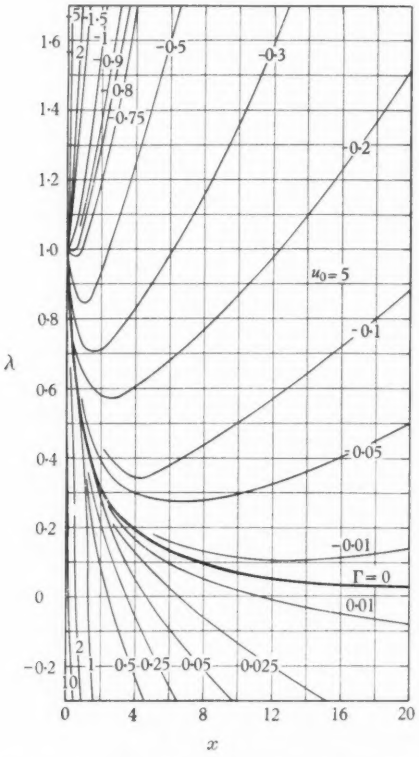

FIGURE 15. The variation of plume buoyancy λ with height x and atmospheric lapse rate Γ. Parameter u_0 is initial plume velocity.

This calculation should be continued to such a value of x that if a new range is again started, u_0 has one of the 5 available values. This value of x, given to the first order in x, is

$$x = \frac{4u_0(u_0^* - u_0)}{5 + 2u_0^2(\Gamma-2)}, \tag{25}$$

where u_0, Γ are values appropriate to the short range being computed and u_0^* is the nearest u_0 for one of the available solution graphs.

To illustrate the method of use of the solutions herein presented, the following problem is solved. Suppose a fire of 10 m diameter releases heat at the rate

10^8 cal/sec. Suppose, in agreement with some rough measurements, the upward velocity just above the flames is $\bar{u} = 3$ m/sec.

Atmospheric conditions chosen are those which existed over Seattle, Washington on 1 August 1957. The temperature, potential temperature and piecewise constant lapse rate are shown in figure 16.

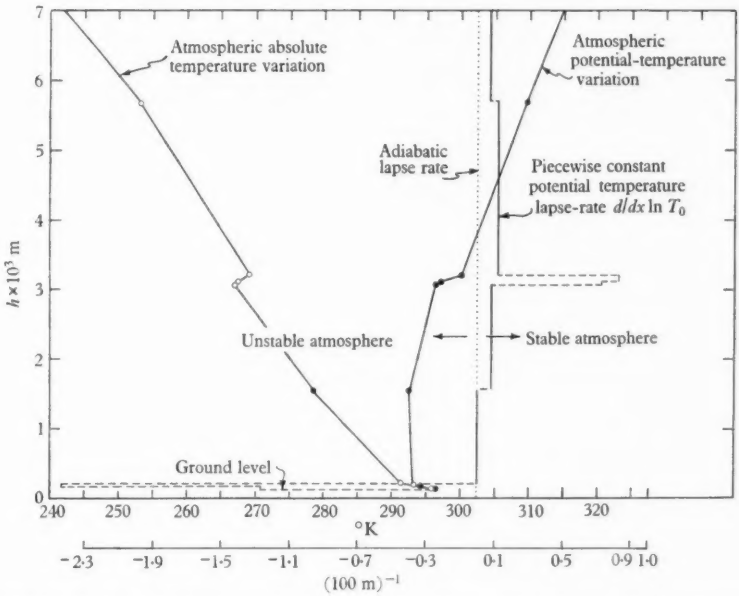

FIGURE 16. Variation of temperature, potential temperature and potential temperature lapse-rate with height above sea level on 1 August 1957, Seattle, Washington.

By (18) and the given data, one finds that at the ground level ($h = 125$ m above sea level) the buoyancy value is

$$\frac{\Delta\gamma_{00}}{\gamma_{00}} = 0{\cdot}614,$$

and, by (19), using $\alpha = 0{\cdot}1$, that $u_0 = 0{\cdot}13$, $\Gamma = -0{\cdot}021$. This completes the first line of table 1. The value $u_0 = 0{\cdot}13$ does not correspond to any of the available solution curves. The nearest is $u_0 = 0{\cdot}2$. Equation (25*a*) indicates that, at $x = 0{\cdot}007$ diameters, a new start would result in $u_0 = 0{\cdot}2$. Now equations (24) give line 2 of table 1 while line 3 gives the starting values for use with the solution curves.

The height of the top of the first lapse-rate range is 52 m. Thus $\bar{x}$ varies from 0 to 51·3 m, or in dimensionless form, from 0 to 64. The solution curves now give values for u, b, λ at $x = 0{\cdot}64$, $u_0 = 0{\cdot}2$, $\Gamma = -0{\cdot}017$. Thus line 4 of table 1 can be completed.

The next lapse-rate range begins at $h = 52$ m and ends at 75 m. This range is computed as above except that interpolation between $u_0 = 1$ and $u_0 = 2$ is more

convenient than use of (25). Additional lapse-rate ranges are computed in the same manner up to range 5 where the velocity falls to zero. Thus we find that at $h = 2180$ m the column stops rising. The buoyancy falls essentially to zero at a height of 704 m and goes negative at a height of about 1400.

The resultant changes in the column velocity, diameter and buoyancy are plotted in figure 17.

h m above ground	Range	$\bar{x}$ m	x initial range diam.	Γ	u range dimensionless	u initial dimensionless	$\bar{u}$ m/sec	b initial range diam.	b fire diam.	$\bar{b}$ m	λ fraction of initial range value	λ fraction of initial fire value	λ local density difference ratio
0	1	0	0	− 0·021	0·13	0·13	3·0	1	1	10	1	1	0·614
0·7	1	0·7	0·007	− 0·021	0·183	0·183	4·2	0·80	0·8	8	0·99	0·99	0·608
0·7	2	—	0	− 0·017	0·20	—	—	1	0·8	—	1	—	—
52	2	51·3	0·64	− 0·017	0·63	0·573	13·1	0·80	0·64	6·4	0·45	0·446	0·274
52	3	—	0	− 0·057	1·07	—	—	1	0·64	—	1	0·446	—
75	3	23	0·36	− 0·057	1·05	0·561	12·9	1·12	0·72	7·2	0·7	0·31	0·190
75	4	—	0	≃ 0	1·186	—	—	1	—	—	1	—	—
579	4	504	7	≃ 0	0·636	0·301	7·0	5·16	3·72	37·2	0·062	0·028	0·017
579	5	—	0	—	1·132	—	—	1	—	—	1	—	—
951	5	372	1	0·021	1·132	0·251	5·8	1·51	5·62	56·2	0·43	0·020	0·012
1395	5	816	2·19	0·021	0·808	0·215	5·0	2·29	8·54	85·4	0·221	0·0042	0·002
1395	6	—	—	—	1·164	—	—	1	—	—	1	—	—
1600	6	205	0·24	2·76	1·164	0·18	4·2	2·55	9·5	95·0	—	−0·04	−0·025
2180	6	785	0·92	—	0	0	0	∞	∞	∞	—	−0·3	−0·18

TABLE 1

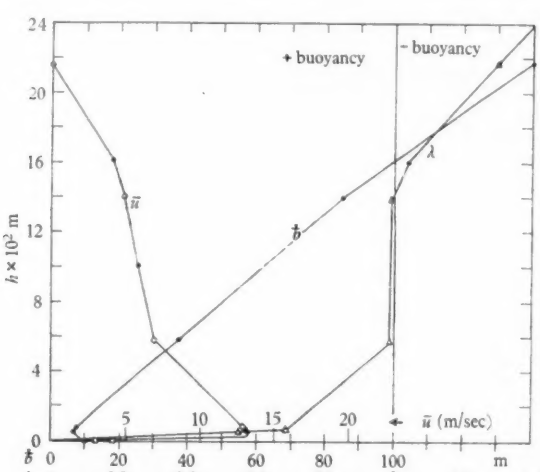

FIGURE 17. Properties of buoyancy plume in atmosphere of figure 16 due to 10 m diameter fire liberating 10^5 k cal/sec energy. Initial values: $\bar{b} = 10$ m, $\bar{u} = 3$ m/sec, $(\Delta\gamma_0/\gamma_0)_0 g = 0{\cdot}602$.

Appendix

If terms are not neglected, equations (6), (7), (8), are replaced by

$$\frac{\partial}{\partial \bar{x}}\rho_0 ur + \frac{\partial}{\partial r}\rho_0 vr - \rho_0 \frac{ru}{kp}\rho_{\infty 0} g\left(\frac{p}{p_0}\right)^{1/k} = 0, \tag{1a}$$

$$r\left(u\frac{\partial u}{\partial \bar{x}} + v\frac{\partial u}{\partial r}\right) = r\frac{\Delta\gamma_0}{\gamma_0}g + \frac{1}{\rho_0}\frac{\partial}{\partial r}r\tau_0, \tag{2a}$$

$$r\left(u\frac{\partial T_0}{\partial \bar{x}} + v\frac{\partial T_0}{\partial r}\right) = \frac{ru\rho_{\infty 0}g}{p}\left(\frac{p}{p_0}\right)^{1/k}\left\{T_0\frac{k-1}{k} - \frac{p_0}{\rho_0 c_p}\right\} - \frac{1}{\rho_0 c_p}\frac{\partial}{\partial r}(rq_0). \tag{3a}$$

Introducing the ideal gas relation between T_0 and $\Delta\gamma_0/\gamma_0$,

$$T_0 = T_{\infty 0}\frac{\Delta\gamma_0}{\gamma_0} + T_{\infty 0},$$

equation $3a$ becomes

$$r\left(u\frac{\partial}{\partial \bar{x}}\frac{\Delta\gamma_0}{\gamma_0} + v\frac{\partial}{\partial r}\frac{\Delta\gamma_0}{\gamma_0}\right) + ur\frac{d}{dx}\ln T_{\infty 0} = -ru\frac{\Delta\gamma_0}{\gamma_0}\frac{d}{dx}\ln T_{\infty 0}$$
$$+ ru\rho_{\infty 0}g\left(\frac{p_0}{p}\right)^{(k-1)/k}\left[\frac{k-1}{k}\frac{\rho_{\infty 0}}{\rho_0} - \frac{1}{\rho_0 c_p T_{\infty 0}}\right] - \frac{1}{\rho_0 c_p T_{\infty 0}}\frac{\partial}{\partial r}(rq_0). \tag{4a}$$

Following the steps of derivation and definition of mean and dimensionless quantities as in the paper, assuming ρ_0 constant in $1a$, and further noting that

$$\frac{k-1}{k} = \frac{R}{c_p} = \frac{p_0}{c_p T_0 \rho_0},$$

R being the gas constant per unit mass, we find that equations (20), (21), (22) become

$$\frac{d}{dx}b^2 u = bu - b^2 ux^*,$$

$$\frac{d}{dx}b^2 u^2 = b^2\lambda - b^2 u^2 x^*,$$

$$\frac{d}{dx}b^2 u\lambda = -b^2 u\Gamma - b^2 u\lambda\,(\delta^* - x^*),$$

where

$$\delta^* = \frac{b_0}{\alpha}\frac{d}{d\bar{x}}\ln T_{\infty 0} \quad \text{and} \quad x^* = \frac{b_0}{\alpha}\frac{\rho_{\infty 0}}{kp}g\left(\frac{p}{p_0}\right)^{1/k} = \frac{b_0 g}{\alpha k R T_{\infty 0}\left(\frac{p}{p_0}\right)^{(k-1)/k}}.$$

x^* is a measure of the variation of the potential density with height and in view of the equation (1) is given as an explicit function of $(p_0/p)^{(k-1)/k}$. x^* does not become important unless we are dealing with large fires and large heights (large pressure ratios). For example, for a fire size of $10k$ and for $(p_0/p) \approx 4$, $x^* = 0{\cdot}3$. This pressure ratio corresponds almost to the top of the troposphere. For most fires and an atmosphere of several stable and unstable lapse rates, this height will never be reached and x^* will therefore be even less important. δ^* can be neglected compared with Γ, as is apparent from their definition, for temperatures $T_0 \ll 2T_{\infty 0}$.

This research was supported by the United States Air Force under Contract No. AF49(638)-29, monitored by the Air Force Office of Scientific Research, Air Research and Development Command. The authors gratefully acknowledge this support.

REFERENCES

MORTON, B. R. 1957 *J. Fluid Mech.* **2**, 127.
MORTON, B. R. 1959 *J. Fluid Mech.* **5**, 151.
MORTON, B. R., TAYLOR, G. I. & TURNER, J. S. 1956 *Proc. Roy. Soc.* A, **236**, 1.
PRIESTLY, C. H. B. & BALL, F. K. 1955 *Quart. J. R. Met Soc.* **81**, 144.
ROUSE, H., YIH, C. S. & HUMPHERIES, H. W. 1952. *Tellus*, **4**, 201.
SCHMIDT, W. 1941 *Z. angew Math. Mech.* **21**, 265, 351.

Propagation of waves of finite amplitude along a duct of non-uniform cross-section

By JAN ROŚCISZEWSKI
Pierce Hall, Harvard University

(Received 15 August 1959 and in revised form 16 February 1960)

This paper is concerned with the propagation of a simple wave along a duct of initially constant and then slowly varying cross-section. The equations of motion are linearized in the deviations from the simple wave solution. The solution for the propagation of a centred simple rarefaction wave is obtained in closed form and compared with the results of step-by-step calculations. The results are also found to be good when the area change is not small. Some remarks on boundary-layer influence are included.

1. Introduction

In this paper, the method of small parameters is applied to the system of partial differential equations which govern unsteady flow through ducts of variable cross-section (see Rudinger 1950)

$$\frac{\partial r}{\partial \alpha} \equiv \frac{\partial r}{\partial t} + (V+a)\frac{\partial r}{\partial x} = -\frac{a}{2}\frac{D \ln A}{Dt} + \frac{a}{2(k-1)c_p}\frac{\partial S}{\partial \alpha} + F_1(a, V, x, t) \tag{1}$$

$$\frac{\partial s}{\partial \beta} \equiv \frac{\partial s}{\partial t} + (V-a)\frac{\partial s}{\partial x} = -\frac{a}{2}\frac{D \ln A}{Dt} + \frac{a}{2(k-1)c_p}\frac{\partial S}{\partial \beta} + F_2(a, V, x, t), \tag{2}$$

where

$$r = \frac{a}{k-1} - \frac{V}{2}, \quad s = \frac{a}{k-1} + \frac{V}{2}$$

are the Riemann invariants, V is the velocity of flow, a the velocity of sound, A the cross-section area of the duct, S the specific entropy, α and β the characteristic directions, c_p the specific heat at constant pressure, and F_1, F_2 the coefficients representing the influence of the boundary layer.

2. A centred rarefaction wave in a duct of slowly varying cross-section

Neglecting boundary-layer influence, assuming that

$$A = A(x,t) = A^0 + \epsilon_A(x,t),$$

where $\epsilon_A \ll A^0$, and representing all parameters as the sum of parameters corresponding to a simple wave and disturbances caused by area change; we write $V = V^0 + \epsilon_V$ where $\epsilon_V \ll V^0$, $a = a^0 + \epsilon_a$ where $\epsilon_a \ll a^0$, $r = r^0 + \epsilon_r$ where $\epsilon_r \ll r^0$, and

$s = s^0 + \epsilon_s$ where $\epsilon_s \ll s^0$. After substituting these relations into (1) and (2) we get

$$\frac{\partial \epsilon_r}{\partial \alpha} \equiv \frac{\partial \epsilon_r}{\partial t} + (V^0 + a^0)\frac{\partial \epsilon_r}{\partial t} = -\frac{V^0 a^0}{2}\frac{D \ln \epsilon_A}{Dt} \equiv -\frac{V^0 a^0}{2}\psi(x,t), \tag{3}$$

$$\frac{\partial \epsilon_s}{\partial \beta} \equiv \frac{\partial \epsilon_s}{\partial t} + (V^0 - a^0)\frac{\partial \epsilon_s}{\partial t} = -\frac{V^0 a^0}{2}\psi(x,t), \tag{4}$$

where $\psi(x,t)$ is a given function of x and t.

These equations are independent linear differential equations of the first order. The coefficients of these equations can be calculated (see Courant & Friedrichs 1948) by the use of the simple wave relations (see figure 1). We get

$$V^0 = \frac{2}{k+1}\left[\frac{x}{t} - (k-1)s^0\right], \tag{5}$$

$$a^0 = \frac{k-1}{k+1}\left(\frac{x}{t} + 2s^0\right). \tag{6}$$

We thus obtain

$$\frac{\partial \epsilon_r}{\partial t} + \frac{x}{t}\frac{\partial \epsilon_r}{\partial x} = -\frac{k-1}{k+1}\left[\left(\frac{x}{t}\right)^2 - (k-3)\frac{x}{t}s^0 - 2(k-1)s^{0^2}\right]\psi(x,t), \tag{7}$$

$$\frac{\partial \epsilon_s}{\partial t} + \left[\frac{3-k}{k+1}\frac{x}{t} - \frac{4(k-1)}{k+1}s^0\right]\frac{\partial \epsilon_s}{\partial x} = -\frac{k-1}{k+1}\left[\left(\frac{x}{t}\right)^2 - (k-3)\frac{x}{t}s^0 - 2(k-1)s^{0^2}\right]\psi(x,t). \tag{8}$$

Integrating the first equation, we find the characteristics are

$$\frac{x}{t} = c = \text{const.}, \tag{9}$$

and along these characteristics

$$\epsilon_r = \frac{k-1}{k+1}\left[\frac{x}{t} - (k-3)s^0 - \frac{2t}{x}(k-1)s^{0^2}\right]\Psi + C_\alpha\left(\frac{x}{t}\right), \tag{10}$$

where $$\Psi \equiv \Psi(x,t) = \int \psi\left(x, \frac{x}{c}\right)dx,$$

and the C_α are constants which take a different value on each characteristic α. This value we can calculate from the condition that for $x = L + 0$, $\epsilon_r = 0$.

Assuming for simplicity that $\Psi \equiv \Psi(x)$, we get

$$\epsilon_r = -\frac{k-1}{k+1}\left[\frac{x}{t} - (k-3)s^0 - \frac{2t}{x}(k-1)s^{0^2}\right]\Psi(x) + \frac{k-1}{k+1}\left[\frac{L}{t} - (k-3)s^0 - \frac{2t}{L}(k-1)s^{0^2}\right]\Psi(L+0). \tag{11}$$

If, for the sake of example, $A/A_0 = e^{Kx}$, where K is constant, then

$$\epsilon_r = -\frac{k-1}{k+1}\left[\frac{x-L}{t} + \frac{2t(x-L)}{xL}(k-1)s^{0^2}\right]K. \tag{12}$$

A solution in closed form for ϵ_r could also have been obtained for a non-centred wave. Integrating equation (8), we find the β-characteristics of the centred wave are given by

$$x = C_1 t^{(3-k)/(k+1)} - 2s^0 t, \tag{13}$$

where $C_1 = \text{const.}$ along each β-characteristic.

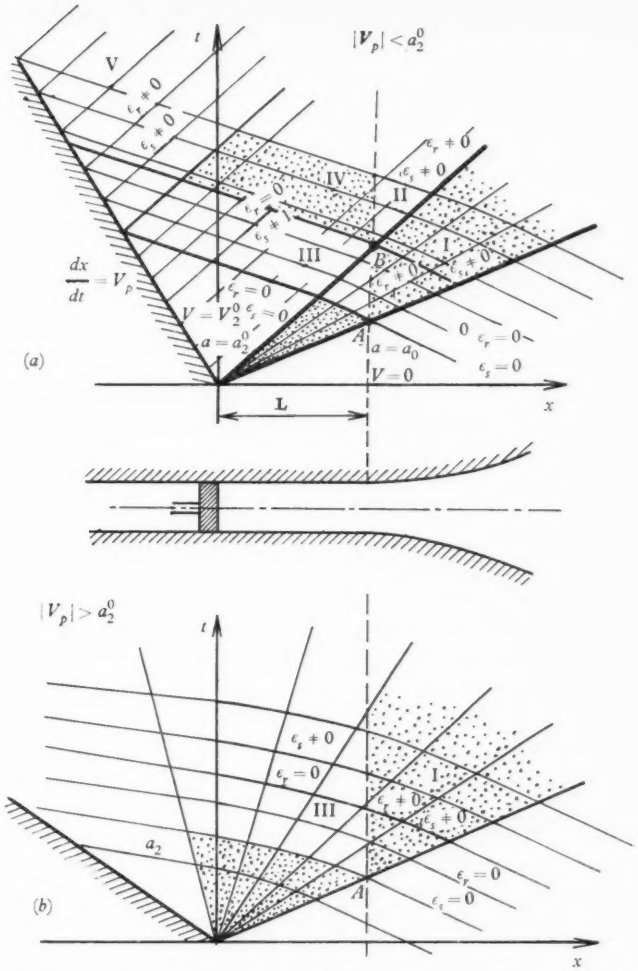

FIGURE 1. Propagation of a centred rarefaction wave through a duct of slowly variable cross-section. (*a*) Subsonic flow behind the rarefaction wave. (*b*) Supersonic flow behind the rarefaction wave.

It is of interest that we get a wave in which the characteristics as given by equations (9) and (13) are the same as for a simple wave (in a duct of constant cross-section). To the present approximation, the α and β characteristics coincide for waves in a duct with constant or slowly varying cross-section.

The change of ϵ_s along the β-characteristics is given by

$$\epsilon_s = -\frac{k-1}{k+1}\int \{[C_1 t^{[2(1-k)/(k+1)]} - 2s^0]^2 - (k-3)[C_1 t^{[2(k-1)/(k+1)]} - 2s^0]s^0 - 2(k-1)s^{0^2}\}\psi\, dt. \tag{14}$$

For simplicity we shall evaluate this integral only for a special duct with shape prescribed by

$$A = A^0 e^{Kx}, \tag{15}$$

where $K = \text{const}$.

We get, after substituting for C_1 from (13),

$$\epsilon_s = -\frac{k-1}{k+1}(x+2s^0t)\left[\frac{x+2s^0t}{(5-3k)t} - \frac{k+1}{3-k}s^0\right]K + C_\beta, \tag{16}$$

where C_β is constant along the β-characteristic and can be calculated from the boundary conditions on the front of the wave; namely, $V = 0$, $a = a_0$, $\epsilon_s = 0$ for $x/t = a_0$. Then we obtain

$$C_\beta = \frac{2Ka_0^2(k+1)t}{(5-3k)(3-k)}. \tag{17}$$

Equations (12) and (16) give the values of the deviation of the flow parameters from the simple wave solution in region I prescribed by $x \geqslant L$ (see figure 1) and

$$\frac{x}{a_0 + \frac{1}{2}(k+1)V_0^2} \geqslant t \geqslant \frac{x}{a_0},$$

where V_2^0 is the velocity on the back of the centred wave. In the special case when $|V_2^0| > a_2^0$, point B (figure 1*b*) is at infinity.

For the case of subsonic flow behind the centred wave, there is a reflected wave-region III (see figure 1*a*). In this region, $\epsilon_r = 0$ but $\epsilon_s \neq 0$. Along the β-characteristics, $\epsilon_s = C_\beta = \text{const}$. The values of C_β are the same as at the points of intersection of the β-characteristics with the vertical line $x = L$. These values are given by equations (16) and (17)

$$C_{\beta AB} = -\frac{k-1}{k+1}(L+2s^0t_{AB})\left[\frac{L+2s^0t_{AB}}{(5-3k)t_{AB}} - \frac{k+1}{3-k}s^0\right]K + \frac{2a_0^2K(k+1)t_{AB}}{(5-3k)(3-k)}. \tag{18}$$

For an arbitrary point (L, t_{AB}), by the use of equation (13), the equation of the characteristic at the back of the centred wave, i.e. $x/t = V_2^0 + a_2^0$, and equation (25), we can calculate for given t the corresponding co-ordinate x lying on the β-characteristic which intersects the vertical line $x = L$ at the point (L, t_{AB}):

$$x - L = (L+2s^0t_{AB})\left[\left(\frac{k+1}{k-1}\frac{t_{AB}}{L+2s^0t_{AB}}a_2^0\right)^{(3-k)/[2(1-k)]} - 1\right]$$
$$+ (V_2^0 - a_2^0)t + 2s^0t_{AB} - \frac{k+1}{k-1}a_2^0\left[\frac{t_{AB}^{(3-k)/(k+1)}}{L+2s^0t_{AB}}\frac{k+1}{k-1}a_2^0\right]^{(k+1)/[2(1-k)]}. \tag{19}$$

For the case of subsonic flow behind a centred wave ($|V_2^0| < a_2^0$), we can calculate the flow parameters in region II (figure 1*a*) from the system of equations similar to (3) and (4) but with constant coefficients

$$\frac{\partial\epsilon_r}{\partial\alpha} \equiv \frac{\partial\epsilon_r}{\partial t} + (V_2^0 + a_2^0)\frac{\partial\epsilon_r}{\partial x} = -\frac{V_2^0a_2^0}{2}\psi, \tag{20}$$

$$\frac{\partial\epsilon_s}{\partial\beta} \equiv \frac{\partial\epsilon_s}{\partial t} + (V_2^0 - a_2^0)\frac{\partial\epsilon_s}{\partial x} = -\frac{V_2^0a_2^0}{2}\psi. \tag{21}$$

Then we find from equation (20) that the α-characteristics are straight lines

$$x = (V_2^0 + a_2^0)\,t + x_{0\alpha}, \tag{22}$$

where $x_{0\alpha}$ is the co-ordinate of the point of intersection of the α-characteristic with the x-axis. Along these characteristics

$$\epsilon_r = -\frac{V_2^0 a_2^0}{2} K \frac{x}{V_2^0 + a_2^0} + C_\alpha, \tag{23}$$

where C_α is a constant along each characteristic which can be calculated from the boundary condition $\epsilon_r = 0$ when $x = L$. Then we get

$$\epsilon_r = -\frac{V_2^0 a_2^0}{2} K \frac{x - L}{V_2^0 + a_2^0}. \tag{24}$$

The characteristics of equation (21) can be written in the form

$$x = (V_2^0 - a_2^0)\,t + x_{0\beta}, \tag{25}$$

where $x_{0\beta}$ is the co-ordinate of the point of intersection of the β-characteristic with the x-axis. Along these characteristics, we have

$$\epsilon_s = -\frac{V_2^0 a_2^0}{2} K t + C_\beta. \tag{26}$$

The constants C_β are calculated from the compatibility conditions for the solutions (16) and (26) along the rear boundary of the centred wave in regions I and II. We then have for $x_b = (V_2^0 + a_2^0)\,t_b$, the relation

$$-\frac{V_2^0 a_2^0}{2} K t_b + C_\beta = -a_2^0 t_b \left[\frac{k+1}{k-1}\frac{a_2^0}{5-3k} - \frac{k+1}{3-k} s^0\right] K + \frac{2a_0^2 K(k-1)}{(5-3k)(3-k)} t_b.$$

The co-ordinates (x, t) of an arbitrary point lying in region II on the β-characteristic through the point (x_b, t_b) on the back of the centred wave satisfy

$$\frac{x_b - x}{t_b - t} = V_2^0 - a_2^0,$$

so that

$$t_b = \frac{x - (V_2^0 - a_2^0)\,t}{2a_2^0}.$$

Then finally we have

$$\epsilon_s = -\frac{V_2^0 a_2^0}{3-k} K t + \frac{K(x - V_2^0 t)}{(3-k)\,a_0}\left[\frac{2(k+1)\,(a_0^2 - a_2^{0^2})}{5-3k} + (k-1)\,V_2^0 a_2^0\right]. \tag{27}$$

Equations (24) and (27) then give the flow parameters in region II (figure 1*a*).

In region IV (figures 1*a*), $\epsilon_r = 0$, and ϵ_s takes a constant value along β-characteristics which is equal to the value at the points of intersection of the β-characteristic with $x = L$. Then in region IV, we get

$$\epsilon_s = -\frac{V_2^0 a_2^0}{3-k} K\left(t - \frac{x-L}{V_2^0 - a_2^0}\right) + \frac{K\left(L - V_2^0 t + \dfrac{x-L}{V_2^0 - a_2^0} V_2^0\right)}{(3-k)\,a_2^0}\left[\frac{2(k+1)\,(a_0^2 - a^{0^2})}{5-3k} + (k-1)\,V_2^0 a_2^0\right]. \tag{28}$$

When the β-characteristics reach the moving piston, the boundary condition along the piston path, $x/t = V_2^0 = \text{const}$, gives $\epsilon_V = \epsilon_r - \epsilon_s = 0$. Then we have a reflected wave (region V on figure 1*a*) in which the α-characteristics are given by $dx/dt = V_2^0 + a_2^0$, and along which $\epsilon_r = \text{const}$. The value of ϵ_r is equal to the value of ϵ_s for the β-characteristic passing through the point where the α-characteristic meets the piston path.

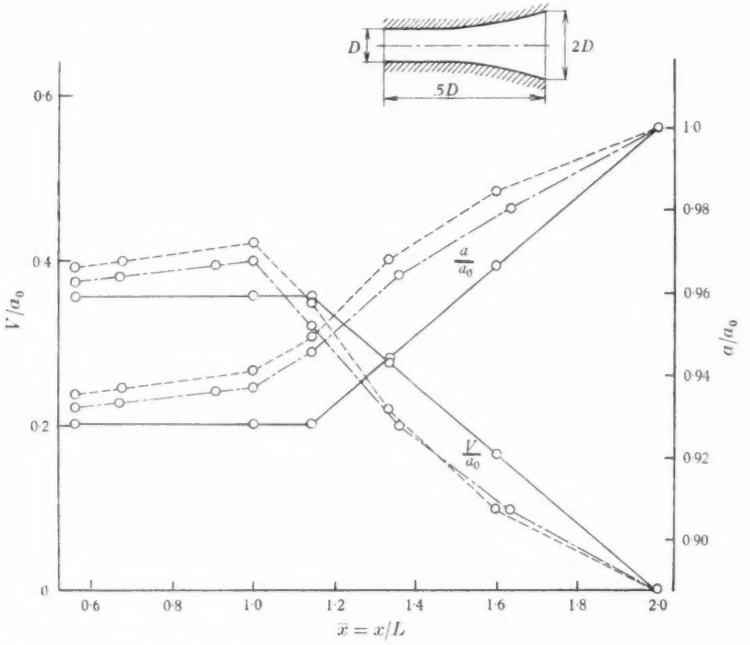

FIGURE 2. Comparison of the present method with a step-by-step calculation of the velocity and velocity of sound in a centred wave along a tube of variable cross-section given by $A/A_0 = e^{1\cdot384(x/L)}$, when $a_0 t/L = 2$. ----, Step-by-step calculations; —·—, linearized theory; ——, simple wave.

A comparison of the present method with step-by-step calculations† using equations (1) and (2) is shown in figures 2 and 3 for $K = 1{\cdot}384$ and $k = 1{\cdot}4$, and for $tL/a_0 = 2$ and $tL/a_0 = 2{\cdot}5$. The solid lines correspond to the simple wave solution for $A = A^0 = \text{const}$.

We thus find reasonably good results for a duct of non-slowly varying cross-section, in which K has a value such that when $\bar{x} = 5$, the cross-section area of the duct increases four times ($A/A_0 = 4$).

3. The boundary-layer influence on the simple wave

This problem was discussed by Owczarek (1956), who supposed that the boundary layer caused only surface friction and a production of entropy. In fact, the boundary-layer influence is more complicated, because of the change in

† These computations were made by P. Kijkowski.

the effective duct cross-section area. A more detailed consideration, based on the three principal equations of mechanics, of the boundary-layer influence in the special case of shock-tube flow was given by Rościszewski (1959). Below, we

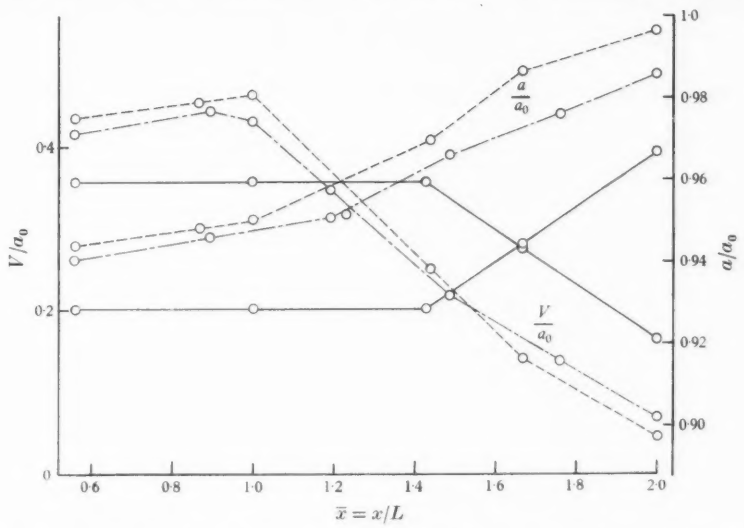

FIGURE 3. Comparison of the present method with a step-by-step calculation of the velocity and velocity of sound in a centred wave along a tube of variable cross-section given by $A/A_0 = e^{1\cdot384(x/L)}$, when $a_0 t/L = 2\cdot5$. ----, Step-by-step calculations; —·—, linearized theory; ——, simple wave.

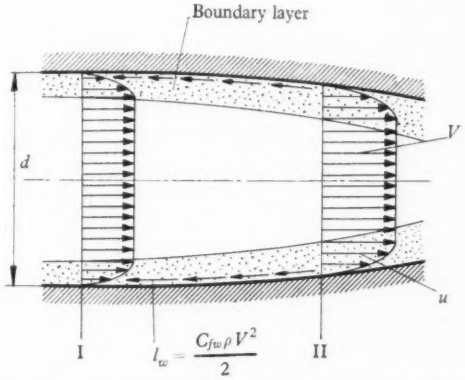

FIGURE 4. Boundary-layer influence on unsteady flow in a duct of slowly varying cross-section.

shall generalize this theory for the arbitrary one-dimensional unsteady flow. We shall assume that the boundary-layer thickness is very small in comparison with the duct diameter, and that the pressure is constant in each cross-section. We then apply the three basic equations of mechanics to the control volume between sections I and II of the tube (figure 4) of variable cross-section. We

assume the variation of duct cross-section to be a small quantity of the same order as the variation of boundary-layer thickness.

The conservation of mass gives

$$\left[\iint_A \rho u dA\right]_{\mathrm{I}} - \left[\iint_A \rho u dA\right]_{\mathrm{II}} = \frac{\partial}{\partial t}\left\{\int_{x_{\mathrm{I}}}^{x_{\mathrm{II}}}\left[\iint_A \rho dA\right]dx\right\},$$

where u and ρ are the velocity and density in a given cross-section. We note that

$$\iint_A \rho^i w^j dA = (A - \pi\delta_{ij} d)\bar{\rho}^i V^j,$$

where V and $\bar{\rho}$ are constant in a given cross-section and are the velocity and density outside of boundary layer, and

$$\delta_{ij} = \int_0^{\delta}\left(1 - \frac{\rho^i u^j}{\bar{\rho}^i V^j}\right)dy. \tag{29}$$

In particular $\delta_{11} \equiv \delta^*$ is the well-known boundary-layer displacement thickness.

Finally we get† for $x_{\mathrm{I}} \to x_{\mathrm{II}}$,

$$\frac{D\bar{\rho}}{Dt} + \bar{\rho}\frac{\partial V}{\partial x} = -\bar{\rho}\frac{D\ln A}{Dt} + \frac{4\bar{\rho}}{d}\left(V\frac{\partial\delta^*}{\partial x} + \frac{\partial\delta_{10}}{\partial t}\right). \tag{30}$$

The momentum equation gives

$$\begin{aligned}(Ap)_{\mathrm{I}} - (Ap)_{\mathrm{II}} + \int_{x_{\mathrm{I}}}^{x_{\mathrm{II}}} p\frac{\partial A}{\partial x}dx - \int_{x_{\mathrm{I}}}^{x_{\mathrm{II}}} \pi d\frac{\bar{\rho}V^2}{2}C_{fw}dx \\ = \left[\iint_A \rho u^2 dA\right]_{\mathrm{II}} - \left[\iint_A \rho u^2 dA\right]_{\mathrm{I}} + \frac{\partial}{\partial t}\left\{\int_{x_{\mathrm{I}}}^{x_{\mathrm{II}}}\left[\iint_A \rho u dA\right]dx\right\},\end{aligned}$$

where C_{fw} is the surface friction coefficient $\left(\tau = \frac{\bar{\rho}V^2}{2}C_{fw}\right)$. Using equation (29) we get for $x_{\mathrm{I}} \to x_{\mathrm{II}}$,

$$\frac{DV}{Dt} + \frac{1}{\bar{\rho}}\frac{\partial p}{\partial x} = -\frac{2C_{fw}V^2}{d} - \frac{4V^2}{d}\frac{\partial(\delta^* - \delta_{12})}{\partial x} - \frac{4V}{d}\frac{\partial(\delta_{10} - \delta^*)}{\partial t}. \tag{31}$$

The energy equation gives

$$\left[\iint_A i_0\rho u dA\right]_{\mathrm{II}} - \left[\iint_A i_0\rho u dA\right]_{\mathrm{I}} + \frac{\partial}{\partial t}\left\{\int_{x_{\mathrm{I}}}^{x_{\mathrm{II}}}\left[\iint_A \rho E dA\right]dx\right\} = -\pi d\int_{x_{\mathrm{I}}}^{x_{\mathrm{II}}} q_w dx,$$

where

$$i_0 = \frac{u^2}{2} + \frac{k}{k-1}\frac{p}{\rho}$$

is the stagnation enthalpy,

$$E = \frac{u^2}{2} + \frac{1}{k-1}\frac{p}{\rho} \quad \text{and} \quad q_w$$

is the heat flow through the duct wall per unit time per unit area. Using equations (29) and (31), and

$$\frac{S - S_0}{C_V} = \ln\frac{p}{\rho^k},$$

† Assuming $A = \frac{1}{4}\pi d^2$.

we get for $x_{II} \to x_I$,

$$\frac{1}{C_p}\frac{DS}{Dt} = \frac{2(k-1)}{da^2}V^3\left[\frac{2}{k-1}\frac{a^2}{V^2}\frac{\partial\delta_{01}}{\partial x} + \frac{1}{V}\left(1-\frac{2}{k-1}\frac{a^2}{V^2}\right)\frac{\partial\delta_{10}}{\partial t} + \left(1-\frac{2}{k-1}\frac{a^2}{V^2}\right)\frac{\partial\delta^*}{\partial x}\right.$$
$$\left. -\frac{2}{V}\frac{\partial\delta^*}{\partial t} - 2\frac{\partial\delta_{12}}{\partial x} + \frac{1}{V}\frac{\partial\delta_{12}}{\partial t} + \frac{\partial\delta_{13}}{\partial x} + C_{fw}\right] - \frac{4q_w(k-1)}{\rho a^2 d}. \quad (32)$$

Using equations (29), (31) and (32), we can express the coefficients F_1, F_2 in equations (1) and (2) as

$$F_{1,2} = \frac{2V^2}{d}\left[\left(\pm 1 - \frac{k-1}{2}\frac{V}{a}\right)\frac{\partial\delta^*}{\partial x} + \left(\mp 1 - \frac{k-1}{a}V\right)\frac{\partial\delta_{12}}{\partial x} - \frac{a}{V}\frac{\partial\delta_{01}}{\partial x}\right.$$
$$-\frac{k-1}{2}\frac{V}{a}\frac{\partial\delta_{13}}{\partial x} - \left[\pm\frac{1}{V} - (k-1)\frac{1}{a}\right]\frac{\partial\delta^*}{\partial t} - \frac{1}{V}\left(\frac{k-1}{2}\frac{V}{a}\mp 1\right)\frac{\partial\delta_{10}}{\partial t}$$
$$\left. -\frac{k-1}{2}\frac{1}{a}\frac{\partial\delta_{12}}{\partial x} \pm \frac{c_{fw}}{2}\left[1\mp(k-1)\frac{V}{a}\right] + \frac{(k-1)q_w}{\rho a V^2}\right]. \quad (33)$$

We assume that the boundary-layer parameters δ_{ij}, c_{fw} and q_w are given on the basis of the solution of the boundary-layer equations with the velocity in the duct given by the ideal flow solution. This is a good approximation when the boundary layer is thin. For the case when it is not so, we can apply the method of successive approximation.

In particular, by making use of the theory of the non-steady boundary layer caused by a simple wave and of equation (33), it is possible to compute (as before) the boundary-layer influence on the centred wave. For example, it is possible to employ Backer's (1957) results which are obtained by the assumption of constant pressure, density and temperature in a given cross-section. In this case, using a very close approximation to Backer's formula (43) ($g = 4\eta + 2\eta^2$) for laminar flow and Rayleigh's approximation for turbulent flow, we obtain the solution in closed form for the centred wave. All the boundary-layer characteristics in this case depend in a simple manner of $\eta = 1 - x/a_0 t$ and t.

The integrals on the right-hand side of the equations obtained, which are similar to equation (14), can be solved in closed form. Backer's results can be used only for the weak waves (a small velocity of flow) because of the assumption of constant density in a cross-section.

For a more general solution of the problem discussed it is necessary to solve the unsteady compressible boundary layer, with the assumption of a simple wave potential flow and a heat conducting duct wall.

REFERENCES

Backer, E. 1957 *Ing. Archiv.* **25**, .

Courant, R. & Friedrichs, K. O. 1948 *Supersonic Flow and Shock Waves.* New York: Interscience.

Owczarek, J. 1956 *Quart. J. Mech. Appl. Math.* **9**, 143.

Rościszewski, J. 1959 *J. Aero-Space Sci.* **26**, 388.

Rudinger, G. 1950 *Wave Diagrams for Nonsteady Flow in Ducts.* New York: Van Nostrand.

REVIEWS

Fluid Dynamics. By D. E. Rutherford. Edinburgh: Oliver and Boyd, 1959. 226 pp. 10*s*. 6*d*.

Hydrodynamics. By D. H. Wilson. London: Edward Arnold (Publishers) Ltd., 1959. 149 pp. 30*s*.

When Sir Horace Lamb's *Hydrodynamics* was first published in 1879, fluid dynamics was a sufficiently compact science to make it possible for an author to record most of the known principles and many of their more important applications between the covers of a single volume. During the subsequent half-century the subject grew to such an extent that, when the last edition of Lamb's famous book appeared in 1932, it was, despite its greatly increased content, already a rather unbalanced account of the subject as a whole. And during the last quarter-century the scope and depth of the science has increased beyond all recognition, making the idea of a single all-embracing treatise quite obsolete.

But the idea of an elementary textbook, designed to give students of theoretical fluid dynamics a broad introduction to the whole subject, is not obsolete. Indeed, it must never become so if the teaching of fluid dynamics in standard university courses is to retain its usefulness. The writing of such a book, however, presents the author with a very difficult problem, that of choosing appropriate material. Moreover, he is not entitled here, as he may be in the writing of a monograph or more advanced treatise, to let his own interests dictate the choice. For the relative space devoted to each topic will be regarded by the student as a measure of the relative importance of each topic, so that if the student is to get a reasonably well-balanced picture of the modern subject the choice of material is of comparable importance with the way it is presented. Dr Rutherford is therefore to be congratulated for producing a book which gets away from the idea that elementary fluid dynamics consists mainly of techniques for solving problems concerned with the irrotational flow of a liquid. This, indeed, is the chief virtue of the book under review. So many books dealing almost exclusively with potential flow have been published over the years that one almost feels that Lamb's great book has, through no fault of its author, cast a shadow, rather than a light, over the teaching of the subject.

Nevertheless, Dr Rutherford's choice of material is not as well balanced as it might be. Of the five chapters, the first (39 pages) deals with the basic concepts, the next two (90 pages) with non-viscous incompressible flow, the fourth (62 pages) with compressibility, and the last (29 pages) with viscosity. By almost any standards, viscosity has here received far less than its fair share of attention, and this becomes even more apparent when one examines the content in more detail. It seems strange, for instance, that a book which can find space for the transonic modification of linearized compressible-flow theory contains only a descriptive account of boundary-layer theory, culminating in the remark that many features of this theory are unsatisfactory. And surely much of the point in teaching the elements of viscous flow is to give the student some sort of mechanistic explana-

tion of the more artificial devices of non-viscous flow theory, such as Joukowski's hypothesis in aerofoil theory. Yet, in this particular connexion, we read (p. 67) only that the fluid velocity is infinite at the trailing edge 'unless we adopt' this hypothesis.

Dr Rutherford is at his best when treating the more formal parts of the subject. His style of presentation is then brilliantly clear, and in this respect the high standards of the University Mathematical Texts are certainly maintained. He is at his worst, and occasionally it is quite a bad worst, when discussing general principles and their background ideas. It is especially unfortunate, for instance, that we read near the beginning of the book (p. 4) that non-viscous flow theory 'will lead to results which approximate to the motion of those parts of a real fluid which are far from rigid boundaries'. Someone who is already familiar with the theory of laminar flow at large Reynolds numbers might be able to twist the meaning of these words into a description of the truth; but the raw student, with only three pages behind him, will take them literally and thereby gain a completely false picture of the role of non-viscous flow theory in fluid dynamics. Many other potential sources of misunderstanding occur throughout the book, though perhaps none is as serious as the one just mentioned. Typical examples are the failure to qualify the statement of Kelvin's circulation theorem (p. 34) to allow for the important class of rotational flows caused by gravity, the absence of any discussion of the thermodynamic significance of the purely formal definition of pressure in viscous flow (p. 199), and the curious use of the low Reynolds number approximation to neglect the 'stretching' terms, but not the 'convection' terms in the three-dimensional vorticity equation (p. 206). Less important, but nevertheless annoying, is the repeated mis-spelling of the name of Osborne Reynolds, in the form 'Reynold's number', in the last chapter.

The book as a whole leaves one with the impression that it has been written by a naturally lucid author who is, on this occasion, writing outside his normal field of study.

By comparison, Mr Wilson's *Hydrodynamics* follows a traditional pattern much more closely: it is what it claims to be, an introduction to classical hydrodynamics written for students of mathematics and theoretical physics. The opening pages are concerned with vector analysis and the connectivity of spaces, and throughout the following chapters on equations of motion, two-dimensional motion, two-dimensional vortex motion, conformal representation, and axisymmetrical motion, the formal mathematical spirit of these first few pages seems to persist. In fact, these chapters tend to read like a mathematical essay based on a set of axioms to which the underlying physical ideas are quickly reduced, and there is a danger here that the student will forget that he is reading about fluids rather than a class of vector fields satisfying certain constraints. However, the analysis itself is both well presented and suitably up-to-date (it includes the relatively recent circle and sphere theorems of Milne-Thomson, Weiss and Butler). The principal omission from this introductory account of classical hydrodynamics is the theory of wave motion, and it might have been better, for the sake of homogeneity at least, to replace the final brief chapter on viscosity by one on waves.

The most serious drawback of Mr Wilson's book is the one already implied at the beginning of this review, that a study of classical hydrodynamics by itself cannot nowadays be regarded as an adequate introduction to fluid dynamics. If an undergraduate were able to spend the whole of his time studying only fluid dynamics, a book of this kind might well be a suitable text for the appropriate courses; but for a course whose length reflects the legitimate demands of other subjects, such an unbalanced account cannot be recommended.

IAN PROUDMAN

Turbulent Transfer in the Lower Atmosphere. By C. H. B. PRIESTLEY. University of Chicago Press, 1959. 130 pp. 28*s*.

The scientific study of the vertical transfer of heat and water vapour in the lower atmosphere dates effectively from 1911 when the liner *Titanic* struck an iceberg in fog on its maiden voyage across the Atlantic and foundered. It hardly needed this fatality for meteorologists to realise the importance of transfer processes, but the event led to the *Scotia* expedition to the Newfoundland Grand Banks in which G. I. Taylor participated. His observations laid the foundations of the theory of turbulent transfer in the atmosphere and of air-mass modification deriving from the transfers (as recorded in the early papers in volume 2 of *Scientific Papers*, by G. I. Taylor). Water vapour (latent heat) is wholly supplied and sensible heat partly supplied to the atmosphere from below by turbulent process, and the total of this supply of energy, deriving ultimately of course from the sun, is the main source of power for the atmospheric engine. The flux of momentum from air to surface is a concomitant of the energy fluxes and provides the only external force, other than gravity and mountain drag, to which the lower atmosphere is subjected.

Taylor's theory was expressed in terms of an eddy transfer coefficient related empirically to some representative wind and difference of temperature in the vertical, and was applied to transfer processes over more or less deep layers. That was followed, in the decade or so before the last war and immediately after, by the application of boundary-layer knowledge, primarily to the lower part of the affected layer in which turbulent fluxes could be assumed independent of height. Attention was directed particularly to the determination of surface fluxes from the vertical variation of macroscopic (mean) properties, of wind speed, temperature and vapour pressure. The quantitative effect of thermal or density stratification on the transfer process did not, however, readily appear.

Dr Priestley, who has led an active group on transfer study near Melbourne over most of the post-war period, now provides us with a monograph which takes up the story of transfer at roughly the above stage and describes the recent theoretical and observational developments, largely in terms of the work of his group. The accent again falls on transfer in the constant flux layer, now with particular reference to mechanism and to the effects of thermal stratification, and mainly in respect of heat transfer. But the behaviour of deep layers is also critically considered.

Following the introduction, the author first discusses the eddy flux and its measurement near the surface, enlarging separately on the shearing stress in relation to the wind profile, and on heat convection in relation to the temperature profile. There is then a chapter on the spectrum of turbulence and the structure of free convection followed by a theoretical treatment of buoyant motion, the latter along the lines of Priestley's recent work but with attention paid also to Morton, Taylor & Turner (*Proc. Roy. Soc.* A, **234**, 1956, 1). Special aspects arising in the study of evaporation are considered briefly and the book then concludes with a thoughtful discussion of the application of transfer theory to what is commonly called synoptic meteorology, the concern being with 'the pattern in space and time of the surface heating or, more generally, that of the total energy source' in relation to typical weather systems.

The direct measurement of energy and momentum fluxes at the earth's surface itself is usually difficult and often impossible, for which reason the general tendency is towards measurements of fluxes *near* the earth's surface by the co-variance technique, the vertical flux of heat, for example, being given by $\rho c_p \overline{w'T'}$, where w' is the vertical component of eddy velocity, T' the associated temperature anomaly and ρc_p the heat capacity per unit volume. These measurements, however, are also far from simple, as is now well known, and reliable values are only to be obtained from instruments with a wide frequency response and much labour. The efforts of Priestley's group to make representative measurements over a wide range of stability (or of Richardson number) are to be highly commended. Yet the fact that a majority of these measurements missed, by selective sampling in frequency, significant fractions of the fluxes (up to about 30 %), indicates the scope for much further effort. Moreover, there is evidence now from more than one source that the spectral form of the momentum and heat flux covariances may be materially different, so that the ratio of eddy viscosity to eddy diffusivity which is inferred from the fluxes and gradients may be distinctly uncertain. One does not regret the author's attempt to assemble inferences from the data, whose limitations are not glossed over, but some of the inferences at least must temporarily remain in doubt.

No work of consequence has been done in the laboratory on heat transfer in boundary layers whose structure is affected by the heat transfer or thermal stratification in the layer, on account of the difficulty in obtaining large (positive or negative) Richardson numbers in the laboratory. Priestley, therefore, can only appeal to observation in the real but uncontrolled and somewhat 'messy' atmosphere for empirical relations concerning forced convention which can provide a test of theory. The case is otherwise for free convection from plane surfaces, with the work of Malkus and Townsend among others, but the author has not seen fit to consider this in relation to the atmospheric data and theory except for passing reference to Townsend. Perhaps the laboratory studies need to be taken further before they can be used effectively in the meteorological problem.

The current position regarding the relation of vertical fluxes near the earth's surface to the 'external' parameters, the latter depending on the problem posed, is that there is a reasonably valid body of knowledge available for conditions

sufficiently near neutral static stability and, for heat flux only, in conditions so unstable that free convection obtains. Some understanding of the intermediate (general) condition and the case of extreme stability begins to appear, but theory is halting and good observation still needed. Priestley gives an admirable account of the position and shows how theory and recent observation are leading to better understanding of the relevant mechanisms. If he implies greater penetration than is perhaps justified, that is excusable in one who has made, directly and indirectly, so considerable an impression on the subject. The reader must keep his wits about him and he may then be promised a stimulating experience, in which physical intuition and discipline will be found the master of mathematical detail. One would have liked an author's prospect at the conclusion of each main section, but its absence encourages the reader to supply his own and thereby perhaps to balance his own view against Priestley's as to just how far the subject has got. The aspects of dynamical meteorology which characterize the subject and make it strange to fluid dynamicists, namely, those arising from rotational and baroclinic effects, are largely absent here, and it is to be hoped that they will look carefully at this monograph. A fluid dynamicist can read it out of his own experience and perhaps, as a result, assist the meteorologist in his tremendous task.

P. A. Sheppard

INDEX

AXFORD, W. I. The oscillating plate problem in magneto hydrodynamics, 97

BARTHEL, JAMES, R. and LYKOUDIS, PAUL S. The slow motion of a magnetized sphere in a conducting medium, 307

CLARKE, JOSEPH H. The force on wing-fuselage combinations in supersonic flow, 210

DE WIEST, ROGER, J. M. Unsteady flow through an underdrained earth dam, 1

ELLISON, T. H. A note on the velocity profile and longitudinal mixing in a broad open channel, 33

ELLISON, T. H. and TURNER, J. S. Mixing of dense fluid in a turbulent pipe flow. Part 1. Overall description of the flow, 514

ELLISON, T. H. and TURNER, J. S. Mixing of dense fluid in a turbulent pipe flow. Part 2. Dependence of transfer coefficients on local stability, 529

EMMONS, H. W. *See* MURGAI

FREEMAN, N. C. On a singular point in the Newtonian theory of hypersonic flow, 109

FRIEDMAN, M. P. An improved pertubation theory for shock waves propagating through non-uniform regions, 193

GRAEBEL, WILLIAM PAUL. The stability of a stratified flow, 321

HASIMOTO, HIDENORI. Steady longitudinal motion of a cylinder in a conducting fluid, 61

HOWELLS, I. D. The effect of turbulence and magnetic field on electron density fluctuations in the ionosphere, 545

HUNTER, C. On the collapse of an empty cavity in water, 241

KELLER, JOSEPH B. *See* TADJBAKHSH

LIGHTHILL, M. J. Dynamics of a dissociating gas. Part 2. Quasi-equilibrium transfer theory, 161

LONGUET-HIGGINS, M. S. Mass transport in the boundary layer at a free oscillating surface, 293

LONGUET-HIGGINS, M. S. and STEWART, R. W. Changes in the form of short gravity waves on long waves, and tidal currents, 565

LYKOUDIS, PAUL S. *See* BARTHEL

MACK, LESLIE M. The compressible viscous heat-conducting vortex, 284

MAULL, D. J. Hypersonic flow over axially symmetric spiked bodies, 584

MOLLÖ-CHRISTENSEN, ERIK and NARASIMHA, RODDAM. Sound emission from jets at high subsonic velocities, 49

MORTON, B. R. Laminar convection in uniformly heated vertical pipes, 227

MURGAI, M. P. and EMMONS, H. W. Natural convection above fires, 611

NARASIMHA, RODDAM. *See* MOLLÖ-CHRISTENSEN

PACK, D. C. A note on the breakdown of continuity in the motion of a compressible fluid, 103

PALM, ENOK. On the tendency towards hexagonal cells in steady convection, 183

PAPADOPOULOS, V. M. A line source on an interface between two media, 41

RAYMOND, JOSEPH L. Piston theory applied to strong shocks and unsteady flow, 509

ROŚCISZEWSKI, JAN. Calculations of the motion of non-uniform shock waves, 337

ROŚCISZEWSKI, JAN. Propagation of waves of finite amplitude along a duct of non-uniform cross-section, 625

ROSENBLAT, S. Flow between torsionally oscillating disks, 388

SAFFMAN, P. G. On the effect of the molecular diffusivity in turbulent diffusion, 273

SCHUBAUER, G. B. and SPANGENBURG, W. G. Forced mixing in boundary layers, 10

SHERMAN, FREDERICK S. Shock-wave structure in binary mixtures of chemically inert perfect gases, 465

SPANGENBERG, W. G. *See* SCHUBAUER

SPENCE, D. H. Velocity and enthalpy distributions in the compressible turbulent boundary layer on a flat plate, 368

STEWART, R. W. *See* LONGUET-HIGGINS

STEWARTSON, K. On the motion of a non-conducting body through a perfectly conducting fluid, 82

TADJBAKHSH, IRADJ and KELLER, JOSEPH B. Standing surface waves of finite amplitude, 442

TOWNSEND, A. A. The development of turbulent boundary layers with negligible wall stress, 143

TURCOTTE, DONALD L. The melting of ice in a hot humid stream of air, 123

TURNER, J. S. *See* ELLISON

URSELL, F. On Kelvin's ship-wave pattern, 418

VAN BLERKOM, RICHARD. Magneto hydrodynamic flow of a viscous fluid past a sphere, 432

WARREN, C. H. E. An experimental investigation of the effect of ejecting a coolant has at the nose of a bluff body, 400

WILLIAMS, W. E. Exact solutions of the magneto hydrodynamic equations, 452

WINTER, D. F. T. Multiple shock compression using a piston of finite weight, 264

YIH, CHIA-SHUN. Gravity waves in a stratified fluid, 481

REVIEWS

Advanced Mechanics of Fluids, 156

Aerodynamik des Flugzeuges. Band 1, 158

Journal of Nuclear Energy. Part C. Plasma Physics—Accelerators—Thermonuclear Research, 160

Fluid Mechanics, 315

Fluid Dynamics, 634

Hydrodynamics, 634

Turbulent Transfer in the Lower Atmosphere, 636

JOURNAL OF FLUID MECHANICS

The JOURNAL OF FLUID MECHANICS exists for the publication of theoretical and experimental investigations of all aspects of the mechanics of fluids, and is issued in four parts per volume.

EDITOR

DR G. K. BATCHELOR

Department of Applied Mathematics and Theoretical Physics, University of Cambridge, Free School Lane, Cambridge, England

ASSISTANT EDITORS

DR T. B. BENJAMIN, DR I. PROUDMAN, DR P. G. SAFFMAN

Department of Applied Mathematics and Theoretical Physics, University of Cambridge, Free School Lane, Cambridge, England

ASSOCIATE EDITORS

PROF. G. F. CARRIER

Pierce Hall, Harvard University, Cambridge 38, *Massachusetts, U.S.A.*

DR W. C. GRIFFITH

Research and Development Laboratory, Missile Systems Division, Lockheed Aircraft Corporation, Palo Alto, California, U.S.A.

M. J. LIGHTHILL

Royal Aircraft Establishment, Farnborough, Hampshire, England

PROF. R. R. LONG

School of Engineering, The Johns Hopkins University, Baltimore 18, *Maryland, U.S.A.*

Authors wishing to have papers published in the JOURNAL should communicate them to any one of the persons named above, choosing one in their own country where possible.

Authors are urged to ensure that their papers are written clearly and attractively, in order that their work will be readily accessible to readers.

Manuscripts should be typed in double spacing on one side of the paper only, with references listed at the end in alphabetical order of authors. Drawings should be done on a large scale in Indian ink on tracing cloth or drawing paper, the lettering being shown clearly in pencil for reproduction by the printer; the list of captions should be typed at the end of the manuscript. Proofs of papers from overseas will usually be despatched to authors by airmail. There is no charge for publication. Authors are entitled to receive 50 offprints of a paper in the JOURNAL free of charge, and additional offprints can be purchased if ordered in advance.

SUBSCRIPTIONS

The subscription price for a volume of four parts is £5. 10*s*. net, post free, payable in advance; separate parts 30*s*. net, plus postage. Subscriptions may be sent to any bookseller, or to the Cambridge University Press, Bentley House, 200 Euston Road, London, N.W. 1.

Subscribers in the United States should send their orders to the Cambridge University Press, American Branch, 32 East 57th Street, New York 22. The subscription price per volume is $18.50, post free, payable in advance; separate parts $5.00, plus postage.

Quotations for available back volumes and parts may be obtained on application to the Cambridge University Press.

Particulars of the

JOURNALS

Published by the Cambridge University Press, may be had from

THE MANAGER
CAMBRIDGE UNIVERSITY PRESS
BENTLEY HOUSE
200 EUSTON ROAD
LONDON, N.W. 1

★

Inquiries for Advertisement space in any of the journals published by the Cambridge University Press should be addressed to

THE
ADVERTISEMENT DEPARTMENT
CAMBRIDGE UNIVERSITY PRESS
BENTLEY HOUSE
200 EUSTON ROAD
LONDON, N.W. 1

The Aeronautical Research Council of Great Britain has sponsored the following books on Fluid Dynamics published by the Clarendon Press:

Incompressible Aerodynamics

An Account of the Theory and Observation of the Steady Flow of Incompressible Fluid past Aerofoils, Wings, and other Bodies

Edited by BRYAN THWAITES

The first of a new series sponsored by the Aeronautical Research Council, this is a comprehensive review of certain flows of incompressible fluid which are of special importance to aeronautics. Many of the theories described are also being increasingly applied to other fields of knowledge and technology. (FLUID MOTION MEMOIRS, *Illustrated 75s net*

FORTHCOMING:

Laminar Boundary Layers
by L. ROSENHEAD *(ed.)*

ALREADY PUBLISHED:

Modern Developments in Fluid Dynamics, Vols. I & II (1938),
by S. GOLDSTEIN *(ed.)*

High Speed Flow, Vols. I & II (1953),
by L. HOWARTH *(ed.)*

Compressible Airflow: Tables (1952),
by L. ROSENHEAD *(ed.)*

Compressible Airflow: Graphs (1957),
by L. ROSENHEAD *(ed.)*

Oxford UNIVERSITY PRESS

JOURNAL OF FLUID MECHANICS

Volume 8, Part 4 August 1960

CONTENTS

Gravity waves in a stratified fluid
by CHIA-SHUN YIH *page* 481

Piston theory applied to strong shocks and unsteady flow
by JOSEPH L. RAYMOND 509

Mixing of dense fluid in a turbulent pipe flow. Part 1. Overall description of the flow
by T. H. ELLISON and J. S. TURNER 514

Mixing of dense fluid in a turbulent pipe flow. Part 2. Dependence of transfer coefficients on local stability
by T. H. ELLISON and J. S. TURNER 529

The effect of turbulence and magnetic field on electron density fluctuations in the ionosphere
by I. D. HOWELLS 545

Changes in the form of short gravity waves on long waves and tidal currents
by M. S. LONGUET-HIGGINS and R. W. STEWART 565

Hypersonic flow over axially symmetric spiked bodies
by D. J. MAULL 584

The hydrodynamic stability of a thin film of liquid in uniform shearing motion
by JOHN W. MILES 593

Natural convection above fires
by M. P. MURGAI and H. W. EMMONS 611

Propagation of waves of finite amplitude along a duct of non-uniform cross-section
by JAN ROŚCISZEWSKI 625

REVIEWS

Fluid Dynamics 634

Hydrodynamics 634

Turbulent Transfer in the Lower Atmosphere 636

INDEX TO VOLUME 8 639

#482

Printed in Great Britain at the University Press, Cambridge
(Brooke Crutchley, University Printer)